Design Tool for a Ground-Coupled Ventilation System

Mohammad Omar Alfadil

Dissertation submitted to the Faculty of the Virginia Polytechnic Institute and State University

in partial fulfillment of the requirements for the degree of

Doctor of Philosophy
in
Architecture and Design Research

James R. Jones, Chair
Saad A. Ragab
Elizabeth J. Grant
Demetri P. Telionis
Robert P. Schubert

March, 2019
Blacksburg, Virginia

Keywords: Ground-coupled ventilation system, earth to air tunnel heat exchanger, geo-exchange system, and geothermal energy

Design Tool for a Ground-Coupled Ventilation System

Mohammad Omar Alfadil

Abstract

Ground-coupled ventilation (GCV) is a system that exchanges heat with the soil. Because ground temperatures are relatively higher during the cold season and lower during the hot season, the system takes advantage of this natural phenomenon. This research focused on designing a ground-coupled ventilation system evaluation tool of many factors that affect system performance. The tool predicts the performance of GCV system design based on the GCV system design parameters including the location of the system, pipe length, pipe depth, pipe diameter, soil type, number of pipes, volume flow rate, and bypass system. The tool uses regression equations created from many GCV system design simulation data using Autodesk Computational Fluid Dynamics software. As a result, this tool helps users choose the most suitable GCV system design by comparing multiple GCV systems' design performances and allows them to save time, money, and effort.

Design Tool for a Ground-coupled Ventilation System

Mohammad Omar Alfadil

General Audience Abstract

Ground-coupled ventilation (GCV) is a system that exchanges heat with the soil. Because ground temperatures are relatively higher during the cold season and lower during the hot season, the system takes advantage of this natural phenomenon. This research focused on designing a ground-coupled ventilation system evaluation tool of many factors that affect system performance. The tool predicts the performance of GCV system design based on the GCV system design parameters including the location of the system, pipe length, pipe depth, pipe diameter, soil type, number of pipes, volume flow rate, and bypass system. The tool uses equations created from many GCV system designs' simulation data using simulation software. As a result, this tool helps users choose the most suitable GCV system design by comparing multiple GCV system designs' performance and allows them to save time, money, and effort.

Dedication

I dedicate this dissertation to my family:

My father, for supporting and encouraging me;

My mother, for her great sacrifice and prayer;

My lovely wife and children, for their care, support, and patience.

I love you all.

Acknowledgments

I would like to express my sincere gratitude to my advisor, Dr. James R. Jones, for his continuous support, patience, motivation, and immense knowledge during my Ph.D. studies. His guidance helped me at all times during the research and while I was writing this thesis, and I cannot imagine having a better advisor and mentor for my dissertation.

In addition to Dr. Jones, I would like to thank Drs. Saad A. Ragab, Demetri P. Telionis, Elizabeth J. Grant, and Robert P. Schubert for their insightful comments and encouragement. I also would like to thank them for their excellent questions, which motivated me to widen my research and approach it from various perspectives.

I offer many thanks to my colleagues, Bandar Alkahlan, Mohammed Aloshan, Naif Altahlawi, Soo Jeong Jo, Seyedreza Fateminasab, Sana Alrqaibat, Amos Kalua, and Alsaleh Sugati, for their warm words and support.

I would like to give special thanks to my friends, Karim Abdelatty and Saad Alabdulkareem, for helping me code the tool, and Ibrahim Khalfallah, Majed Alarif, Hassan Almani, and my uncle Abdulaziz Althqeb for helping me install the instruments.

Table of Contents

CHAPTER 1: INTRODUCTION **1**

1.1 BACKGROUND 1

1.2 GCV SYSTEM OVERVIEW 2

1.2.1 GCV System Types *3*

1.2.2 Factors Affecting the GCV System *4*

1.2.3 GCV System Design *5*

1.2.4 Opportunity to Reduce Cooling and Heating *6*

1.2.5 Heat Transfer *8*

1.3 PROBLEM STATEMENT 9

1.4 RESEARCH QUESTIONS 10

1.5 RESEARCH GOAL AND OBJECTIVES 10

1.6 RESEARCH SIGNIFICANCE AND CONTRIBUTION TO BODY OF KNOWLEDGE 11

1.7 RESEARCH METHODS 12

1.8 RESEARCH CONTRIBUTION 13

CHAPTER 2: LITERATURE REVIEW **14**

2.1 ENERGY USE IN BUILDINGS 14

2.2 VERTICAL AND HORIZONTAL GCV SYSTEMS 15

2.3 SOLAR CONCRETE MASONRY HOUSE 17

2.3.1 GCV System *24*

2.4 GCV SYSTEM DESIGN 26

2.5 GCV SYSTEM EFFICIENCY 29

2.6 FUNGUS AND BACTERIA IN THE GCV SYSTEM 30

2.7 GROUND AIR HEAT EXCHANGE SOFTWARE (GAEA) 31

2.8 FUNDAMENTAL HEAT TRANSFER 40

2.8.1 Exogenous Variables *42*

2.8.2 Endogenous Variables *50*

2.9 COMPUTATIONAL FLUID DYNAMICS (CFD) 56

2.9.1 Fluid Flows *57*

2.9.2 CFD Predictions *57*

2.9.3 CFD Analysis Process *58*

2.10 AUTODESK CFD VALIDATION 63

2.10.1 Turbulent pipe flow *63*

2.10.2 Flow around a cylinder array *64*

2.10.3 Flow through an overheated cylinder *66*

2.11 CONCLUSION 68

CHAPTER 3: RESEARCH DESIGN 69

3.1 OVERVIEW 69

3.1.1 Methods *69*

3.1.2 Computer Prediction Software *70*

3.1.3 Research Design Strategy *71*

3.2 MONITORING THE GCV SYSTEM AT THE SOLAR CM HOUSE 72

3.3 CFD AND GAEA MODEL FOR THE SOLAR CM HOUSE 72

3.4 GCV PARAMETER MODELING 73

3.4.1 Modeling *75*

3.5 SIMULATION DATA ANALYSIS, REGRESSION ANALYSIS AND VALIDATION 77

3.5.1 Regression Validation *77*

3.6 TOOL DEVELOPMENT 78

3.6.1 Creating the GCV System Evaluation Tool *78*

3.6.2 Tool Validation *80*

3.7 RIYADH GCV SYSTEM 80

CHAPTER 4: MONITORING THE GCV SYSTEM AT THE SOLAR CM HOUSE 82

4.1.1 GCV System in the Solar CM House 83

4.1.2 Equipment Installation and Data Collection 84

CHAPTER 5: CFD AND GAEA MODEL FOR THE SOLAR CM HOUSE 88

5.1 CFD MODEL FOR THE SOLAR CM HOUSE 88

5.1.1 Finding the Appropriate CFD Program 88

5.1.2 Simulation of the GCV System at the Solar CM House 92

5.2 GAEA MODEL FOR THE GCV SYSTEM AT THE SOLAR CM HOUSE 108

5.3 CFD AND GAEA MODELS VALIDATION 115

5.4 SUMMARY 120

CHAPTER 6: GCV SIMULATIONS 121

6.1 SIMULATION VARIABLES 121

6.2 GCV SYSTEM SIMULATION PROCESS 127

6.2.1 Modeling GCV system designs 127

6.2.2 Simulation boundary conditions 129

6.2.3 Model simulations 132

6.3 SUMMARY 134

CHAPTER 7: SIMULATION DATA AND REGRESSION ANALYSIS 135

7.1 SIMULATION DATA ANALYSIS 135

7.2 REGRESSION ANALYSIS 143

7.3 REGRESSION VALIDATION 148

7.4 SUMMARY 150

CHAPTER 8: GCV SYSTEM EVALUATION TOOL 151

8.1 TOOL DEVELOPMENT 151
8.1.1 Tool input *153*
8.1.2 Tool processing *154*
8.1.3 Tool output *156*
8.2 TOOL VALIDATION 158
8.3 TOOL GUIDELINES 163
8.3.1 Building ventilation volume requirements *163*
8.3.2 Tool inputs *168*
8.3.3 Tool processing *170*
8.3.4 Tool output *172*
8.4 SUMMARY 175
CHAPTER 9: RIYADH GCV SYSTEM 176
9.1 OVERVIEW 176
9.2 IN-SITU RIYADH DATA COLLECTION 176
9.3 RIYADH GCV SYSTEM DESIGN 180
9.4 SUMMARY 185
CHAPTER 10: CONCLUSION 186
10.1 METHODOLOGY 186
10.2 RESEARCH FINDINGS 188
10.2.1 *GAEA, CFD simulation, GCV tool accuracy* *188*
10.2.2 *GCV system variable relations* *190*
10.2.3 *Regression equation* *191*
10.2.4 *GCV system evaluation tool* *192*
10.2.5 Riyadh GCV system *193*
10.3 THE CONTRIBUTIONS TO THE BODY OF KNOWLEDGE 194

10.4 FUTURE USES FOR THIS RESEARCH 194

REFERENCES 196

APPENDICES 201

APPENDIX A: GCV SYSTEM AT SOLAR CM HOUSE INSPECTION 201

APPENDIX B: BOUNDARY CONDITIONS: 202

Different volume flow rates 202

Different soil temperatures 206

APPENDIX C: GCV SYSTEM CLOSED LOOP DESIGN 210

APPENDIX D: SOIL TEMPERATURE CHARGED AT SOLAR CM HOUSE 211

Chapter 1: Introduction

1.1 Background

Energy is a basic requirement for life. At present, the growth of energy use in the world continues to affect the supply of energy resources, global warming, and climate change. According to the International Energy Agency (2015), annual primary energy consumption has increased 20% and atmospheric carbon dioxide (CO_2) levels have increased 1.8% over the past two decades. Using renewable energy sources and technologies to achieve increased energy efficiency has the potential to reduce this annual energy consumption, particularly for buildings (Pérez-Lombard, Ortiz, & Pout, 2008).

In developed countries, energy consumption of buildings comprises 20 to 40% of total energy use. HVAC systems alone account for nearly half of the energy consumption in these buildings and represent between 10 and 20% of total energy consumption in developed countries. One possible solution to this increased demand on energy resources is the integration of a systems approach that relies on such high-energy efficiency systems as ground-coupled ventilation (GCV) to reduce energy consumption for heating and cooling buildings (Pérez-Lombard et al., 2008).

1.2 GCV System Overview

Thinking thoroughly about our habitat stimulates creativity. Many innovative ideas stem from our need to live in changing habitats, and the natural world provides illustrations of creative solutions that can improve our lives. For example, termites, or “white ants,” employ a stunning design strategy to ensure their colonies’ survival, in which they build tunnels in their mounds to control the air temperature before the air arrives at the farm core (“The Animal House ~ The Incredible Termite Mound | Nature | PBS,” 2011). Figure 1-1 depicts a termite mound. After World War II, scientists noticed that the air released from the ventilation tunnels of underground shelters was at a different temperature than the outside air. Since then, researchers have developed a system to help cool and heat a building using the ground. Ground-coupled ventilation (GCV) is a system that exchanges heat with the soil by forcing air through buried pipes in the earth. As the ground temperature is more stable than the air temperature, the ground temperature changes more slowly, such that it is higher during the cold season and lower during the hot season. Figure 1-2 shows a schematic GVC system in the cold season (Alghamdi, 2008).

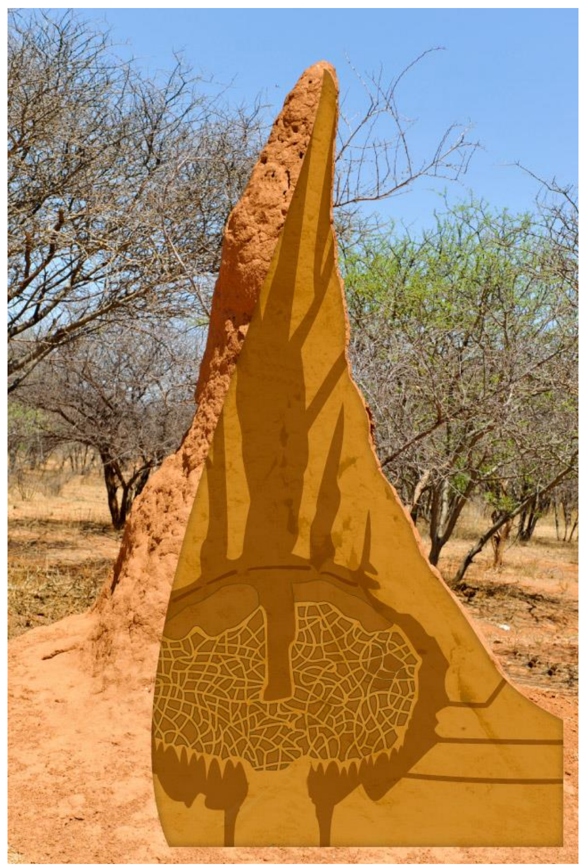

Figure 1-1: A Termite “White Ant” Mound (photograph by “The Animal House ~ The Incredible Termite Mound | Nature | PBS,” 2011 modified by author)

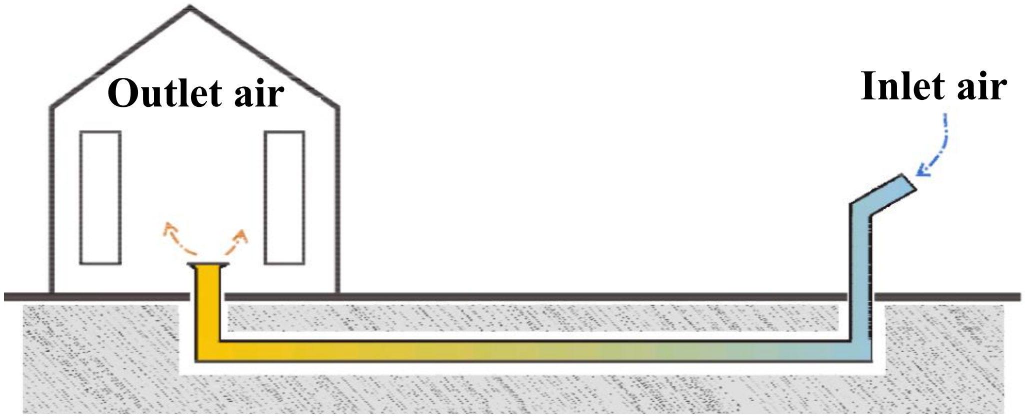

Figure 1-2: Schematic Image of a GCV System (Alghamdi, 2008)

1.2.1 GCV System Types

There are two types of ground-coupled ventilation systems, the open loop system (Figure 1-3) and the closed loop system (Figure 1-4). The open loop system forces the outdoor air through the ground into the indoor environment. In contrast, the closed loop system circulates indoor air through the ground and does not rely on fresh air (Taylor, 2008).

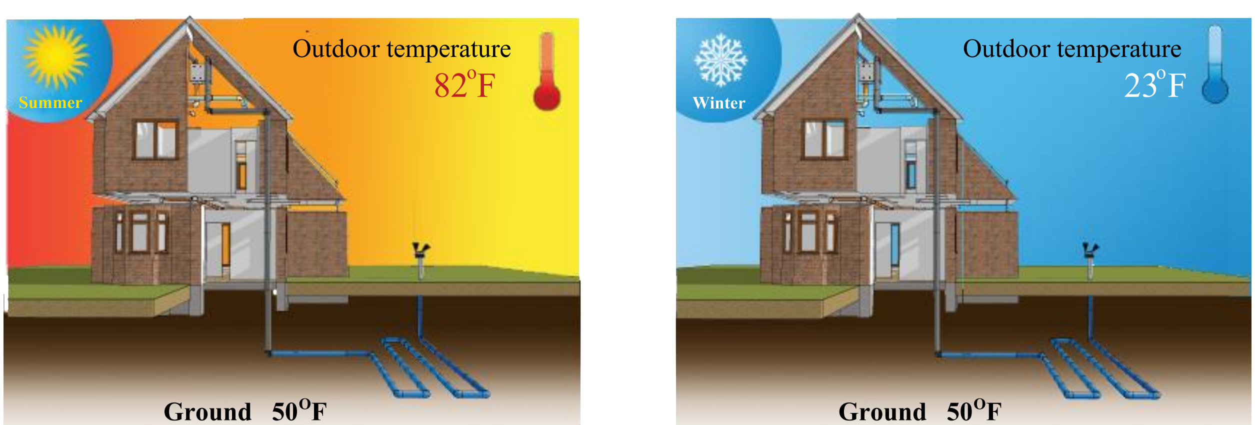

Figure 1-3: An Open Loop System

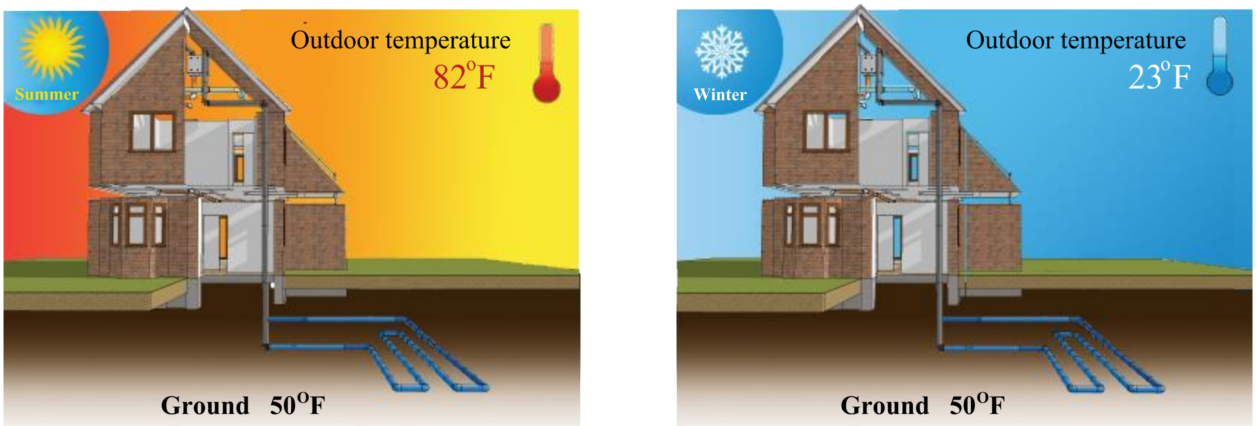

Figure 1-4: A Closed Loop System

1.2.2 Factors Affecting the GCV System

There are many factors that influence the performance of a GCV system, including site, design, air residence time, heating and cooling loads, and location (Figure 1-5).

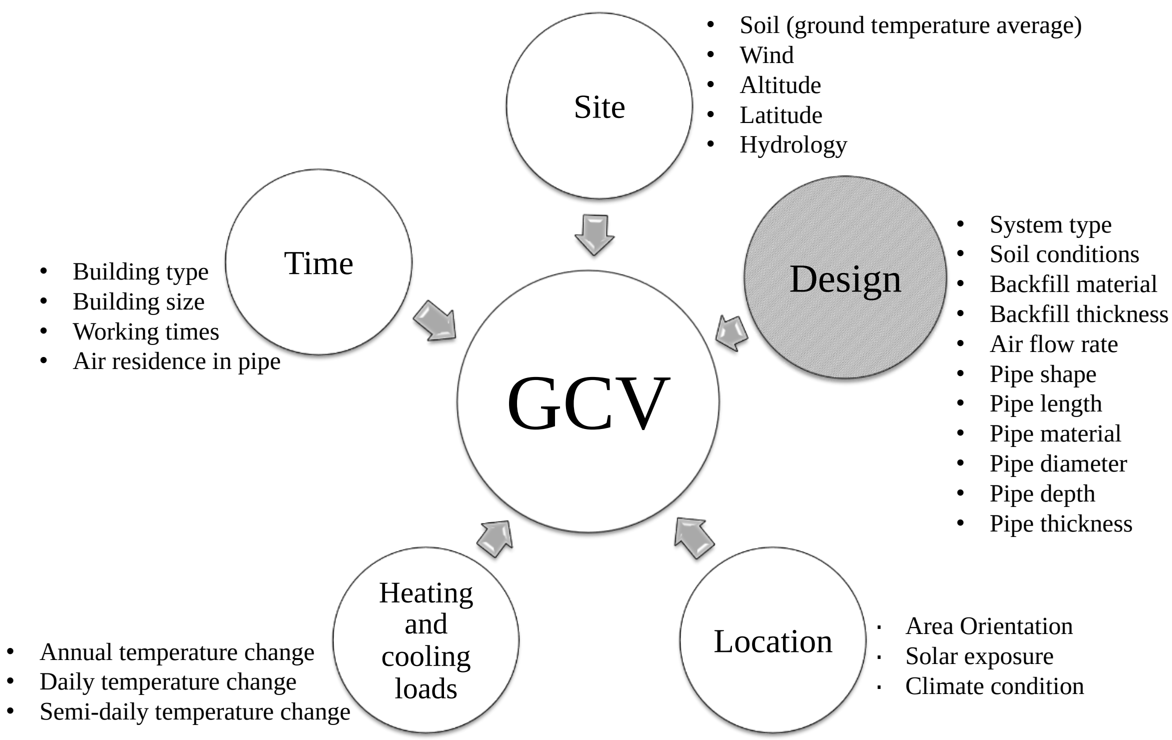

Figure 1-5: Factors Influencing Ground-Coupled Ventilation Systems

1.2.3 GCV System Design

GCV system design differs from place to place and climate to climate. Many factors affect the system's performance. Figure 1-6 represents these GCV system design factors. Designing a GCV system for high performance is rather complicated because all factors need to be compatible.

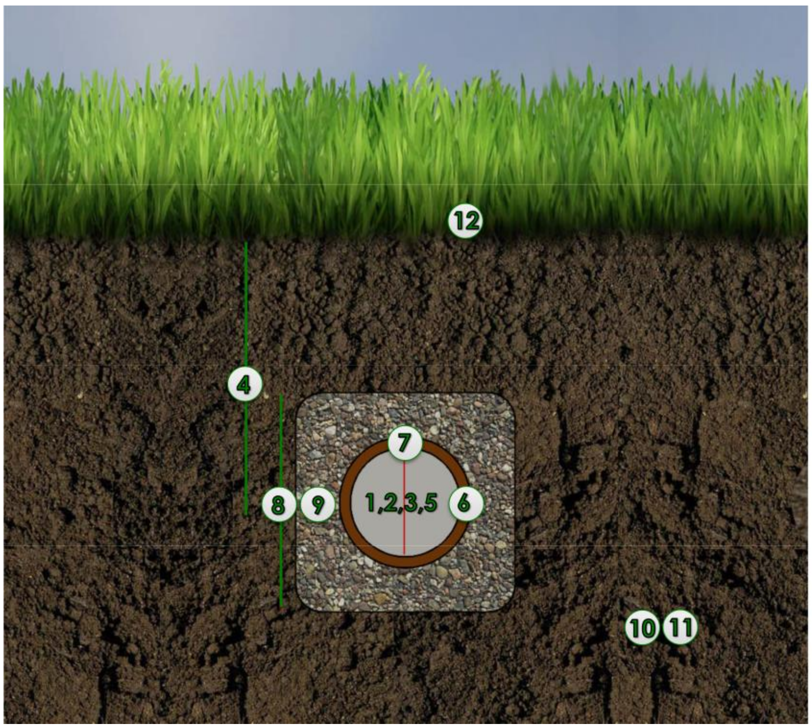

Research Variables:

1. Airflow rate
2. Air Temperature
3. Pipe Length
4. Pipe Depth
5. Pipe Diameter
6. Pipe Thickness
7. Pipe Material
8. Backfill Thickness
9. Backfill Material
10. Soil Type
11. Ground Temperature
12. Ground Shading

Figure 1-6: Design Variables in a GCV System (Alghamdi, 2008)

1.2.4 Opportunity to Reduce Cooling and Heating

GCV systems rely on heat transference. Ground and air temperatures are the fundamental factors that affect heat transference in these systems, second to the overall system design. The ability to reduce cooling and heating varies from place to place. For example, the GCV system at the Solar Concrete Masonry (CM) House at Virginia Tech is 84.4 feet long, 7.5 inches in diameter, 4 to 9.8 feet deep, and has a volumetric air flow of 118 ft^3/min (velocity 100 feet/min). The system cooled the air temperature on average by between 20°F to 25°F on July 24th, 2017 as Figure 1-7 shows. If we look at a hot region such as Riyadh, Saudi Arabia, the highest air temperature is 115°F, but the ground temperature at 19.5 feet deep is 75°F (Figure 1-8). If we use GCV systems in Riyadh, what are the potential reductions of air temperature? Moreover, what is the appropriate GCV system design for Riyadh, Saudi Arabia? This research pursued the answers to these questions.

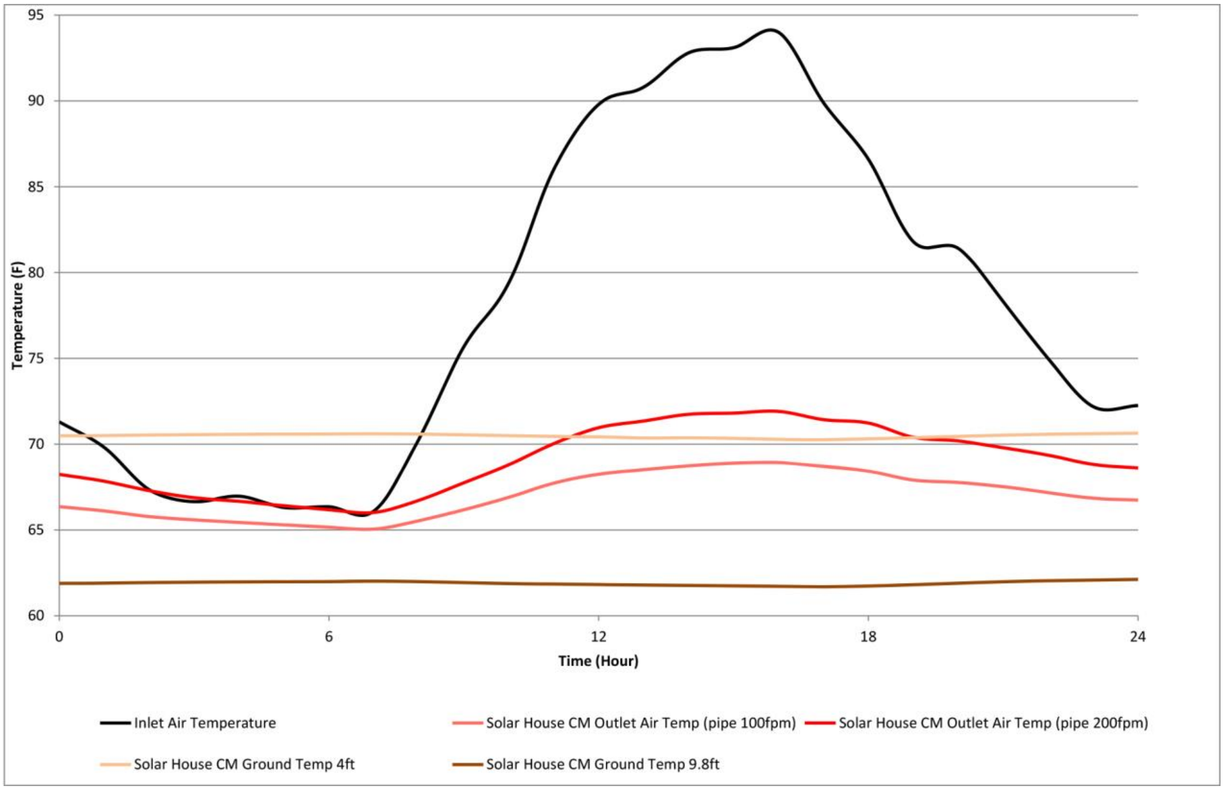

Figure 1-7: GCV System Performance on Jul 24th at Solar CM House

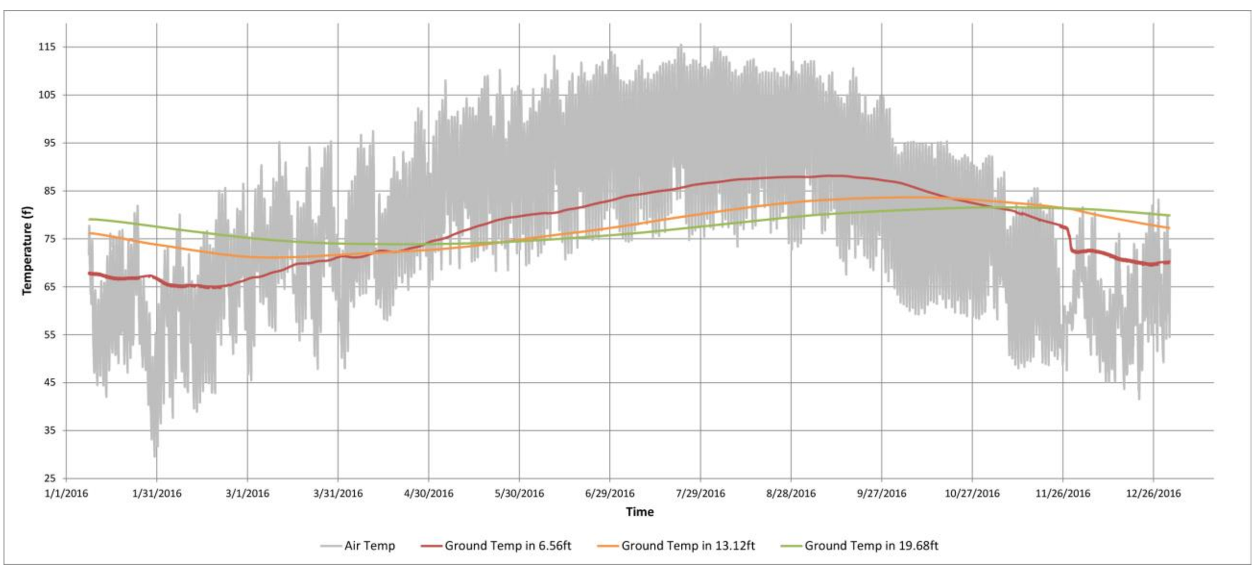

Figure 1-8: Air and Ground Temperature at Different Depths in Riyadh, Saudi Arabia

1.2.5 Heat Transfer

Heat transfer is a natural phenomenon where heat is exchanged between two objects. Heat can be transfered in three fundamental ways: conduction, convection, and radiation. In an open-loop GCV system, the outdoor air enters a pipe that is buried in the ground. Typically, the temperature of the outdoor air and the soil that surrounds the pipe differ. Because of this temperature difference between the pipe surface and airflow, heat is exchanged at the interior surface of the tube by convection. The rate of heat flow changes along the length of the tube not only because the temperature varies from tube inlet to tube outlet, but also because the temperature of the soil surrounding the tube varies. Three other factors also contribute to the complexity of the system: first, the ground temperature varies depending on the depth below the surface (Figure 1-9). Second, the heat exchange rate between the air, the tube surface, and the soil change along the length of the tube. Third, the thermal response time of the ground temperature relative to the air varies with depth (Reysa, 2005; Trząski & Zawada, 2011).

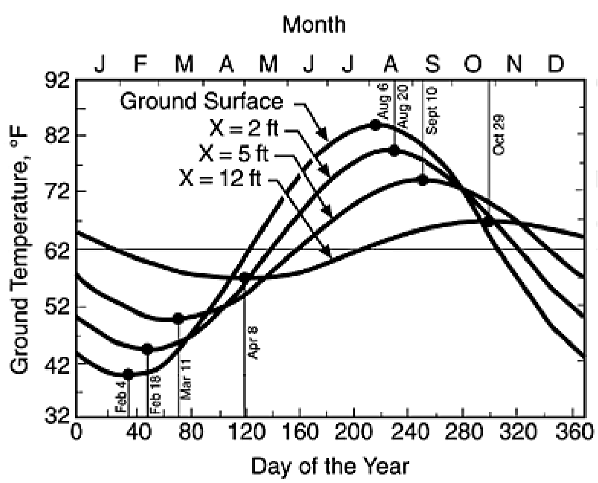

Figure 1-9: Soil Temperature Distribution by Depth in Virginia (Reysa, 2005)

1.3 Problem Statement

Oil is a main source of energy in the Middle East, and particularly in Saudi Arabia. The Saudi government has invested heavily in reducing energy consumption because there is a limited supply of oil. Therefore, renewable energy is promoted as an alternative. HVAC systems are usually the highest energy consumers in buildings. In the hot season, power consumption rises as air conditioning use increases. This raises the question of how to achieve mechanical cooling or heating in our buildings without high energy consumption. GCV systems are one of many options that have the potential to reduce energy consumption. However, most buildings in Saudi Arabia do not use this system. The adoption of GCV systems in Saudi Arabia may contribute significantly to energy conservation if the system performs well.

Unfortunately, although GCV systems can be applied in different places in the world, there is no standard design for the system because many variables affect the performance of the system. GCV system design also varies from place to place and each design performs differently. The principal variables in the system are ground and air temperature. Moreover, designing a GCV system that considers pipe length, depth, material, and air-flow rate are mediating factors for heat exchange between the ground and air. Therefore, there is no standard design for the system at this time. Another problem is that, at present, predicting the GCV system design performance in temperature change requires complex simulation. Thus, if there are many different GCV system designs, it will be time consuming to predict the performance of all of them. The goal of this research was to find solutions to these two problems by developing a new design assistance tool.

1.4 Research Questions

The performance of the GCV system depends on location, climate, and several system variables. Because Riyadh, Saudi Arabia does not use this system currently, the research sought to answer the following questions:

- Does the GCV system significantly reduce air temperature in Riyadh, Saudi Arabia for a case study?
- What is the relation between GCV system variables?

1.5 Research Goal and Objectives

Research Goal

The goal of this research was to develop a design assistance tool that predicts the performance of the GCV system by determining the relations between each variable. This research sought to achieve these following goals:

- Create a GCV system evaluation tool that predicts air temperature change under a typical range of variables that affect GCV system performance.
- Apply the new tool for the design of a GCV system for a non-residential case study in Riyadh, Saudi Arabia to present the recommended GCV system design.

Research Objectives

- Monitor the GCV system at the Solar CM House in-situ at Virginia Tech.
- Validate the Ground Air Heat Exchange software (GAEA) and computational fluid dynamic (CFD) models' output by comparing their output to the GCV system at Solar CM House.
- Apply CFD simulation parametrically for multiple GCV system variables to determine air temperature change between the inlet and outlet.
- Conduct a regression analysis for the CFD models designs to predict temperature change.
- Collect air and ground temperature data in-situ in Riyadh.

1.6 Research Significance and Contribution to Body of Knowledge

The outcome of this research will be a design assistance tool for GCV systems. This research will add to the existing body of knowledge in two ways (see Figure 1-10). First, as there is no standard design for GCV systems, this research will create a new design assistance tool for GCV systems. Second, in the current situation, predicting the GCV system design performance using computer simulation is time consuming. Using the new tool will save considerable time in predicting GCV system design performance. Therefore, this research is significant because the new tool will save time, money, and effort (International Energy Agency, 2015; Pérez-Lombard et al., 2008).

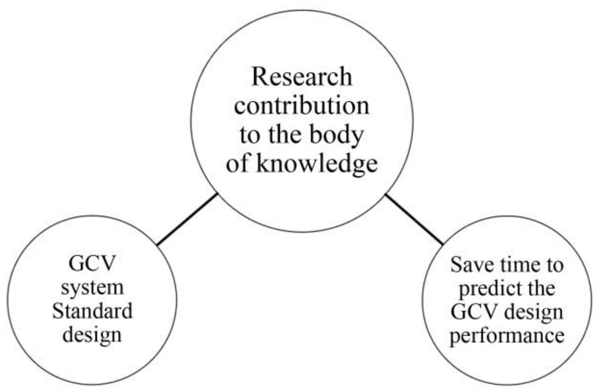

Figure 1-10: Research Contribution to the Body of Knowledge.

As mentioned previously, oil is a primary source of energy in the Middle East, and thus, the Saudi government has invested heavily in reducing energy consumption because the oil supply is limited. Based on crown prince Prince Mohammad bin Salman’s 2030 vision to adopt alternative energy sources, the outcomes of this research will be used in Saudi Arabia to achieve part of his vision by reducing energy consumption by using geo-exchange energy in the buildings (Al-Saud, 2016).

1.7 Research Methods

Achieving the research objectives and determining the possible thermal performance of GCV systems required several steps. These include computational fluid dynamic (CFD) modeling, data collection, and analysis, as shown in Figure 1-11. Additional details regarding variables and methods are discussed in Chapter three.

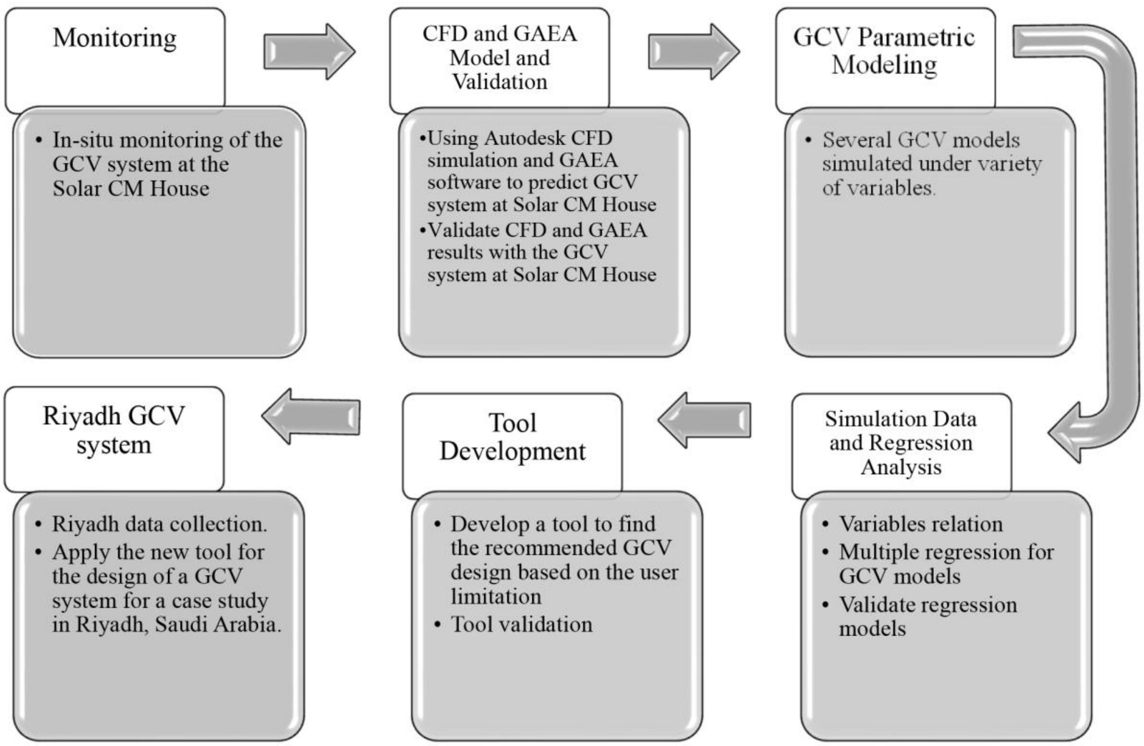

Figure 1-11: Research Methodology

1.8 Research Contribution

The goal of this research was to develop a tool that predicts the performance of a GCV system. The tool works by inputting the system variables including air and soil temperatures, soil type, volume airflow, pipe length, pipe depth, and pipe diameter into the tool. The tool then allows the designer to choose by comparing different GCV system designs. Figure 1-12 shows the interface of the tool. For now, this tool is a standalone tool, but in the future, it could be integrated into energy software to calculate the GCV system cost.

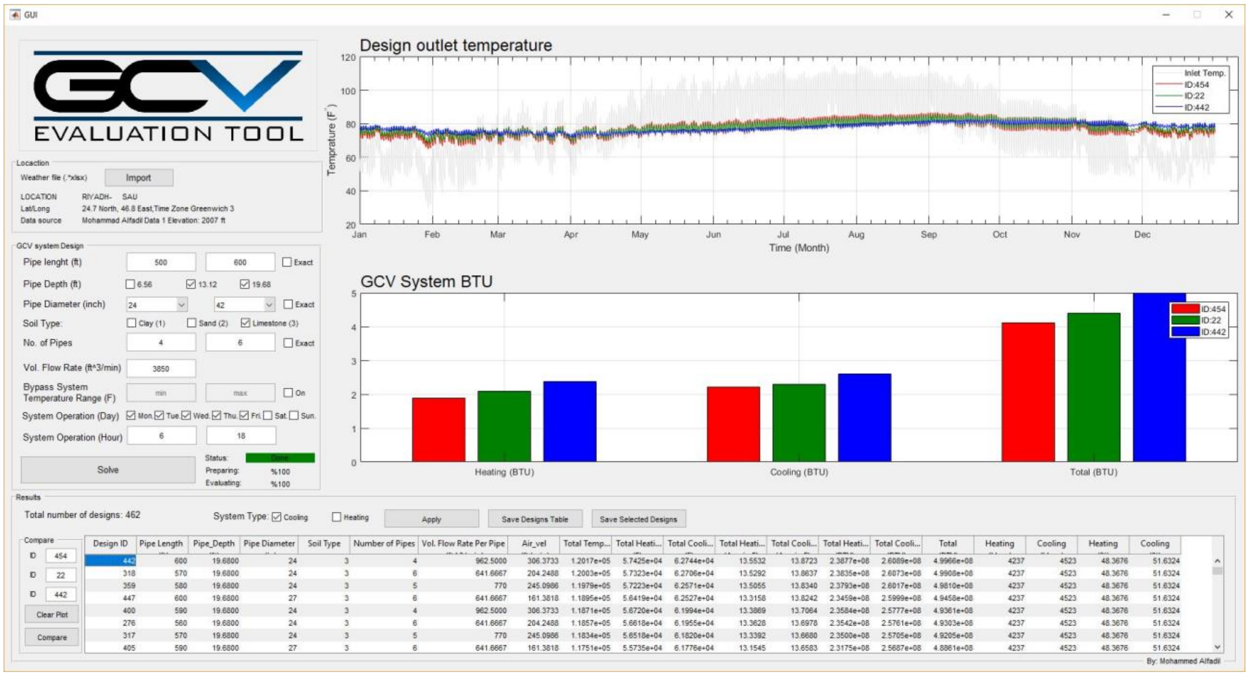

Figure 1-12: GCV Tool Interface

Chapter 2: Literature Review

This chapter examines the scholarship concerning energy use in buildings, past studies of GCV systems, ground air heat exchange (GAEA) software, GCV system fundamental heat transfer factors, and information on computational fluid dynamics (CFD) and fluid mechanics.

2.1 Energy Use in Buildings

Buildings can be divided into external, internal, and ventilation load dominated with respect to energy consumption. Figure 2-1 shows the breakdown of buildings according to energy consumption. Residential energy consumption is greater than that of commercial buildings because there are many more residential buildings in terms of economic growth, the building sector's expansion, and the spread of building services, particularly heating, ventilation, and air conditioning (HVAC) systems. As Table 1 illustrates, HVAC systems are the largest energy consuming systems in both residential and commercial buildings, as maintaining indoor conditions within the thermal comfort zone is the main concern in design and construction of most buildings (Pérez-Lombard et al., 2008).

Table 1: Breakdown of Energy Consumption by Building Type
(Pérez-Lombard et al., 2008, p. 296)

Final energy consumption (%)	Commercial	Residential	Total
USA	18	22	40
UK	11	28	39
EU	11	26	37
Spain	8	15	23
World	7	16	24

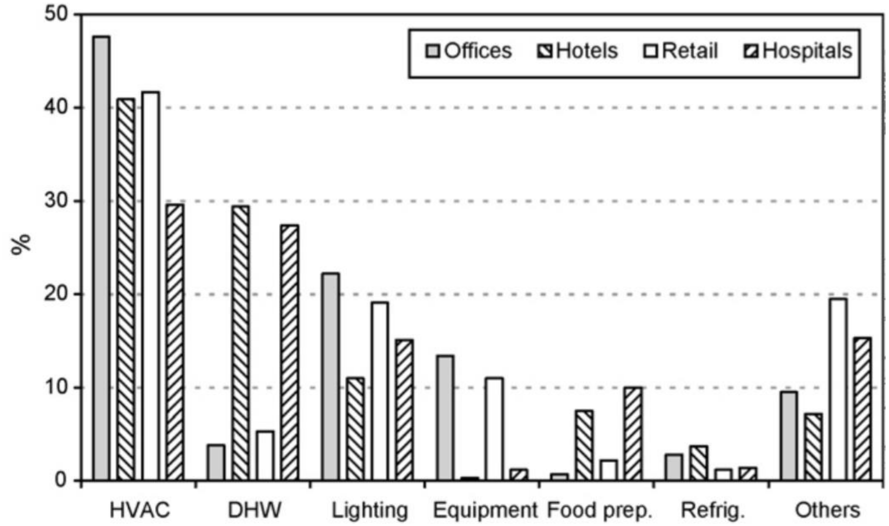

Figure 2-1: Consumption by Energy Use for Different Building Types in the USA (Pérez-Lombard et al., 2008, p. 397)

HVAC systems account for nearly half of energy consumption in buildings. One solution to this problem could be an integrated systems approach that relies on highly efficiency (such as GCV) systems to achieve thermal comfort (Pérez-Lombard et al., 2008).

2.2 Vertical and Horizontal GCV systems

A GCV system can be designed with either a vertical or horizontal layout. Table 2 shows a comparison between four parameters in the two designs: construction, cost, size, and performance efficiency. The principal differences are construction and land costs. For example, a tower with a large plot of land has two options. First, due to the large ventilation requirement a horizontal design will require most of the land to be used for the system; therefore, the site needs to be designed to include the system while considering such surrounding elements as buildings and landscape—particularly if the land is expensive. Second, although a vertical design would use less area on the site, the construction cost is higher. Based on these considerations, it is possible to choose the most appropriate design for a given building. As the outcome of this research, the tool addresses horizontal systems performance based on the tool inputs.

Table 2: Vertical and Horizontal GCV System Comparison

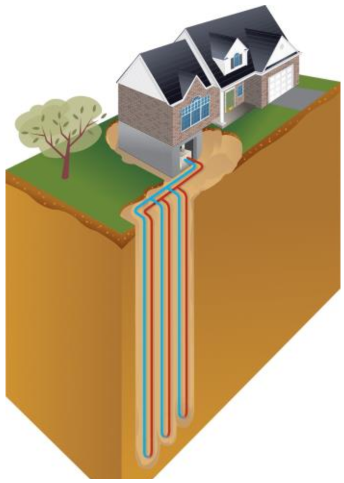

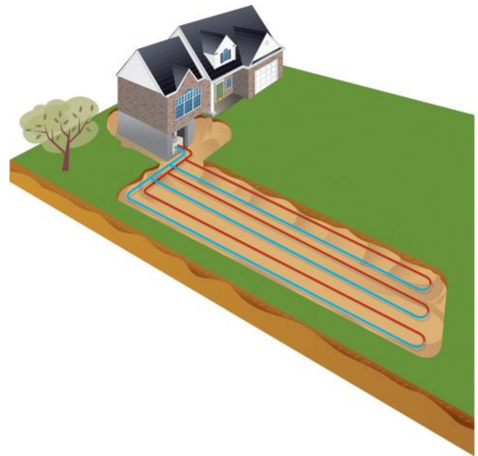

Parameter	Vertical GCV system	Horizontal GCV system
Construction	Digging process needs special equipment to reach the desired depth, particularly if the pipe diameter is large.	Digging process can be done using conventional digging machines.
Cost	Construction costs will be higher than for the horizontal design, but it is good for a small plot of land.	Construction costs will be cheaper than for the vertical system, but it will occupy a large land space if the system is large.
Size	Requires a large vertical area of land if the system is large.	Requires a large horizontal area of land if the system is large.
Performance efficiency	The systems' performance will be the same if they reach a constant level of ground temperature, which is greater than 26 feet.	

2.3 Solar Concrete Masonry House

The Solar Concrete Masonry (CM) House was built at Virginia Tech in the 1980s and is located in the Environmental System Laboratory facility. The solar CM consists of two units connected by a hallway. The first unit measures 16 ft. x 16 ft. and the second unit measures 16 ft. x 24 ft., with a 10 ft. ceiling height. Each unit has a solar heating system and GCV, as seen in Figure 2-2 to Figure 2-7. This building is unique because it has an integrated air-to-air heat exchanger tower, multifunction solar wall, and GCV system. The multifunction solar wall is located to the south. In the cold season, the wall works as passive solar heating to heat throughout the building, as shown in Figure 2-7. In the hot season, the GCV system cools the building and helps remove heat from the south wall, as illustrated in Figure 2-8 (Riley & Schubert, 1985).

The air-to-air heat exchange tower, seen in Figure 2-9, provides the fresh air and removes pollutants and moisture without adding excessively to the building's heating load. With the heat exchangers, the exhaust air is used to precondition the fresh intake air. The intake and exhaust air pass each other to exchange heat along opposite sides of a thin metal membrane. In the warm season, the cool exhaust air precools the warm intake air, while in the cold season, the warm exhaust air preheats the cold intake air.

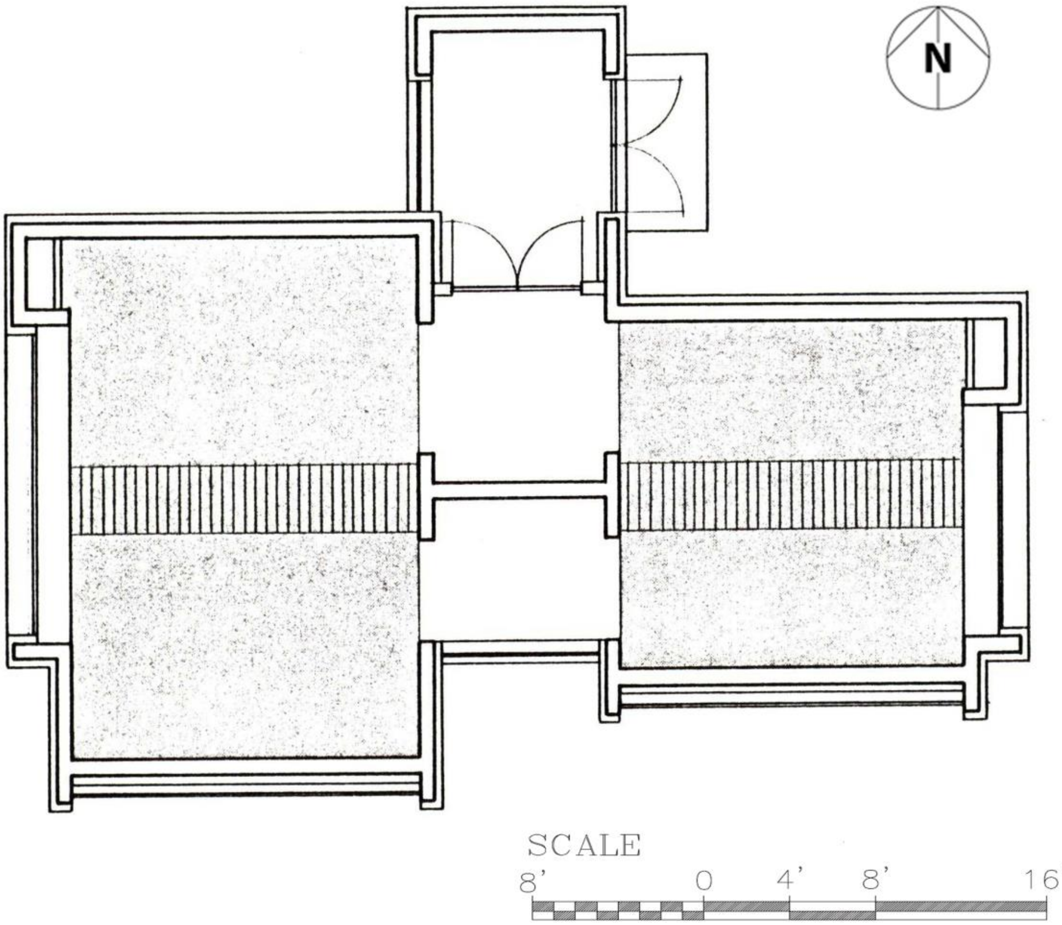

Figure 2-2: Solar CM House Plan (Riley & Schubert, 1985)

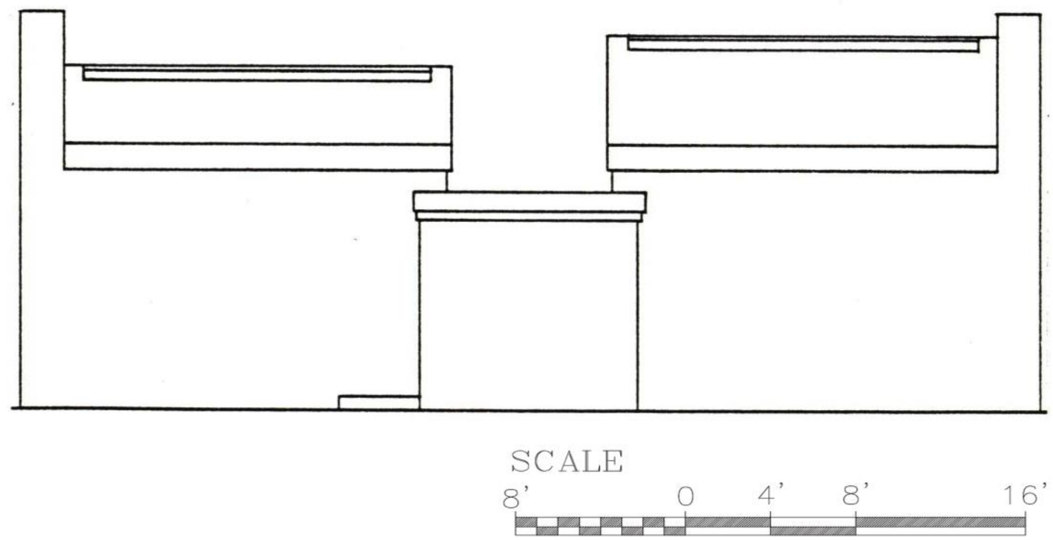

Figure 2-3: Solar CM House North Elevation (Riley & Schubert, 1985)

Figure 2-4: Solar CM House South Elevation (Riley & Schubert, 1985)

Figure 2-5: Solar CM House East Elevation (Riley & Schubert, 1985)

Figure 2-6: Solar CM House West Elevation (Riley & Schubert, 1985)

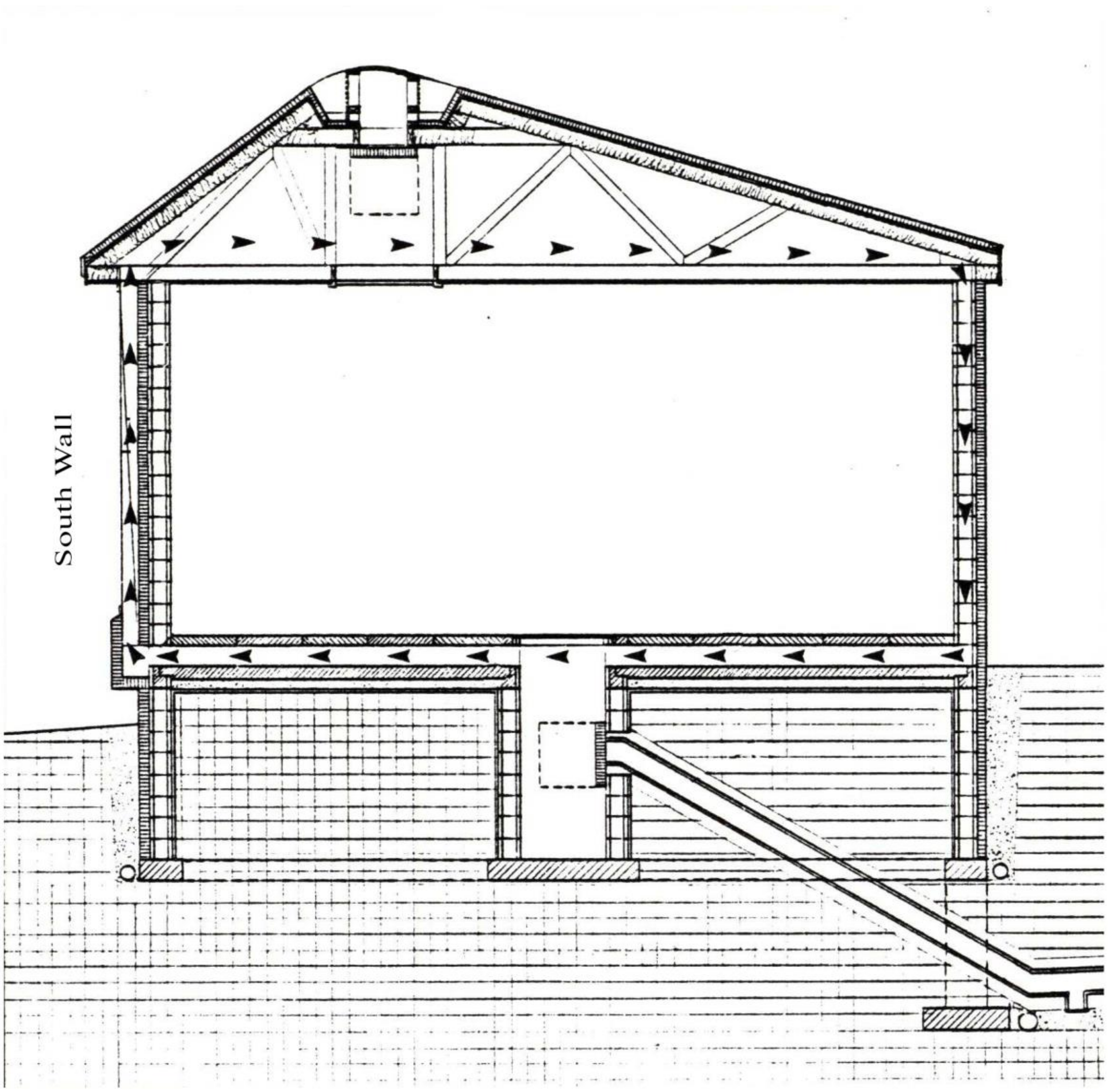

Figure 2-7: Solar CM House Passive Solar Heating Mode (Riley & Schubert, 1985)

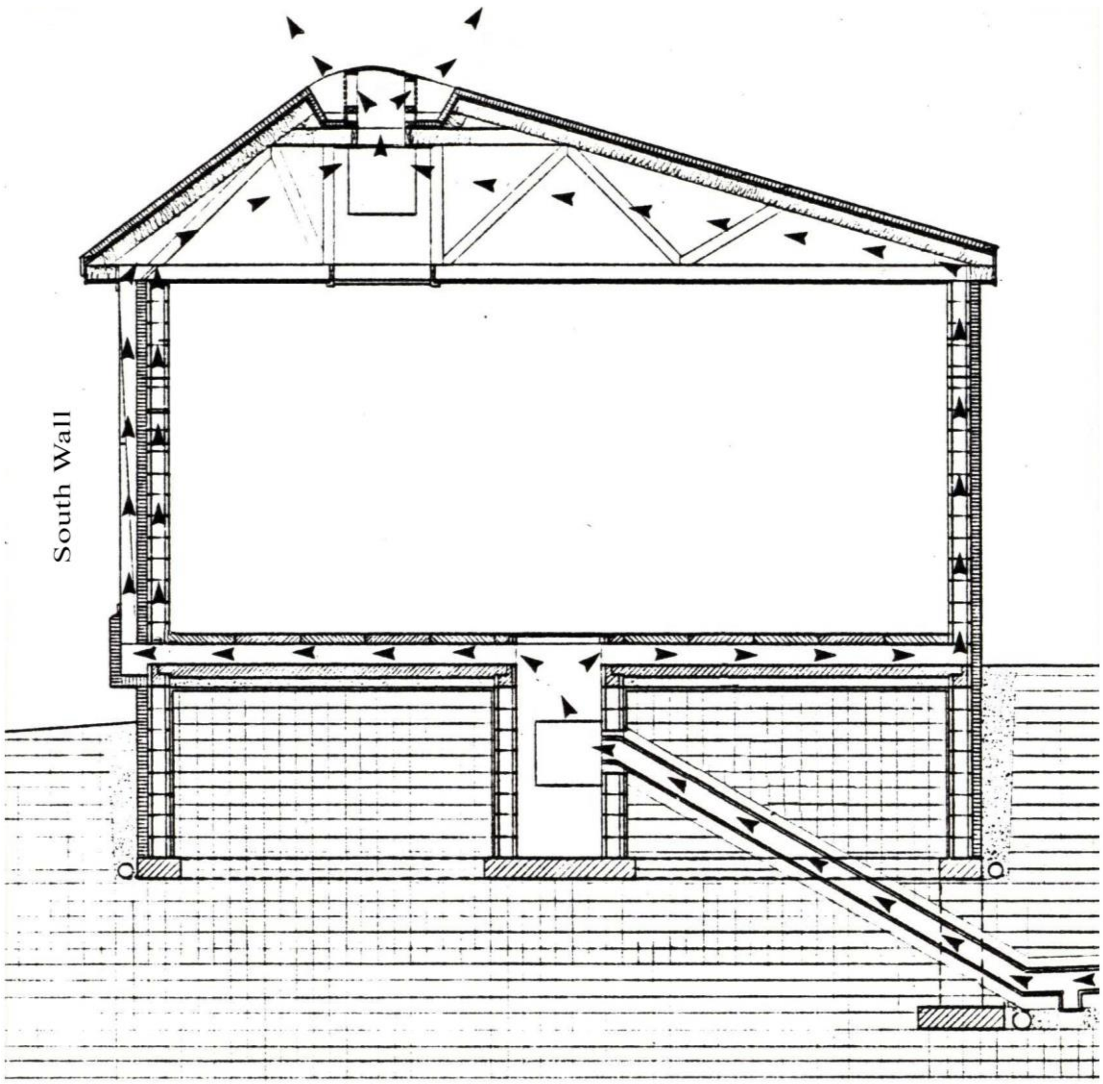

Figure 2-8: Solar CM House Passive Cooling Mode (Riley & Schubert, 1985)

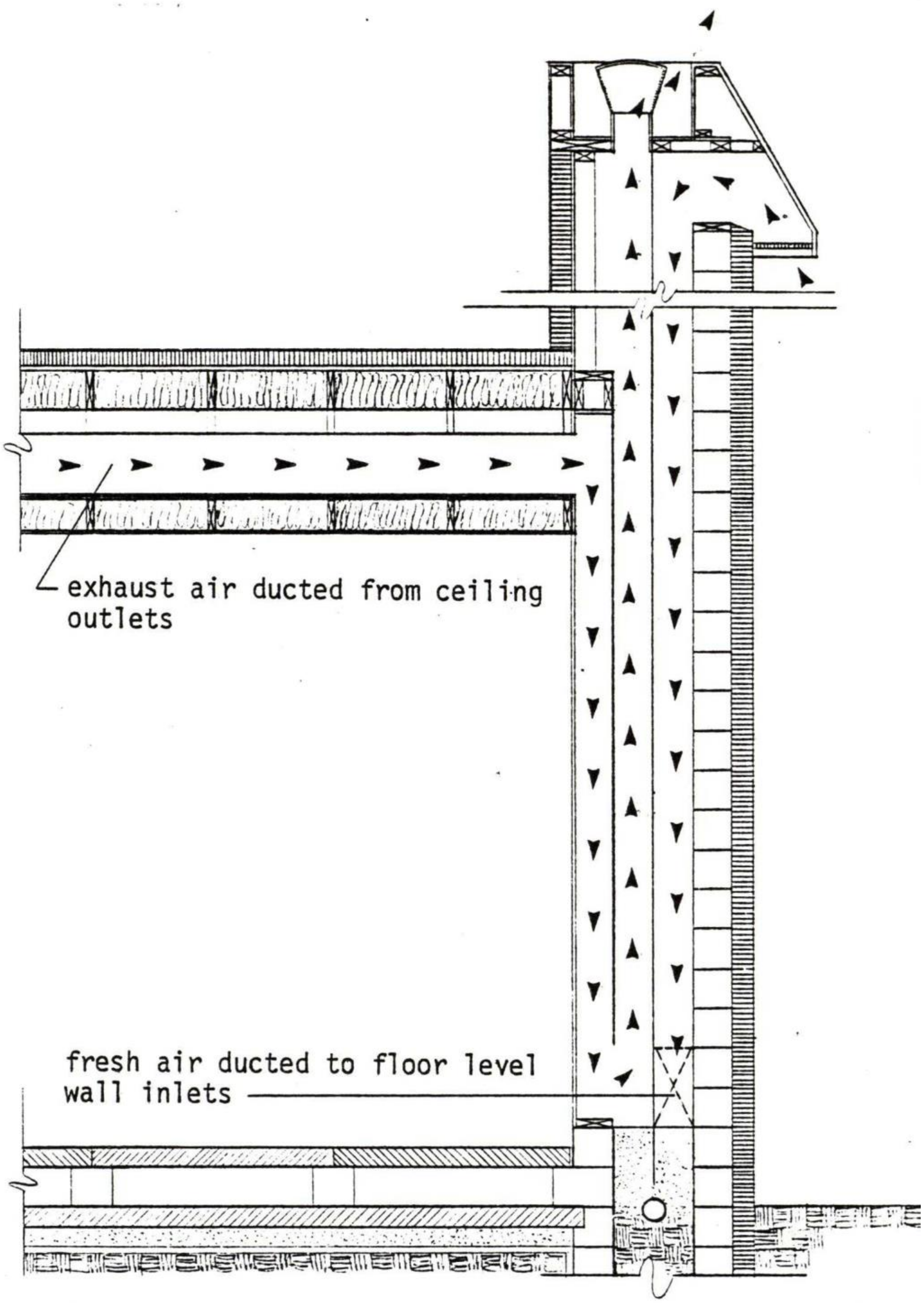

Figure 2-9: Solar CM House Air to Air Heat Exchanger Tower (Riley & Schubert, 1985)

2.3.1 GCV System

Since the 1980s, there has been considerable investment in the study of GCV systems and their potential to reduce energy consumption in buildings. For example, Alghamdi's (2008) research used computational fluid dynamics to simulate a GCV system. His goal was to determine the accuracy of alternative CFD modeling techniques by comparing the simulated results with data measured from an as-built system. Alghamdi's process was divided into three stages: experimental, CFD simulation, and data analysis. For the first, the experimental, he monitored the GCV system at the Solar CM House, which has four pipes each with different air flow rates (Figure 2-10). The experimental method included not only soil sample analysis, but also the recording of thermocouple sensors located in the pipes and the ground. Secondly, he used CFD simulation to model the system performance. Finally, Alghamdi compared the experimental data with the CFD simulation results using multiple means comparison (Fisher's LSD methods).

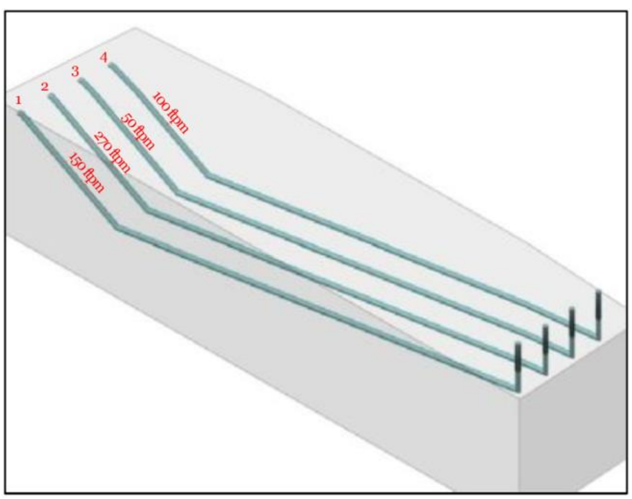

Figure 2-10: GCV Systems' Four Pipes with Different Air Flow
(Alghamdi, 2008)

Figure 2-11: Solar CM House in 2007 (photo by Robert Schubert)

Figure 2-12: Vitrified Clay Pipes Used in the Solar CM House GCV System and the Gravel Backfill (photo by Robert Schubert)

Alghamdi's results were specific to the variables at that site. In the analysis (2008), both experimental monitoring and the CFD results confirmed a negative relation between heat transfer and air velocity (i.e., the higher the air velocity, the less the air temperature difference between the inlet and outlet). Further, the research demonstrated that CFD simulation results were consistent with the as-built data.

2.4 GCV System Design

Trząski and Zawada (2011) used simulation to modify a GCV system in a single-family home in Poland. The system consisted of two 25m parallel PVC pipes with a 160mm diameter and 3.6mm thickness that were buried to a depth increasing from 1.1m at the inlet to 1.6m at the outlet. The inlet air is drawn through a single pipe, and then, the air is split into two parallel pipes. There is a collector at the end of the pipes that couples both outdoor air flows and the GCV system outlet to the building ventilation system. Inlet and outlet air temperature, air flow, solar radiation, and ground temperature were measured to verify the accuracy of the simulation model, which is shown in Figure 2-13.

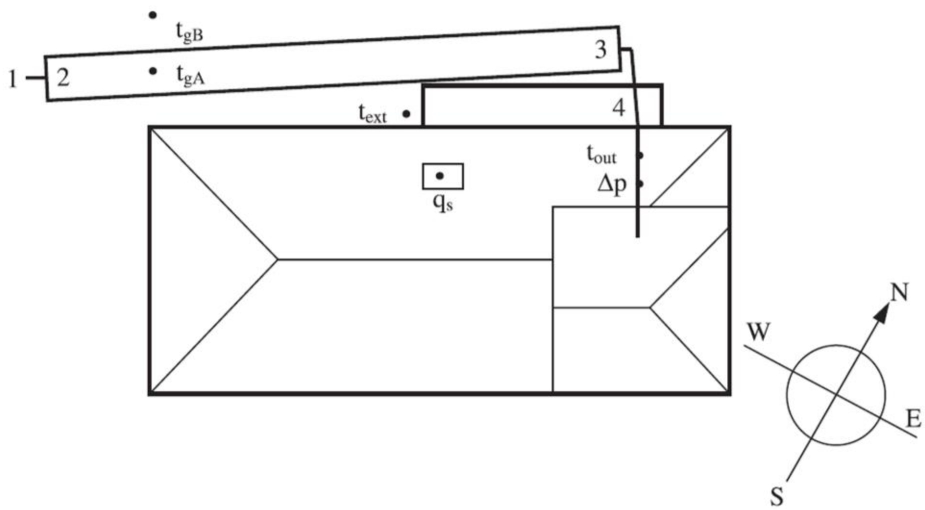

Figure 2-13: Plan View of GCV System Site Measurements (Trząski & Zawada, 2011, p. 1439)

- t_{gA}, t_{gB} location of the ground temperature measurement
- t_{ext} location of the outdoor air temperature measurement
- q_s location of solar radiation intensity measurement
- t_{out} location of the heat exchanger outlet temperature measurement
- Δ_P location of the pressure difference measurement

After verifying the reliability of the simulation model, the authors used the simulation to vary several system parameters (Figure 2-14). Their comparative results between the base and the modified models were shown as the percentage difference in the heating and cooling consumptions as the system parameters changed, as noted in Table 3. The heat exchange efficiency varied widely depending on the system design. As shown, the changes to the bypass, pipe length, depth, and number of pipes increased the system's heating and cooling consumption. Conversely, the shade factor increases the cooling efficiency. By using automatic air bypass, the GCV system is more efficient because it allows the ventilation system to intake outside air directly thus bypassing the GCV system. The benefits of the bypass system are shown in Figure 2-15.

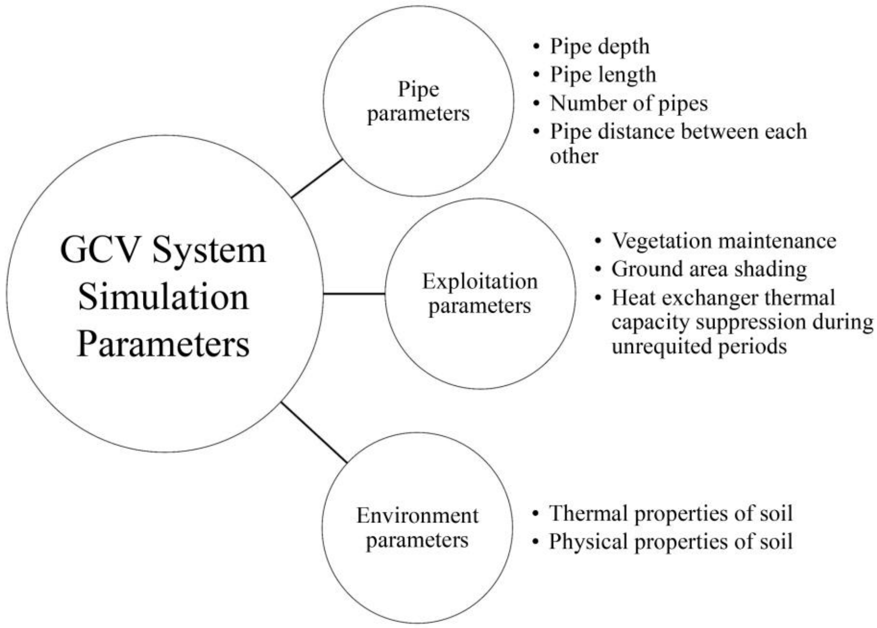

Figure 2-14: Simulation Parameters Used to Modify an Actual GCV System

Table 3: Modifications' Possible Effect on Heat Exchanger's Heating and Cooling Potential (Trząski & Zawada, 2011, p. 1444)

No.	Parameter	Base case	Modification	Heating	Cooling
1	Bypass	No	Automatic	+19.1%	+136.5%
2	Soil type	Sandy clay loam	Sand	+5.0%	−29.9%
3	Ground cover type	Grass lawn	Bare ground	+0.4%	−58.4%
4	Shading factor	0%	100%	−4.4%	+181.1%
5	Length	35 m	45 m	+18.1%	+19.5%
6	Depth	1.75 m	2.25 m	+8.0%	+93.2%
7	Diameter	200 mm	280 mm	−1.6%	−4.6%
8	Number of pipes	1	2	+22.6%	+26.0%
9	Distance between pipes	1 m	1.5 m	+3.3%	+3.9%

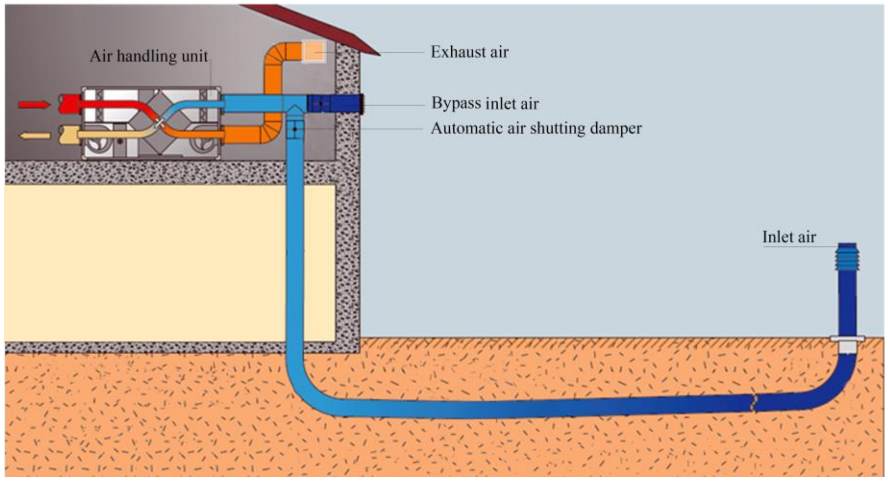

Figure 2-15: Air Bypass in the GCV System

2.5 GCV System Efficiency

The efficiency of the GCV system can be determined based on energy consumption, temperature reduction, and cost. For example, Figure 2-16 shows a comparison between two high schools in York County, Virginia, one with a traditional HVAC system and the other with a GCV system. The county found that the utility costs for the GCV system were approximately $60,000 less per year than the traditional heating and cooling system in these schools ("York County School Division - Green YCSD Geothermal Heating & Cooling," 2016).

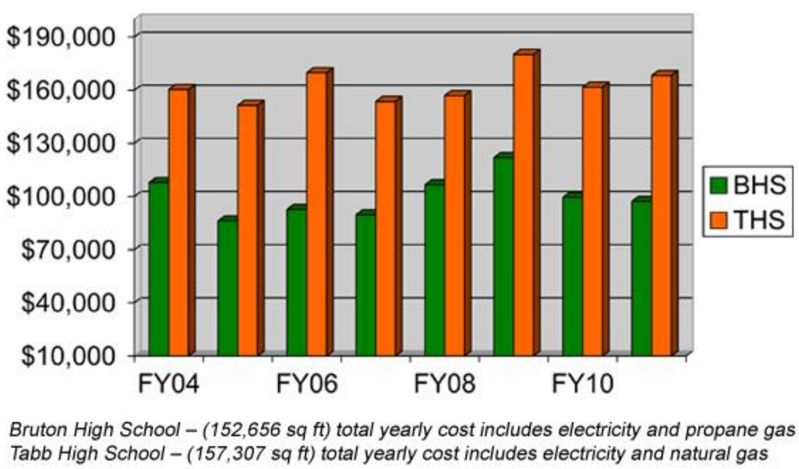

Figure 2-16: Energy Consumption for GCV System vs. HVAC System
("York County School Division - Green YCSD Geothermal Heating & Cooling," 2016)

2.6 Fungus and Bacteria in the GCV System

Air quality is an important aspect to consider when using a GCV system. Relative humidity and changes in air temperature are factors that can have adverse effects on the health of the building's occupants, as buried air tubes can be a favorable environment for some forms of microbial contamination (Ager & Tickner, 1983). Flückiger, Monn, Lüthy, and Wanner conducted a study "…to determine if microbial growth does occur in existing ground-coupled air systems of different ages and design, and if the supply air might thus become contaminated with a concomitant risk of a health hazard" (1998, pp. 197–198). They examined three different GVC systems in Switzerland for one year; the systems ranged in age from 1 to 13 years old. Data were collected quarterly to monitor seasonal differences, and air samples were taken from several locations: in the outdoor air near the inlet, before the filter units close to the outlet, and in the outlet near the supply air. The air temperature and relative humidity were recorded from the samples.

In general, the researchers found that the concentration of bacteria and fungi in the air in the underground pipes was lower than that in the outdoor air. However, they cautioned that this result cannot be applied to buildings of vastly different sizes. The authors found that the greater the volume of air in the pipes, the more microorganisms were present in the air tube. This study found no differences in microbe concentration between plastic, concrete pipes, and the age of the system (Flückiger et al., 1998).

2.7 Ground Air Heat Exchange Software (GAEA)

In Europe, residential buildings occasionally have GCV systems, and GAEA software can be used to estimate change in air temperature. Benkert, Heidt, and Schöler (1997) created the GAEA software, which uses equations to calculate soil and air temperature and the heat exchange between the air and ground.

The software uses several steps to determine a system's performance. Figure 2-17 shows these steps, from inputting pipe parameters to determining the system performance. The software accommodates a range of system pipe parameters, including length, depth, diameter, number of pipes, the distance between the pipe and the building, and the location of the fan. As a second step, the soil type may be specified using soil properties of density, thermal conductivity, and heat capacity. Because the software was developed in Germany, climate data for Europe are supported, or the user can enter climate data manually by using the max, min, and mean temperatures to draw the temperature curve over the year as a third step. The fourth step entails inputting the HVAC system parameters including building volume, air change rate, and ventilation flow to determine the required ventilation rate. Further, the "automatic bypass" can be controlled by using a temperature range or for certain days of operation when the outside air temperature is more beneficial than the GCV system air. The fifth step is cost, in which the software calculates the total cost and energy use with and without the system. Finally, the system's performance can be displayed by year or day with reference to all of the previous system inputs. Moreover, it includes an option to show a recommended system given by the pipe parameters and the system cost. Figure 2-17 to Figure 2-26 show the GAEA software steps and interface (Benkert et al., 1997).

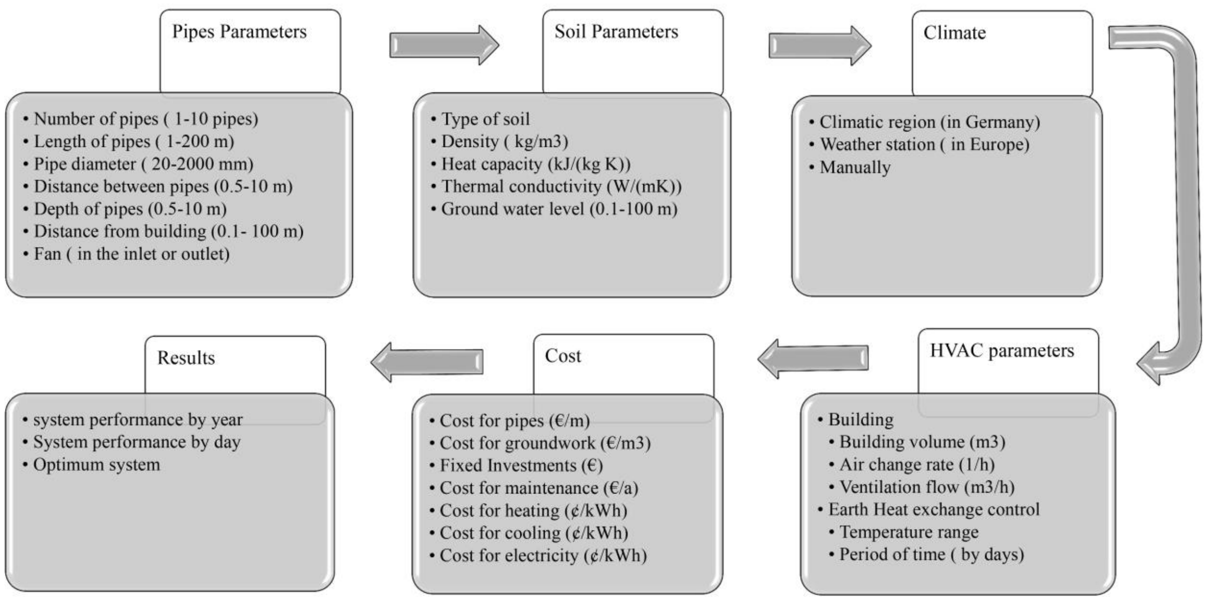

Figure 2-17: GAEA Software Steps

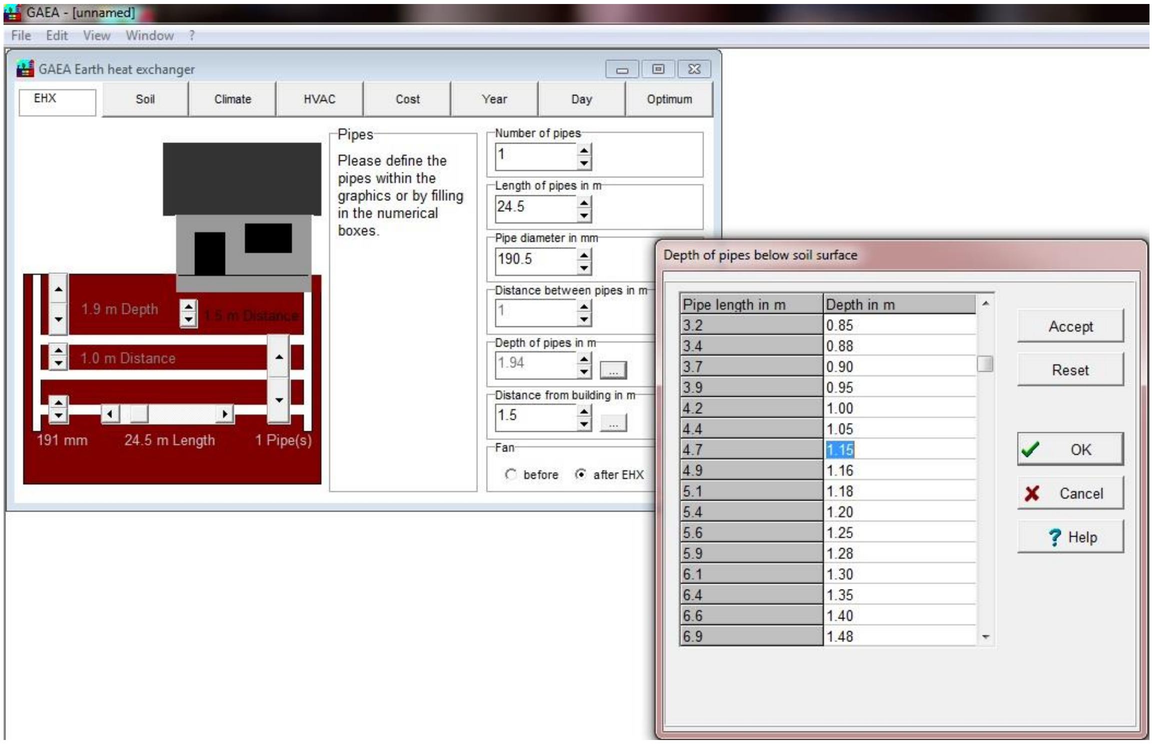

Figure 2-18: Pipe Parameters

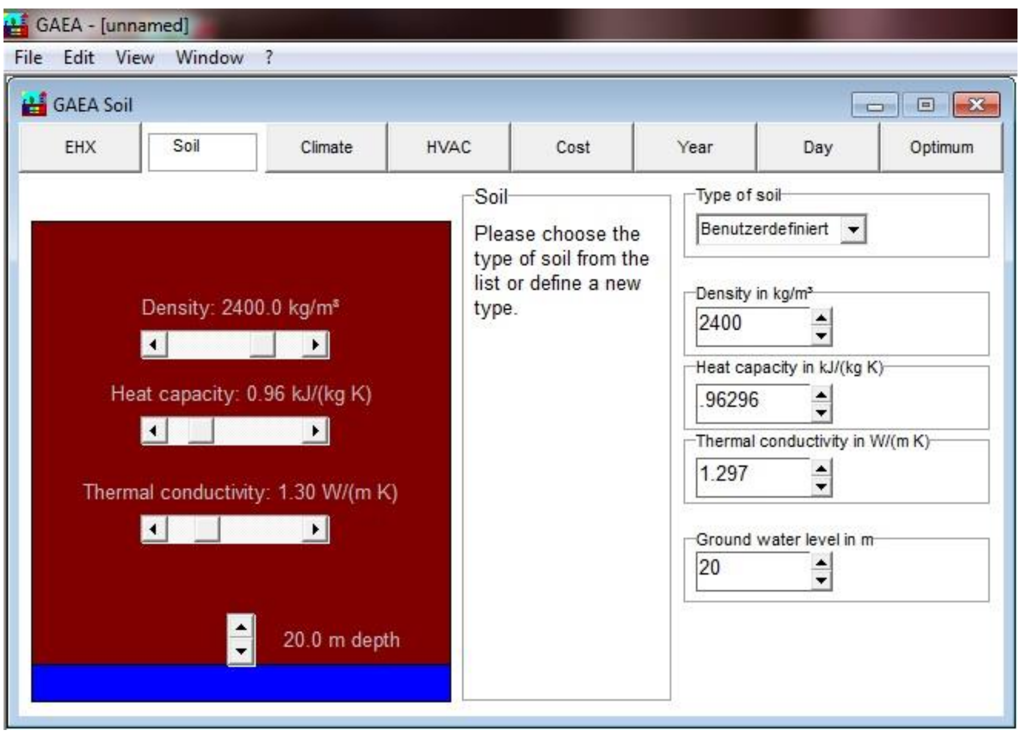

Figure 2-19: Soil Parameters

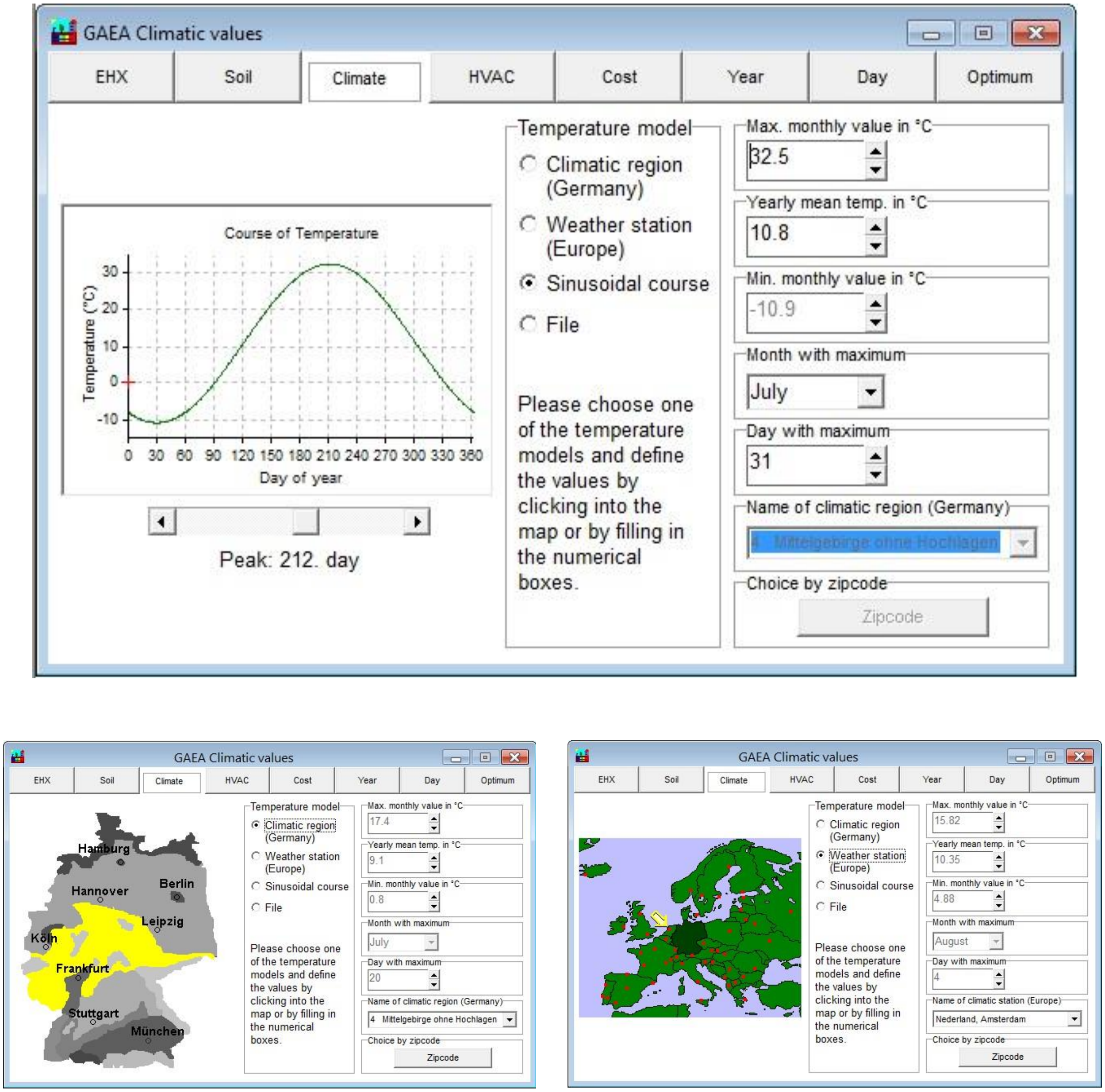

Figure 2-20: Climate Parameters

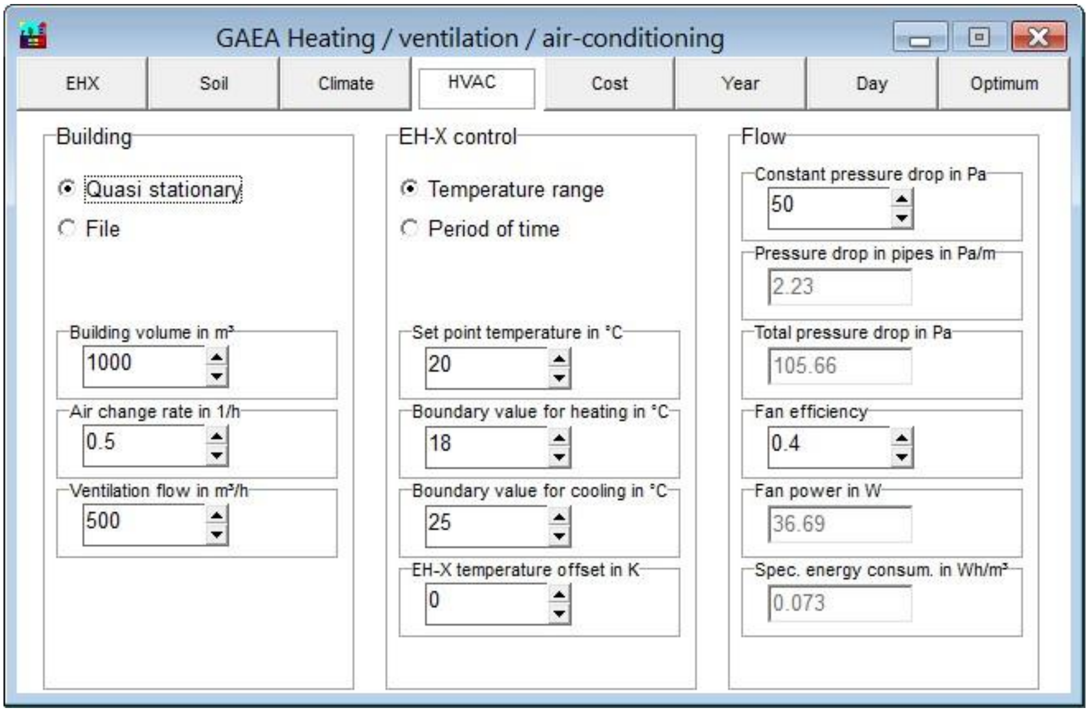

Figure 2-21: HVAC Parameters

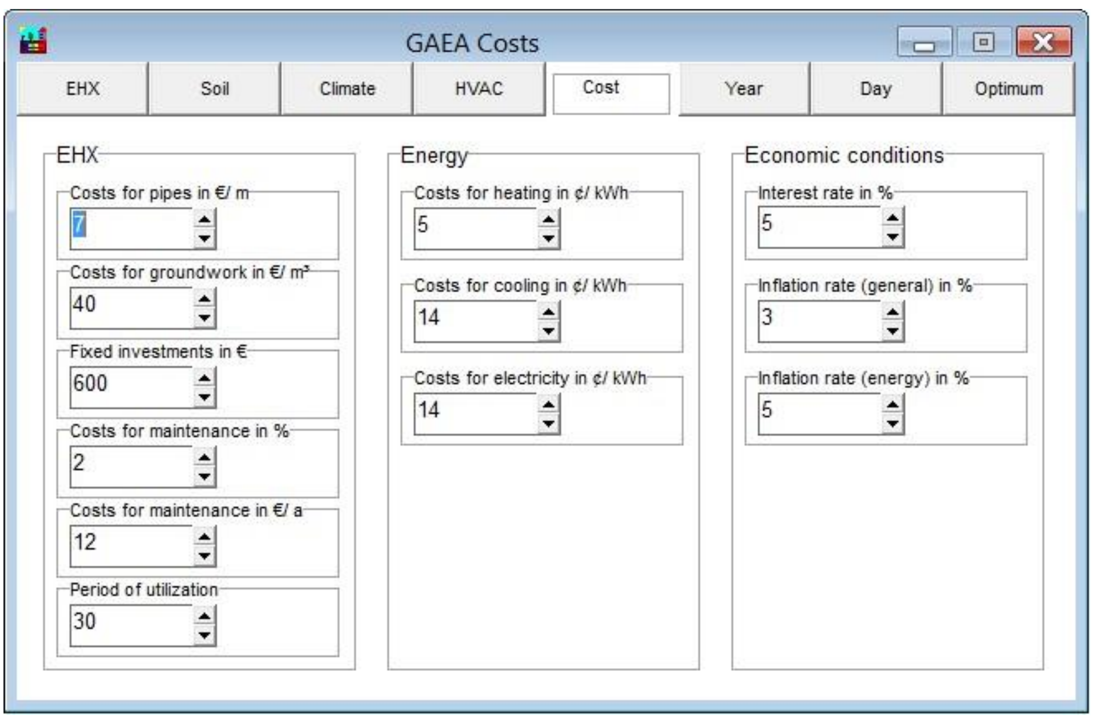

Figure 2-22: Cost Parameters

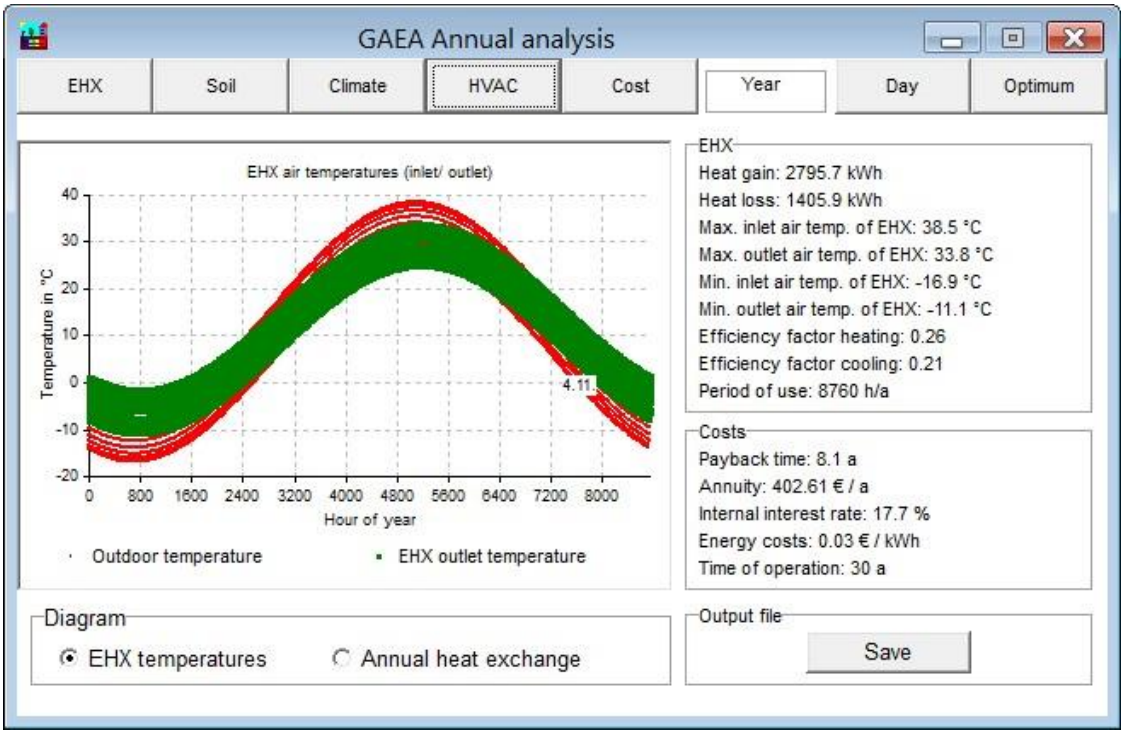

Figure 2-23: Annual System Performance

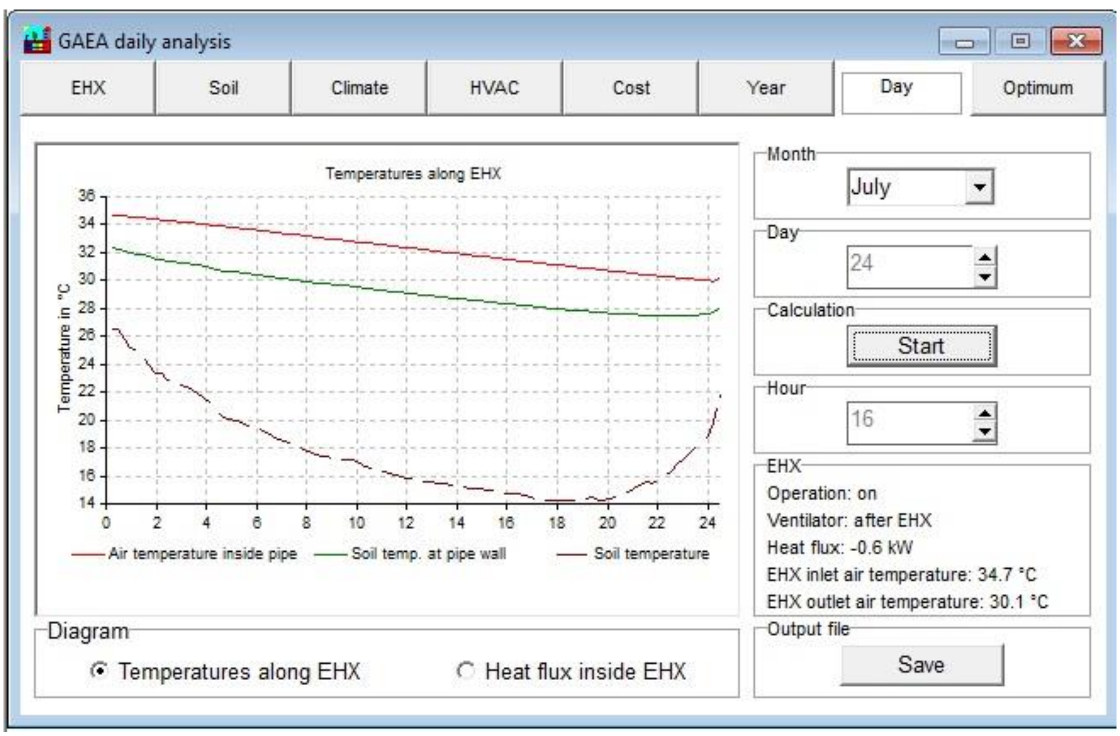

Figure 2-24: Daily System Performance

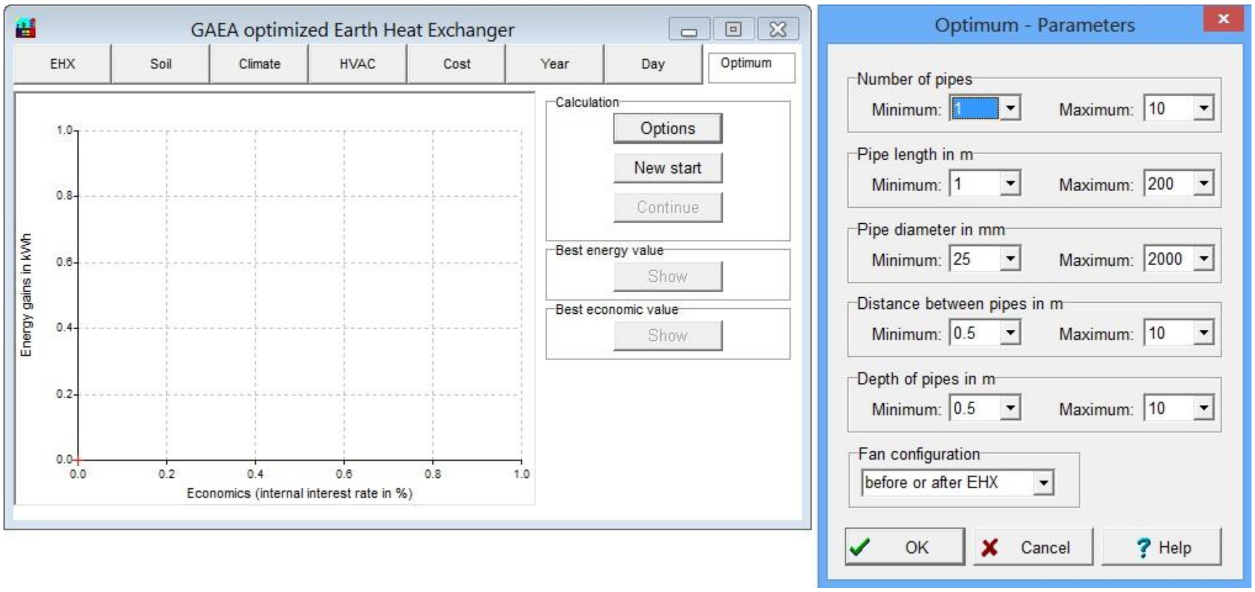

Figure 2-25: Optimum Design Limitations

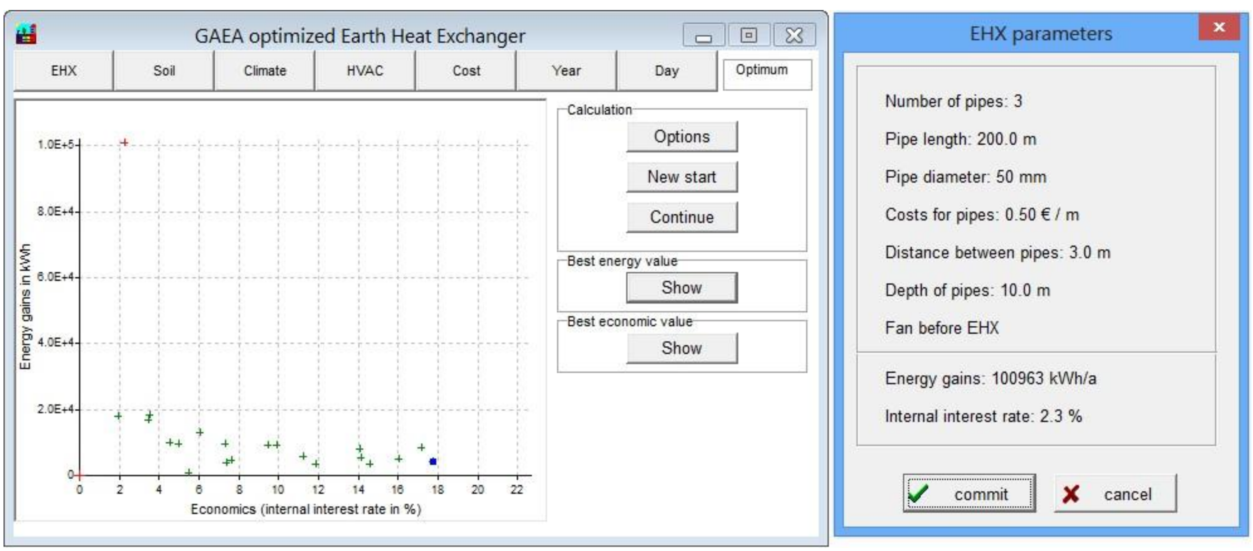

Figure 2-26: Optimum Design (Best Energy Value)

The GAEA software uses an equation derived from physics to calculate the heat exchange between the air and soil, after the user inputs a set of parameters used to calculate heat transfer. Table 4 shows the GAEA software equation used to predict the GCV system performance. At the time of this writing, the GAEA program is still in its first stage of development (Albers, 1991). The GAEA software was used in this research by comparing an actual GCV system with a predicted GCV system to improve the accuracy prediction of a GCV system performance. More information can be found in Chapter five.

Table 4: Physics Equation for GAEA Software

Equation name	Equation	Nomenclature
Heat transfer ratio from earth surface to pipe and from airflow to pipe wall.	$\cup^* = 2\pi \frac{\lambda}{\cup_L} * \frac{1}{\ln\left(\frac{S_0}{R_0} + \sqrt{\left(\frac{S_0}{R_0}\right)^2 - 1}\right)}$	• $\cup^*$ Conductance ratio of heat transfer from earth surface-pipe-airflow to pipe surface. • λ Thermal conductivity of ground in W/(m K) • $\cup_L$ Heat transfer coefficient per length of wall of pipe between bulk air and wall in W/(m K) • S_0 Depth of pipe center under surface in m • R_0 Radius of pipe in m
Earth temperature at the pipe wall not affected by pipe	$\vartheta_{E,0}(t) = \vartheta_m + (\vartheta_{max} - \vartheta_m) * e^{-\xi} \cos\left(2\pi \frac{t}{t_0} - \xi\right)$	• $\vartheta_{E,0}$ Earth temperature at the wall of the pipe not influenced by pipe in °C • ϑ_m Annual mean value of ambient air temperature in °C • ϑ_{max} Annual maximum value of ambient air temperature in °C • ξ Dimensionless parameter for "thermal depth" of pipe • t Time in seconds • t0 Suration of year in seconds (1a≈31.5x106 s) • t/t0 Fraction of a year (with t/t0 equal zero for maximum ambient air temperature)
Thermal depth	$\xi = S_0 \sqrt{\frac{\pi \rho c}{t_0 \lambda}}$	• ρc Volumetric heat capacity of ground in J/(m3 K)
Ground temperature at pipe wall	$\vartheta_{E,W} = \frac{\cup^* \vartheta_{E,0} + \vartheta_{A,P}}{\cup^* + 1}$	• $\vartheta_{E,0}$ Earth temperature at the wall of the pipe in °C • $\vartheta_{A,P}$ Air temperature inside the pipe in °C
Ambient air temperature	$\vartheta_{A,0}(t) = \vartheta_m + (\vartheta_{max} - \vartheta_m) * \cos\left(2\pi \frac{t}{t_0}\right)$	• $\vartheta_{A,0}(t)$ Ambient air temperature in °C at time t in s
Heat exchange for each segment	$Q_W = \Delta Z * \cup_L * \left(\vartheta_{E,W} - \vartheta_{A,P}\right)$	• Q_W Heat flow from earth through wall of pipe to air in pipe in W • ΔZ Length of segment in m
Heat exchange coefficient per length of pipe wall	$\cup_L = 2\pi R_0 h_i$	• h_i Heat transfer coefficient at the inner surface of pipe in W/(m2 K)
Heat transfer coefficient at the inner surface of pipe	$h_i = \frac{\lambda_{A,P} Nu}{2 * R_0}$	• $\lambda_{A,P}$ Thermal conductivity of air in pipe in W/(m K) • Nu Nusselt number of air in pipe
Nusselt number	$Nu = 0.0214 * (Re^{0.8} - 100) * Pr^{0.4}$	• Re Reynolds number of air in pipe • Pr Prandtl number of air (typically: Pr = 0,72)

2.8 Fundamental Heat Transfer

Heat can be exchanged between two objects via conduction, convection, and radiation. Conduction is energy transfer from more energetic particles in a substance to adjacent, less energetic ones as a result of particle interaction. Convection is energy transfer between a solid surface and nearby liquid or gas in motion, and involves the combined effects of conduction and fluid motion. Both conduction and convection occur in the GCV system, as shown in Figure 2-27. When the air enters the GCV system pipe, it exchanges heat with the pipe's surface by convection. Then, the heat is transferred from the internal to external surface of the pipe and finally to the surrounding soil by conduction. Heat is exchanged from the air to the pipe and soil, and the converse, depending upon which is hotter at the time. Because soil generally has low thermal conductivity (compared to metal) and high heat capacity, the air will tend to not overcharge the soil with too much heat over time. This suggests that the GCV system can cool or heat the air. Figure 2-28 shows the heat transfer variables in the GCV system. These variables can be classified as exogenous variables (external to the system) and endogenous variables (internal to the system), which are listed in Figure 2-29 (Cengel, 2012).

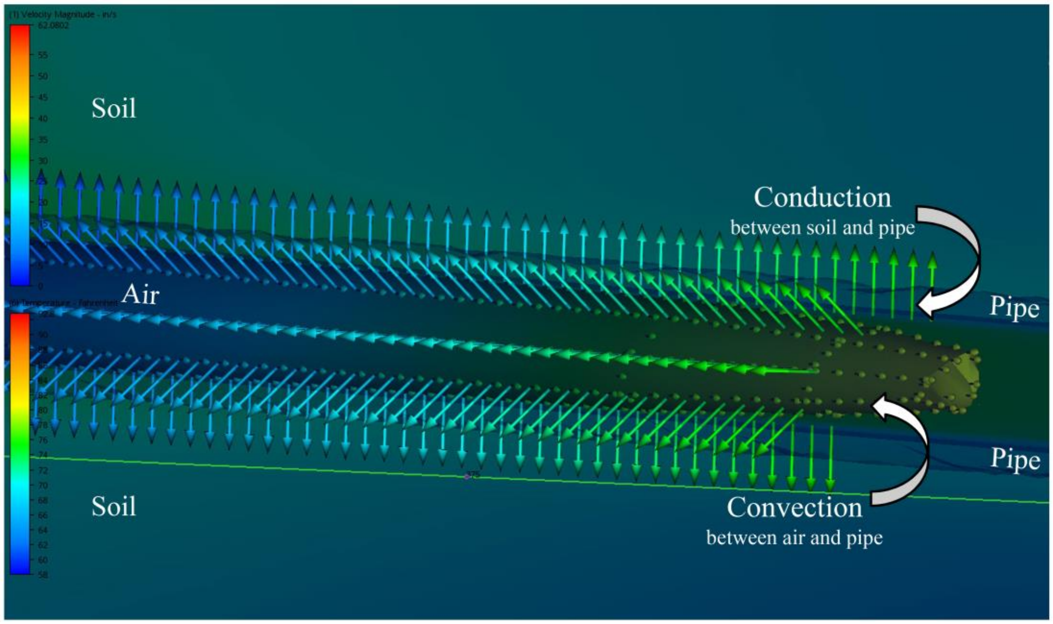

Figure 2-27: Conduction and Convection in the GCV system

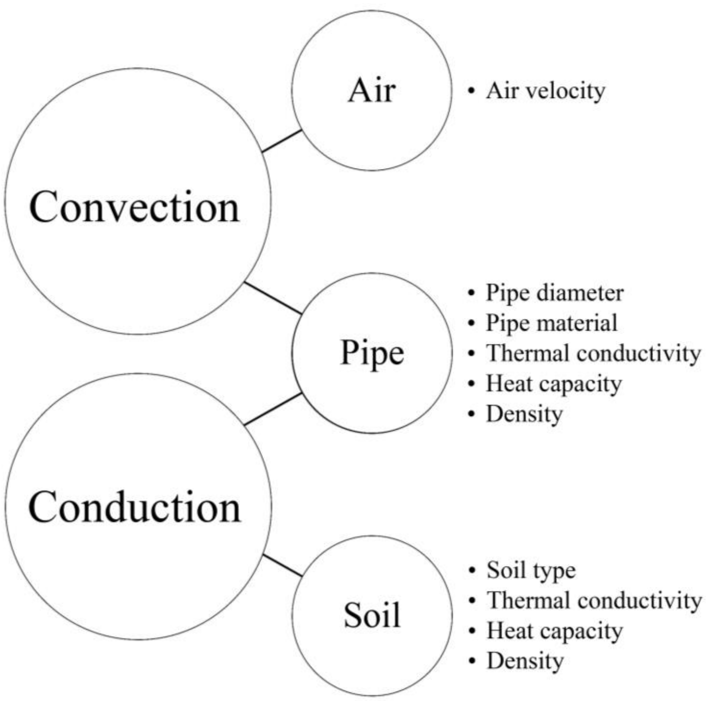

Figure 2-28: Heat Transfer Variables in the GCV System

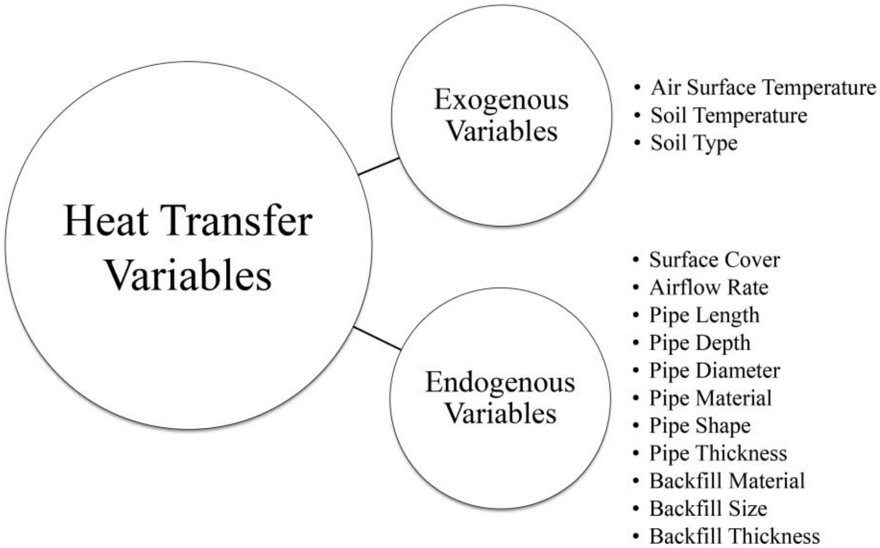

Figure 2-29: GCV System Heat Transfer Variables

2.8.1 Exogenous Variables

The GCV system exchanges heat between the air, pipe, and ground. The exchange of heat from the air in the pipe and the surrounding soil is first from convection along the interior surface of the pipe and then by conduction through the pipe to the soil. The GCV system performance relies on three main exogenous variables for heat exchange: soil type, soil temperature, and air temperature.

Air Temperature

Air temperature is the first variable that affects the GCV system performance and heat exchange with the pipe. Geographical location and site conditions are the principal factors that affect air temperature. Daily, monthly, and annual air temperatures vary based on the geographical location, which can be approximated by using longitude and latitude coordinates. Further, at the site, the surrounding characteristics in the region—such as mountains, creeks, and lakes—affect changes in air temperature.

Soil Temperature

Soil temperature changes monthly or daily as a function of incidental solar radiation, rainfall, seasonal variations in overlying air temperature, shade, vegetation cover, soil type, and depth. Soil temperatures deep in the ground are more stable and lag significantly behind seasonal changes in the overlying air temperature because the soil has a higher heat capacity than the air. The range of seasonal changes in the ground temperature depends on the soil type and depth below the ground surface. In Virginia, the amplitude of soil temperature at the surface varies between 20-25°F, depending on the type of vegetation cover (Figure 2-30), and soil temperature becomes more stable at increased depth. The soil temperature remains constant year round at depths greater than about 26 feet below the surface, which corresponds approximately to the water temperature in ground wells that are 30 to 50 feet deep (Reysa, 2005).

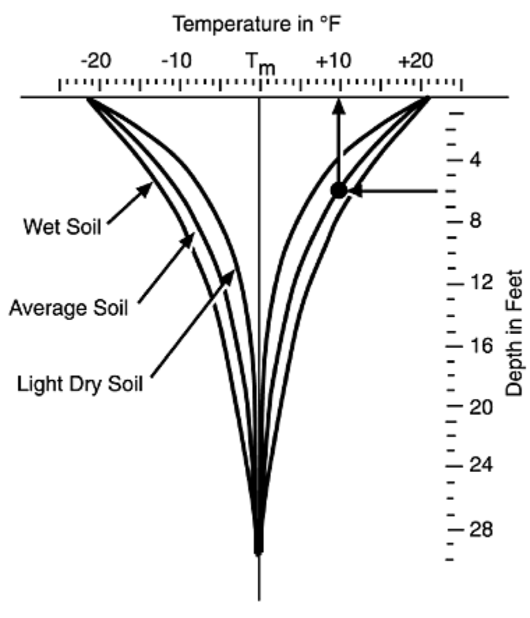

Figure 2-30: Seasonal Soil Temperature Changes in Virginia (Reysa, 2005)

When a GCV system is installed, it is important to know the expected seasonal changes for the soil temperature. The gain in thermal performance may outweigh the cost of installing a GCV system in deeper troughs, as deeper soil has lower temperature and is more stable (Figure 2-31).

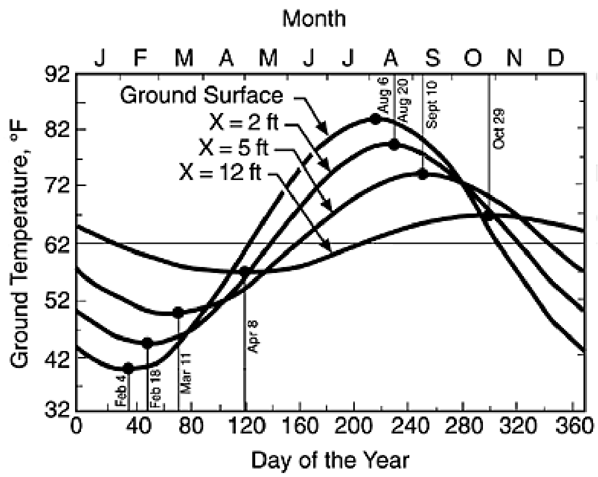

Figure 2-31: Soil Temperature Distribution by Depth in Virginia (Reysa, 2005)

Soil Thermal Properties

The thermal properties of the soil influence the heat exchange efficiency in heat capacity and thermal conductivity. Heat capacity indicates a soil's ability to store heat energy. In general, the greater the heat capacity, the more heat can be collected. To allow analysis of a wide range of soil types, Equation 1 adopts a soil textural classification proposed by the Polish Society of Soil Science (Figure 2-32). The "texture" of a particular soil indicates its content of sand, silt, and clay particles. These particle dimensions are [2000 mm, 50 mm], [50 mm, 2 mm] and [2 mm, and so on], respectively. This classification system assigns each soil to one of sixteen classes (Trząski & Zawada, 2011). The sixteen soil types' assumed properties are presented in Table 5. Soil parameters vary even more because of moisture content. It is relatively easy to determine soil thermal capacity and density based on dry soil and water properties (M De Paepe & Janssens, 2003; Michel De Paepe, 2002).

Equation 1: Heat capacity (M De Paepe & Janssens, 2003; Michel De Paepe, 2002)

$$c = \frac{(1-n).c_{\mathrm{dry}} + x_u.c_w + (x - x_u).c_i}{\rho}$$

$$\rho = \rho_{\mathrm{dry}} + x.\rho_w$$

Where:

- c Heat capacity
- c_{dry} Dry soil heat capacity, J/(kg K)
- c_w Water heat capacity, J/(kg K)
- c_i Ice heat capacity, J/(kg K)
- x Total water volume fraction, m^3/m^3
- x_{u} Unfrozen water volume fraction, m^3/m^3
- ρ_{dry} Dry soil density, kg/m^3
- ρ_w Water density, kg/m^3

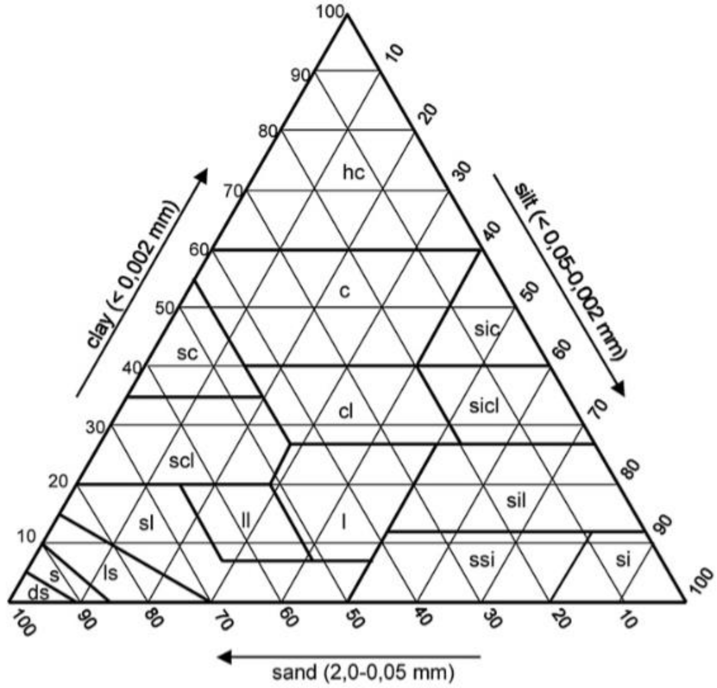

Figure 2-32: Soil Classification Textural Triangle (Trząski & Zawada, 2011, p. 1438)

Table 5: Assumed Parameters for Soil Textural Classes (Trząski & Zawada, 2011, p. 1438)

No.	Soil type	Symbol	Sand (%)	Silt (%)	Clay (%)	Quartz content (%)	Porosity (%)
1	Detached sand	ds	95	3	2	85	35.7
2	Sand	s	90	5	5	81	36.5
3	Loamy sand	ls	80	15	5	77	37.5
4	Sandy loam	sl	65	30	5	69	39.0
5	Light loam	ll	58	27	15	63	40.7
6	Loam	l	42	40	18	54	42.6
7	Sandy clay loam	scl	60	27	13	64	40.3
8	Clay loam	cl	33	35	32	45	44.9
9	Silty clay loam	sicl	10	55	35	33	47.5
10	Sandy silt	ssi	29	65	6	52	42.7
11	Silt	si	10	85	5	43	44.5
12	Silt loam	sil	19	60	21	42	45.2
13	Sandy clay	sc	55	5	40	52	43.5
14	Silty clay	sic	10	45	45	29	48.5
15	Clay	c	23	27	50	34	47.7
16	Heavy clay	hc	20	10	70	25	50.0

Thermal conductivity is an important soil property that must be known to design a GCV system, and indicates the rate at which heat will be transferred between the ground pipe and the surrounding soil. The thermal conductivity properties for the soil and rock are significant values that determine the length of the system pipe for heat exchange, which in turn affects the installation cost as well as system performance. There are several methods to estimate soil thermal conductivity. According to Johansen (1981), the most accurate method to calculate soil thermal conductivity between saturated and dry soil is Equation 2. Dry thermal conductivity for natural soil can be determined based on Equation 3 (Gauthier, Lacroix, & Bernier, 1997).

Peters-Lidard et al. (1998) and Farouki (1981) concurred that the most accurate method over the full range of saturation is that proposed by Johansen. According to their research, deviations in saturation over 0.2 are within the 35% range, while for saturations under 0.2, the method underestimates thermal conductivity by between 5 and 15%.

Equation 2: Soil thermal conductivity (Farouki, 1981)

$$\lambda = K_e\left(\lambda_{\mathrm{sat}} - \lambda_{\mathrm{dry}}\right) + \lambda_{\mathrm{dry}}$$

Where:

- λ_{sat} Saturated thermal conductivity, W/m K
- λ_{dry} Dry thermal conductivity, W/m K
- K_e Kersten number

Equation 3: Dry thermal conductivity for natural soil (Gauthier et al., 1997)

$$\lambda_{\mathrm{dry}} = \frac{0.135\rho_{\mathrm{dry}} + 64.7}{2700 - 0.947\rho_{\mathrm{dry}}}$$

Where:

- ρ_{dry} Dry density, kg/m^3

In cases where there are no measurement data, dry soil density can be calculated from the porosity *n*, assuming the same soil weight (Equation 4) (Hollmuller & Lachal, 2001):

Equation 4: Soil density (Hollmuller & Lachal, 2001)

$$\rho_{\text{dry}} = (1 - n)2700$$

Where:

- n Soil porosity, m^3/m^3

Porosity, quartz content, and the unfrozen water fraction affect saturated thermal conductivity in natural soils (Equation 5) (Kumar, Ramesh, & Kaushik, 2003):

Equation 5: Saturated thermal conductivity (Kumar et al., 2003)

$$\lambda_{\text{sat}} = (\lambda_q^q \lambda_o^{1-q})^{1-n} \lambda_i^{n-x_u} \lambda_w^{x_u}$$

Where:

- λ_i Thermal conductivity of ice, W/m K
- λ_w Thermal conductivity of water, W/m K
- x_u Unfrozen water volume fraction, m^3/m^3
- λ_q Quartz thermal conductivity, W/m K
- λ_o Other minerals' thermal conductivity, W/m K
- q Volumetric quartz content, m^3/m^3

The Kersten number is a function only of the degree of saturation, S_r, and phase of water: for fine unfrozen soils (over 5% of fraction up to 2 μm) (Mihalakakou, Santamouris, Lewis, & Asimakopoulos, 1997).

Equation 6: Kersten number (Mihalakakou et al., 1997)

$$K_e = \begin{Bmatrix} 0 & \text{dla} & S_r \leq 0.1 \\ \log S_r + 1 & \text{dla} & S_r > 0.1 \end{Bmatrix}$$

Equation 7: Kersten number for unfrozen coarse soils (up to 5% of fraction up to 2 μm) (Mihalakakou, Santamouris, & Asimakopoulos, 1994).

$$K_e = \begin{Bmatrix} 0 & \text{dla} & S_r \leq 0.05 \\ 0.7\log S_r + 1 & \text{dla} & S_r > 0.05 \end{Bmatrix}$$

For frozen soils:

$$K_e = S_r$$

Where:

- S_r Degree of saturation

At this time, heat transfer can be calculated using software. For example, CFD includes all of the heat transfer equations and is used to calculate heat transfer for each mesh cell based on the soil properties. The most accurate heat transfer results can be determined if the mesh is sufficiently fine, as the CFD calculates heat transfer for many cells.

2.8.2 Endogenous Variables

GCV systems depend primarily on three endogenous variables: air to ground heat exchange, system design, and materials. All of these variables should be compatible to address the GCV system design's potential for exchanging heat.

Air to Ground Tube Heat Exchange

Air in the pipe exchanges heat with the surrounding surfaces by convection, and the pipe and the soil affect heat transfer by conduction. Figure 2-33 shows the airflow temperature effect on the pipe surface. Air close to the pipe surface changes temperature the most, and also varies with the air velocity; the pipe has a higher velocity in the center and decreases gradually toward the pipe surface. This determination is based on Alghamdi's (2008) comparison of GCV systems with various air flows, in which he compared air flows of 50fpm, 100fpm, 150fpm, and 270fpm. As a result, at lower flow rates, the air resides in the pipe longer leading to more heat exchange with the pipe surface (see Figure 2-34). Pipe diameter also is another factor that determines the heat exchange efficiency. On the one hand, if the pipe diameter decreases, heat transfer between the air volume and the surrounding soil will increase. On the other hand, increasing the air volume flow in the pipe will decrease the heat transfer between the air and pipe surface. This suggests that the best way to increase the heat transfer efficiency between the air and the soil is to have a set of parallel pipes as opposed to only one, as shown in Figure 2-35. That leads to more heat exchange between the air and the surrounding soil if the total air volume passed through multiple pipes instead of one pipe (Cengel, 2012; Trząski & Zawada, 2011).

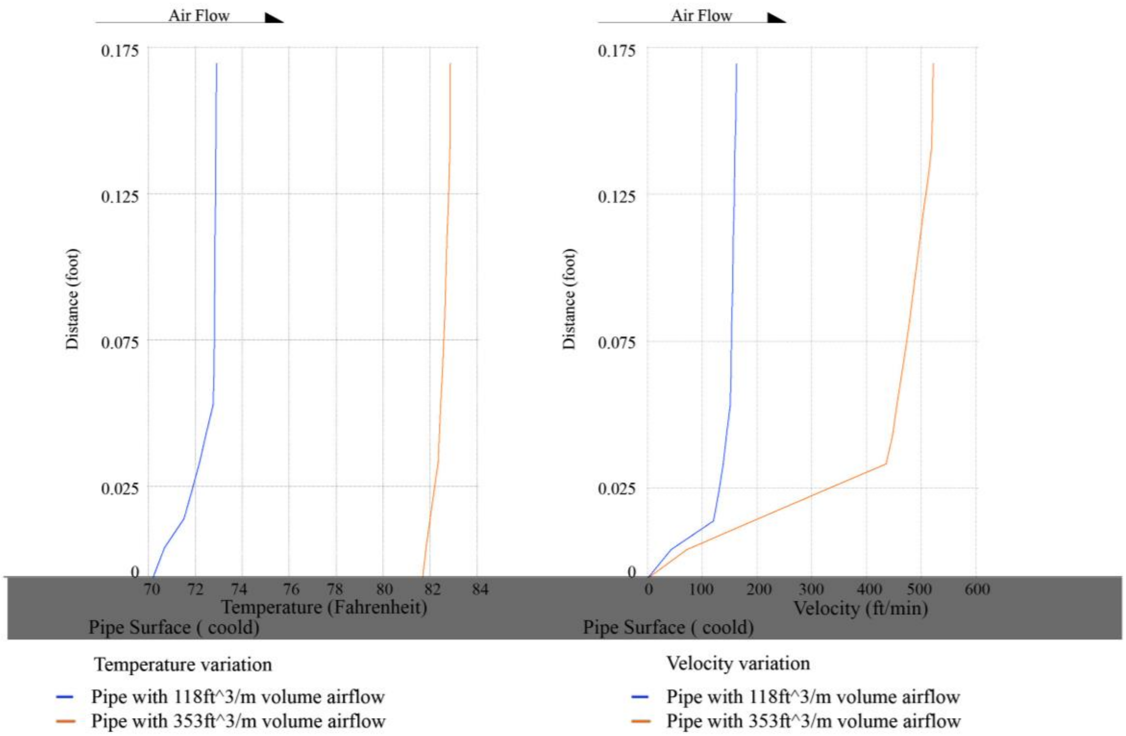

Figure 2-33: Air Velocity and Temperature Variation

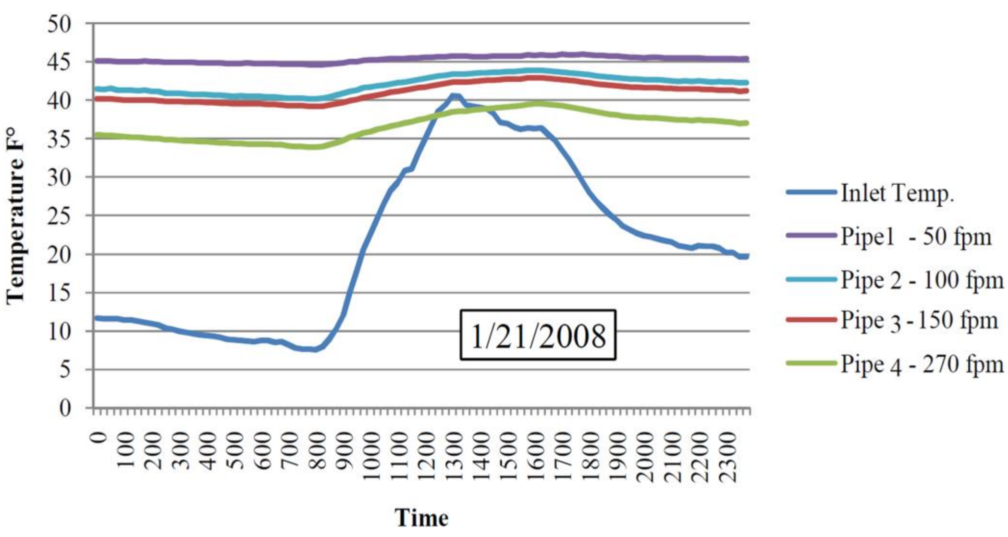

Figure 2-34: Temperature Change over 24-hour Period (01/21/2008) (Alghamdi, 2008, p. 32)

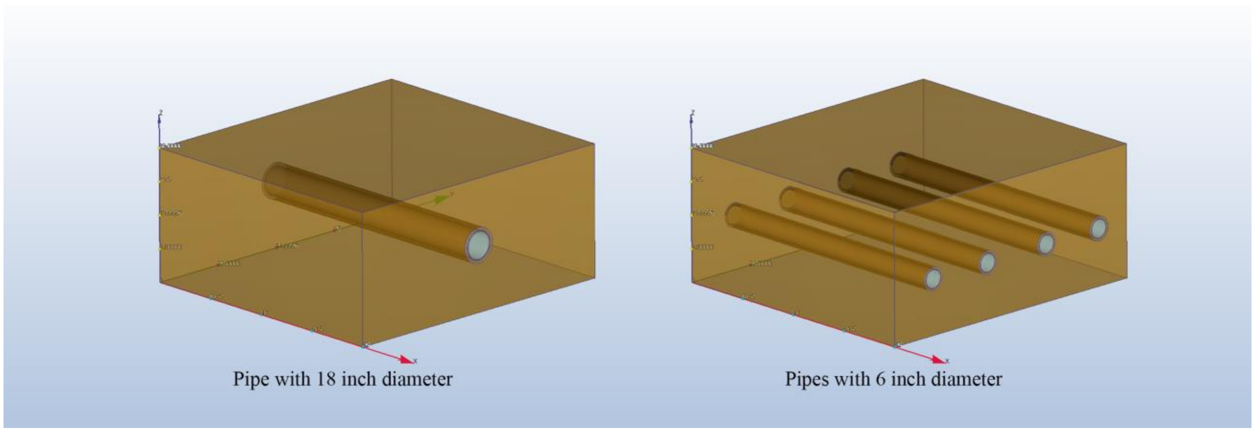

Figure 2-35: Increasing Heat Exchange Surface Between Airflow and the Surrounding Soil

Convective heat transfer should be calculated for each section of the pipe based upon the enthalpy of the air entering and the air-ground energy transfer balance, which is calculated from the surrounding properties of the soil, the convective heat transfer coefficient, and the pipe's thermal resistance. The convective heat transfer coefficient is calculated according to the airflow type (e.g., laminar, transitioning, or turbulent) (Equation 8) (Bojic, Trifunovic, Papadakis, & Kyritsis, 1997).

Equation 8: Reynolds' number (Bojic et al., 1997)

$$Nu = \begin{cases} 0.17\mathrm{Re}^{0.33}.\mathrm{Gr}^{0.1}.\mathrm{Pr}^{0.43} & \text{for} \quad \mathrm{Re}<2400 \\ \mathrm{K}_0.\mathrm{Pr}^{0.43} & \text{for} \quad 2400\leq\mathrm{Re}\leq10000 \\ 0.021\mathrm{Re}^{0.8}.\mathrm{Pr}^{0.43} & \text{for} \quad \mathrm{Re}>10000 \end{cases}$$

Where:

- Re Reynolds' number
- Pr Prandtl's number
- Gr Grashoff's number
- K_0 Coefficient dependent on the Reynolds' number

System Design and Materials Heat Exchange

The GCV system design and pipe materials are important factors for heat transfer because they constitute the heat flow path between the soil and airflow. Each material has thermal properties through which heat will flow. The more conductive the material, the faster heat will flow through it. In GCV systems, due to thermal conductivity, the material type is important for the system to perform well (Table 6). Pipes and types of backfill material in GCV systems should be chosen appropriately to serve their function and work together for all modes of thermal heat transfer.

Table 6: Materials Thermal Conductivity

Thermal conductivity W/(m K)	
Material/Substance	**Temperature - 25^oC**
Concrete, dense	1.0 - 1.8
Concrete, lightweight	0.1 - 0.3
Concrete, medium	0.4 - 0.7
Concrete, stone	1.7
Gravel	0.7
Ground or soil, dry area	0.5
Ground or soil, moist area	1
Ground or soil, very dry area	0.33
Ground or soil, very moist area	1.4
Limestone	1.26 - 1.33
Sandstone	1.7
Soil, clay	1.1
Soil, saturated	0.6 - 4
Soil, with organic matter	0.15 - 2
Water	0.58

Pipe depth, length, wall thickness, and backfill thickness affect GCV system performance. Pipe and backfill thickness, as well as material type, affect heat transfer conductivity between soil and airflow. Pipe depth is related to soil temperature. When the pipe is buried deeper, the soil temperature will be more constant. Pipe length also is related to heat exchange with the airflow. The longer the air resides in the pipe, the greater the heat exchange and change in air temperature. All design factors must be compatible in the GCV system to achieve its best performance.

Mathematical Formula

To model the heat transfer between airflow and surrounding soil, the ground volume can be divided into separate cross-sections. Assuming three axes (X, Y, Z), Figure 2-36 shows that where X is the horizontal axis normal to the heat exchanger axis, Y is the vertical axis, and Z is the horizontal axis parallel to the heat exchanger axis. The heat transfer equation based on enthalpy for each section (two-dimensional model) is as follows (Equation 9) (Ahmed, Miller, & Gidado, 2009):

Equation 9: Heat transfer for each section (Ahmed et al., 2009)

$$\frac{\partial}{\partial \tau}(c.\rho.T) = \frac{1}{\lambda}\left(\frac{\partial^2 T}{\partial x^2} + \frac{\partial^2 T}{\partial y^2}\right)$$

Where:

- c Soil heat capacity, J/(kg K)
- ρ Soil density, kg/m^3
- λ Soil thermal conductivity, W/mK
- T Temperature, C^o
- x, y Coordinates, m

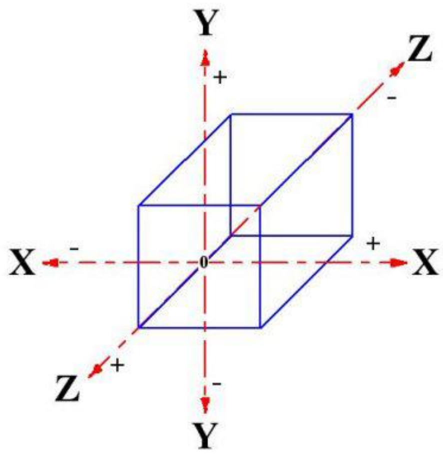

Figure 2-36: Ground Heat Transfer Cross-Sections

To determine soil temperature, a finite element method is used for each cross-section. The model uses a different rectangular grid in which a stepped curve approximates the round shape of a pipe cross-section (Figure 2-37). To increase the computing speed, both the size of the elements and the time step are set to achieve the desired accuracy. In CFD, this cross-section grid is the mesh-size cell that is used to determine soil temperature.

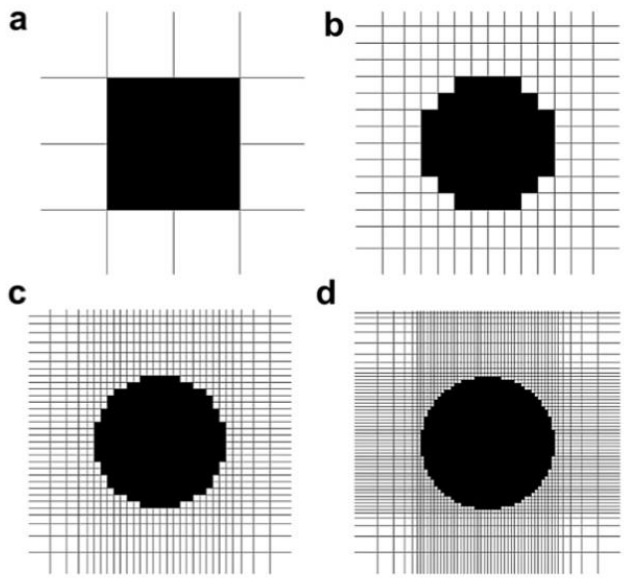

Figure 2-37: Sample Stepped-Curve Approximation of a Pipe Cross-Section (200 mm Diameter) with Element Size of (a) 100mm, (b) 25mm, (c) 10mm, (d) 5mm

Heat transfer calculations in GCV systems is complicated because many factors affect the process. Further, probability error calculation is possible because heat transfer is calculated in a multi-section of the GCV system. Now, with the computer software available, all of the heat transfer calculations can be performed using the CFD program, which is faster, more accurate, and produces fewer errors.

2.9 Computational Fluid Dynamics (CFD)

CFD is the art of presenting a set of algebraic equations that can be solved using computers. Among other uses, CFD helps architects design comfortable and safe living environments, improve vehicle design, and predict fluid flows. Such mathematical models as those with partial differential equations, numerical methods of discretization and solution techniques, and other software tools are all critical components of these pre-processing and post-processing utilities.

CFD provides an understanding of the difficulty and expense involved in studying flow patterns through experimental techniques. CFD cannot replace direct measurements completely, but it can and does reduce the amount of experimentation needed and the cost overall. Table 7 compares experiments and CFD simulations (Kuzmin, 2014).

Table 7: Experiments vs. CFD Simulations

Experiments	**Simulations**
Quantitative description of flow phenomena using measurements:	Quantitative prediction of flow phenomena using CFD software:
• For one quantity at a time	• For all desired quantities
• At a limited number of points and time instants	• With high resolution in space and time
• For a laboratory-scale model	• For the actual flows domain
• For a limited range of problems and operation conditions	• For virtual problem and realistic operating conditions
Error sources: measurement errors, flow disturbances by the probes	Error sources: modeling, discretization, iteration, and implementation
Expensive	Cheaper
Slow	Faster
Sequential	Parallel
Single-purpose	Multiple-purpose
Equipment and personnel are difficult to transport.	CFD software is portable and easy to both use and modify

2.9.1 Fluid Flows

Partial differential equations that represent conservation laws for mass, momentum, and energy control both gas and liquid flows. Fluid flows are a fundamental element of rain, wind, hurricanes, floods, and fires. Further, they influence air pollution, contaminant transport, heat transfer, ventilation, and air conditioning in buildings, cars, and more propulsive systems or objects that interact with the surrounding air or water. These complex flows also occur in furnaces and heat exchangers. Fluids have many properties that are outlined in Table 8 (Kuzmin, 2014):

Table 8: Fluid Properties

Macroscopic properties		**Classification of fluid flows**	
ρ	Density	Viscous	Inviscid
μ	Viscosity	Compressible	Incompressible
p	Pressure	Steady	Unsteady
T	Temperature	Laminar	Turbulent
V	Velocity	Single-phase	Multiphase

2.9.2 CFD Predictions

CFD uses a computer to solve mathematical equations and make predictions using a process that entails four steps:

1. The human being (analyst) states the problem to be solved.
2. Scientific knowledge (models, methods) is expressed mathematically.
3. The computer code (software) that embodies this knowledge provides detailed instructions (algorithms) for the computer hardware, which then performs the actual calculations.
4. The analyst inspects and interprets the simulation's results.

CFD simulation results are not 100% reliable. The input may have involved guesswork or inaccuracy. Further, the computing power available always limits the results' accuracy (Kuzmin, 2014).

2.9.3 CFD Analysis Process

CFD analysis involves eight steps:

- Problem statement
- Mathematical model
- Discretization process:
    - Mesh generation
    - Space discretization
    - Time discretization
- Multi-solution
- CFD software
- Simulation run
- Post-processing
- Verification

Problem Statement

Several questions can help a researcher identify a problem statement in CFD analysis (Kuzmin, 2014). For example:

- What is known about the flow problem already?
- What physical phenomena must be taken into account?
- What is the geometry of the domain and operating conditions?
- Are there any internal obstacles, free surfaces, or interfaces?
- Is the flow laminar or turbulent?
- What is the CFD analysis' objective?
    - Computation of integral quantities (lift, drag, yield)
    - Snapshot of field data for velocities and concentrations
    - Shape optimization designed to improve performance
- What is the easiest, least expensive, and fastest way to achieve the goal?

Mathematical Model

The following steps should be considered when developing a mathematical model:

1. Choose a suitable flow model and reference frame.
2. Identify the force that causes and influences the fluid's motion.
3. Define the computational domain to solve the problem.
4. Express conservation laws for the mass, momentum, and energy.
5. Simplify the governing equations to reduce computational time:
    a. Use current flow information.
    b. Check flow directions and symmetries.
    c. Disregard those terms that do not affect the results.
    d. Model the effect of small-scale fluctuations that cannot be captured.
    e. Integrate knowledge of measurement data and CFD results.
6. Add constitutive relations and specify original materials and boundary conditions.

Discretization Process

The partial differential equations (PDE) system can be transformed into a set of algebraic equations:

1. Mesh generation (decomposition into cells or elements):
    a. Structured or unstructured, triangular or quadrilateral?
    b. CAD tools + grid generators (Delaunay or advancing front?)
    c. Mesh size and adaptive refinement in interesting flow regions
2. Space discretization (approximation of spatial derivatives):
    a. Finite differences, volumes, and elements
    b. High vs. low order approximations
3. Time discretization (approximations of temporal derivatives):
    a. Explicit vs. implicit schemes, stability constraints.
    b. Local stepping time and control steps time

Multi-Solution

Algebraic equations for the simulation must be solved iteratively:

- For outer iterations, the solution values from the previous iteration are used to update the discrete problem's coefficients. This eliminates the nonlinearities by a Newtonian-like method and allows governing equations to be solved in a segregated fashion.
- For inner iterations, the resulting sequence of linear subproblems is solved typically by an iterative method (conjugate gradients, multigrain), because direct solvers are prohibitively expensive.
- It is necessary to check the residual, relative solution changes and other convergence criteria indicators to ensure that the iterations converge.

CFD Software

At present, CFD software cannot be used blindly without a basic understanding of the underlying numerics. Many CFD software programs are available on the market—ANSYS CFX, Fluent, Star-CCM++, Autodesk CFD, and FEMLAB. Each has its functions and properties that will be compared in Chapter five to determine the CFD program most appropriate for the research.

CFD Simulation

The computing times for a flow simulation depend on the following (Kuzmin, 2014):

- The numerical algorithms and data structures
- Linear algebra tools, stopping criteria for iterative solvers
- Discretization parameters (mesh quality and size, time step)
- Time cost per step and convergence rates for outer iterations
- Programming language (most CFD codes are written in Fortran)
- Many other elements (hardware, victimization, parallelization, etc.)

The quality of the simulation results depends on:

- The mathematical model and underlying assumptions
- Approximation type, the stability of the numerical scheme
- Mesh, time step, error indicators, stopping criteria, etc.

Post Processing and Analysis

The simulation results are post-processed to extract the information desired from the computed flow field:

- Calculation of quantities derived (stream function, vorticity)
- Calculation of integral parameters (lift, drag, total mass)
- Visualization (representation of numbers as images)
    - 1D data: function values connected by straight lines
    - 2D data: streamlines, contour levels, color diagrams
    - 3D data: cutline, cut plane, isosurfaces, isovolumes
    - Arrow plots, particle tracing, animations
- Systematic data analysis using statistical tools
- Debugging, verification, and validation of the CFD model

Verification of CFD Codes

Verification requires looking for errors in the models' implementation:

- Examine the computer programming by checking the source code visually, documenting it, and testing the underlying subprograms individually.
- Examine iterative convergence by monitoring the residuals, relative changes in integral quantities, and checking whether the tolerance prescribed is achieved.
- Examine consistency (check whether relevant conservation principles are satisfied).
- Examine grid convergence: As the mesh and/or the time step are refined, the spatial and temporal discretization errors, respectively, should approach zero asymptotically.
- Compare the computational results with analytical and numerical solutions for standard benchmark configurations.

Validation entails checking the adequacy of the model for practical purposes. As (Kuzmin, 2014) explained, “The goal of verification and validation is to ensure that the CFD code produces reasonable results for a certain range of flow problems.” Therefore, validation was used to ensure the right equations were solved:

- Verify the code to ensure that the numerical solutions are correct.
- Compare results with experimental data available (check for measurement errors) to check whether the reality is represented sufficiently accurately.
- Perform a sensitivity analysis and parametric study to assess the inherent uncertainty attributable to an insufficient understanding of physical processes.
- Try using different models, geometry, and initial or boundary conditions.
- Report the findings and document model limitations and parameter settings.

2.10 Autodesk CFD Validation

Autodesk CFD needs to be, and has been, validated in many cases as a tool to predict fluid flow and heat transfer. These cases compared Autodesk CFD with experimental and numerical calculation examples, such as the following:

2.10.1 Turbulent pipe flow

In this example, a 2D circular pipe was analyzed to verify the ability of Autodesk CFD to model fluid flow and turbulence with the numerical calculations shown in Figure 2-38. The results of Autodesk CFD and White’s (1994) numerical calculations can be compared in a pressure drop, as shown in Table 9 (Autodesk, 2015c).

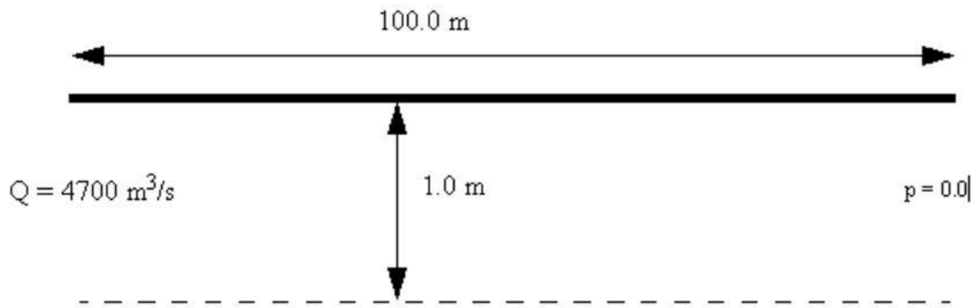

Figure 2-38: Geometry and Boundary Conditions (Autodesk, 2015c)

Table 9: Turbulent Pipe Flow Results (Autodesk, 2015c)

	Benchmark	2013: Build 20120131	% Error	2014: Build 20130102	% Error
ΔP	4.0e5 Pa	397495.70 Pa	0.550	397744.82 Pa	0.488

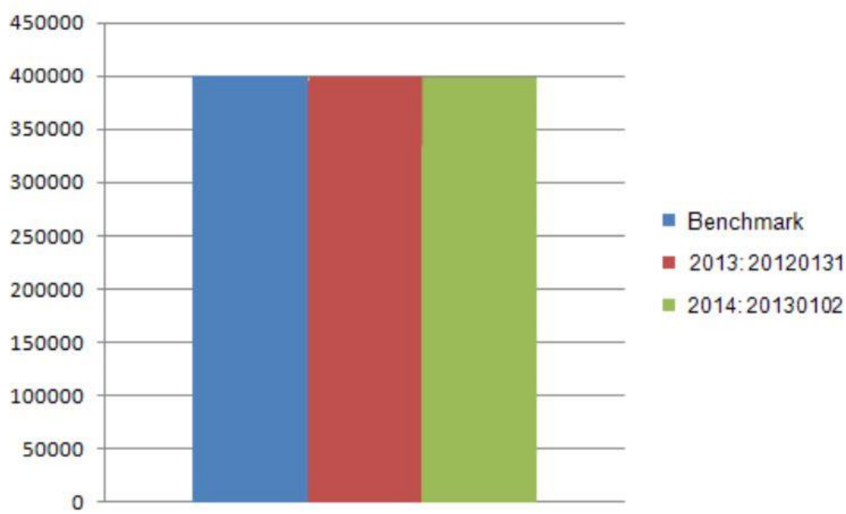

2.10.2 Flow around a cylinder array

A cylinder array's geometry is a channel with a rectangular cross-section and seven cylinders. The two types of fluid tested included a Newtonian and non-Newtonian fluid. The non-Newtonian fluid is one that does not follow Newton's law of viscosity. The pressure drop across the channel that Autodesk CFD calculated was compared to the measured data in Table 10 (Autodesk, 2015b; Georgiou, Momani, Crochet, & Walters, 1991, pp. 231–260).

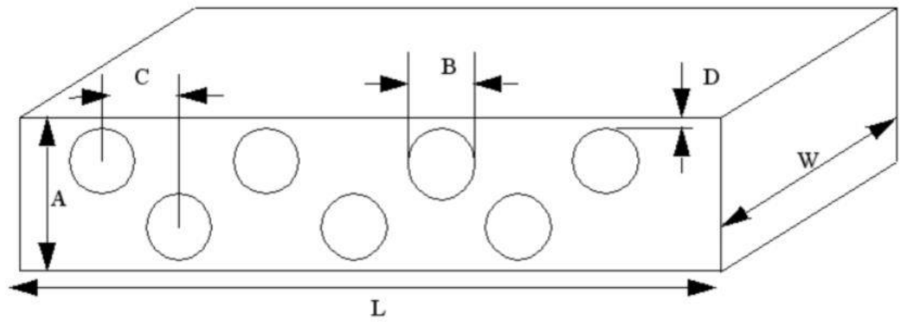

Where A = 2.3 cm., B = 1.25 cm., C = 3.375 cm., D = 0.35 cm., L = 32.6 cm., W = 2.5 cm.

Figure 2-39: Cylinder Array Geometry (Autodesk, 2015b)

Table 10: Flow Around a Cylinder Array Results (Autodesk, 2015b)

	Benchmark ΔP (Pa)	2013: Build 20120131	% Error	2014: Build 20130102	% Error
Newtonian					
$\dot{Q}$ = 30 cc/s	4200	4325.57	2.98	4329.32	3.07
Non-Newtonian					
$\dot{Q}$ = 30 cc/s	3400	3578.62	5.25	3599.45	5.87

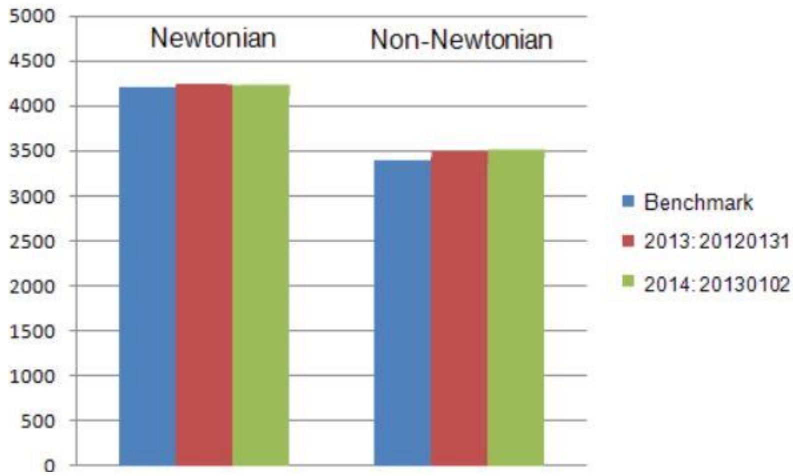

2.10.3 Flow through an overheated cylinder

A model was created to determine the flow through an overheated circular cylinder with an infinitely long axis (Figure 2-40) immersed in a laminar flow with a Reynolds' number of 50 (based on the cylinder's diameter). The cylinder had a fixed temperature 100^{o}K higher than that of the fluid. This model was analyzed to verify Autodesk CFD fluid flow and heat transfer modeling capabilities by comparing two expressions of the Nusselt number, which is the heat transfer ratio from convection to conduction across the normal boundary. One was an experimental correlation from Holman (1981), while the other was an analytical derivation. Table 11 shows the results comparison (Autodesk, 2015a).

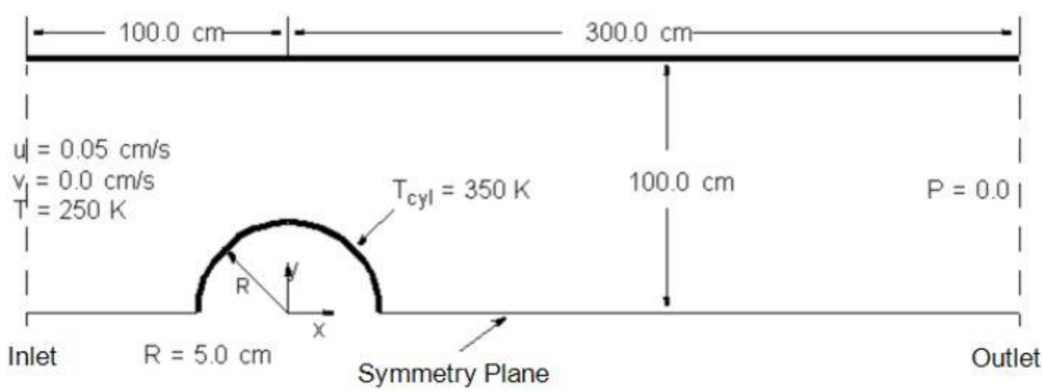

Figure 2-40: Flow Through an Overheated Cylinder Geometry (Autodesk, 2015a)

Table 11: Flow Through an Overheated Cylinder Results (Autodesk, 2015a)

Benchmark	2013: Build 20120131	% Error	2014: Build 20130102	% Error
Nue = 8.29	Nua = 8.268	0.257	Nua = 8.229	0.735

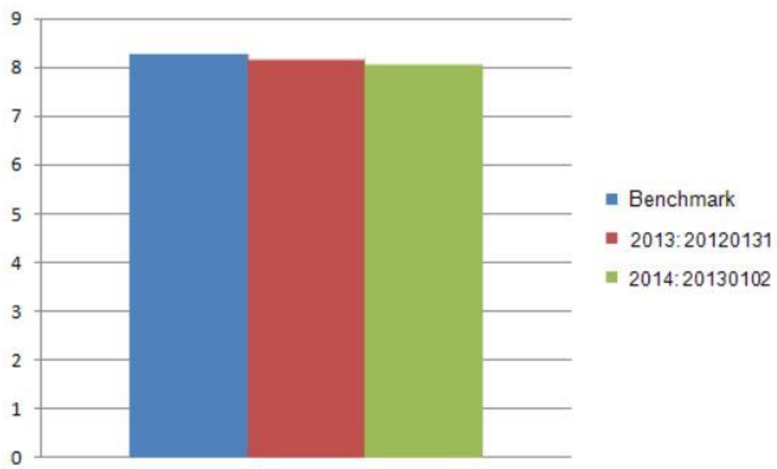

Based on the three examples above, the Autodesk CFD results were validated with experimental cases and numerical calculation. Accordingly, Autodesk CFD was used as a simulation tool in this research.

2.11 Conclusion

This research contributes to the body of knowledge in four points. First, since the HVAC system is the highest energy consumption in most buildings, by using the GCV system, energy consumption may reduce. Second, because the GCV system design varies from place to place, there is no standard design for GCV systems. The outcome of this research is a GCV system tool that predicts the performance of a GCV system and helps to determine the recommended GCV system design for a given building. Third, the GCV evaluation tool helps the designer to save time predicting the performance of the GCV system. Fourth, the GCV system evaluation tool is more accurate than the GAEA tool because it relies on regression equations that were derived from parametric GCV modeling from CFD.

Chapter 3: Research Design

3.1 Overview

Energy consumption is both an economic and environmental issue. A GCV system depends on geothermal energy to maintain a comfortable ambient temperature, and thus, can drastically reduce demands on such non-renewable energy sources as oil—particularly in Saudi Arabia. The primary goal of this research was to create a tool to evaluate GCV system designs. In order to achieve this goal, in-situ GCV system monitoring and CFD as a simulation tool were used. While many factors affect GCV system performance, this study focused primarily on design and examined pipe parameters (pipe length, depth, and diameter), soil type, and airflow velocity of the GCV system. These factors will be discussed later in more detail (International Energy Agency, 2015).

3.1.1 Methods

The study used quantitative methods to achieve the research goals. There are three ways to collect data from a GCV system. First, one can monitor existing GCV systems in-situ using instruments located within the system. Second, one can experiment by building different GCV systems with a range of variables. Third, one can predict GCV system performance using such computer software as CFD or GAEA. Table 12 shows the advantages and disadvantages of all three options. After comparing these methods, computer prediction software was selected as the most appropriate option because it has unlimited design conditions, low cost, requires less effort, and obtains results in a shorter time compared to the other methods.

Table 12: Advantages and Disadvantages of Data Collection Options

Method	Advantages	Disadvantages
In-situ monitoring	Actual results	Expensive equipment cost Not enough GCV system examples
Experimental	Actual results	Long time Much effort High cost Limited conditions
Computer prediction	Short time Less effort Low cost Unlimited design conditions	Predicted results Should validate results

3.1.2 Computer Prediction Software

Computer software can predict GCV system performance, which can save time, cost, and effort when compared to the other methods of collecting data. As previously mentioned, two types of software can be used to predict GCV system performance, CFD and GAEA. CFD software depends on simulated fluid flow and heat exchange to predict GCV system performance, while GAEA uses less rigorous equations to calculate heat exchange in GCV systems. Both CFD and GAEA must be validated with an as-built GCV system to determine the accuracy of the results from each software.

3.1.3 Research Design Strategy

As stated, because the results of the CFD and GAEA are predictions, the results must be validated with an actual GCV system. The research design was divided into six phases: first, monitor the GCV system in the Solar CM House in-situ; second, simulate a CFD model and a GAEA model of the GCV system at Solar CM House and compare the predictions with the in-situ data; third, design several different GCV systems using Autodesk CFD; fourth, use the results from the simulations for the different CFD models to perform a regression analysis that predicts the temperature differences between inlet and outlet and then validate the regression model; fifth, develop a GCV system evaluation tool to predect the GCV system performance using the regression models; and sixth, apply the tool to the design of a GCV system for Riyadh, Saudi Arabia. All of these steps will be summarized in this chapter.

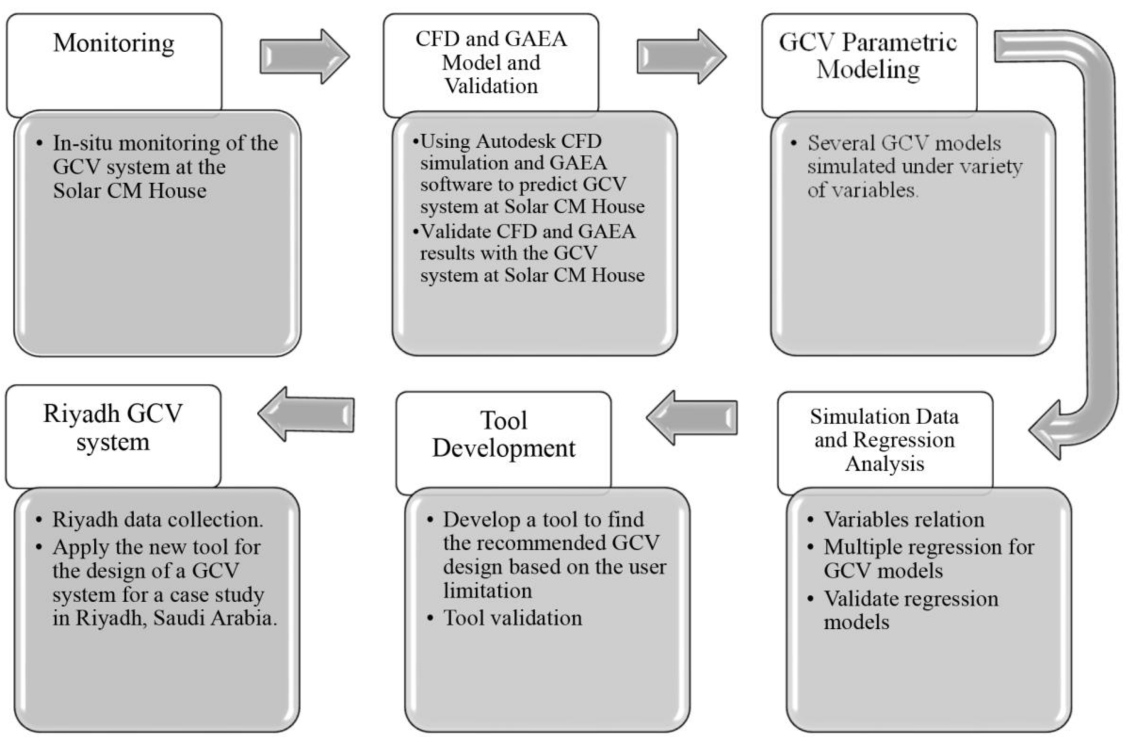

Figure 3-1: Summary of Research Design Phases

3.2 Monitoring the GCV System at the Solar CM House

The first phase of the research was to monitor the GCV system at the Solar CM House. The GCV system is an open loop system consisting of clay pipe, gravel backfill, and on-site soil. Several variables were monitored including air flow velocity, air temperatures, and ground temperatures as Figure 3-2 shows. The GCV system was monitored for eight months. Chapter four presents in greater details the monitoring of the GCV system at the Solar CM House.

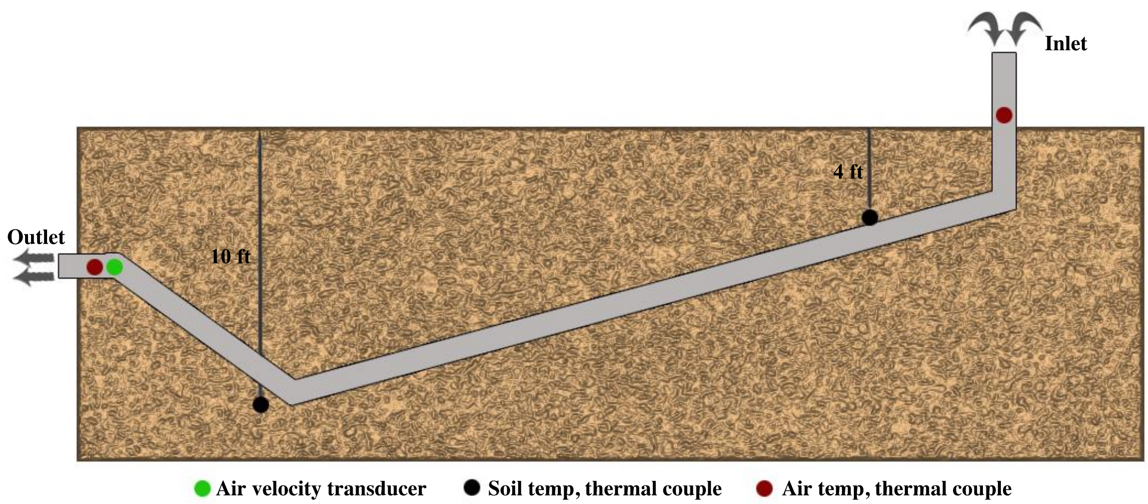

Figure 3-2: Instrument Locations at Solar CM House

3.3 CFD and GAEA Model for the Solar CM House

The second phase of the research was to determine the accuracy of the CFD and GAEA as predictive tools. Both CFD and GAEA models were developed for the design and properties of the GCV system at the Solar CM House. In the end, the CFD and GAEA model were validated by comparing the outlet temperatures for three selected days. Chapter five discusses the CFD and GAEA model and validation.

3.4 GCV Parameter Modeling

The third phase of the research consisted of parametrically evaluating the GCV system performance for both exogenous and endogenous variables. Exogenous variables include air temperature, ground temperature, and soil type. Endogenous variables include air velocity, pipe length, depth, thickness, and diameter—each of which has boundary levels that limited the research. Other variables were considered fixed during the simulations. Table 13 shows a summary of the GCV system variables and limitations that were included in this research. More details about the variables can be found in Chapter six.

Table 13: Research Limitation Variables

Variable	Variable in this research	Reason	Limitation	Limitation reason
Air temperature	Yes	Air temperature is the main factor of the system	5-115 F	Air temperature limitation covers hot and cold season for different locations.
Ground temperature	Yes	Ground temperature is a primary factor of heat exchange.	35-95 F	Ground temperature limitation covers hot and cold season for different locations.
Soil type	Yes	Thermal properties of the soil affect ground temperature	Sand- Clay-Limestone	These are the main soil type that have different properties
Airflow velocity	Yes	Airflow is the only variable we can change after designing the system.	50-450 fpm	There is no efficiency on airflow under 50 f/m., nor noise sound if the airflow is under 450 fpm.
Pipe length	Yes	Pipe length impacts air residency.	50-450 ft.	Lengths shorter than 50 ft. will be inefficient. Lengths longer than 450 ft. will occupy too much space.
Pipe diameter	Yes	Pipe diameter impacts air volume	6”-48”	Readily available in the marketplace
Pipe thickness	Correlated	Pipe thickness variation depends on the pipe diameter base on pipe manufacturers standard.	0.73"-5.10"	
Pipe depth	Correlated	Pipe depth correlated with ground temperature	Center of the soil boundary	
Pipe material	Fixed	This research will use clay pipe because of its high thermal conductivity.	Clay pipe	
Pipe shape	Fixed	Most pipes have a circular cross-section. Rectangular and square pipes will not be covered.	Circular cross-section	
Backfill size	Fixed	Changing Backfill size will not significantly affect the GCV system performance. 10” gravel thickness with 1” average diameter will be used.	10"	
Backfill material	Fixed	Gravel is the appropriate material for heat transfer and pipe protection.	Gravel	
Ground shading	Fixed	All GCV systems in this research will assume a shaded system to ensure the greatest impact during the hot season	Shaded	

3.4.1 Modeling

The GCV system was modeled using the Autodesk CFD simulation program based on the system's endogenous variables, some of which affect the GCV system performance more than others. Furthermore, a set of 75 models was designed based on these variables, which contained three levels of soil type and five levels of each pipe diameter and length, as Table 14 shows. To save time, airflow velocity variances were simulated in one model, although the distance between pipes was considered as 40 feet so that the pipes did not affect each other. Each model was simulated 84 times rather than 420 times because airflow velocity was merged into one design.

Moreover, the total number of simulations run for the GCV system models was 6,300 rather than 31,500 simulations to predict temperature reduction according to changes in air and ground temperature (air temperature 5-115^{o}F and ground temperature 35-95^{o}F, respectively). Figure 3-3 shows the GCV models' distribution based on the research variables. The results of all simulations are given in Chapter six.

Table 14: Models of Boundary Condition Variables

Variable	Min value											Max value	Unit
Air flow	50		150			250			350			450	fpm
Pipe length	50		150			250			350			450	feet
Pipe diameter	6		12			24			36			48	inch
Soil type	Clay					Sand						Limestone	
Air temperature	5	15	25	35	45	55	65	75	85	95	105	115	Fahrenheit
Ground Temperature	35		45		55		65		75		85	95	Fahrenheit

Figure 3-3: GCV Design Distribution-Based Research Variables

3.5 Simulation Data Analysis, Regression Analysis and Validation

The simulation data were analyzed in the fourth phase of this research to determine the relations between the GCV system variables through regression analysis of all of the GCV simulations data. The regression analysis was performed with JMP software. There are many types of regression analyses, but multiple linear regression was the most appropriate for this research because the relations between all variables was determined to be linear. As an outcome from the regression analyses, a regression model for a cooling and heating system was presented to predict the outlet air temperature of the GCV system. Chapter seven discusses in more detail the simulation data, regression analysis, and model validation.

3.5.1 Regression Validation

Next, the GCV system regression models were validated. The models used 90% of the samples to predict temperature change for the cooling and heating systems. By using a cross-section validation, the remaining 10% were randomly selected from the dataset to compare the simulation’s output air temperature to the regression models under the same variable conditions. Then, the model was applied to the tool to predict the temperature reduction in the GCV system.

3.6 Tool Development

The fifth phase of the research was to create the GCV system evaluation tool for predicting the system performance. Then, this tool was validated by comparison with in-situ data from the Solar CM House. Chapter eight provides more details about the GCV system tool.

3.6.1 Creating the GCV System Evaluation Tool

The GCV system evaluation tool is a standalone application that was created using the MATLAB program. The tool was divided into five phases (Figure 3-4). First, the GCV system design information or the limitations for the design variables were input. The input information included the weather file, pipe length, depth, diameter, number of pipes, soil type, and the volume flow rate that the building required. Second, the tool generated a list of all possible combinations of the input information for the GCV system. Third, the performance of all of the GCV system designs throughout the year was calculated and the regression equations were used to predict the outlet temperature. Fourth, the recommended GCV system design was determined based on the system type that had the maximum temperature differences between the inlet and outlet. In the fifth phase, the results of all GCV system designs were presented based on the selected system type, with graphs that showed the performance of the system over the year and bar charts of cooling and heating energy in British Thermal Units (BTU).

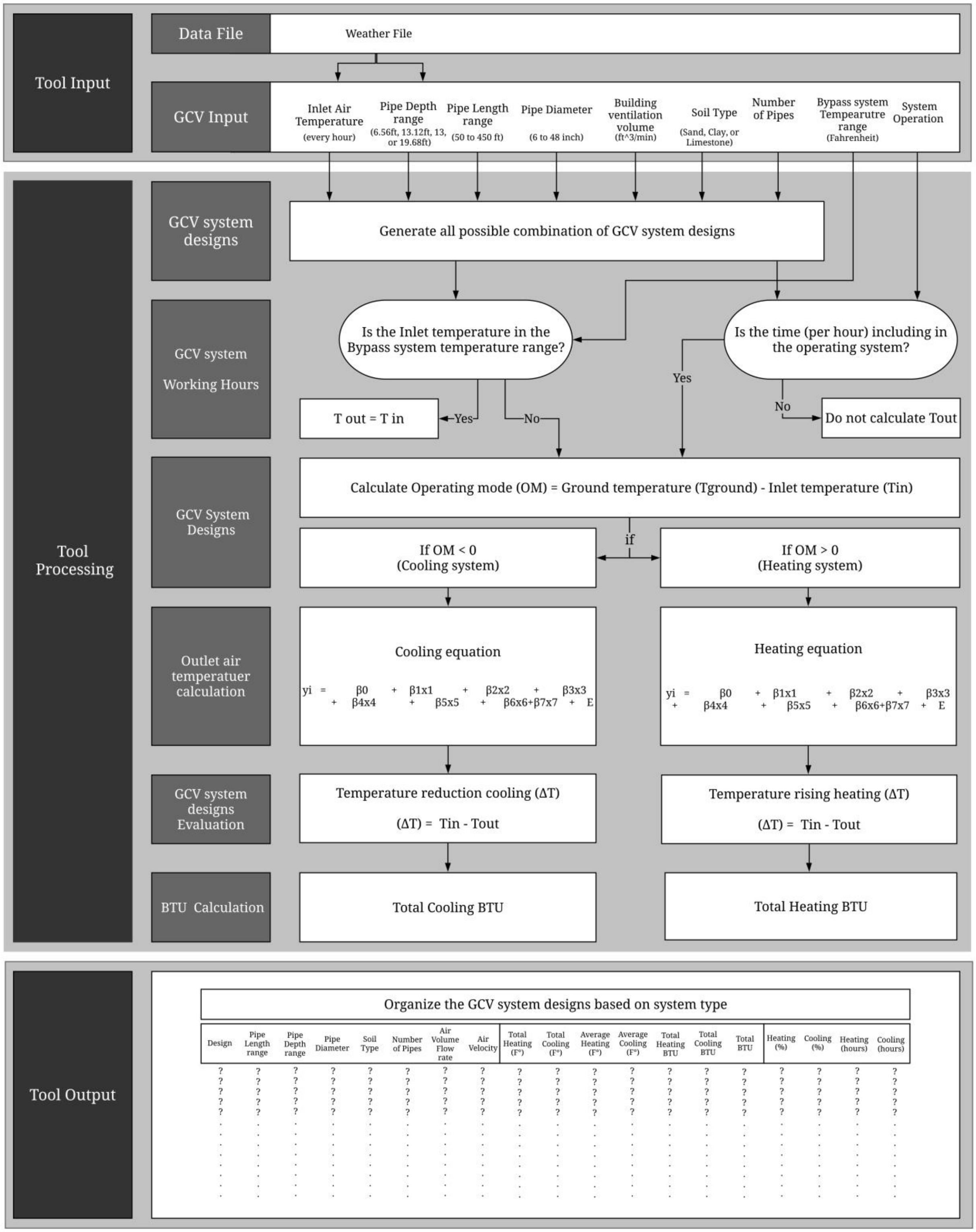

Figure 3-4: GCV System Tool Steps

3.6.2 Tool Validation

After the GCV system evaluation tool was created, it had to be validated by comparing the predicted performance of the GCV system tool with the GCV system at the Solar CM House. This comparison was made on July 24th, Oct 25th, and Dec 20th in 2016 and was based on the outlet temperature.

3.7 Riyadh GCV System

The sixth phase of the research was to answer the research question: What is the recommended GCV design for Riyadh, Saudi Arabia? Based on Prince Mohammad bin Salman's 2030 vision to adopt alternative energy, this research attempted to introduce GCV systems in Riyadh, Saudi Arabia to achieve part of his vision of energy reduction in buildings. After the GCV system tool was validated, it could be used to find the best recommended GCV system design for non-residential buildings in Riyadh. In-situ collection of air and ground temperature data was required to apply the weather file into the tool, after which it was possible to identify the best recommended design.

Riyadh in-situ data collection

Because the weather data file for Riyadh is old (based on 1983), updated data were required. Further, because the weather file did not include the ground temperature at certain depths, air and ground temperatures at different depths were collected in-situ over the course of an entire year. These data included the ambient air and ground temperatures at 6.56 feet, 12.13 feet, and 19.68 feet deep, respectively. To ensure accurate results, the data were collected every five minutes.

Finding a GCV System for Riyadh, Saudi Arabia

To determine the GCV system design that produced the greatest temperature reduction, several steps were taken (Figure 3-5). First, the minimum ventilation required for the building was calculated. The energy modeling software, eQUEST, was used to calculate the required heating and cooling system and ventilation rate. In the second step, GCV system variables were input. Each variable had a limited range to restrict the system designs. In the third step, a range of the possible designs were processed based on the input, the predicted outlet temperature for each design was calculated, and then the temperature change for all of the GCV system designs was calculated. The fourth step was to show the tool's output by listing the GCV system designs based on their type and sorting them based on the greatest temperature change. In addition, the results were presented as graphs of the GCV system outlet temperature, as well as bar charts of the cooling and heating energy in BTU. These steps were used in an office building as a case study to determine the GCV system design to answer the research question. Chapter nine discusses the GCV system performance in a case study in detail.

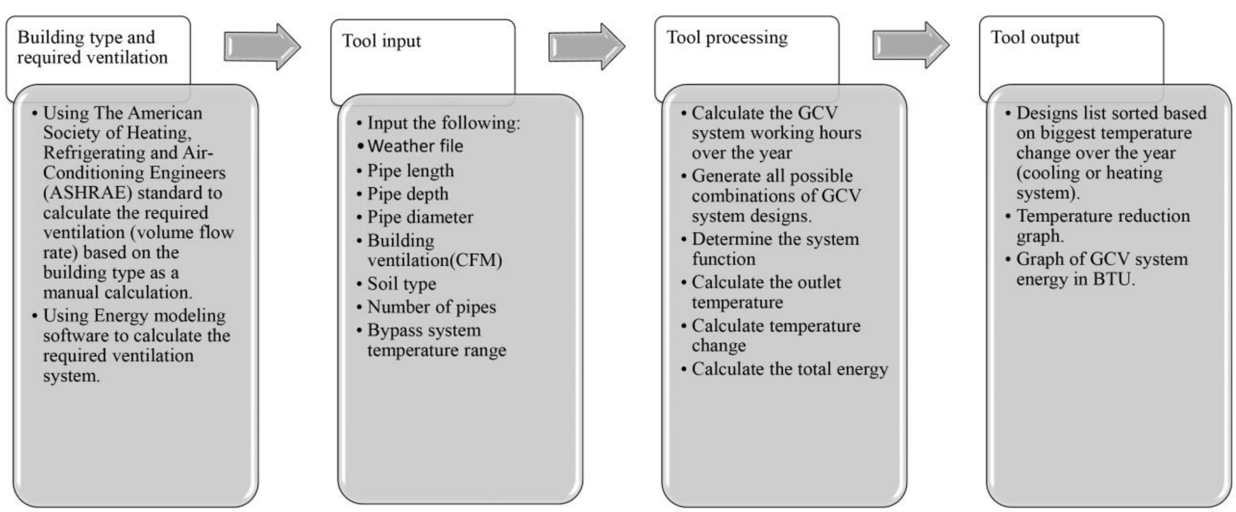

Figure 3-5: Steps to Use the GCV System Design Tool

Chapter 4: Monitoring the GCV System at the Solar CM House

The Solar CM House was the appropriate GCV system case study to monitor because it is easily accessible to Virginia Tech researchers. It is located in the Environmental Systems Laboratory facility, an unoccupied building, and is serviced regularly both by inspection and maintenance service professionals. Further, its GCV system is well designed and documented. The Solar CM House consists of two units connected by a hallway (Figure 4-1). The first unit measures 16 ft. x 16 ft. and the second unit measures 16 ft. x 24 ft., with a 10 ft. ceiling height. Each unit has a separate GCV system (four pipes per unit) that is incorporated into the floor and along the building envelope. This GCV system is an open loop system consisting of clay pipes, gravel backfill, and on-site soil.

Figure 4-1: Solar CM House (photograph by author)

4.1.1 GCV System in the Solar CM House

The pipes are made of vitrified clay with an inner diameter of 7.5 inches and a wall thickness of 1.5 inches. Each pipe has a total length of 84.4 feet and contains 18 segments. The external end of the pipes is capped to protect the system from rain, insects, and other pests (Figure 4-2). There is a joint segment mid-way down the tube to collect water. All the pipes are surrounded with a 1-inch average diameter gravel backfill approximately 10 inches thick. The ground is covered with grass and wild weeds. Because the GCV system is more than thirty years old, the pipes were inspected for cracks, fungus, and mold. The Sterrett Facilities Complex and Environmental Health and Safety at Virginia Tech have the equipment and workforce necessary to inspect and maintain the system. The results show that there were neither cracks in the surface of the pipes nor mold or bacteria. With this information, it was possible to begin installing the instruments.

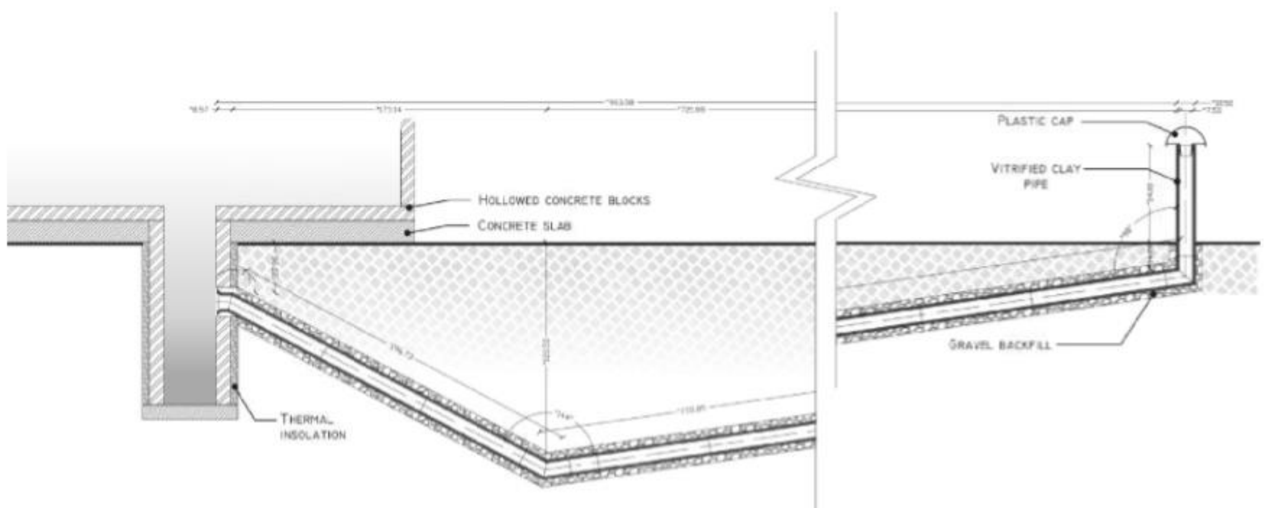

Figure 4-2: Ground-Coupled Ventilation System at Solar CM House (Alghamdi, 2008)

4.1.2 Equipment Installation and Data Collection

It was necessary to monitor several variables in the GCV system at the Solar CM House. Readings of airflow velocity, air temperatures, and ground temperatures were recorded every five minutes. Two pipes with different airflow velocities were also monitored. To obtain the correct results, each variable required a special setup to gather data on:

- **Ground temperature:** two sensors were installed 4 feet and 10 feet underground
- **Air temperature:** inlet and outlet air temperature for each pipe
- **Airflow velocity:** the air velocity was 100 fpm in the first pipe, and 200 fpm in the second pipe

All of these instruments were then connected to a CR3000 Micro data-logger. Table 15 describes the instruments and their functions, while Figure 4-3 shows their locations within the GCV system.

Table 15: Instrument Types Used in the Research

Data	Pipe 1	Pipe 2	Instrument	Notes
Air velocity	Air velocity of 100 fpm	Air velocity of 200 fpm	Blackhawk variable speed fan (Model 11)	A Blackhawk variable speed fan (model 11) will be installed in the interior end of each pipe to control the flow rate.
		Air velocity on the surface	Air velocity transducer (TSI 8475 model)	In each outlet of the pipe at the cinter there is an air velocity transducer (TSI 8475 model) to measure air velocity. Also there is an air velocity transducer close to pipe 2 surface.
Air temperature	Inlet temperature	Inlet temperature	Thermocouple (Type T)	In each end of the pipe, a Thermocouple will be installed three feet inside the pipe to get stable air temperature.
	Outlet temperature	Outlet temperature	Thermocouple (Type T)	
Ground temperature		Ground temperature at 4 ft	Thermocouple (Type T)	Two thermocouples will be buried 4 ft. and 10 ft. under the ground, to know temperature differences in depth.
		Ground temperature at 10ft	Thermocouple (Type T)	

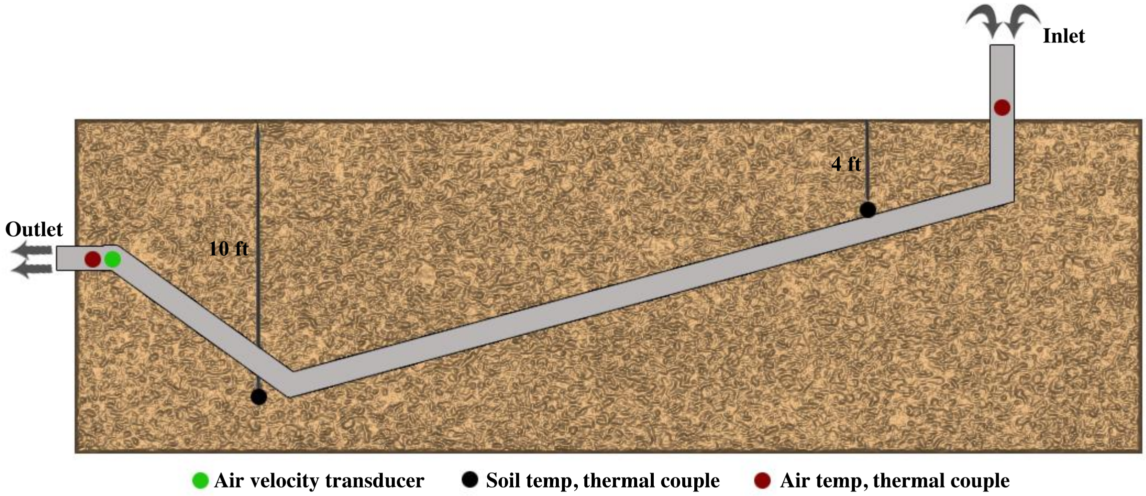

Figure 4-3: Instrument Locations at Solar CM House

Data Collection

The GCV system at the Solar CM House was monitored for eight months. The data-logger recorded the data every five minutes with a sampling interval of 3 seconds to determine the maximum, minimum, sample, and average every five minutes. Table 16 shows the results.

Table 16: GCV Time and Data at Solar CM House

Data/Time	Inlet Temperature								Outlet Temperature							
	Pipe (100 fpm)				Pipe (200 fpm)				Pipe (100 fpm)				Pipe (200 fpm)			
	Avg	Max	Min	Smp	Avg	Max	Min	Smp	Avg	Max	Min	Smp	Avg	Max	Min	Smp
6/7/2016 14:30	83.2	83.6	82.9	83.6	81.1	81.6	80.8	81.6	60.95	61.01	60.88	60.97	63.27	63.34	63.18	63.34
6/7/2016 14:35	83.5	83.9	83.1	83.4	81.1	81.7	80.2	80.9	61.02	61.07	60.96	61.06	63.33	63.42	63.21	63.42
6/7/2016 14:40	83.6	84.4	83	84.3	81.2	82.2	80.5	82.2	61.04	61.11	60.98	61.07	63.38	63.52	63.28	63.51
6/7/2016 14:45	84.3	84.5	84	84.5	81.8	82.4	81.3	82.3	61.05	61.12	60.98	61.07	63.49	63.55	63.42	63.52
6/7/2016 14:50	84.2	84.6	83.7	83.9	81.6	82.3	80.9	81.2	61.02	61.11	60.95	60.95	63.48	63.57	63.38	63.44
6/7/2016 14:55	83.9	84.3	83.6	83.8	81.4	81.9	80.8	80.8	60.97	61.04	60.93	61	63.46	63.53	63.4	63.45
6/7/2016 15:00	84.2	84.6	83.8	84.5	81.4	81.9	80.8	81.9	60.95	61.03	60.92	60.97	63.48	63.57	63.4	63.56
6/7/2016 15:05	84.9	85.4	84.2	84.2	82.2	83	81.5	81.5	61.06	61.14	60.98	61.04	63.62	63.71	63.54	63.55
6/7/2016 15:10	84.4	84.7	84.1	84.7	81.5	81.9	81.2	81.9	60.98	61.06	60.9	60.96	63.54	63.57	63.48	63.53
6/7/2016 15:15	84.6	84.9	84.2	84.2	81.8	82.4	81.3	81.3	60.95	61.02	60.89	60.94	63.58	63.67	63.5	63.54
6/7/2016 15:20	84.2	84.7	83.6	84.5	81.4	82.1	80.6	82.1	60.92	61.02	60.85	60.9	63.57	63.67	63.48	63.58
6/7/2016 15:25	84.7	84.9	84.5	84.5	81.9	82.2	81.5	81.7	60.94	61.01	60.89	60.91	63.64	63.67	63.6	63.62
6/7/2016 15:30	84.4	84.8	83.9	83.9	81.6	82.1	80.7	80.8	60.94	60.99	60.9	60.9	63.64	63.69	63.51	63.51
6/7/2016 15:35	84.1	84.6	83.7	84.6	81.2	81.9	80.7	81.7	60.88	60.92	60.84	60.87	63.58	63.67	63.5	63.67
6/7/2016 15:40	84.7	85.3	84.2	84.2	81.7	82.6	80.9	81	60.92	60.99	60.85	60.88	63.65	63.75	63.56	63.56
6/7/2016 15:45	84.1	84.4	83.9	84.1	81.1	81.5	80.9	81.5	60.85	60.89	60.81	60.86	63.6	63.64	63.55	63.63
6/7/2016 15:50	84.2	84.4	83.9	84.1	81.4	81.7	81.1	81.4	60.9	60.95	60.85	60.89	63.65	63.69	63.59	63.62
6/7/2016 15:55	83.8	84.2	83.6	84	81.1	81.5	80.7	81.4	60.87	60.91	60.78	60.8	63.61	63.66	63.55	63.61
6/7/2016 16:00	83.6	83.9	83.4	83.6	80.8	81.3	80.3	80.7	60.82	60.85	60.76	60.79	63.58	63.65	63.52	63.56
6/7/2016 16:05	83.5	83.7	83.3	83.5	80.5	81	80.1	80.5	60.77	60.82	60.72	60.77	63.55	63.6	63.49	63.56
6/7/2016 16:10	83.7	84.1	83.4	83.5	80.7	81.1	80.4	80.6	60.79	60.84	60.75	60.77	63.57	63.62	63.52	63.59
6/7/2016 16:15	82.6	83.5	81.8	82.3	79.41	80.5	78.44	79.31	60.7	60.79	60.61	60.65	63.43	63.59	63.3	63.4
6/7/2016 16:20	81.9	82.7	81.3	82.1	79.01	79.99	77.86	79.01	60.65	60.73	60.58	60.69	63.37	63.46	63.25	63.42
6/7/2016 16:25	81.7	82.7	81.1	82.7	78.99	80.3	78.31	80.3	60.65	60.71	60.61	60.7	63.37	63.52	63.29	63.52
6/7/2016 16:30	83.2	83.6	82.7	82.9	80.4	81.1	79.78	79.94	60.75	60.84	60.69	60.8	63.56	63.63	63.5	63.51
6/7/2016 16:35	82.9	83.4	82.5	82.5	79.6	80.3	79	79.03	60.71	60.78	60.67	60.71	63.47	63.54	63.41	63.42
6/7/2016 16:40	82.4	82.8	81.9	81.9	78.89	79.45	78.42	78.46	60.7	60.74	60.64	60.66	63.4	63.49	63.33	63.33
6/7/2016 16:45	81.8	82.1	81.4	81.6	78.16	78.7	77.53	78.05	60.66	60.71	60.61	60.63	63.32	63.38	63.25	63.28
6/7/2016 16:50	81.4	81.8	81.1	81.2	77.63	78.06	77.31	77.34	60.62	60.67	60.56	60.6	63.25	63.32	63.18	63.2
6/7/2016 16:55	81.1	81.5	80.7	80.9	77.34	77.8	76.87	77.06	60.6	60.65	60.55	60.55	63.2	63.26	63.12	63.15
6/7/2016 17:00	81	81.4	80.7	80.8	76.83	77.1	76.54	76.54	60.57	60.65	60.52	60.59	63.13	63.17	63.11	63.14
6/7/2016 17:05	80.7	80.9	80.3	80.3	76.2	76.71	75.54	75.57	60.54	60.61	60.48	60.48	63.04	63.13	62.96	62.98
6/7/2016 17:10	79.97	80.3	79.61	79.67	75.69	76.05	75.49	75.5	60.51	60.57	60.46	60.46	62.95	63.03	62.9	62.93
6/7/2016 17:15	79.46	79.73	79.02	79.02	75.36	75.63	75.04	75.1	60.47	60.53	60.43	60.45	62.9	62.96	62.83	62.85
6/7/2016 17:20	78.92	79.31	78.54	79.15	74.94	75.43	74.59	75.43	60.42	60.46	60.37	60.43	62.83	62.85	62.8	62.84
6/7/2016 17:25	78.42	79.4	77.84	77.96	74.87	75.58	74.44	74.63	60.39	60.46	60.33	60.36	62.8	62.88	62.75	62.79
6/7/2016 17:30	77.76	78.46	77.25	77.29	74.8	75.16	74.34	74.85	60.33	60.39	60.29	60.31	62.77	62.84	62.73	62.81
6/7/2016 17:35	76.95	77.59	76.57	76.57	74.79	75.13	74.54	74.77	60.28	60.34	60.23	60.24	62.76	62.81	62.7	62.74
6/7/2016 17:40	76.11	76.56	75.69	75.8	74.6	74.85	74.2	74.68	60.2	60.25	60.14	60.16	62.7	62.74	62.66	62.71
6/7/2016 17:45	75.52	75.85	75.2	75.4	74.7	74.93	74.39	74.82	60.14	60.18	60.09	60.11	62.7	62.74	62.65	62.69
6/7/2016 17:50	75.15	75.41	74.84	75.11	74.7	75.16	74.14	74.99	60.11	60.14	60.08	60.12	62.69	62.74	62.64	62.74
6/7/2016 17:55	75.18	75.29	74.97	75.16	75.27	75.54	74.91	75.28	60.11	60.16	60.07	60.09	62.76	62.8	62.72	62.73
6/7/2016 18:00	74.83	75.17	74.58	74.58	75.08	75.44	74.61	74.88	60.05	60.11	60.01	60.01	62.7	62.76	62.67	62.71
6/7/2016 18:05	74.36	74.71	73.65	73.65	74.61	75.31	73.22	73.22	60.01	60.05	59.95	59.95	62.65	62.74	62.52	62.54
6/7/2016 18:10	73.38	73.68	73.01	73.63	73.3	73.83	72.67	73.53	59.93	59.97	59.85	59.95	62.48	62.55	62.4	62.52
6/7/2016 18:15	73.35	73.69	73.01	73.03	73.2	73.6	72.8	72.97	59.92	59.96	59.89	59.9	62.48	62.54	62.43	62.43
6/7/2016 18:20	73.16	73.41	72.96	73.2	73	73.37	72.64	73.26	59.89	59.93	59.87	59.91	62.44	62.49	62.39	62.47
6/7/2016 18:25	73.35	73.52	73.14	73.33	73.14	73.38	72.84	72.98	59.91	59.94	59.87	59.89	62.46	62.49	62.41	62.45
6/7/2016 18:30	73.11	73.32	72.88	73.08	72.82	73.24	72.23	72.74	59.89	59.91	59.85	59.89	62.4	62.46	62.35	62.4
6/7/2016 18:35	72.98	73.08	72.77	72.89	72.75	73.07	72.39	72.73	59.86	59.89	59.83	59.86	62.37	62.41	62.31	62.37
6/7/2016 18:40	72.77	72.96	72.43	72.75	72.57	72.81	72.17	72.78	59.82	59.86	59.78	59.82	62.33	62.37	62.29	62.3
6/7/2016 18:45	72.53	72.82	72.21	72.24	72.34	72.79	71.63	72.08	59.79	59.82	59.76	59.77	62.29	62.33	62.21	62.24
6/7/2016 18:50	72.2	72.4	71.91	71.91	72.12	72.48	71.55	71.84	59.77	59.84	59.73	59.75	62.25	62.31	62.2	62.21
6/7/2016 18:55	71.97	72.42	71.7	72.36	72.11	72.76	71.47	72.38	59.72	59.76	59.69	59.74	62.22	62.3	62.16	62.3
6/7/2016 19:00	72.42	72.71	72.23	72.5	72.49	72.86	71.98	72.46	59.74	59.77	59.71	59.74	62.27	62.32	62.24	62.27

Data/Time	Ground Temperatuer								Airflow Velocity											
	4 feet				9.8 feet				Pipe (100 fpm)				Pipe (200 fpm)				Pipe (200 fpm) Surface			
	Avg	Max	Min	Smp	Avg	Max	Min	Smp	Avg	Max	Min	Smp	Avg	Max	Min	Smp	Avg	Max	Min	Smp
6/7/2016 14:30	61.89	61.92	61.83	61.88	56.32	56.35	56.28	56.33	102	106	98	98	200	203	197	198	134	136	132	132
6/7/2016 14:35	61.89	61.94	61.83	61.89	56.34	56.52	56.3	56.32	104	111	93	111	202	207	196	205	135	140	131	138
6/7/2016 14:40	61.88	61.9	61.82	61.87	56.29	56.32	56.26	56.27	105	122	97	117	202	212	196	207	135	143	131	140
6/7/2016 14:45	61.86	61.88	61.84	61.85	56.26	56.28	56.25	56.25	104	113	92	98	202	207	193	200	134	139	128	131
6/7/2016 14:50	61.84	61.86	61.81	61.84	56.24	56.26	56.22	56.24	105	113	97	103	202	207	195	203	135	138	130	134
6/7/2016 14:55	61.82	61.84	61.8	61.82	56.23	56.24	56.2	56.22	105	117	96	102	202	207	196	203	134	138	130	137
6/7/2016 15:00	61.81	61.83	61.79	61.8	56.22	56.24	56.2	56.23	104	111	92	107	202	207	195	202	134	139	129	134
6/7/2016 15:05	61.8	61.82	61.78	61.81	56.22	56.23	56.2	56.21	106	125	94	110	203	217	195	206	135	147	130	137
6/7/2016 15:10	61.79	61.81	61.77	61.79	56.2	56.23	56.19	56.2	104	118	96	101	202	211	195	200	134	140	130	133
6/7/2016 15:15	61.78	61.8	61.77	61.78	56.2	56.2	56.17	56.18	104	121	90	107	202	212	193	203	134	142	127	136
6/7/2016 15:20	61.78	61.8	61.77	61.77	56.19	56.21	56.17	56.17	106	116	98	105	203	208	198	200	135	139	132	135
6/7/2016 15:25	61.77	61.79	61.76	61.77	56.18	56.2	56.17	56.19	105	112	96	106	202	210	195	203	135	141	131	135
6/7/2016 15:30	61.77	61.79	61.76	61.77	56.18	56.19	56.16	56.17	106	119	97	103	202	211	195	201	135	142	131	134
6/7/2016 15:35	61.76	61.79	61.74	61.76	56.17	56.19	56.15	56.16	105	115	94	105	202	210	193	203	135	141	129	135
6/7/2016 15:40	61.76	61.77	61.74	61.75	56.16	56.18	56.15	56.15	103	114	95	101	201	207	194	198	133	139	128	133
6/7/2016 15:45	61.75	61.77	61.73	61.75	56.16	56.17	56.14	56.15	102	113	94	98	201	207	196	196	134	138	130	130
6/7/2016 15:50	61.75	61.77	61.73	61.74	56.15	56.17	56.13	56.15	106	119	95	107	201	208	193	201	134	139	127	133
6/7/2016 15:55	61.74	61.76	61.73	61.73	56.14	56.15	56.12	56.12	106	122	96	103	201	211	194	202	133	142	128	133
6/7/2016 16:00	61.73	61.75	61.7	61.73	56.13	56.14	56.11	56.13	104	114	96	105	201	207	197	203	134	138	129	135
6/7/2016 16:05	61.72	61.74	61.71	61.71	56.12	56.14	56.1	56.12	103	114	91	97	200	208	194	197	133	138	129	131
6/7/2016 16:10	61.72	61.74	61.7	61.72	56.11	56.13	56.1	56.11	103	110	89	104	200	204	189	201	133	136	126	133
6/7/2016 16:15	61.72	61.74	61.7	61.72	56.11	56.12	56.09	56.1	104	112	94	97	200	205	189	196	134	139	127	133
6/7/2016 16:20	61.73	61.74	61.71	61.73	56.11	56.12	56.09	56.11	103	112	88	105	200	206	189	202	134	139	126	134
6/7/2016 16:25	61.72	61.74	61.7	61.71	56.1	56.12	56.09	56.1	105	116	92	98	201	207	193	198	135	140	129	132
6/7/2016 16:30	61.72	61.73	61.7	61.72	56.1	56.13	56.09	56.11	103	118	75	104	200	209	180	200	133	139	120	134
6/7/2016 16:35	61.72	61.73	61.7	61.71	56.1	56.11	56.08	56.09	102	110	91	109	201	206	191	206	134	140	127	140
6/7/2016 16:40	61.71	61.73	61.7	61.71	56.09	56.11	56.07	56.08	104	114	97	105	202	206	199	203	136	141	133	136
6/7/2016 16:45	61.71	61.74	61.7	61.71	56.09	56.11	56.08	56.1	105	113	94	112	202	206	195	204	137	141	130	141
6/7/2016 16:50	61.71	61.73	61.69	61.71	56.09	56.11	56.07	56.1	104	113	93	107	201	208	191	204	136	140	131	136
6/7/2016 16:55	61.7	61.73	61.69	61.7	56.09	56.11	56.07	56.08	105	123	96	105	202	212	194	202	136	144	129	138
6/7/2016 17:00	61.7	61.72	61.69	61.7	56.08	56.1	56.07	56.09	106	120	97	105	202	208	196	199	137	143	133	138
6/7/2016 17:05	61.69	61.71	61.68	61.69	56.07	56.09	56.06	56.06	104	114	97	98	200	208	193	196	136	142	131	133
6/7/2016 17:10	61.69	61.71	61.67	61.68	56.07	56.08	56.05	56.07	105	120	92	103	200	207	191	197	136	141	128	134
6/7/2016 17:15	61.68	61.7	61.66	61.7	56.06	56.08	56.04	56.05	106	118	93	106	199	208	193	199	136	143	130	136
6/7/2016 17:20	61.67	61.7	61.64	61.67	56.05	56.07	56.03	56.04	105	113	94	102	200	204	194	198	137	141	131	135
6/7/2016 17:25	61.66	61.68	61.65	61.67	56.04	56.06	56.03	56.05	105	120	88	103	199	204	187	197	136	141	129	134
6/7/2016 17:30	61.67	61.69	61.65	61.66	56.04	56.05	56.02	56.05	105	114	97	111	199	204	192	202	137	141	131	140
6/7/2016 17:35	61.66	61.68	61.65	61.67	56.03	56.05	56.01	56.03	106	116	92	107	199	205	191	198	137	141	130	136
6/7/2016 17:40	61.66	61.68	61.64	61.66	56.02	56.04	56	56.01	105	117	89	101	198	205	186	195	135	140	126	135
6/7/2016 17:45	61.65	61.66	61.63	61.63	56.01	56.03	56	56	106	117	99	103	198	203	193	198	136	140	131	135
6/7/2016 17:50	61.64	61.65	61.62	61.64	56	56.03	55.99	56.01	108	122	103	119	200	209	195	205	137	143	133	140
6/7/2016 17:55	61.63	61.65	61.61	61.62	55.99	56.02	55.97	55.98	108	121	99	109	200	206	192	200	137	141	131	135
6/7/2016 18:00	61.61	61.63	61.59	61.6	55.95	55.98	55.93	55.94	106	115	96	112	198	204	191	198	135	140	129	136
6/7/2016 18:05	61.6	61.62	61.58	61.61	55.93	55.96	55.9	55.93	108	112	100	107	200	204	193	200	136	141	131	139
6/7/2016 18:10	61.61	61.63	61.59	61.63	55.94	55.96	55.92	55.96	109	121	98	107	199	209	191	199	138	144	131	137
6/7/2016 18:15	61.63	61.65	61.61	61.65	55.96	55.99	55.94	55.98	107	112	100	103	198	203	193	195	137	140	133	135
6/7/2016 18:20	61.64	61.66	61.62	61.64	55.98	56.01	55.97	55.97	108	115	101	107	198	202	194	198	138	142	133	139
6/7/2016 18:25	61.64	61.66	61.63	61.64	55.99	56.01	55.97	55.99	107	116	92	108	199	203	191	199	137	141	131	138
6/7/2016 18:30	61.65	61.66	61.63	61.65	55.99	56.01	55.97	55.97	108	118	100	108	199	205	195	198	138	142	134	136
6/7/2016 18:35	61.63	61.66	61.61	61.63	55.98	56.01	55.96	55.99	108	120	103	109	199	206	194	198	138	145	135	137
6/7/2016 18:40	61.63	61.65	61.61	61.63	55.97	56	55.95	55.95	108	117	97	106	198	204	191	197	137	143	132	136
6/7/2016 18:45	61.62	61.64	61.6	61.64	55.96	55.99	55.95	55.98	107	114	100	109	199	204	192	199	138	141	131	138
6/7/2016 18:50	61.63	61.65	61.6	61.62	55.96	55.98	55.94	55.97	111	133	102	111	200	223	193	201	140	157	135	142
6/7/2016 18:55	61.63	61.65	61.6	61.64	55.96	55.98	55.94	55.95	110	121	98	111	199	205	191	200	138	145	130	138
6/7/2016 19:00	61.63	61.64	61.61	61.63	55.95	55.97	55.93	55.94	110	117	103	108	199	205	193	198	139	142	134	136

Figure 4-4: GCV System Performance at Solar CM House

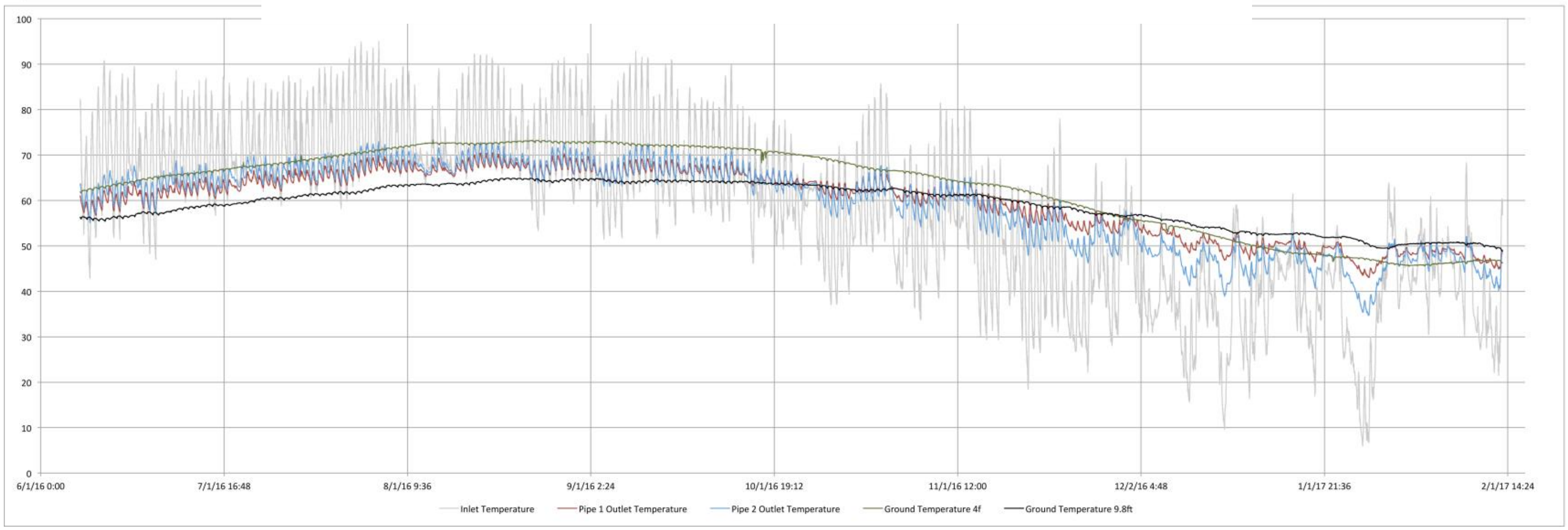

Chapter 5: CFD and GAEA Model for the Solar CM House

This chapter discusses simulating the GCV system at the Solar CM House using CFD and GAEA to see how well the tool predicted the outlet temperature. The chapter begins by describing the CFD model, followed by the GAEA model. Finally, the results from these models were compared with the actual GCV system.

5.1 CFD Model for the Solar CM House

5.1.1 Finding the Appropriate CFD Program

Many CFD programs with a variety of uses and characteristics are available at this time. Table 17 compares the features of several CFD programs (STAR-CCM+, Ansys CFX, Fluent, AcuSolve, and Autodesk CFD). This comparison indicates that Autodesk CFD was the most appropriate for the research project based on its features and the previously presented validation (ANSYS Inc., 2010; Autodesk CFD, 2016; CD-adapco, 2015).

Table 17: CFD Software Comparison

Variables		CD-Adapco STAR-CCM+	Ansys CFX	Ansys Fluent	ACUSIM AcuSolve	Autodesk CFD
Application	General	●	●	●	●	●
	Chemical	●	●	●	●	●
	Aerospace	●	●	●	●	●
	Architectural	●	●	●	●	●
	User-friendly					●
	Other	●	●	●	●	●
Modeling	Software Included	●		●		
	Separate bundle		●		●	●
Meshing Method	2D Meshes	●	●	●	●	●
	3D Meshes	●	●	●	●	●
Boundary conditions	Heat transfer	●	●	●	●	●
	Flux	●	●	●		●
	Radiation	●	●	●	●	●
	Turbulence	●	●	●	●	●
	Convection	●	●	●		●
Custom	Add new codes	●	●	●		●
	Adjust current codes	●	●			●
Misc.	Free license					●
	free customer support					●
	Import/export files	●	●	●	●	●
	Library	●	●	●	●	●
	Tutorials	●	●	●		●
	Special hardware requirements				●	

Autodesk CFD Features

This software met this research's needs on several levels:

Application:

Autodesk CFD implements fluid flow and heat transfer between solids and fluids. The software interface is user-friendly, particularly for an architect. The best feature of this application is that it is compatible with much of the Autodesk software. Thus, the mobility between these applications captures model parts and material properties from a CAD file.

Modeling:

Modeling in Autodesk CFD can be imported from any CAD file. Because Autodesk has specific CAD modeling software (such as AutoCAD, Revit, and Autodesk Inventor), Autodesk CFD does not create models on its own. A model can be exported from any Autodesk software, and Autodesk CFD recognizes model parts and material properties (which helps reduce the time needed to assign parts and material before simulation when there are many models to simulate). Autodesk CFD also is able to generate volume parts, which can be attached to the CAD model using fill and cap functions.

Meshing:

Autodesk CFD uses a triangular mesh shape, which can be generated automatically or manually. The mesh size can be applied to the entire model or to a specific part. Autodesk CFD can determine the mesh size for each part of the model automatically based on the size and domain, which was sufficiently fine enough to solve the simulation problem in this case.

Boundary conditions:

Boundary conditions of Autodesk CFD cover all heat transfer (convection, conduction, and radiation) that was used to determine heat exchange in the GCV system. Boundary conditions can be applied to a part or to a surface and take one or more of the conditions listed in Table 18.

Table 18: Boundary Condition Types

Boundary Conditions			
Velocity	Temperature	Quality	External fan
Rotational velocity	Slip/symmetry	Heat flux	Current
Volume flow rate	Unknown	Total heat flux	Voltage
Mass flow rate	Scalar	Film coefficient	Periodic
Pressure	Humidity	Radiation	Transparent

Customizing:

The user can create and modify codes using algorithms in Autodesk CFD and can use templates and rules to automatically assign materials and boundaries to parts and surfaces for model input. This feature helped save time during the research by automatically providing variable input before simulation.

Processing:

Autodesk CFD works only with Windows operating system and is purported to have a powerful processor and random access memory (RAM) for simulation processing. The hardware can limit the simulation solver based on hardware features (or lack thereof). Conversely, Autodesk provides a cloud solver for large simulations. The student license has one hundred free cloud solvers and, thereafter, the user can purchase a package of additional cloud simulations. The hardware that was used in this research had sufficient capability to carry out the simulation.

Post simulation:

The software performs the post simulation in two steps: by solving fluid flow and then heat transfer. While performing the post simulation, the user can visualize both fluid flow and heat transfer, so if there is any problem or an adjustment is needed, the user can stop or modify the simulation. After the post simulation, Autodesk CFD presents the results visually and in charts. The visual results show fluid flow and heat transfer from the simulation in 2D and 3D, giving an idea of the relation between parts and surfaces in the simulation as well as a comparison between different designs. The chart results show the physical property data for parts and surfaces—for example, minimum, maximum, and mean temperatures are given for a specific part.

Supportive elements:

Autodesk offers a free student license for Autodesk CFD with full software features, whereas the other software described above do not. It also provides self-learning tutorials and an Autodesk community to support and answer questions about using the software. The software contains libraries of fluids and materials that make it possible to add and customize material properties.

5.1.2 Simulation of the GCV System at the Solar CM House

The GCV system at the Solar CM House was simulated based on certain boundary conditions that ensured proper thermal behavior that matched the existing GCV system. The boundary conditions can be divided into four broad categories: air, pipe, backfill, and soil domains. These boundaries allowed for accurate measurements of air and ground temperature, pipe type/thickness, and backfill type/thickness. Table 19 shows the boundary condition for each variable.

The system simulated previously by Alghamdi (2008) included 12 models in which different boundary variables were used to validate the system's performance. Only one model (the mixed model in Table 20) was able to replicate the GCV system's results. Thus, the boundary conditions for this model were used for the simulation in Autodesk CFD.

Table 19: Boundary Conditions Domain Variables and Materials

Domain	Variables
Air	
	Turbulence
	Heat transfer
	Thermal radiation
	Inlet temperature
	Inlet pressure
	Inlet velocity
	Outlet momentum
	Outlet pressure
Pipe	
	Inlet temperature
	Heat transfer
	Thermal radiation
	Roughness
	Thickness
	Diameter
	Material
	Shape
	Length
	Depth
Backfill	
	Inlet temperature
	Heat transfer
	Thermal radiation
	Thickness
	Type
Soil	
	Type
	Land cover
	Inlet temperature
	Heat transfer
	Thermal radiation
	Face A heat transfer
	Face B heat transfer
	Face C heat transfer
	Face D heat transfer
	Face E heat transfer

Figure 5-1: Soil Domain Faces Location

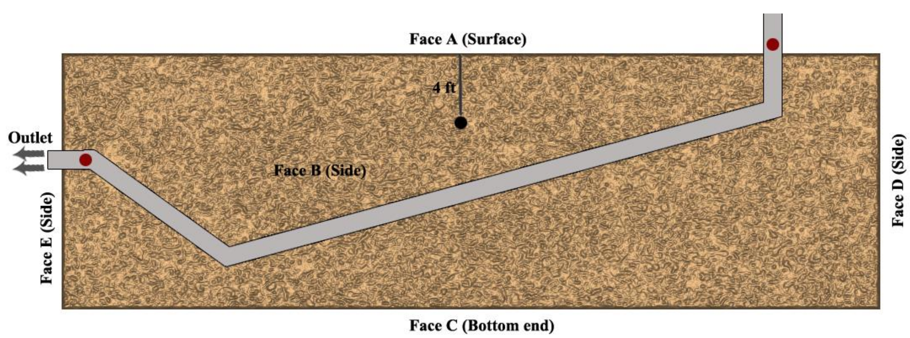

Table 20: Mixed Model (Alghamdi, 2008)

Domain	Elements	Variables
Air		
	Turbulence	**Laminar (none)**
	Heat transfer	Total energy
	Thermal radiation	None
	Inlet temperature	From site data (inlet)
	Inlet pressure	1 Pa
	Inlet velocity	100 fpm
	Outlet momentum	Average static pressure
	Outlet pressure	Average over whole outlet
Pipe		
	Inlet temperature	From site data (soil probe)
	Heat transfer	Thermal energy
	Thermal radiation	None
	Roughness	**Smooth**
Backfill		
	Inlet temperature	From site data (soil probe)
	Heat transfer	Thermal energy
	Thermal radiation	None
	Thickness	**10”**
Soil		
	Inlet temperature	From site data (soil probe)
	Heat transfer	Thermal energy
	Thermal radiation	None
	Face A heat transfer	**Temperature from site data (surface temperature)**
	Face B heat transfer	Adiabatic
	Face C heat transfer	**Temperatuer13.5’ depth soil temperature (CFD simulation)**
	Face D heat transfer	Adiabatic
	Face E heat transfer	Adiabatic

The GCV system model was simulated using a steady-state rather than a transient simulation. This is because, even though the transient simulation captures heat transfer and fluid flow in seconds, it requires considerable simulation time and the results would have been in excess of the research needs. Moreover, the temperature change in the GCV system is not sufficiently significant to warrant collecting temperature changes every minute. Figure 5-2 shows steady state and transient simulation for outlet air and ground temperautre. Because of the limited time available for this research, a steady-state simulation was used to capture heat transfer and fluid flow, which fulfilled the research needs. The boundary conditions domain and material physical properties assumptions were based on Alghamdi's (2008) simulation outcomes, Solar CM House documents, and drawings found in Table 21. Air in the simulation was based on the in-situ measure of airflow and inlet air temperature. The assumed properties of the pipe and backfill were used to determine heat exchange between air and soil. The soil domain used in-situ soil temperature, since the ground temperature varies with depth (Riley, 1984).

The GCV model was simulated at different times of the year to ensure that the simulated performance results matched those of the actual system. The system was simulated for three days (a total of 72 times), as shown in Table 22. These days and times were chosen to represent the performance of the GCV system during both hot and cold seasons, as well as daily changes in the maximum and minimum air temperature. The criteria chosen for these days were based on the weather stability in the days before and after to ensure that no factors, such as rain or storms, affected the performance of the system.

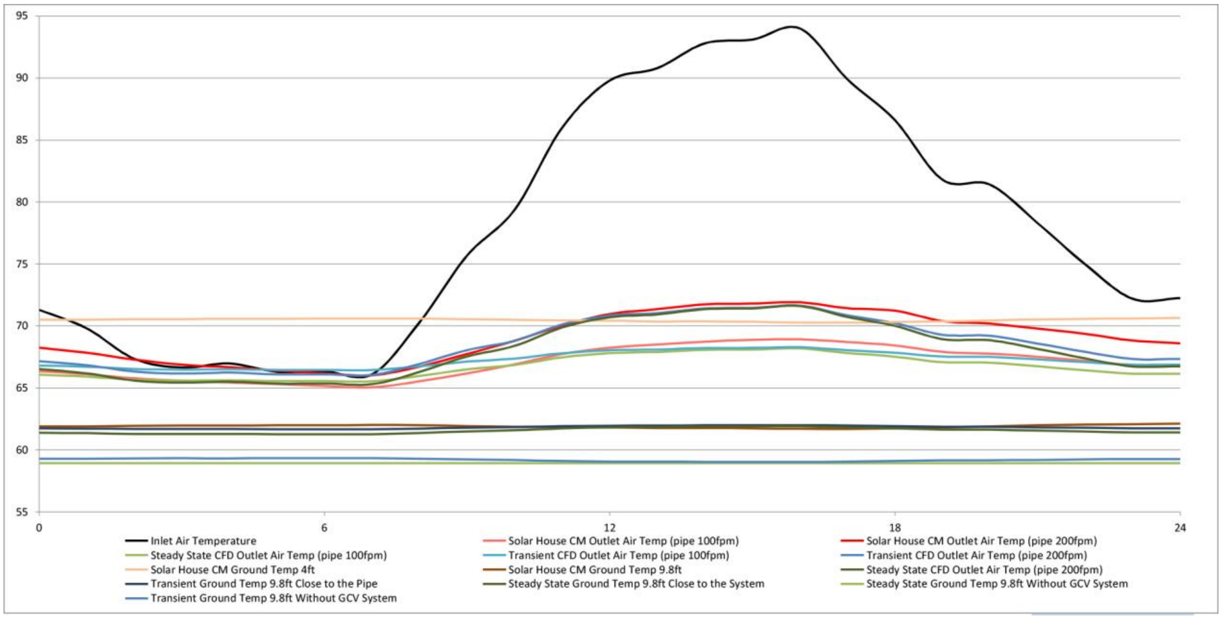

Figure 5-2: Steady State and Transient Simulation for Outlet Air and Ground Temperature on July 24th

Table 21: Boundary Conditions Domain and Physical Properties Assumption for the GCV System

Domain	Elements	Variables	
Air		**Pipe 1**	**Pipe 2**
	Turbulence	k-epsilon	k-epsilon
	Heat transfer	Total energy	Total energy
	Thermal radiation	None	None
	Inlet temperature	From site data (inlet)	From site data (inlet)
	Inlet pressure	Automatic	Automatic
	Inlet velocity	100 fpm	200 fpm
	Outlet momentum	Average static pressure	Average static pressure
	Outlet pressure	Average over whole outlet	Average over whole outlet
	Density	Equation of state	Equation of state
	Conductivity	0.02563 w/m-k	0.02563 w/m-k
	Specific heat	1004 J/kg-k	1004 J/kg-k
	Viscosity	3.79148e-07 lbf-s/ft2	3.79148e-07 lbf-s/ft2
Pipe			
	Heat transfer	Thermal energy	Thermal energy
	Thermal radiation	None	None
	Thickness	As built	As built
	Diameter	As built	As built
	Material	Clay	Clay
	Shape	Cylinder	Cylinder
	Length	As built	As built
	Depth	As built	As built
	Conductivity	1.2 w/m-k	1.2 w/m-k
	Specific heat	900.16 J/kg-k	900.16 J/kg-k
	Density	2 g/cm3	2 g/cm3
Backfill			
	Heat transfer	Thermal energy	Thermal energy
	Thermal radiation	None	None
	Thickness	As built	As built
	Type	Gravel	Gravel
	Conductivity	0.7 w/m-k	0.7 w/m-k
	Specific heat	932 J/kg-k	932 J/kg-k
	Density	2 g/cm3	2 g/cm3
Soil			
	Type	Ultisols	
	Land cover	Mown grass	
	Heat transfer	Thermal energy	
	Thermal radiation	None	
	Conductivity	1.2975 w/m-k	
	Specific heat	962.96 J/kg-k	
	Density	2.4 g/cm3	
	Emissivity	0.92	
	Face 1 heat transfer	Temperature at surface from site data	
	Face 2 heat transfer	Temperature at 13.12' from site data	
	Face 3 heat transfer	Heat flux = 0 BTU/ft2/min	
	Face 4 heat transfer	Heat flux = 0 BTU/ft2/min	
	Face 5 heat transfer	Heat flux = 0 BTU/ft2/min	
	Face 6 heat transfer	Heat flux = 0 BTU/ft2/min	

Table 22: Simulation Days and Times

	GCV System at Solar House CM			Solar House CM Outlet Air Temp (°F)	
Date and Time	Inlet Air Temperature	Ground Temp 4ft	Ground Temp 9.8ft	Pipe 100 fpm	Pipe 200 fpm
7/24/2016 0:00	71.3	70.49	61.89	66.36	68.24
7/24/2016 1:00	69.81	70.5	61.9	66.11	67.84
7/24/2016 2:00	67.35	70.54	61.94	65.78	67.29
7/24/2016 3:00	66.65	70.55	61.96	65.59	66.88
7/24/2016 4:00	66.97	70.58	61.97	65.44	66.67
7/24/2016 5:00	66.31	70.58	61.99	65.3	66.41
7/24/2016 6:00	66.35	70.59	61.99	65.16	66.18
7/24/2016 7:00	66.1	70.61	62.02	65.05	66.02
7/24/2016 8:00	70.3	70.59	61.99	65.54	66.73
7/24/2016 9:00	75.68	70.54	61.93	66.18	67.75
7/24/2016 10:00	79.38	70.49	61.88	66.9	68.8
7/24/2016 11:00	86	70.46	61.85	67.73	70.03
7/24/2016 12:00	89.8	70.43	61.82	68.25	70.96
7/24/2016 13:00	90.8	70.36	61.78	68.51	71.35
7/24/2016 14:00	92.8	70.37	61.78	68.74	71.74
7/24/2016 15:00	93.1	70.34	61.75	68.89	71.81
7/24/2016 16:00	94	70.28	61.71	68.93	71.91
7/24/2016 17:00	89.9	70.26	61.69	68.7	71.43
7/24/2016 18:00	86.6	70.32	61.74	68.43	71.23
7/24/2016 19:00	81.8	70.37	61.81	67.91	70.4
7/24/2016 20:00	81.4	70.45	61.89	67.77	70.19
7/24/2016 21:00	78.3	70.53	61.99	67.52	69.79
7/24/2016 22:00	74.98	70.58	62.04	67.18	69.36
7/24/2016 23:00	72.19	70.61	62.08	66.85	68.82
7/24/2016 23:55	72.25	70.64	62.12	66.74	68.61
10/25/2016 0:00	46.52	66.27	61.96	60.8	58.72
10/25/2016 1:00	46.08	66.24	61.95	60.6	58.37
10/25/2016 2:00	43.33	66.23	61.94	60.31	57.81
10/25/2016 3:00	43.09	66.22	61.95	60.23	57.54
10/25/2016 4:00	40.98	66.21	61.96	60.02	57.03
10/25/2016 5:00	40.94	66.21	61.95	59.87	56.76
10/25/2016 6:00	40.03	66.22	61.93	59.67	56.47
10/25/2016 7:00	38.08	66.21	61.92	59.48	55.99
10/25/2016 8:00	37.02	66.21	61.95	59.26	55.64
10/25/2016 9:00	42.1	66.17	61.88	59.52	56.16
10/25/2016 10:00	49.98	66.09	61.83	60.43	57.6
10/25/2016 11:00	57.35	66.01	61.76	61.02	58.76
10/25/2016 12:00	58.58	65.95	61.7	61.43	59.35
10/25/2016 13:00	63.48	65.9	61.62	61.86	60.3
10/25/2016 14:00	64.44	65.85	61.57	62.27	60.96
10/25/2016 15:00	66.65	65.82	61.55	62.54	61.48
10/25/2016 16:00	65.63	65.75	61.49	62.5	61.52
10/25/2016 17:00	63.57	65.74	61.46	62.24	61.39
10/25/2016 18:00	57.51	65.86	61.6	61.88	60.63
10/25/2016 19:00	53.32	65.97	61.76	61.31	59.81
10/25/2016 20:00	50.17	66.04	61.81	60.98	59.11
10/25/2016 21:00	47.4	66.05	61.82	60.73	58.61
10/25/2016 22:00	45.73	66.05	61.83	60.37	57.94
10/25/2016 23:00	41.69	66.04	61.81	60	57.2
10/25/2016 23:55	41.04	66.04	61.81	59.85	56.84
12/20/2016 0:00	26.21	50.42	53.13	48.41	43.51
12/20/2016 1:00	25.12	50.39	53.1	48.29	43.28
12/20/2016 2:00	24.77	50.38	53.1	48.18	43.11
12/20/2016 3:00	23.83	50.38	53.08	48.09	42.93
12/20/2016 4:00	22.89	50.35	53.1	47.95	42.71
12/20/2016 5:00	21.16	50.35	53.09	47.78	42.28
12/20/2016 6:00	19.51	50.33	53.09	47.46	41.97
12/20/2016 7:00	18.72	50.32	53.09	47.31	41.72
12/20/2016 8:00	17.95	50.31	53.08	47.1	41.49
12/20/2016 9:00	16.78	50.3	53.05	46.88	41.22
12/20/2016 10:00	22.2	50.26	53.02	47.3	41.91
12/20/2016 11:00	27.31	50.2	52.91	47.94	42.68
12/20/2016 12:00	31.51	50.14	52.88	48.41	43.52
12/20/2016 13:00	37.01	50.09	52.83	48.96	44.52
12/20/2016 14:00	38.82	50.01	52.72	49.23	44.95
12/20/2016 15:00	43.29	49.93	52.65	49.67	45.85
12/20/2016 16:00	44.74	49.87	52.58	49.93	46.36
12/20/2016 17:00	43.66	49.87	52.59	49.83	46.46
12/20/2016 18:00	38.1	49.97	52.7	49.44	45.82
12/20/2016 19:00	33.79	50.08	52.8	49.04	45.13
12/20/2016 20:00	30.11	50.12	52.85	48.76	44.54
12/20/2016 21:00	27.59	50.14	52.89	48.52	44.05
12/20/2016 22:00	26.46	50.14	52.9	48.36	43.67
12/20/2016 23:00	28.22	50.15	52.91	48.37	43.75
12/20/2016 23:55	27.89	50.14	52.9	48.33	43.63

CFD Simulation Processing

The simulation followed several steps from modeling the system to visualizing the results. Figure 5-3 shows the simulation steps using the Autodesk CFD software.

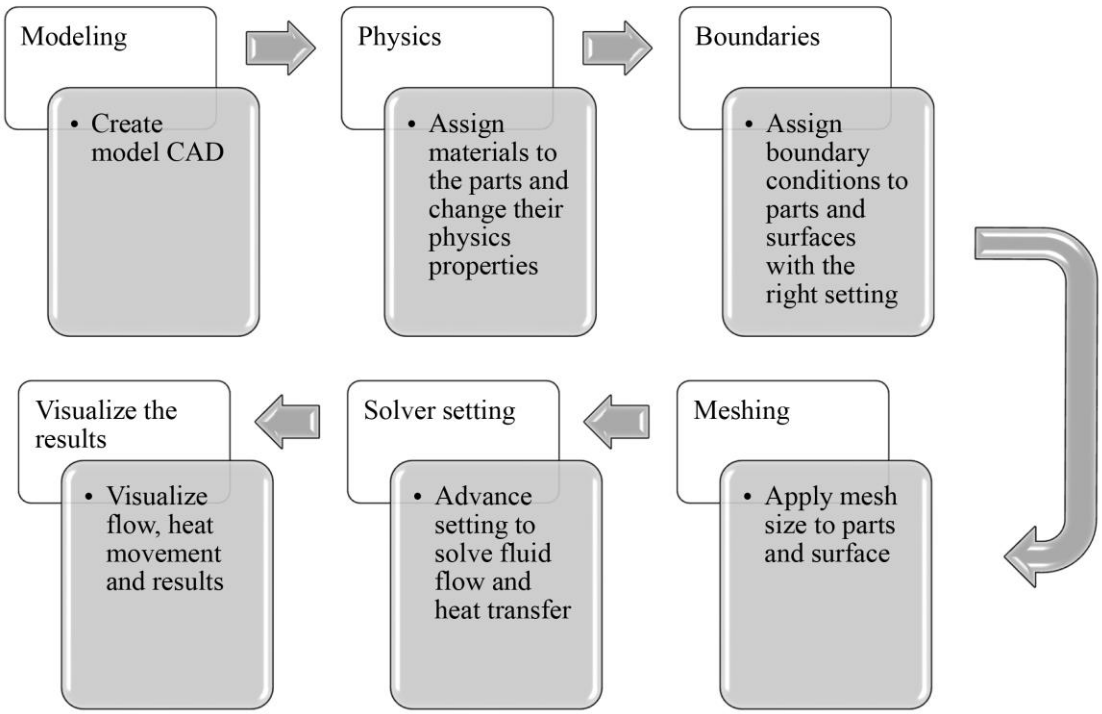

Figure 5-3: CFD Processing

Modeling:

The GCV system modeled used AutoCAD and Inventor Autodesk. The dimensions of the GCV system at the Solar CM House can be found in Figure 5-4. Modeling using Inventor Autodesk helped Autodesk CFD recognize parts and surfaces of the CAD after the file was imported. Additionally, if the CAD model needed minor adjustments, Autodesk CFD can, for example, build volumes to cap the fluid opening using the Void Fill tool (Figure 5-5).

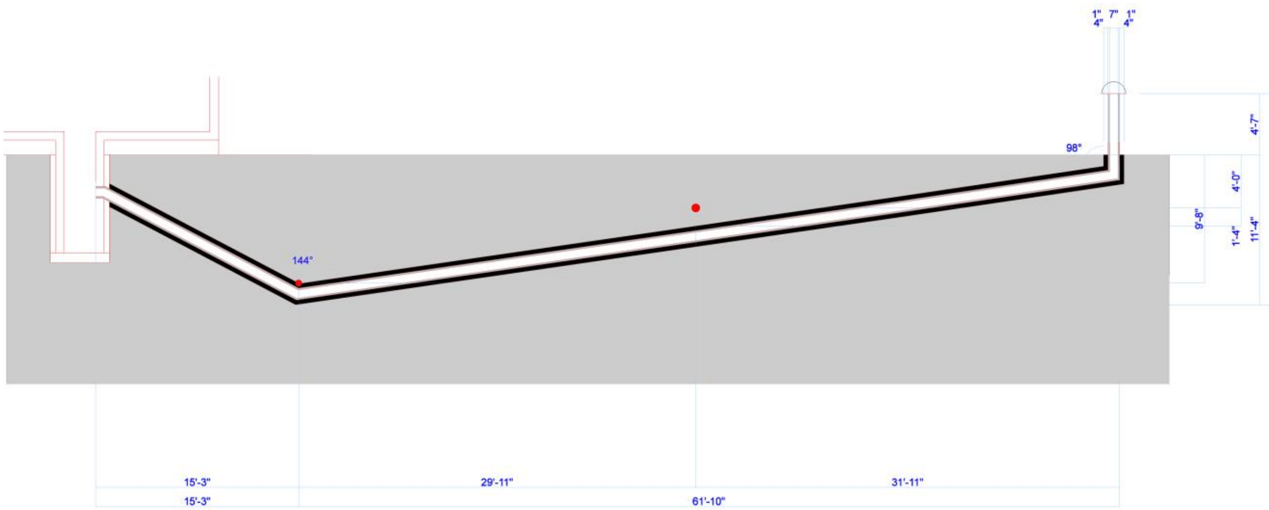

Figure 5-4: Solar CM House Section Dimensions

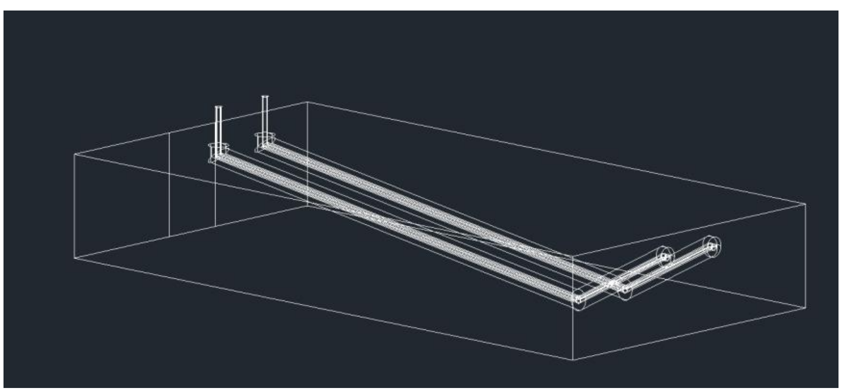

Figure 5-5: Modeling a GCV System in an AutoCAD Program

Physics:

At this point, it was necessary to determine the physical material of the elements. The physical material can be modified in terms of density, viscosity, conductivity, and emissivity (Figure 5-6). The assumed material properties for the Solar CM House used in the research can be found in Table 23.

Table 23: Solar CM House Model Material Properties Assumptions

Material	Density	Thermal Conductivity	Specific heat capacity
Soil	2.4 g/cm3	1.2975 w/m-k	962.96 J/kg-k
Gravel	2 g/cm3	0.7 w/m-k	932 J/kg-k
Vitrified clay	2 g/cm3	1.2 w/m-k	900.16 J/kg-k

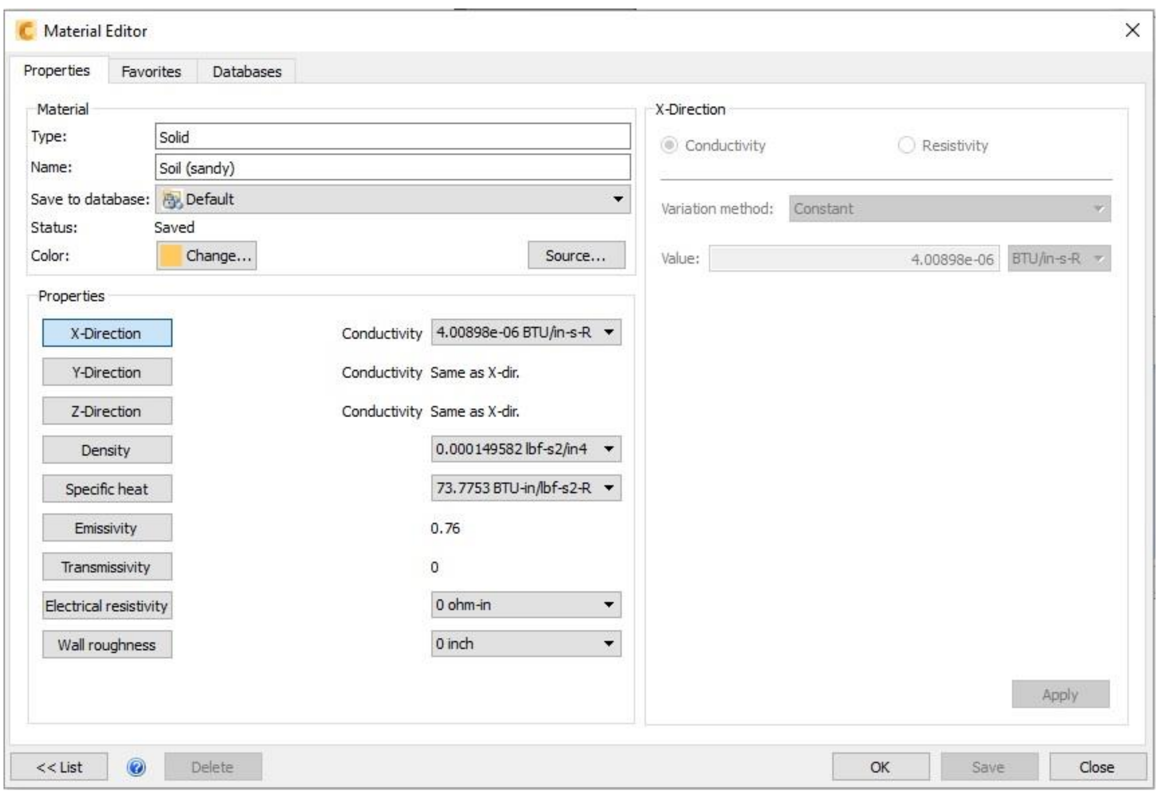

Figure 5-6: Physics Settings

Boundary conditions:

Autodesk CFD sets the boundary types early in the workflow to generate the mesh and provides different types of boundaries (Table 24). Accordingly, the boundary conditions for the GCV model were set for parts and surfaces. The air boundary depends on the inlet temperature from the in-situ measurements and a pressure boundary for the outlet. The boundary condition for the soil temperature was set from the in-situ data on the ground surface and 13.12 ft. deep to capture the soil temperature changes with depth. The Solar CM House model boundary types can be found in Table 25.

Table 24: Boundary Condition Types

Boundary Conditions			
Velocity	Temperature	Quality	External fan
Rotational velocity	Slip/symmetry	Heat flux	Current
Volume flow rate	Unknown	Total heat flux	Voltage
Mass flow rate	Scalar	Film coefficient	Periodic
Pressure	Humidity	Radiation	Transparent

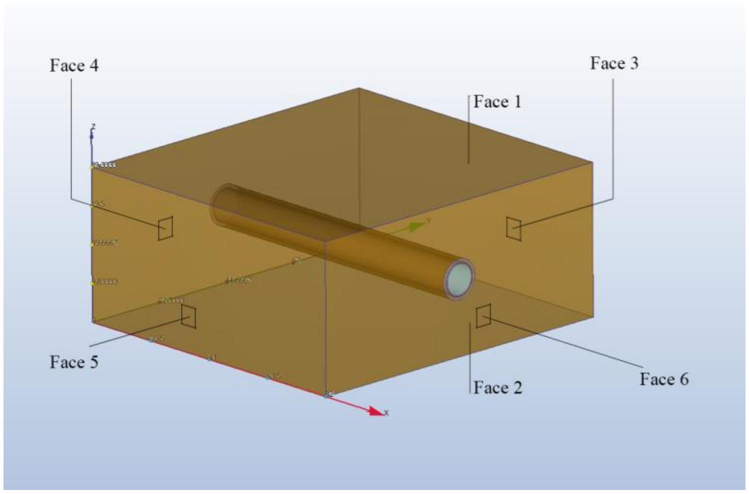

Figure 5-7: Soil Face Domain

Table 25: GCV System Boundary Conditions

Domain	Elements	Variables	
Air		Pipe 1	Pipe 2
	Turbulence	k-epsilon	k-epsilon
	Heat transfer	Total energy	Total energy
	Thermal radiation	None	None
	Inlet temperature	From site data (inlet)	From site data (inlet)
	Inlet pressure	Automatic	Automatic
	Inlet velocity	100 fpm	200 fpm
	Outlet momentum	Average static pressure	Average static pressure
	Outlet pressure	Average over whole outlet	Average over whole outlet
	Density	Equation of state	Equation of state
	Conductivity	0.02563 w/m-k	0.02563 w/m-k
	Specific heat	1004 J/kg-k	1004 J/kg-k
	Viscosity	3.79148e-07 lbf-s/ft2	3.79148e-07 lbf-s/ft2
Pipe			
	Heat transfer	Thermal energy	Thermal energy
	Thermal radiation	None	None
	Thickness	As built	As built
	Diameter	As built	As built
	Material	Clay	Clay
	Shape	Cylinder	Cylinder
	Length	As built	As built
	Depth	As built	As built
	Conductivity	1.2 w/m-k	1.2 w/m-k
	Specific heat	900.16 J/kg-k	900.16 J/kg-k
	Density	2 g/cm3	2 g/cm3
Backfill			
	Heat transfer	Thermal energy	Thermal energy
	Thermal radiation	None	None
	Thickness	As built	As built
	Type	Gravel	Gravel
	Conductivity	0.7 w/m-k	0.7 w/m-k
	Specific heat	932 J/kg-k	932 J/kg-k
	Density	2 g/cm3	2 g/cm3
Soil			
	Type	Ultisols	
	Land cover	Mown grass	
	Heat transfer	Thermal energy	
	Thermal radiation	None	
	Conductivity	1.2975 w/m-k	
	Specific heat	962.96 J/kg-k	
	Density	2.4 g/cm3	
	Emissivity	0.92	
	Face 1 heat transfer	Temperature at surface from site data	
	Face 2 heat transfer	Temperature at 13.12' from site data	
	Face 3 heat transfer	Heat flux = 0 BTU/ft2/min	
	Face 4 heat transfer	Heat flux = 0 BTU/ft2/min	
	Face 5 heat transfer	Heat flux = 0 BTU/ft2/min	
	Face 6 heat transfer	Heat flux = 0 BTU/ft2/min	

Meshing:

Autodesk CFD generates mesh sizing both automatically and manually. According to Kuzmin (2014), the best strategy in meshing is to begin with large-sized base mesh, so that the simulation will not take a long time and will fix the surface mesh in advanced if there is any necessary preparation. Then, Kuzmin recommends setting the basic mesh size to a small number (fine mesh) to make the simulation results more accurate, particularly for the part that the research is interested in and so that the joints between the materials capture heat transfer (Figure 5-8).

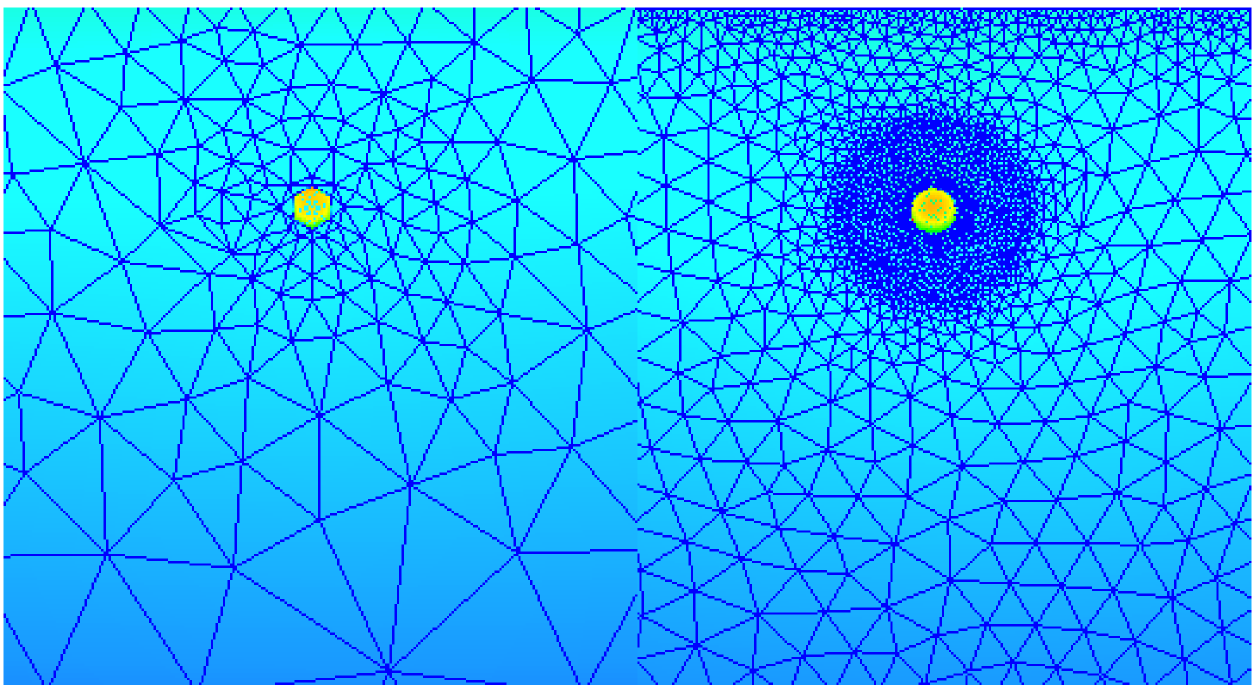

Figure 5-8: Meshing Size

Solver setting:

The solver setting provides more adjustments to the physics of the materials, such as the under-relaxation factor for the segregated flow, radiation depending on the location, and time steps for the simulation. Autodesk CFD performs the simulation in two stages: the first for fluid flow and the second for heat transfer (Figure 5-9).

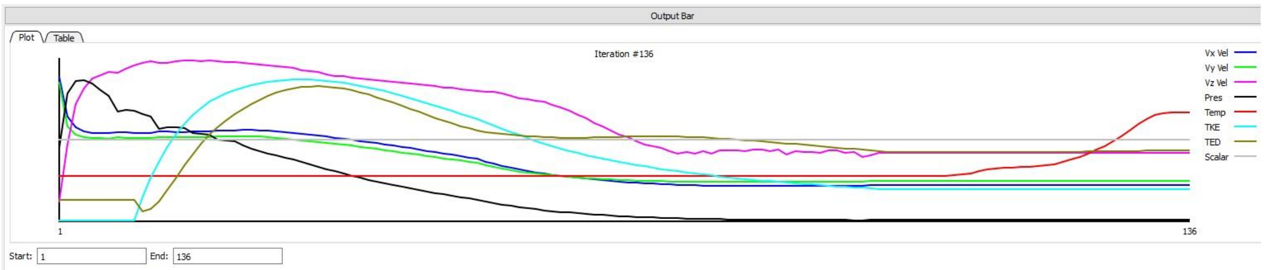

Figure 5-9: Solver Convergence Plot

Visualizing the results:

The last step is to show the fluid flow and heat transfer move in the model. One of the advantages of Autodesk CFD is that it has excellent tools to visualize the results. Moreover, it shows the results for pressure or heat transfer, where the results can be compared between different models. All of these steps were applied to the Solar CM House model for three days (72 hours) to observe the performance of the simulation.

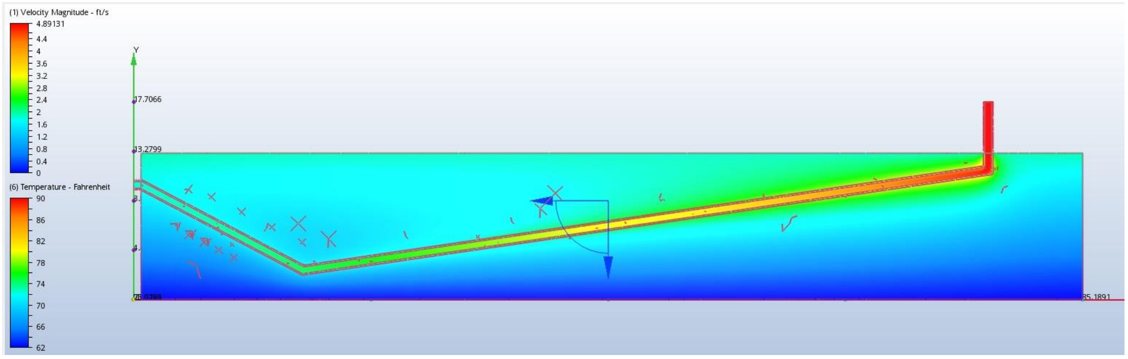

Figure 5-10: Heat Transfer Results in GCV System

Simulation Results

The following figures show the predictions of the CFD simulations with the in-situ data from the GCV system at the Solar CM House on the following days: Jul 24th, Oct 25th and Dec 20th in 2016. Table 26 shows the results (Figure 5-11, Figure 5-12, and Figure 5-13).

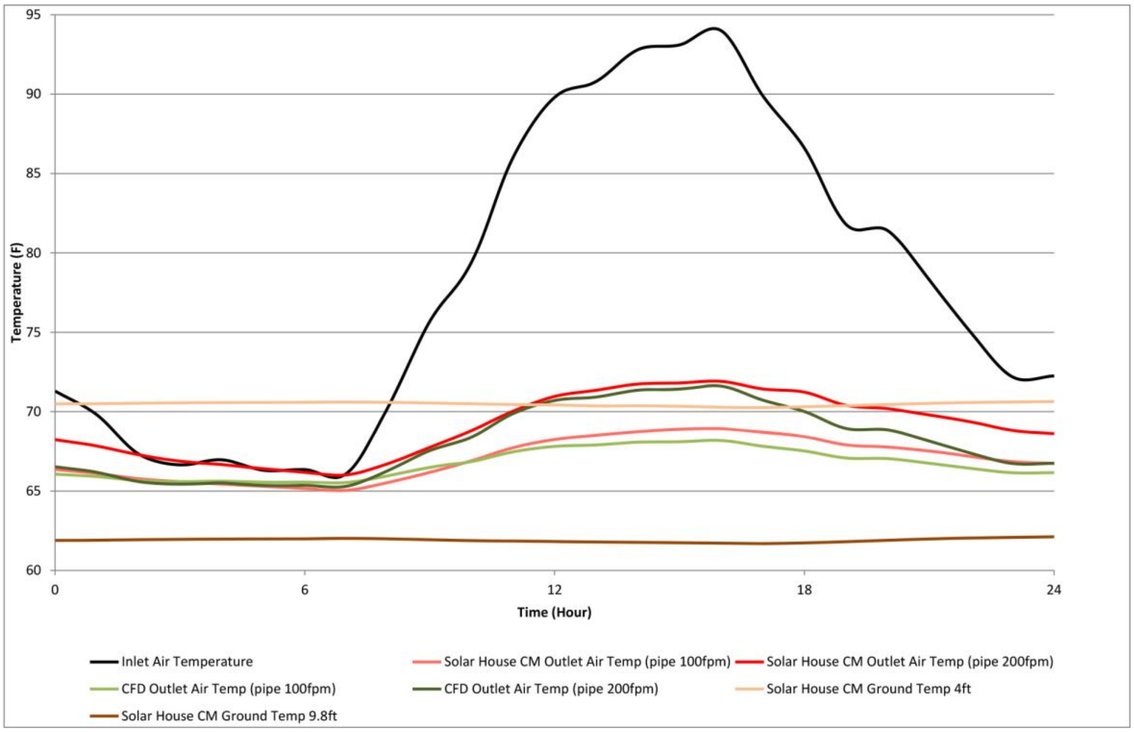

Figure 5-11: CFD Simulation Prediction on Jul 24th

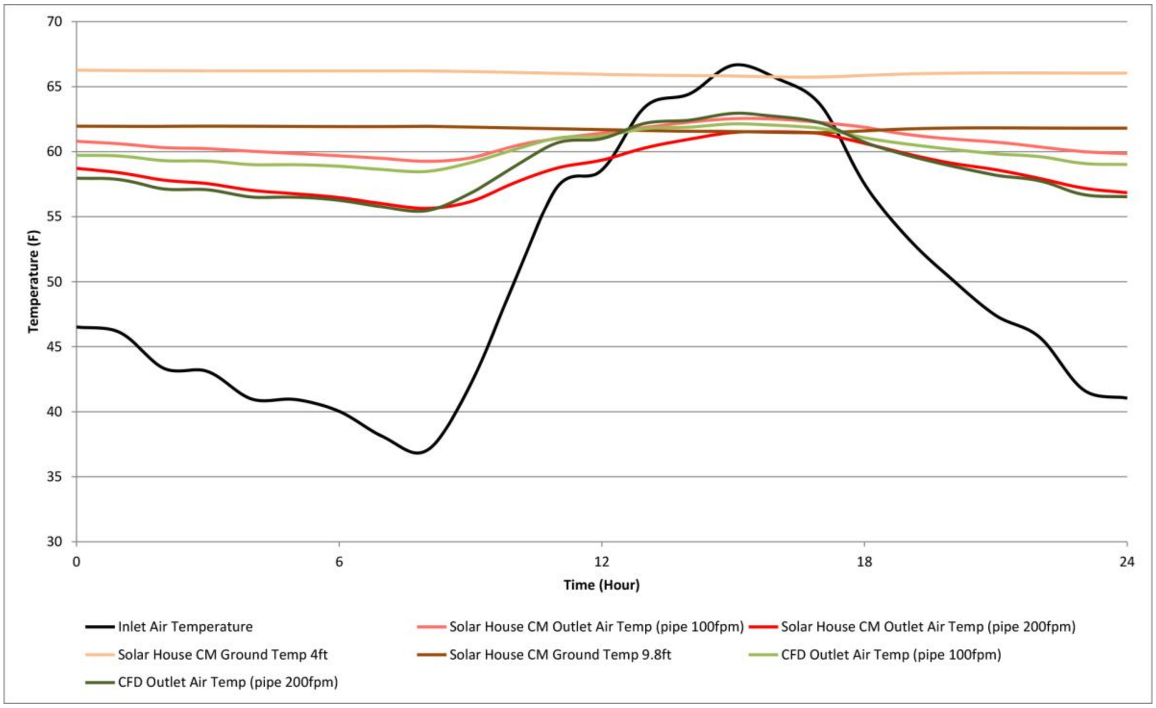

Figure 5-12: CFD Simulation Prediction on Oct 25th

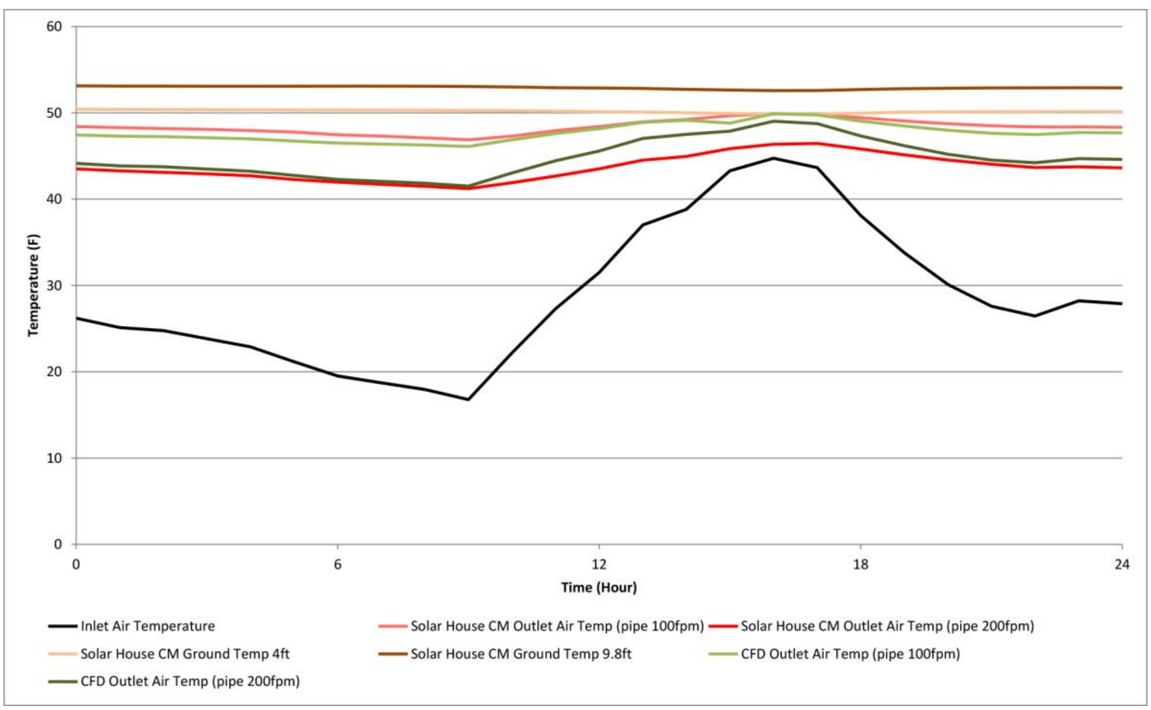

Figure 5-13: CFD Simulation Prediction on Dec 20th

Table 26: GCV System at Solar CM House vs. CFD Outlet Temperature on Three Days

Date		Solar CM House	CFD	Difference
Jul 24th				
Pipe 100 fpm	Min.	65.05	65.54	0.49
Outlet Air Temp (°F)	Max.	68.93	68.18	0.75
	Avg.	67.02	66.69	0.33
	Std dev.	1.31	0.94	0.37
Pipe 200 fpm	Min.	66.02	65.30	0.72
Outlet Air Temp (°F)	Max.	71.91	71.61	0.30
	Avg.	69.06	68.04	1.02
	Std dev.	1.98	2.24	0.26
Oct 25th				
Pipe 100 fpm	Min.	59.26	58.48	0.78
Outlet Air Temp (°F)	Max.	62.54	62.14	0.40
	Avg.	60.77	60.10	0.67
	Std dev.	1.00	1.19	0.18
Pipe 200 fpm	Min.	55.64	55.47	0.17
Outlet Air Temp (°F)	Max.	61.52	62.94	1.42
	Avg.	58.48	58.75	0.27
	Std dev.	1.82	2.43	0.61
Dec 20th				
Pipe 100 fpm	Min.	46.88	46.10	0.78
Outlet Air Temp (°F)	Max.	49.93	49.89	0.04
	Avg.	48.38	47.73	0.65
	Std dev.	0.84	1.06	0.23
Pipe 200 fpm	Min.	41.22	41.51	0.29
Outlet Air Temp (°F)	Max.	46.46	49.03	2.57
	Avg.	43.64	44.76	1.12
	Std dev.	1.52	2.16	0.64

5.2 GAEA Model for the GCV System at the Solar CM House

GAEA software relies on a parametric equation to calculate the GCV system heat exchange. To predict GCV system heat reduction, the design parameters from pipe depth, length, and diameter must be entered. Because the length of the pipe at the Solar CM House changes according to depth (i.e., has a strong slope), GAEA divides the GCV system into hundreds of segments based on length and depth. Figure 5-14 shows the GCV system parameters with pipe depth. The second input in the GAEA tool is the soil properties. In this case, soil properties were the same as those of the soil at Solar CM House, as shown in Figure 5-15. The third input is the temperature range over the year, which depends on the maximum monthly temperature and the annual mean temperature, as Figure 5-16 shows. The fourth input covers air volume and the operation time of the GCV system. The results indicated the daily and annual GCV system temperature reduction; Figure 5-17, Figure 5-18, and Figure 5-19 show the GCV system inlet and outlet temperatures on different days.

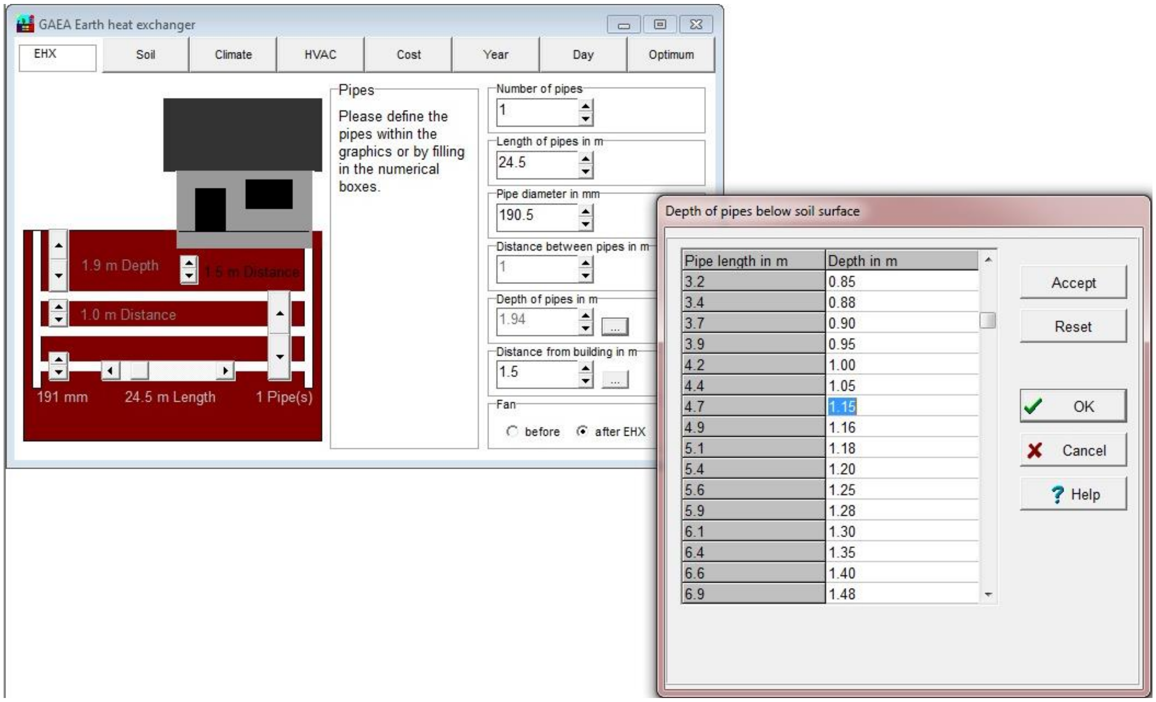

Figure 5-14: GAEA Input for GCV System Design at Solar CM House

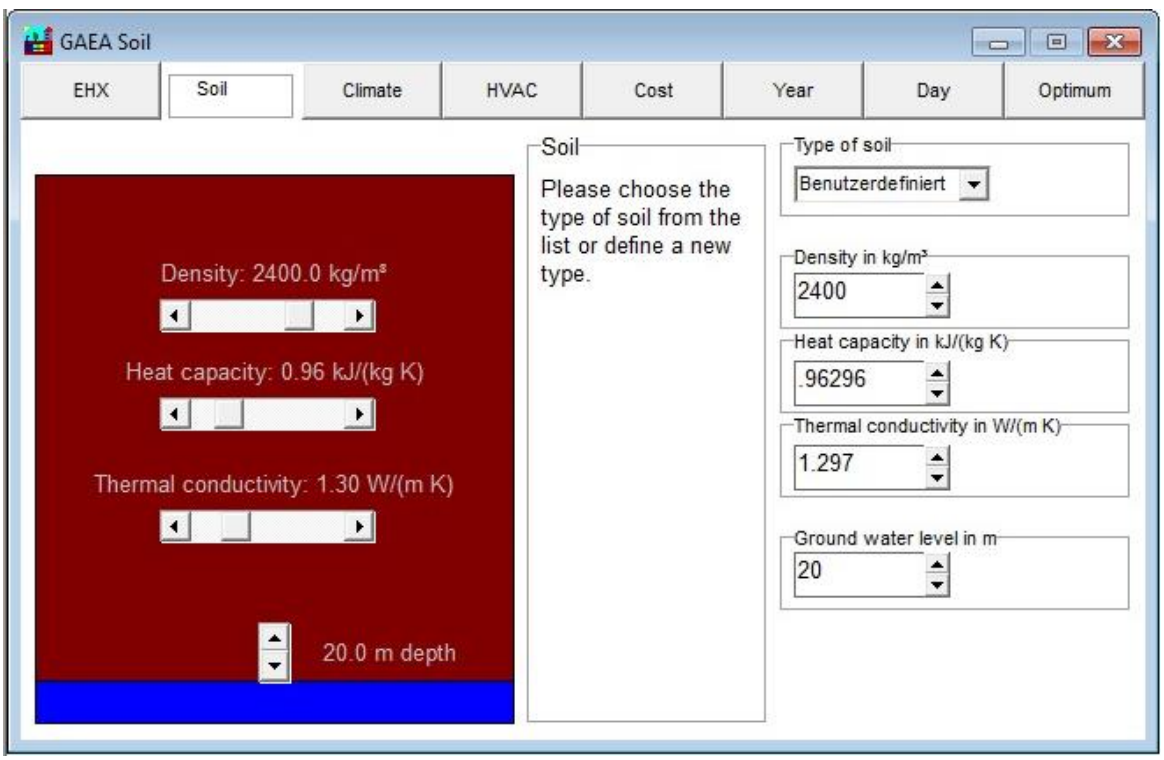

Figure 5-15: GAEA Input for Solar CM House Soil

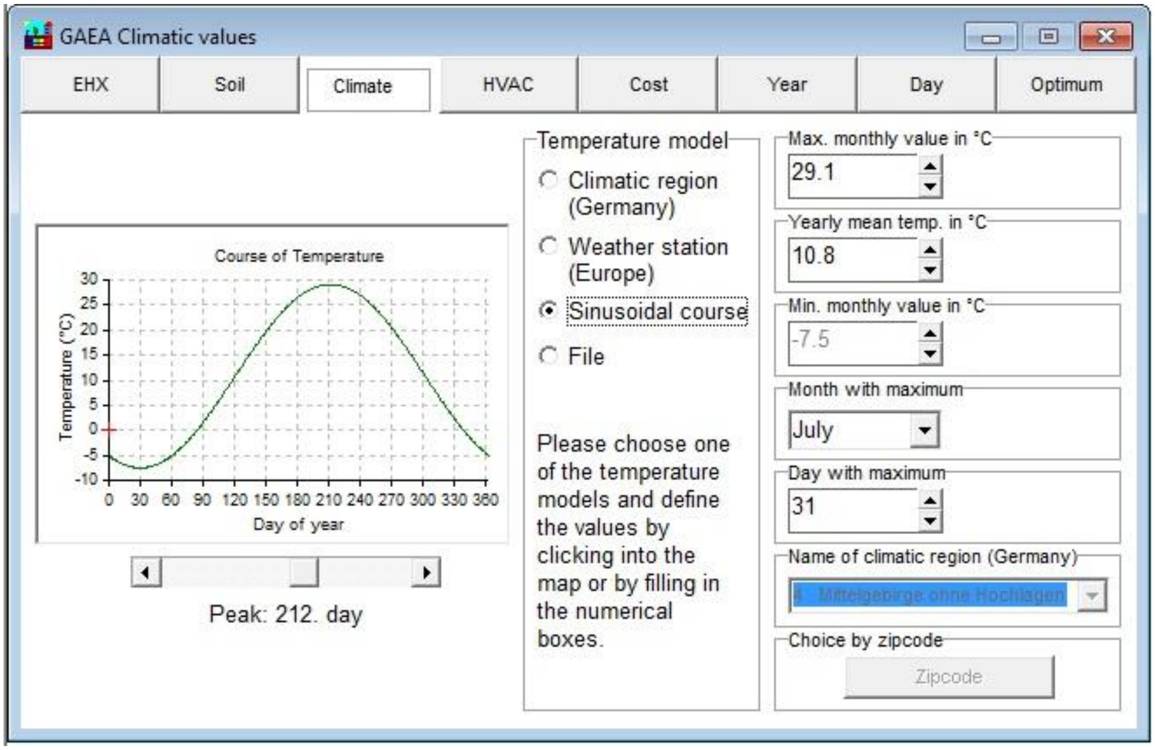

Figure 5-16: Blacksburg, VA's Climate Temperature Range

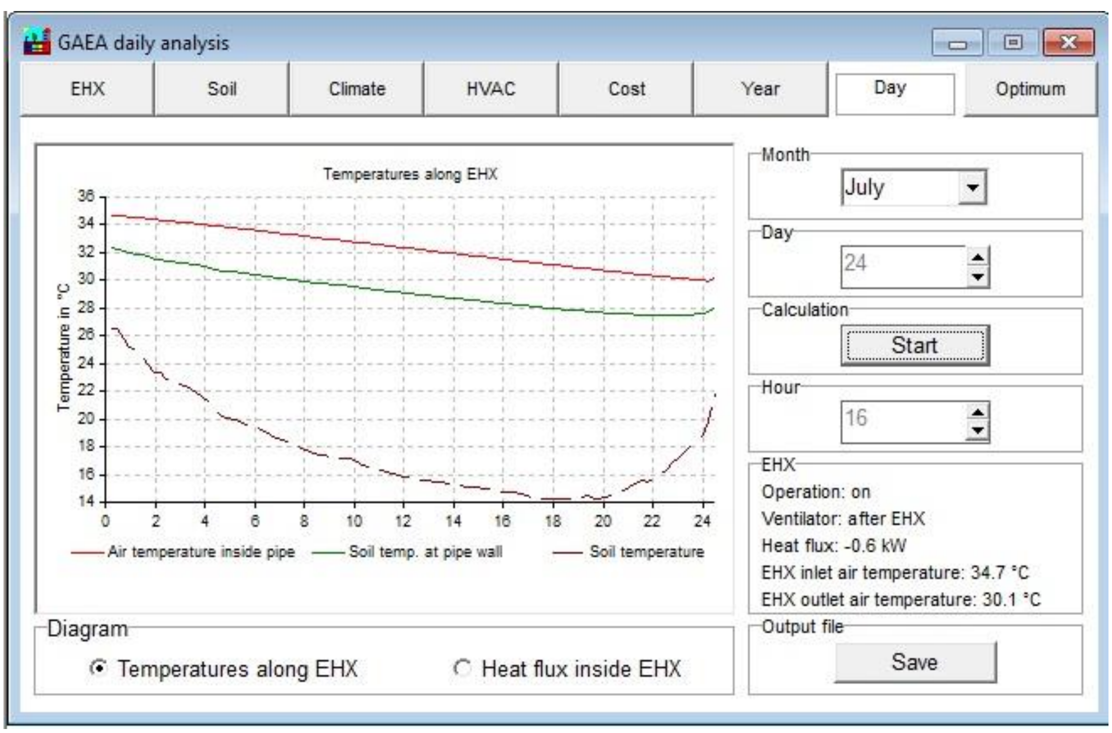

Figure 5-17: GAEA Prediction on Jul 24th

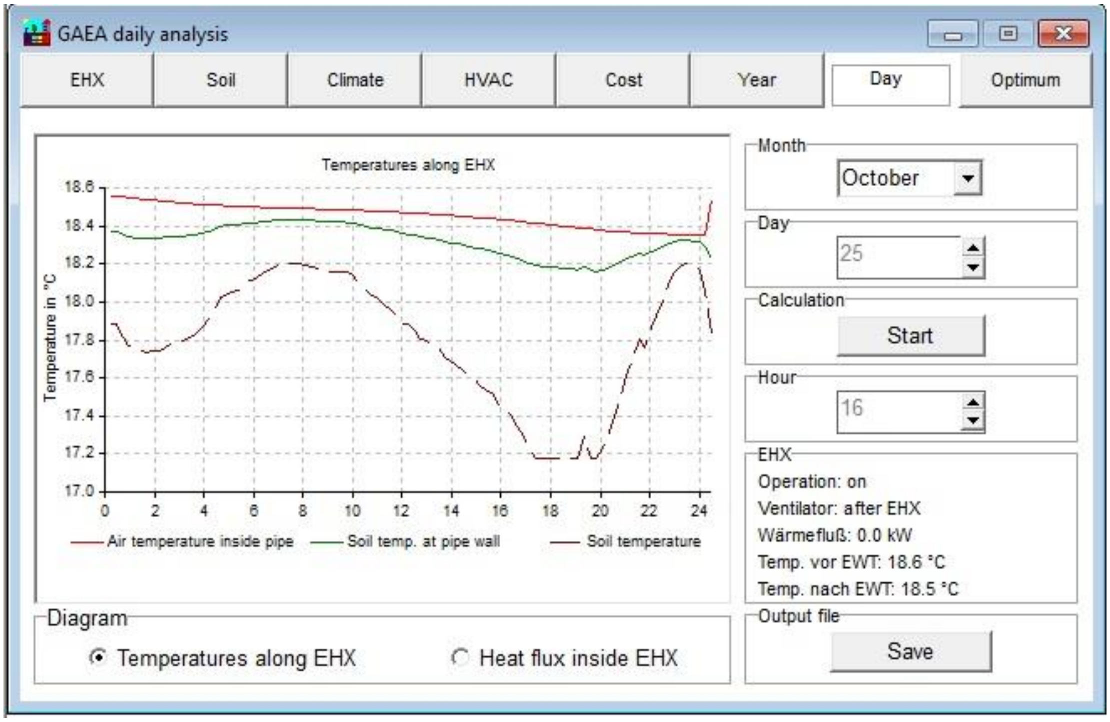

Figure 5-18: GAEA Prediction on Oct 25th

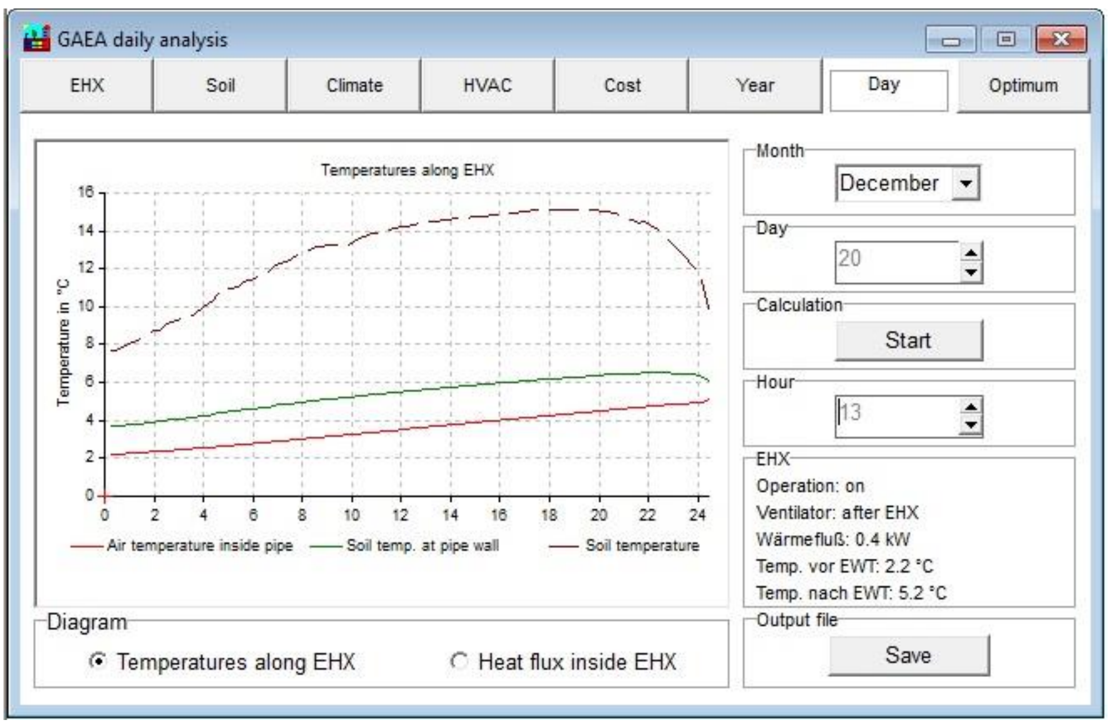

Figure 5-19: GAEA Prediction on Dec 20th

GAEA Results

GAEA software was used to predict the performance every hour over three days for the GCV system at the Solar CM House. A total of 72 points were collected to compare with the as-built GCV system. Table 27 compares the outlet temperature of in-situ GCV measurements to the GAEA predictions (Figure 5-20, Figure 5-21, and Figure 5-22).

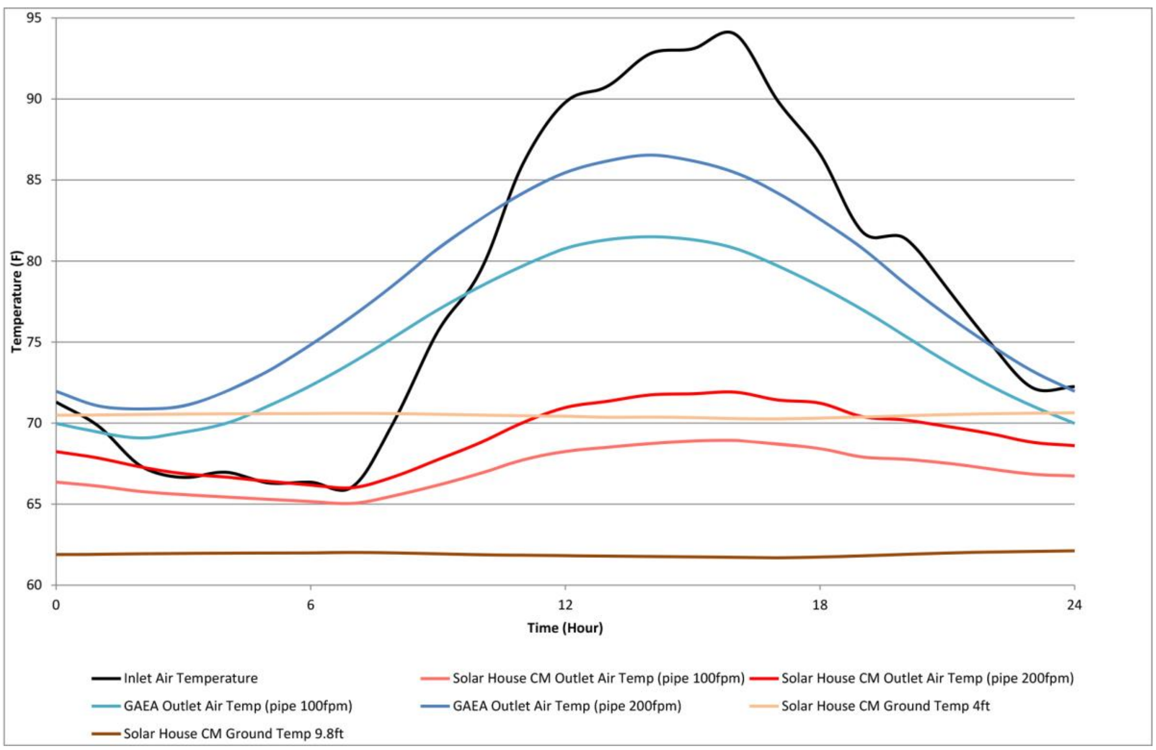

Figure 5-20: GAEA Prediction on Jul 24th

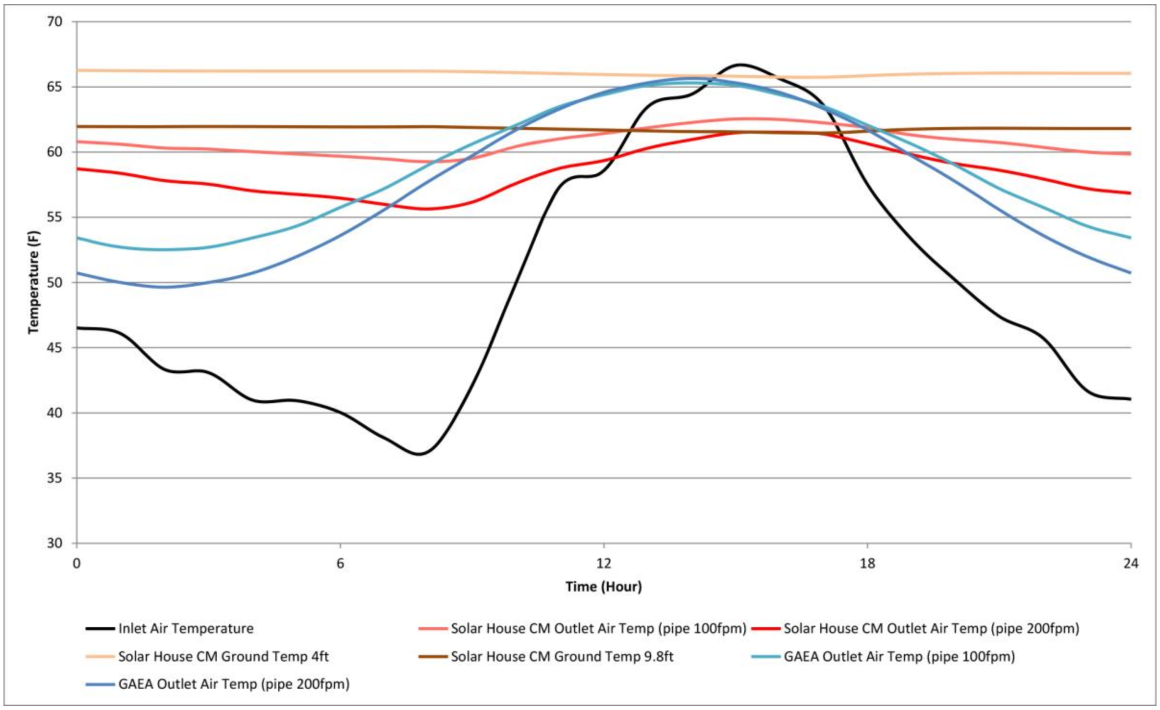

Figure 5-21: GAEA Prediction on Oct 25th

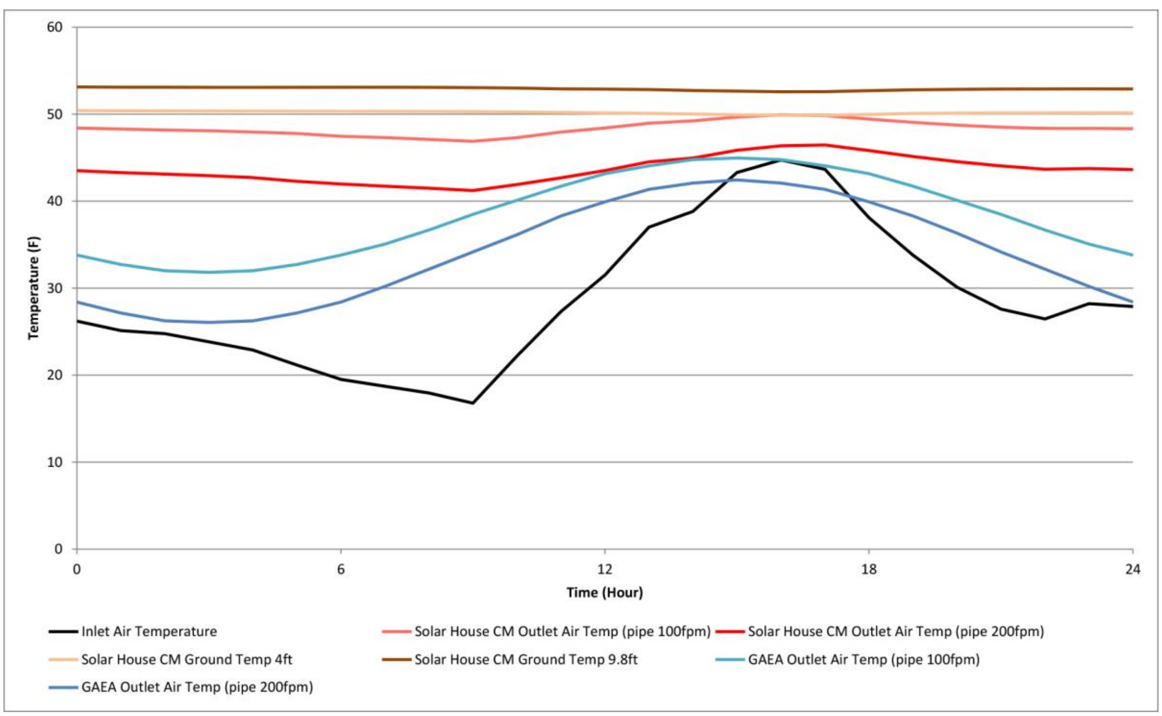

Figure 5-22: GAEA Prediction on Dec 20th

Table 27: GCV System at Solar CM House vs. GAEA Outlet Temperature on Three Days

Date		Solar CM House	GAEA	Difference
Jul 24th				
Pipe 100 fpm	Min.	65.05	69.08	4.03
Outlet Air Temp (°F)	Max.	68.93	81.50	12.57
	Avg.	67.02	75.16	8.13
	Std dev.	1.31	4.50	3.18
Pipe 200 fpm	Min.	66.02	70.88	4.86
Outlet Air Temp (°F)	Max.	71.91	86.54	14.63
	Avg.	69.06	78.42	9.36
	Std dev.	1.98	5.68	3.70
Oct 25th				
Pipe 100 fpm	Min.	59.26	52.52	6.74
Outlet Air Temp (°F)	Max.	62.54	65.30	2.76
	Avg.	60.77	58.70	2.07
	Std dev.	1.00	4.66	3.66
Pipe 200 fpm	Min.	55.64	49.64	6.00
Outlet Air Temp (°F)	Max.	61.52	65.66	4.14
	Avg.	58.48	57.38	1.10
	Std dev.	1.82	5.82	4.00
Dec 20th				
Pipe 100 fpm	Min.	46.88	31.82	15.06
Outlet Air Temp (°F)	Max.	49.93	44.96	4.97
	Avg.	48.38	38.23	10.15
	Std dev.	0.84	4.75	3.92
Pipe 200 fpm	Min.	41.22	26.06	15.16
Outlet Air Temp (°F)	Max.	46.46	42.44	4.02
	Avg.	43.64	33.97	9.67
	Std dev.	1.52	5.90	4.38

5.3 CFD and GAEA Models Validation

The goal of this phase was to validate the GAEA and CFD models predictions for the GCV system performance by comparing the in-situ GCV measurements to the GAEA and CFD outputs. The comparison was based on the outlet air temperature at different airflows (100 fpm and 200 fpm). Table 28 shows the comparison of the outlet air temperatures for three different days to determine the change in the outlet during the hot and cold seasons (Figure 5-23, Figure 5-24, and Figure 5-25). A linear regression model was used to compare the results. Knowing the root mean square error (RMSE) determines which method is most accurate in predicting the performance of the actual GCV system.

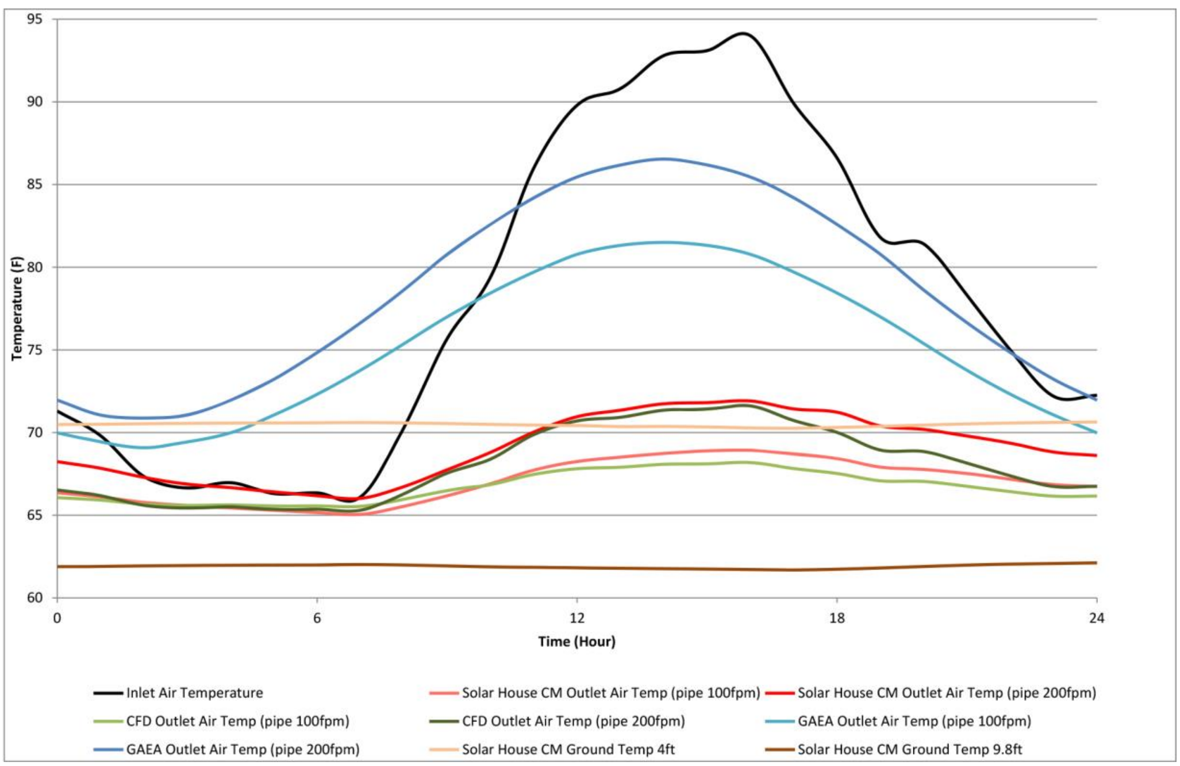

Figure 5-23: GCV System, CFD, and GAEA Performance on Jul 24th

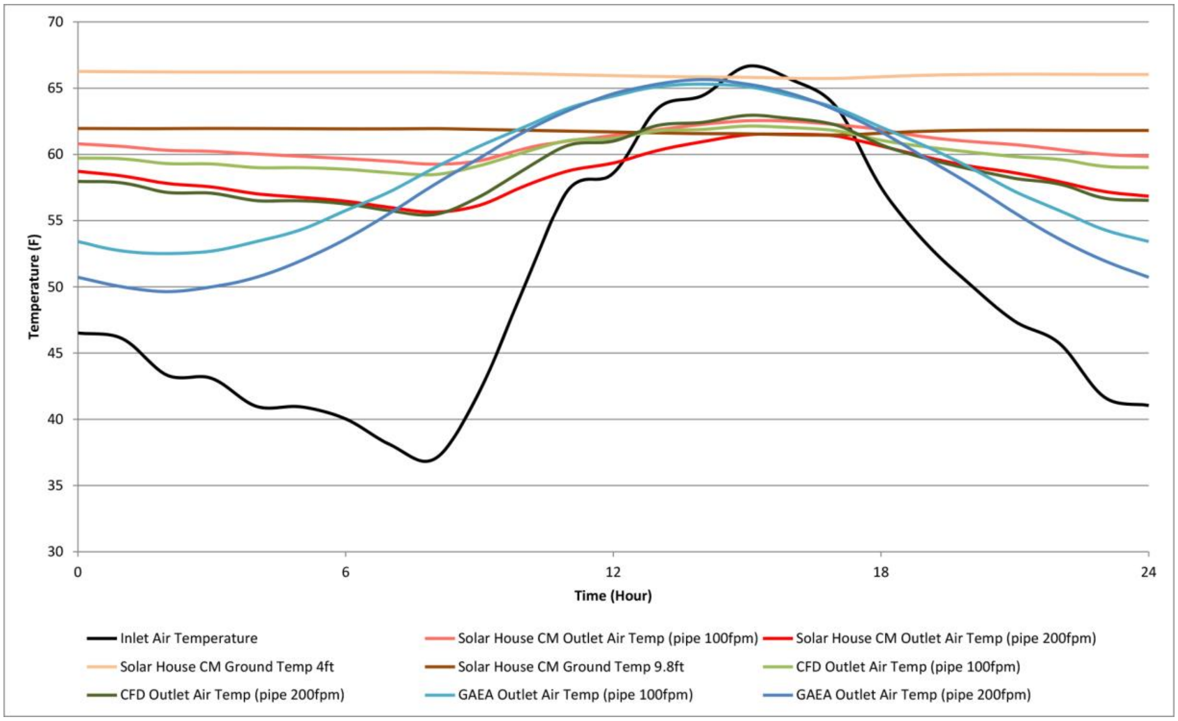

Figure 5-24: GCV System, CFD, and GAEA Performance on Oct 25th

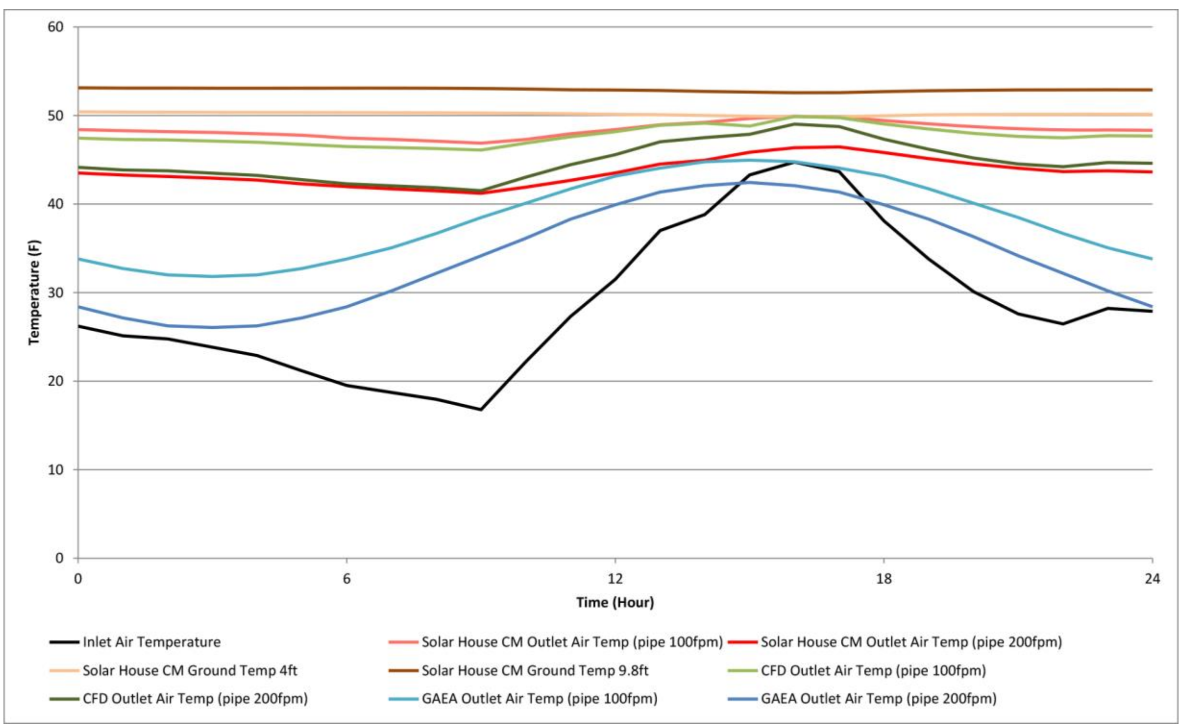

Figure 5-25: GCV System, CFD, and GAEA Performance on Dec 20th

Table 28: GCV Monitoring, CFD Simulation, and GAEA Results for the Three Days

Date		Solar CM House	CFD	Difference	Solar CM House	GAEA	Difference	CFD	GAEA	Difference
Jul 24th										
Pipe 100 fpm	Min.	65.05	65.54	0.49	65.05	69.08	4.03	65.54	69.08	3.54
Outlet Air Temp (°F)	Max.	68.93	68.18	0.75	68.93	81.50	12.57	68.18	81.50	13.32
	Avg.	67.02	66.69	0.33	67.02	75.16	8.13	66.69	75.16	8.46
	Std dev.	1.31	0.94	0.37	1.31	4.50	3.18	0.94	4.50	3.56
Pipe 200 fpm	Min.	66.02	65.30	0.72	66.02	70.88	4.86	65.30	70.88	5.58
Outlet Air Temp (°F)	Max.	71.91	71.61	0.30	71.91	86.54	14.63	71.61	86.54	14.93
	Avg.	69.06	68.04	1.02	69.06	78.42	9.36	68.04	78.42	10.38
	Std dev.	1.98	2.24	0.26	1.98	5.68	3.70	2.24	5.68	3.44
Oct 25th										
Pipe 100 fpm	Min.	59.26	58.48	0.78	59.26	52.52	6.74	58.48	52.52	5.96
Outlet Air Temp (°F)	Max.	62.54	62.14	0.40	62.54	65.30	2.76	62.14	65.30	3.16
	Avg.	60.77	60.10	0.67	60.77	58.70	2.07	60.10	58.70	1.40
	Std dev.	1.00	1.19	0.18	1.00	4.66	3.66	1.19	4.66	3.47
Pipe 200 fpm	Min.	55.64	55.47	0.17	55.64	49.64	6.00	55.47	49.64	5.83
Outlet Air Temp (°F)	Max.	61.52	62.94	1.42	61.52	65.66	4.14	62.94	65.66	2.72
	Avg.	58.48	58.75	0.27	58.48	57.38	1.10	58.75	57.38	1.37
	Std dev.	1.82	2.43	0.61	1.82	5.82	4.00	2.43	5.82	3.39
Dec 20th										
Pipe 100 fpm	Min.	46.88	46.10	0.78	46.88	31.82	15.06	46.10	31.82	14.28
Outlet Air Temp (°F)	Max.	49.93	49.89	0.04	49.93	44.96	4.97	49.89	44.96	4.93
	Avg.	48.38	47.73	0.65	48.38	38.23	10.15	47.73	38.23	9.50
	Std dev.	0.84	1.06	0.23	0.84	4.75	3.92	1.06	4.75	3.69
Pipe 200 fpm	Min.	41.22	41.51	0.29	41.22	26.06	15.16	41.51	26.06	15.45
Outlet Air Temp (°F)	Max.	46.46	49.03	2.57	46.46	42.44	4.02	49.03	42.44	6.59
	Avg.	43.64	44.76	1.12	43.64	33.97	9.67	44.76	33.97	10.79
	Std dev.	1.52	2.16	0.64	1.52	5.90	4.38	2.16	5.90	3.73

Table 29 shows a comparison of the results between the actual GCV system output temperature with CFD simulation and the GAEA method. Based on the RMSE, the results indicate that the CFD method gave more accurate results than the GAEA. Accordingly, this study relied on a CFD simulation method to predict GCV system temperature reduction for the different design variables.

Table 29: Comparison of GCV System's Predicted Performance on the Three Days

		GCV Solar CM House Vs. CFD	GCV Solar CM House Vs. GAEA	GCV Solar CM House Vs. CFD	GCV Solar CM House Vs. GAEA
	Day	Pipe 100 fpm Outlet Air Temp (°F)		Pipe 200 fpm Outlet Air Temp (°F)	
Root mean square error (Degree Fahrenheit)	24-Jul	0.56	9	1.15	10.45
	25-Oct	0.72	4.33	0.9	4.76
	20-Dec	0.73	10.8	1.3	10.63

Figure 5-26: GCV Solar CM House vs. CFD Outlet Temperature on Three Days (200fpm)

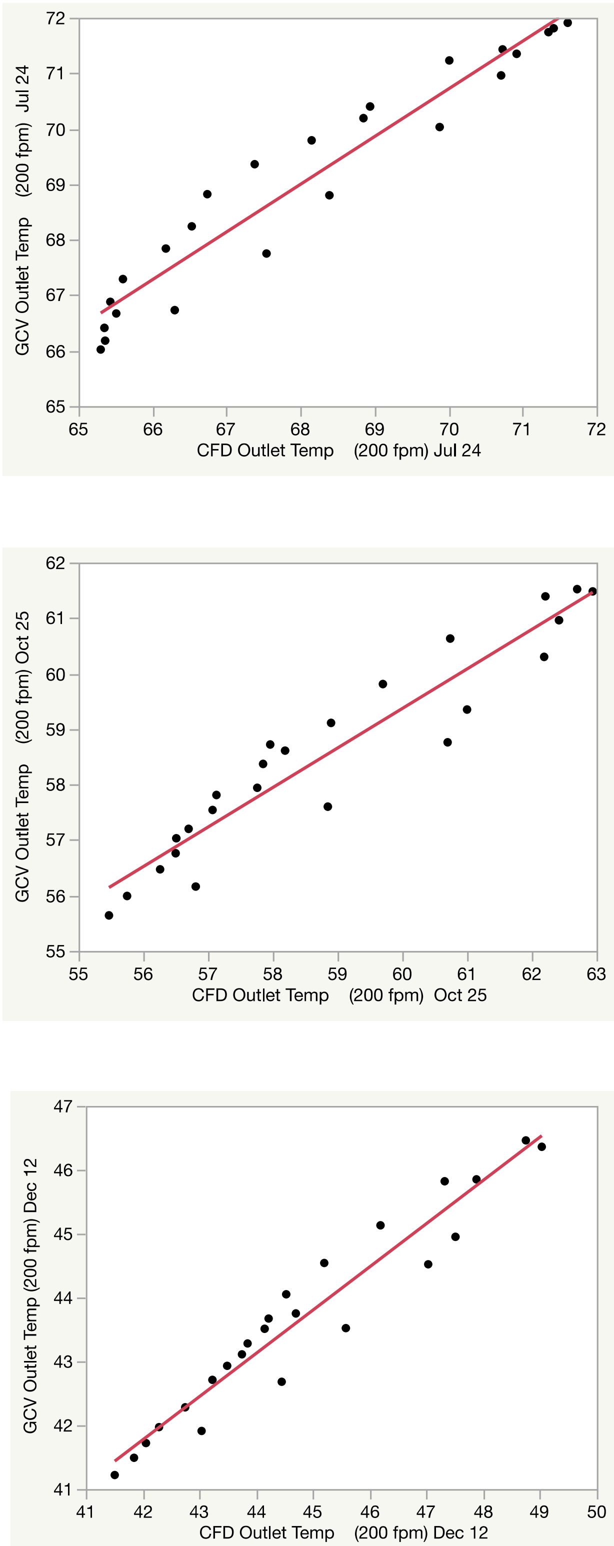

Figure 5-27: GCV Solar CM House vs. GAEA Outlet Temperature on Three Days (200fpm)

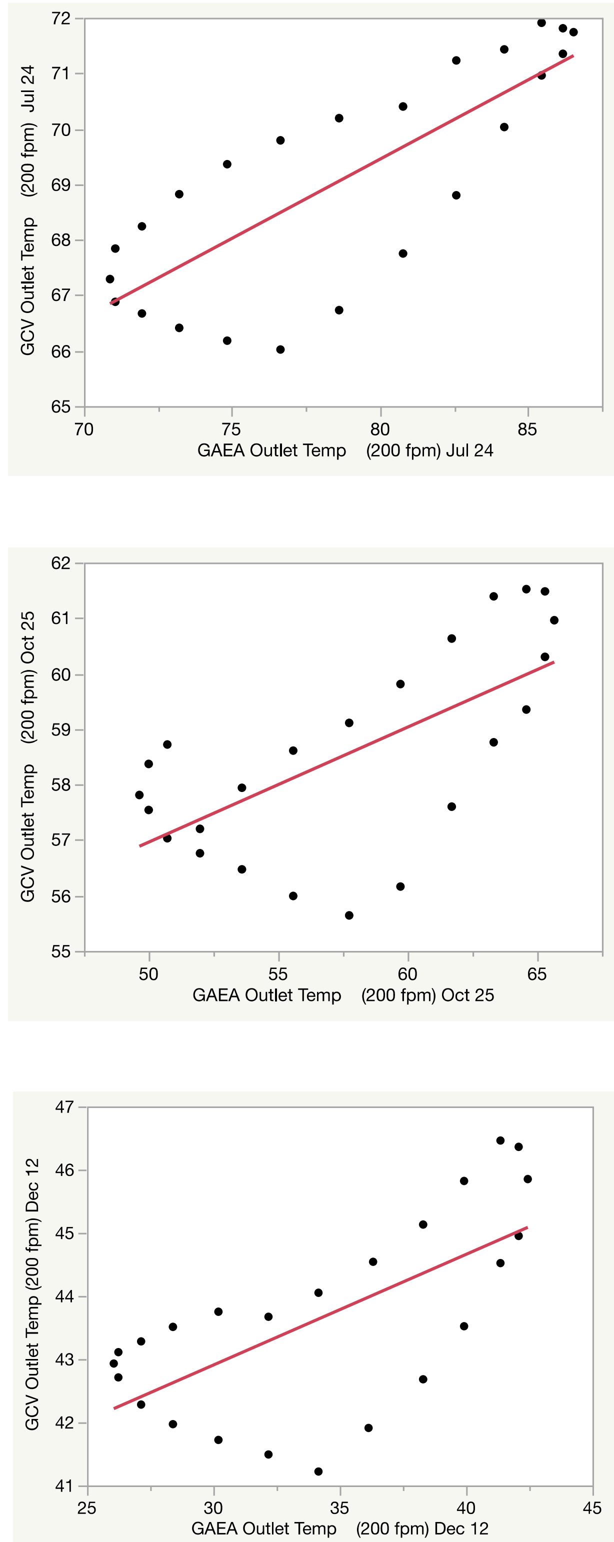

Figure 5-28: GCV Solar CM House vs. CFD Outlet Temperature on Three Days (100fpm)

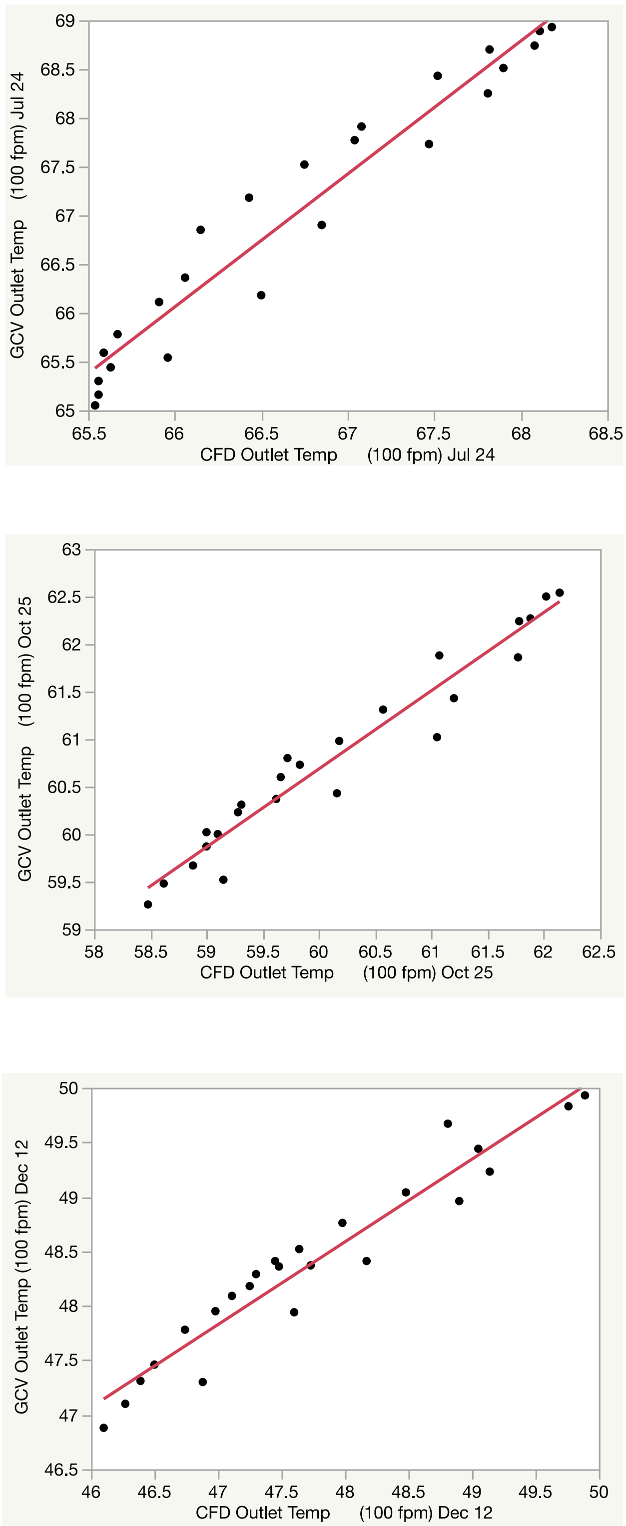

Figure 5-29: GCV Solar CM House vs. GAEA Outlet Temperature on Three Days (100fpm)

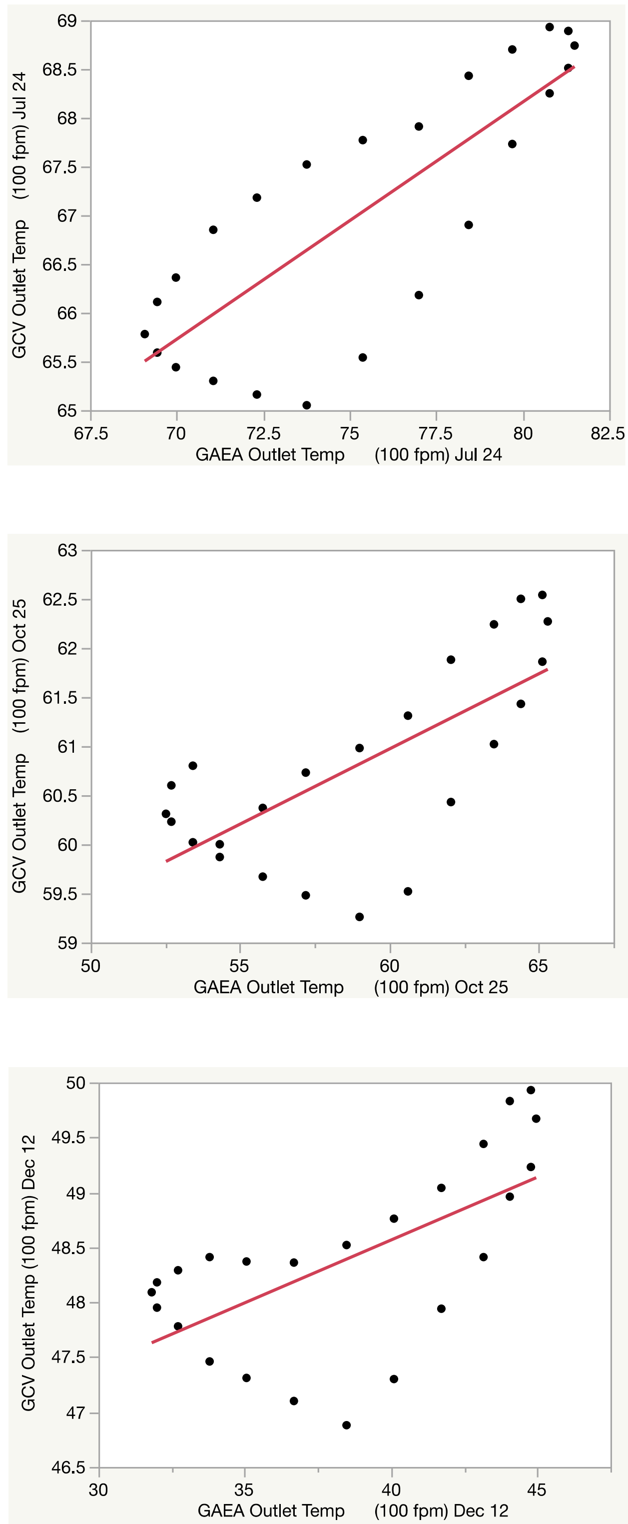

5.4 Summary

This chapter can be summarized as follows:

- **Finding the appropriate CFD program:** compared several CFD programs to find the appropriate CFD program. This comparison indicates that Autodesk CFD was the most appropriate for the research project based on its features and the previously presented validation.
- **Autodesk CFD model:** the GCV system at the Solar CM House was simulated using Autodesk CFD. This simulation was based on certain boundary conditions that ensured proper thermal behavior that matched the existing GCV system for three days.
- **GAEA model:** the GCV system at the Solar CM House was simulated using GAEA software. This software relies on a parametric equation to calculate the GCV system heat exchange, which has been used to predict the performance of the GCV system at the Solar CM House for three days.
- **CFD and GAEA models validation:** both CFD and GAEA models were compared with the in-situ GCV system at the Solar CM House. The comparison was based on the outlet air temperature at different airflows (100 fpm and 200 fpm) for three days. The results in Table 29 showed that the CFD method gave more accurate results than the GAEA. Accordingly, this study relied on a CFD simulation method to predict GCV system temperature reduction for the different design variables.

Chapter 6: GCV Simulations

This chapter discusses the GCV system parametric simulations, which presents the simulation variables and process in addition to the boundary conditions using Autodesk CFD.

6.1 Simulation Variables

Many parameters, both exogenous and endogenous, affect the performance of the GCV system. Exogenous variables include air temperature, ground temperature, and soil type. Endogenous variables include air velocity, pipe length, pipe depth, pipe thickness, and pipe diameter. Table 30 shows a summary of the variables and their limits for this research.

Table 30: Research Limitation Variables

Variable	Variable in this research	Reason	Limitation	Limitation reason
Air temperature	Yes	Air temperature is the main factor of the system	5-115 F	Air temperature limitation covers hot and cold season for different locations.
Ground temperature	Yes	Ground temperature is a primary factor of heat exchange.	35-95 F	Ground temperature limitation covers hot and cold season for different locations.
Soil type	Yes	Thermal properties of the soil affect ground temperature	Sand- Clay-Limestone	These are the main soil type that have different properties
Airflow velocity	Yes	Airflow is the only variable we can change after designing the system.	50-450 fpm	There is no efficiency on airflow under 50 f/m., nor noise sound if the airflow is under 450 fpm.
Pipe length	Yes	Pipe length impacts air residency.	50-450 ft.	Lengths shorter than 50 ft. will be inefficient. Lengths longer than 450 ft. will occupy too much space.
Pipe diameter	Yes	Pipe diameter impacts air volume	6”-48”	Readily available in the marketplace
Pipe thickness	Correlated	Pipe thickness variation depends on the pipe diameter base on pipe manufacturers standard.	0.73"-5.10"	
Pipe depth	Correlated	Pipe depth correlated with ground temperature	Center of the soil boundary	
Pipe material	Fixed	This research will use clay pipe because of its high thermal conductivity.	Clay pipe	
Pipe shape	Fixed	Most pipes have a circular cross-section. Rectangular and square pipes will not be covered.	Circular cross-section	
Backfill size	Fixed	Changing Backfill size will not significantly affect the GCV system performance. 10” gravel thickness with 1” average diameter will be used.	10"	
Backfill material	Fixed	Gravel is the appropriate material for heat transfer and pipe protection.	Gravel	
Ground shading	Fixed	All GCV systems in this research will assume a shaded system to ensure the greatest impact during the hot season	Shaded	

Air, ground temperature, and soil type

GCV systems rely on heat exchange between the air and ground. Air and ground temperatures vary from place to place and from one time to another, and significantly affect the performance of the GCV system. By limiting air temperature to between 5^{o}F and 115^{o}F, and ground temperature to between 35^{o}F and 95^{o}F in this research, the GCV will still be applicable to many locations around the world. Moreover, ground temperature relies on location and soil type. Each soil has its properties in terms of heat conductivity and capacity that affect heat exchange in the GCV system. This research covered three major soil types: clay, limestone, and sand. Table 31 shows the soil type properties ("Thermal Conductivity of some common Materials and Gases," 2015).

Table 31: Soil Type Properties

Material	Density	Thermal Conductivity	Specific heat capacity
Clay	1.7 g/cm3	1.1 w/m-k	1381 J/kg-k
Limeston	2.56 g/cm3	1.3 w/m-k	909 J/kg-k
Sand	1.7 g/cm3	1.7 w/m-k	710 J/kg-k

Airflow velocity

Airflow velocity is the only variable that can be easily changed after the GCV system is installed. In looking at Alghamdi's (2008) comparison of four pipes with different airflows (Figure 6-1), the pipe that had the lowest airflow rate had the greatest heat transfer, due to the longer residence time. In this research, there were five different levels of airflow velocity in the simulations 50, 150, 250, 350, and 450 fpm.

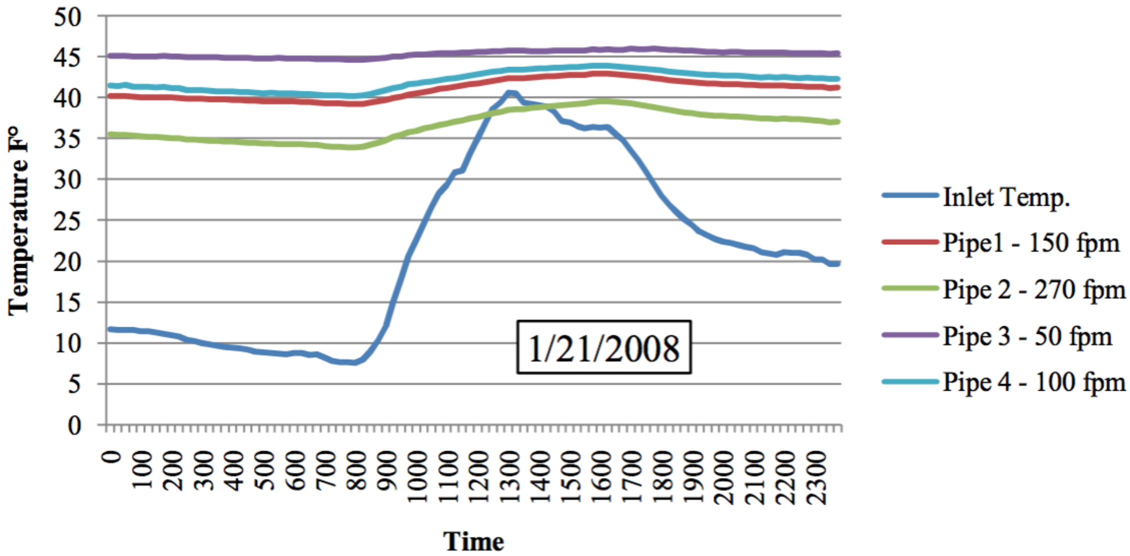

Figure 6-1: 24-hour Period Temperature Change (01/21/2008) (Alghamdi, 2008, p. 32)

Pipe depth and length

Pipe depth and length are important factors that affect heat exchange. Pipe depth is correlated with ground temperature, which remains constant at about 26 feet deep (Reysa, 2005). Therefore, if pipe depth is fixed during the simulation, the surrounding ground temperature will also be constant. Pipe length is correlated with the time that air resides in the pipe, meaning that the longer the pipe, the greater the residence time. In this research, the pipe length ranged from 50, 150, 250, 350 to 450 feet (Givoni, 1998).

Pipe diameter and thickness

Pipe diameter affects system performance as well. Pipe diameter affects the surface area for heat exchange between the air and pipe surface. Pipe thickness also affects heat transfer between the pipe's outer and inner surfaces. Pipe thickness and diameter are correlated positively based on a standard measurement, such that the greater the pipe diameter, the greater the pipe thickness. In this research, there were five levels of pipe diameter: 6, 12, 24, 36, and 48 inches.

However, to limit the number of simulations, pipe thickness was fixed because it is correlated with pipe diameter, which takes the values as Table 32 shows (Mission Rubber Company LLC, 1951).

Table 32: Pipe Diameter and Thickness

Diameter (inch)	4	6	8	10	12	15	18	21	24	27	30	32	36	39	42	48
Thickness (inch)	0.65	0.73	0.98	1.02	1.12	1.52	1.93	2.5	2.52	3.09	3.25	3.15	3.72	3.98	4.31	5.1

Pipe and backfill material

The pipe and backfill material also are important. Each material has its own thermal properties that affect the heat transfer between the air and the ground. This research used a clay pipe and gravel as a backfill material because they commonly used GCV system materials and are affordable. Table 33 shows the pipe and backfill material thermal properties ("Thermal Conductivity of some common Materials and Gases," 2015).

Table 33: Thermal Material Properties

Material	Density	Thermal Conductivity	Specific Heat Capacity	Emissivity
Clay	2.6 g/cm3	1.6 w/m-k	900.16 J/kg-k	0.92
Concrete	2.4 g/cm3	1.4 w/m-k	880 J/kg-k	0.85
Stainless Steel	7.48 g/cm3	16 w/m-k	490 J/kg-k	0.85
Carbon Steel	7.853 g/cm3	54 w/m-k	490 J/kg-k	0.79
Copper	8.1 g/cm3	401 w/m-k	385 J/kg-k	0.78
PVC	0.805 g/cm3	0.19 w/m-k	840 - 1170	0.92
Gravel	2.629 g/cm3	4.8 w/m-k	3307 J/kg-k	0.28

Pipe shape

Pipe shape influences airflow and the cross-section area. Due to its many advantages a circular cross-section is the standard pipe shape.

Backfill size

Based on the GCV performance results by Alghamdi (2008), backfill thicknesses of 8, 10, and 12 inches, respectively, showed no significant difference in performance. Accordingly, the backfill thickness was fixed at 10 inches.

Ground shading

Ground shading affects the ground temperature, particularly during cooling periods. According to Trzaski and Zawada (2011), the GCV system's cooling performance increases 181% if the system is shaded, while heating performance decreases 4.4%. Thus, ground shading is important in hot climates because it significantly affects the performance of the system. In this research, ground shading was fixed because it depends on the ground temperature in the weather file. For example, to predict the performance of the GCV system for shaded ground, the ground temperature from the weather file data must be taken in a shaded condition as well for a non-shaded ground.

.

6.2 GCV System Simulation Process

To determine the GCV system performance, which was determined by the change in the inlet to outlet temperature, the GCV system was processed in three steps. First, the GCV system was described and input to AutoCAD. Second, the materials and boundary conditions were assigned. Third, the simulations were performed and the results were checked.

6.2.1 Modeling GCV system designs

As previously mentioned, several variables affect the GCV system performance and this study focused on six variables: air flow velocity, pipe length, pipe diameter, soil type, air temperature, and ground temperature. Each variable had different levels, as Table 34 shows. Simulations were performed for each combination of variables. This resulted in 375 models. To save time, the variance in air flow velocity was simulated in one model using five pipes with different airflow velocity in each model, so this reduced the number of models to 75, as Figure 6-2 shows. To avoid interaction between pipes, they were spaced at 40 feet. Each of these 75 models had an inlet temperature and ground temperature. In all, 6,300 simulations were performed resulting in 31,500 outlet temperatures from all possible design combinations.

Table 34: GCV System Model Variables and Levels

Variable	Min value											Max value	Unit
Air flow	50		150			250			350			450	fpm
Pipe length	50		150			250			350			450	feet
Pipe diameter	6		12			24			36			48	inch
Soil type	Clay					Sand						Limestone	
Air temperature	5	15	25	35	45	55	65	75	85	95	105	115	Fahrenheit
Ground Temperature	35		45		55		65		75		85	95	Fahrenheit

Figure 6-2: GCV Design Distribution Based on Research Variables

6.2.2 Simulation boundary conditions

For the simulations, the GCV system was divided into four domains: air, pipe, backfill, and soil (Figure 6-3). Each domain had physical properties and boundary conditions to be assigned. For the physical properties, each material in the domain was described by thermal conductivity, heat capacity, and density. For the boundary conditions, six faces must be assigned to the soil, as Figure 6-4 shows. The side faces need to be insulated, and the temperature should be assigned from the top and bottom faces, as Figure 6-5 and Figure 6-6 show. Air boundary conditions, inlet temperature, and air velocity were assigned to the inlet. Pressure and heat flux were assigned in the outlet, as Figure 6-7 shows. When this information is assigned in Autodesk CFD, the software calculates heat transfer by treating these domains as one continuum to satisfy the continuity of temperature and heat flux along the faces between air to pipe, to backfill, and to the soil. The boundary conditions for all possible combinations of the variables in the simulations can be found in Table 35.

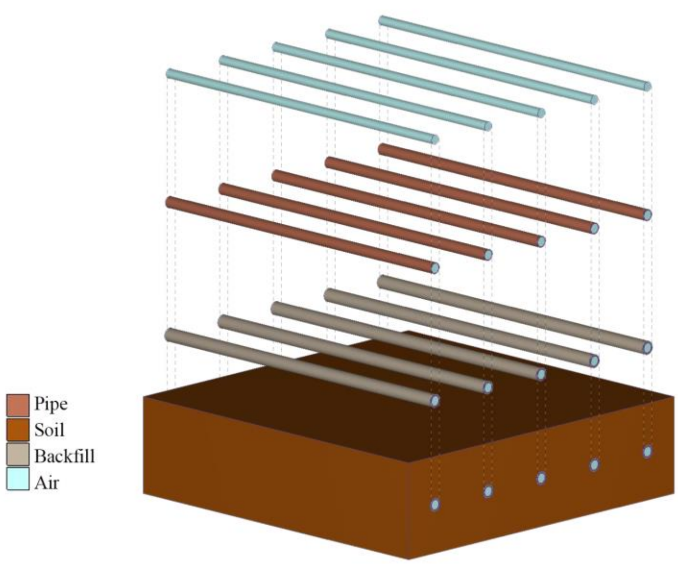

Figure 6-3: Boundary Condition Domains

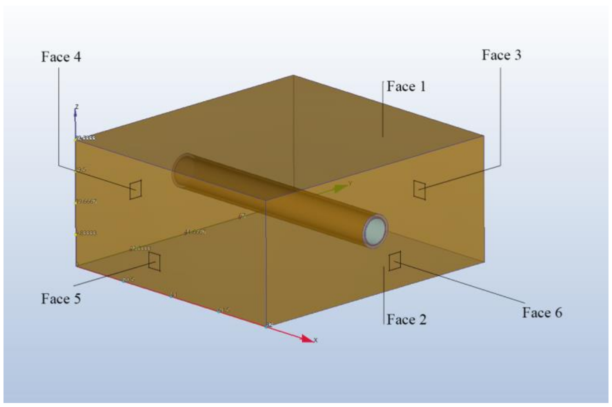

Figure 6-4: Soil Faces

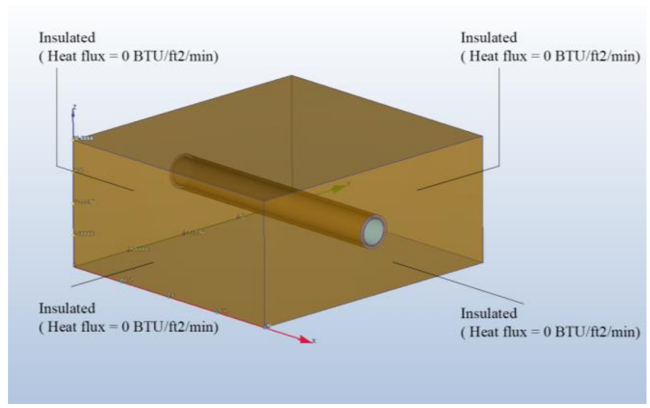

Figure 6-5: Soil Side Boundary Conditions

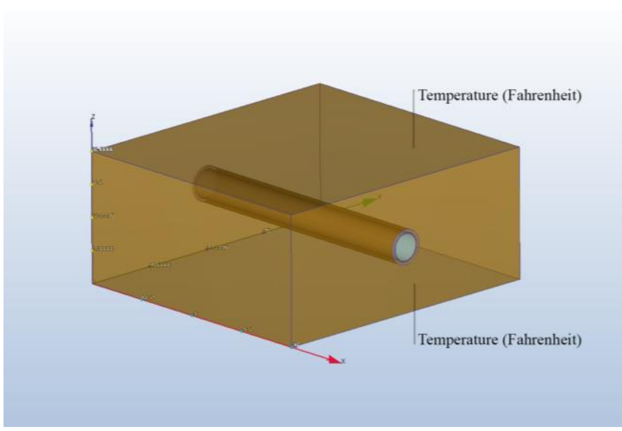

Figure 6-6: Top and Bottom Boundary Conditions

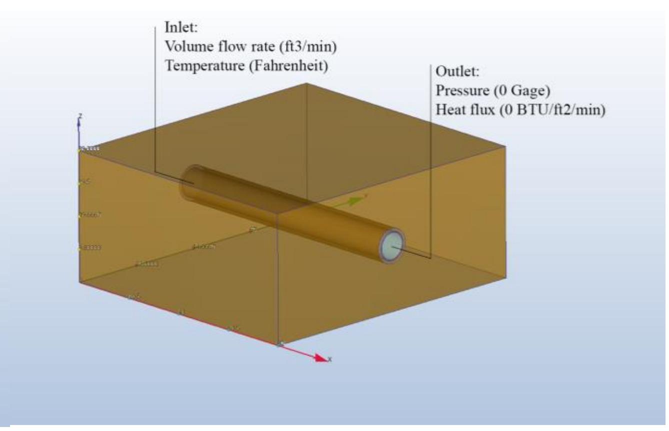

Figure 6-7: Inlet and Outlet Boundary Conditions

Table 35: Boundary Conditions for all GCV System Models

Domain	Elements	Pipe 1	Pipe 2	Pipe 3	Pipe 4	Pipe 5
Air						
	Boundary condition					
	Turbulence	k-epsilon	k-epsilon	k-epsilon	k-epsilon	k-epsilon
	Inlet temperature			**5, 15, 25, 35, 45, 55, 65, 75, 85, 95, 105, and115 Fahrenheit**		
	Inlet air Velocity	**100 fpm**	**200 fpm**	**300 fpm**	**400 fpm**	**500 fpm**
	Outlet heat flux	0 BTU/ft2/min	0 BTU/ft2/min	0 BTU/ft2/min	0 BTU/ft2/min	0 BTU/ft2/min
	Outlet pressure	0 Gage	0 Gage	0 Gage	0 Gage	0 Gage
	Physical properties					
	Density	Equation of state	Equation of state	Equation of state	Equation of state	Equation of state
	Conductivity	0.02563 w/m-k	0.02563 w/m-k	0.02563 w/m-k	0.02563 w/m-k	0.02563 w/m-k
	Specific heat	1004 J/kg-k	1004 J/kg-k	1004 J/kg-k	1004 J/kg-k	1004 J/kg-k
	Viscosity	3.79148e-07 lbf-s/ft2	3.79148e-07 lbf-s/ft2	3.79148e-07 lbf-s/ft2	3.79148e-07 lbf-s/ft2	3.79148e-07 lbf-s/ft2
Pipe						
	Boundary condition					
	Thickness			0.65, 0.73, 0.98, 1.02, 1.12, 1.52, 1.93, 2.5, 2.52, 3.09, 3.25, 3.15, 3.72, 3.98, 4.31, and 5.1 in		
	Diameter			**6,12, 24, 36, and 48 in**		
	Material	Clay	Clay	Clay	Clay	Clay
	Shape	Cylinder	Cylinder	Cylinder	Cylinder	Cylinder
	Length			**50, 150, 250, 350, and 450 feet**		
	Depth	Center of soil domain	Center of soil domain	Center of soil domain	Center of soil domain	Center of soil domain
	Physical properties					
	Conductivity	1.2 w/m-k	1.2 w/m-k	1.2 w/m-k	1.2 w/m-k	1.2 w/m-k
	Specific heat	900.16 J/kg-k	900.16 J/kg-k	900.16 J/kg-k	900.16 J/kg-k	900.16 J/kg-k
	Density	2 g/cm3	2 g/cm3	2 g/cm3	2 g/cm3	2 g/cm3
Backfill						
	Boundary condition					
	Thickness	10 in	10 in	10 in	10 in	10 in
	Type	Gravel	Gravel	Gravel	Gravel	Gravel
	Physical properties					
	Conductivity	0.7 w/m-k	0.7 w/m-k	0.7 w/m-k	0.7 w/m-k	0.7 w/m-k
	Specific heat	932 J/kg-k	932 J/kg-k	932 J/kg-k	932 J/kg-k	932 J/kg-k
	Density	2 g/cm3	2 g/cm3	2 g/cm3	2 g/cm3	2 g/cm3
Soil						
	Boundary condition					
	Type			**Clay, Limestone, and Sand**		
	Face 1 heat transfer			**Temperature = 35, 45, 55, 65, 75, 85, and 95 Fahrenheit**		
	Face 2 heat transfer			**Temperature = 35, 45, 55, 65, 75, 85, and 95 Fahrenheit**		
	Face 3 heat transfer	Heat flux = 0 BTU/ft2/min	Heat flux = 0 BTU/ft2/min	Heat flux = 0 BTU/ft2/min	Heat flux = 0 BTU/ft2/min	Heat flux = 0 BTU/ft2/min
	Face 4 heat transfer	Heat flux = 0 BTU/ft2/min	Heat flux = 0 BTU/ft2/min	Heat flux = 0 BTU/ft2/min	Heat flux = 0 BTU/ft2/min	Heat flux = 0 BTU/ft2/min
	Face 5 heat transfer	Heat flux = 0 BTU/ft2/min	Heat flux = 0 BTU/ft2/min	Heat flux = 0 BTU/ft2/min	Heat flux = 0 BTU/ft2/min	Heat flux = 0 BTU/ft2/min
	Face 6 heat transfer	Heat flux = 0 BTU/ft2/min	Heat flux = 0 BTU/ft2/min	Heat flux = 0 BTU/ft2/min	Heat flux = 0 BTU/ft2/min	Heat flux = 0 BTU/ft2/min
	Physical properties					
	Conductivity			**Clay = 1.1 w/m-k, Limeston = 1.3 w/m-k, Sand = 1.7 w/m-k**		
	Specific heat			**Clay = 1381 J/kg-k, Limeston = 909 J/kg-k, Sand = 710 J/kg-k**		
	Density			**Clay = 1.7 g/cm3, Limeston = 2.56 g/cm3, Sand = 1.7 g/cm3**		

6.2.3 Model simulations

After the GCV system models were designed and input, their performance was simulated. To save time and reduce input errors, there is a ruler setting in Autodesk CFD that helps the user to assign the boundary conditions and physical properties for a set of designs. After inputting each model and assigning the physical properties and boundary conditions, the software simulates the design, and determines outlet temperature for each pipe by presenting a convergence graph and text output at each iteration, as Figure 6-8 shows. At the end of the simulations, there were 31,500 data points for outlet temperatures. These data needed to be analyzed to find the relations between the variables and the regression model. Table 36 shows the simulation data.

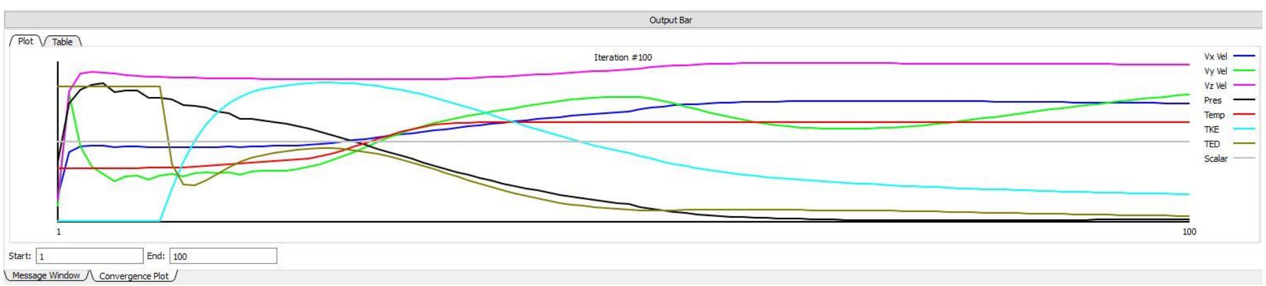

Output Bar

Iteration	Vx Vel	Vy Vel	Vz Vel	Pressure	Temp	TKE	TED	Scalar
1	1.2281e+00	6.9482e-05	-5.6223e-04	3.0802e-01	8.2050e+01	1.4048e-04	9.9475e-01	0.0000e+00
2	1.5613e+00	1.4388e-04	-1.3678e-04	5.8425e-01	8.2050e+01	1.4048e-04	9.9475e-01	0.0000e+00
3	1.6057e+00	1.0929e-04	-6.8642e-05	6.5145e-01	8.2051e+01	1.4048e-04	9.9475e-01	0.0000e+00
4	1.6106e+00	9.5290e-05	-6.2044e-05	6.7479e-01	8.2052e+01	1.4048e-04	9.9475e-01	0.0000e+00
5	1.6090e+00	9.0883e-05	-6.6074e-05	6.8157e-01	8.2054e+01	1.4048e-04	9.9475e-01	0.0000e+00
6	1.5981e+00	8.5715e-05	-6.9051e-05	6.4063e-01	8.2059e+01	1.4048e-04	9.9475e-01	0.0000e+00
7	1.6033e+00	8.8985e-05	-7.4419e-05	6.4878e-01	8.2069e+01	1.4048e-04	9.9475e-01	0.0000e+00
8	1.6038e+00	8.9538e-05	-7.8585e-05	6.4613e-01	8.2084e+01	1.4048e-04	9.9475e-01	0.0000e+00
9	1.5967e+00	8.6784e-05	-8.0230e-05	6.1402e-01	8.2106e+01	1.4048e-04	9.9475e-01	0.0000e+00
10	1.6002e+00	8.9478e-05	-8.2221e-05	6.1275e-01	8.2135e+01	1.4048e-04	9.9475e-01	0.0000e+00
11	1.6009e+00	9.0558e-05	-8.3653e-05	6.0534e-01	8.2163e+01	6.0330e-02	5.2703e-01	0.0000e+00
12	1.5960e+00	8.9193e-05	-8.4207e-05	5.7905e-01	8.2233e+01	1.0904e-01	4.0665e-01	0.0000e+00
13	1.5988e+00	9.1011e-05	-8.5288e-05	5.7380e-01	8.2345e+01	1.4814e-01	4.0213e-01	0.0000e+00

Start: 1 End: 100

Message Window / Convergence Plot

Figure 6-8: Solver Convergence Graph and Text Output at Each Iteration

Table 36: GCV System Simulation Data

Model	soil type	Diameter	soil temp	Pipe length	Velocity f/min	Inlet temp	outlet temp
1	clay	6	35	50	50	5	30.02
2	clay	6	35	50	50	15	31.79
3	clay	6	35	50	50	25	33.45
4	clay	6	35	50	50	35	35.00
5	clay	6	35	50	50	45	36.45
6	clay	6	35	50	50	55	37.81
7	clay	6	35	50	50	65	39.07
8	clay	6	35	50	50	75	40.26
9	clay	6	35	50	50	85	41.36
10	clay	6	35	50	50	95	42.39
11	clay	6	35	50	50	105	43.35
12	clay	6	35	50	50	115	44.24
13	clay	6	35	50	150	5	22.29
14	clay	6	35	50	150	15	26.65
15	clay	6	35	50	150	25	30.89
16	clay	6	35	50	150	35	35.00
17	clay	6	35	50	150	45	39.00
18	clay	6	35	50	150	55	42.88
19	clay	6	35	50	150	65	46.65
20	clay	6	35	50	150	75	50.32
21	clay	6	35	50	150	85	53.88
22	clay	6	35	50	150	95	57.34
23	clay	6	35	50	150	105	60.70
24	clay	6	35	50	150	115	63.97
25	clay	6	35	50	250	5	22.29
26	clay	6	35	50	250	15	26.65
27	clay	6	35	50	250	25	30.89
28	clay	6	35	50	250	35	35.00
29	clay	6	35	50	250	45	39.00
30	clay	6	35	50	250	55	42.88
31	clay	6	35	50	250	65	46.65
32	clay	6	35	50	250	75	50.32
31479	sand	48	95	450	350	25	47.41
31480	sand	48	95	450	350	35	54.49
31481	sand	48	95	450	350	45	61.46
31482	sand	48	95	450	350	55	68.35
31483	sand	48	95	450	350	65	75.14
31484	sand	48	95	450	350	75	81.85
31485	sand	48	95	450	350	85	88.47
31486	sand	48	95	450	350	95	95.00
31487	sand	48	95	450	350	105	101.45
31488	sand	48	95	450	350	115	107.81
31489	sand	48	95	450	450	5	32.98
31490	sand	48	95	450	450	15	40.25
31491	sand	48	95	450	450	25	47.41
31492	sand	48	95	450	450	35	54.49
31493	sand	48	95	450	450	45	61.46
31494	sand	48	95	450	450	55	68.35
31495	sand	48	95	450	450	65	75.14
31496	sand	48	95	450	450	75	81.85
31497	sand	48	95	450	450	85	88.47
31498	sand	48	95	450	450	95	95.00
31499	sand	48	95	450	450	105	101.45
31500	sand	48	95	450	450	115	107.81

6.3 Summary

This chapter can be summarized as follows:

- **Simulation variables:** many parameters, both exogenous and endogenous, affect the performance of the GCV system. These research variables include air temperature, ground temperature, soil type, pipe length, pipe diameter and air flow velocity with limitation. The other variables were fixed.
- **GCV system designs:** the GCV system was designd based on the GCV system variables from pipe length (5 levels), pipe diameter (5 levels) and soil type (3 levels). To save time, the variance in air flow velocity (5 levels) was simulated in one model, which resulted in 75 models. The inlet temperature (12 levels) and ground temperature (7 levels) were inserted to the 75 models to be simulated. In all, 6,300 simulations were performed resulting in 31,500 outlet temperatures from all possible design combinations.
- **Simulation boundary conditions:** the GCV system was divided into four domains: air, pipe, backfill, and soil. Each domain had physical properties and boundary conditions to be assigned. For the physical properties, each material in the domain was described by thermal conductivity, heat capacity, and density. For the boundary conditions, six faces were assigned to the soil. Air boundary conditions, inlet temperature, and air velocity were assigned to the inlet. Pressure and heat flux were found in the outlet. The boundary conditions for all possible combinations of the variables in the simulations can be found in Table 35.
- **Model simulations:** Autodesk CFD was used to simulate all GCV system designs using a ruler setting that helps to assign the boundary conditions and physical properties for a set of designs to determines outlet temperature for each pipe. At the end of the simulations, there were 31,500 data points for outlet temperatures.

Chapter 7: Simulation Data and Regression Analysis

This chapter discusses the simulation results and regression analysis. The analysis of the simulation results was carried out to determine the relations between the GCV system variables. Regression analysis was performed to obtain statistical models that predicted the GCV system performance as inferred by the outlet temperature and difference in inlet and outlet temperatures. Finally, the regression models were validated using 10% of the actual data and compared to the predicted data.

7.1 Simulation Data Analysis

After collecting the 31,500 simulation data points, they were partitioned based on cooling or heating operation, both of which rely on the inlet and ground temperatures. If the inlet temperature is higher than the ground temperature, the system is cooling, while if it is lower than the ground temperature, the system is heating. After partitioning the data, there were 15,750 cooling system data points and 18,375 heating system data points. All data needed to be analyzed to identify the relations between the variables. As Figure 7-1 to Figure 7-14 show, there was linear relation between soil type, pipe diameter, pipe length, soil temperature, inlet temperature, and airflow velocity with outlet temperature for both cooling and heating system. On the one hand, in the cooling system, there were positive linear relations between pipe diameter, airflow velocity, soil temperature, and inlet temperature with outlet temperature. There were negative linear relations between pipe length and outlet temperature, indicating that if pipe length increases, the outlet temperature will decrease, as Figure 7-15 shows. On the other hand, in the heating system, there were negative linear relations between pipe diameter, airflow velocity, soil temperature, and inlet temperature with outlet temperature. Also, there was a positive linear relation between pipe length and outlet temperature, which indicates that if the pipe length increases, the outlet temperature increases as well, as Figure 7-16 shows. To know which variable is the most effective in the system, each variable was standardized to see the effect of each unit variable on the outlet temperature. As Figure 7-15 and Figure 7-16 show, the inlet and outlet temperature was the highest effective variable, followed by pipe diameter, pipe length, and airflow velocity respectively. By checking the interaction between the variables, Table 37 and Table 38 show that there were no high correlations between the pair-wise variables. Figure 7-17 and Figure 7-18 represent the correlation between the variables.

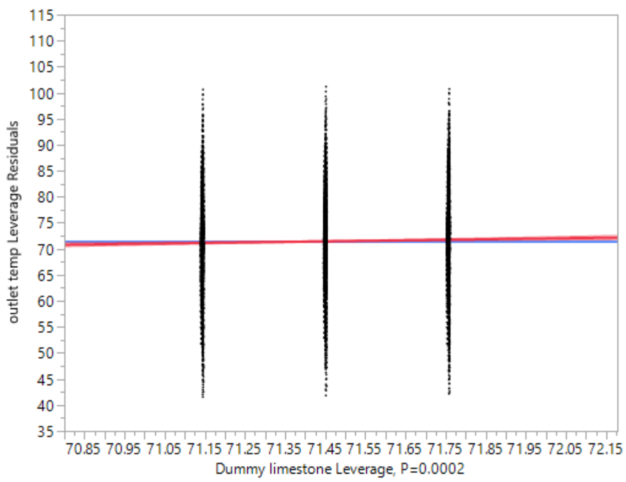

Figure 7-1: The Relation Between the Outlet Temperature and Soil Type (Limestone) in Cooling System

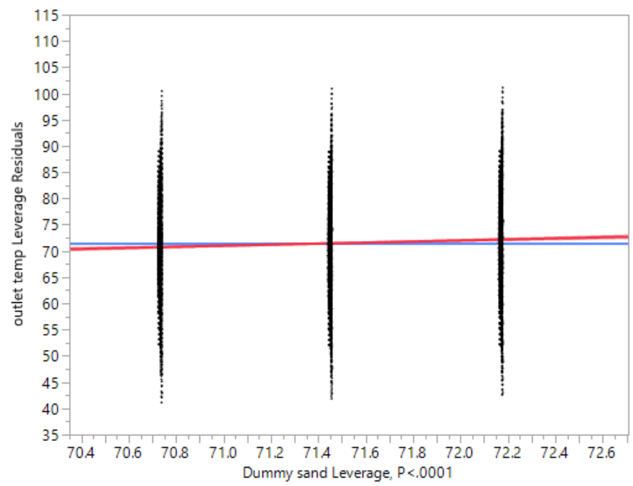

Figure 7-2: The Relation Between the Outlet Temperature and Soil Type (Sand) in Cooling System

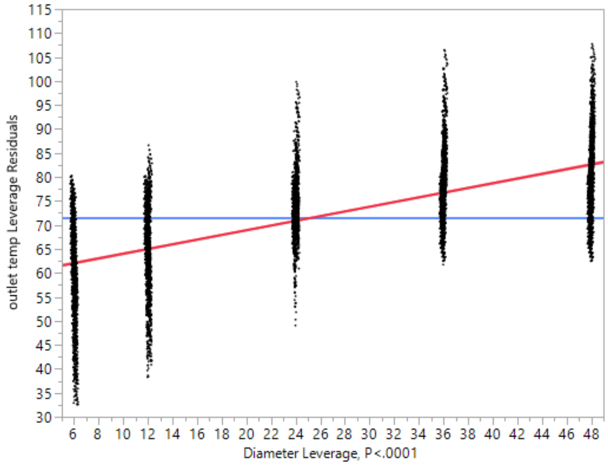

Figure 7-3: The Relation Between the Outlet Temperature and Pipe Diameter in Cooling System

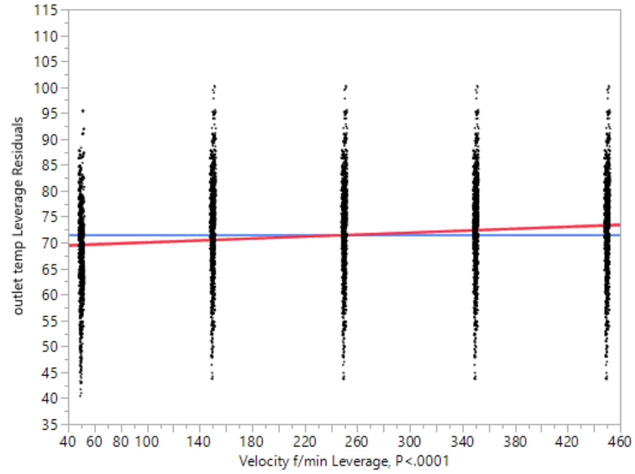

Figure 7-4: The Relation Between the Outlet Temperature and Airflow Velocity in Cooling System

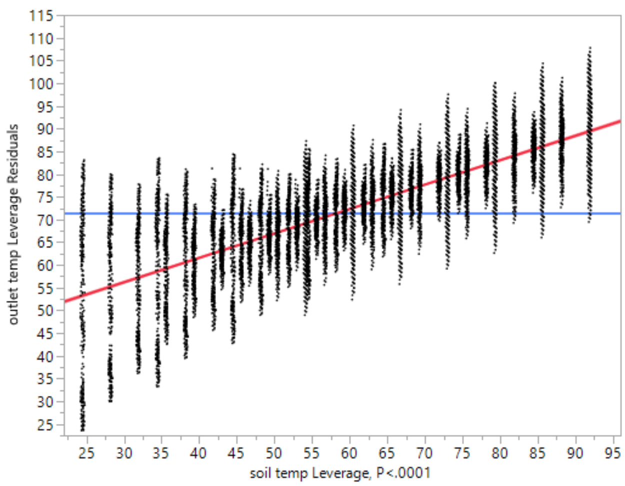

Figure 7-5: The Relation Between the Outlet Temperature and Soil Temperature in Cooling System

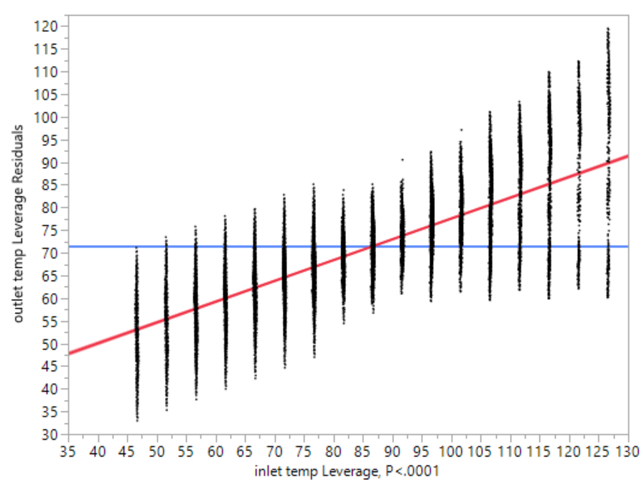

Figure 7-6: The Relation Between the Outlet Temperature and Inlet Temperature in Cooling System

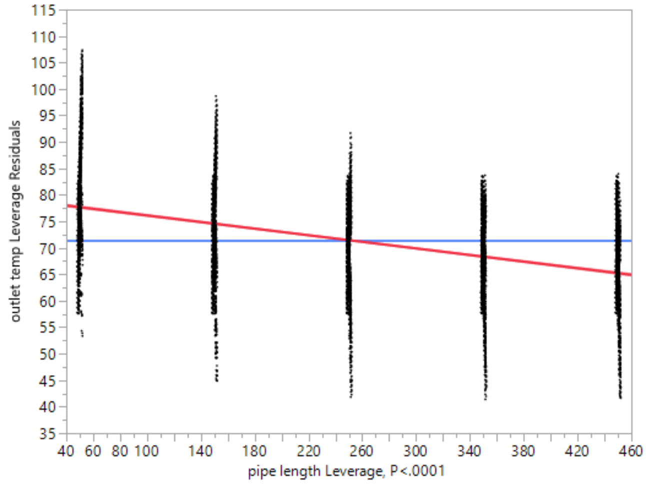

Figure 7-7: The Relation Between the Outlet Temperature and Pipe Length in Cooling System

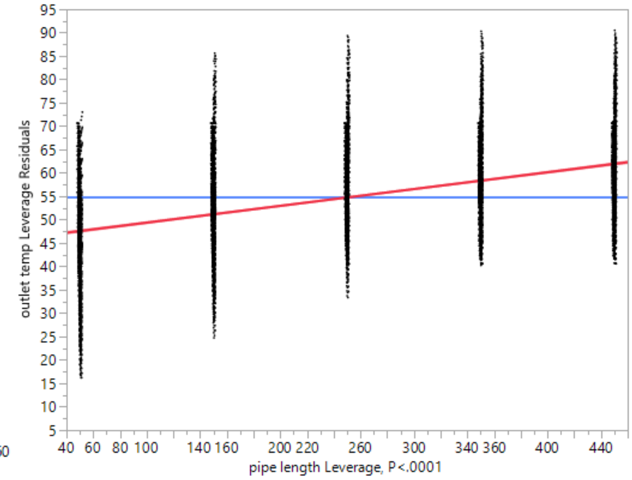

Figure 7-8: The Relation Between the Outlet Temperature and Pipe Length in Heating System

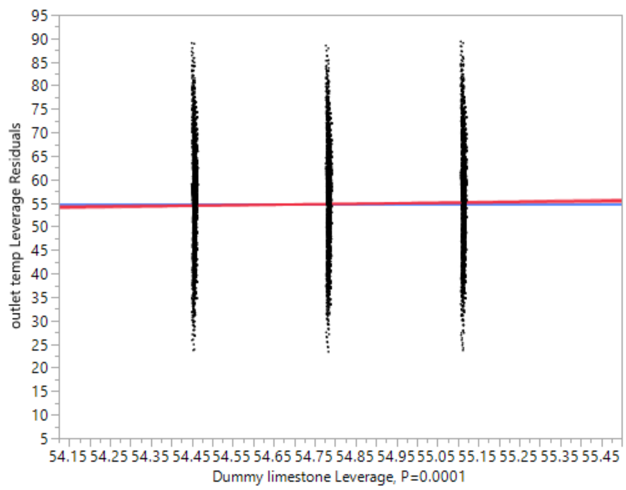

Figure 7-9: The Relation Between the Outlet Temperature and Soil Type (Limestone) in Heating System

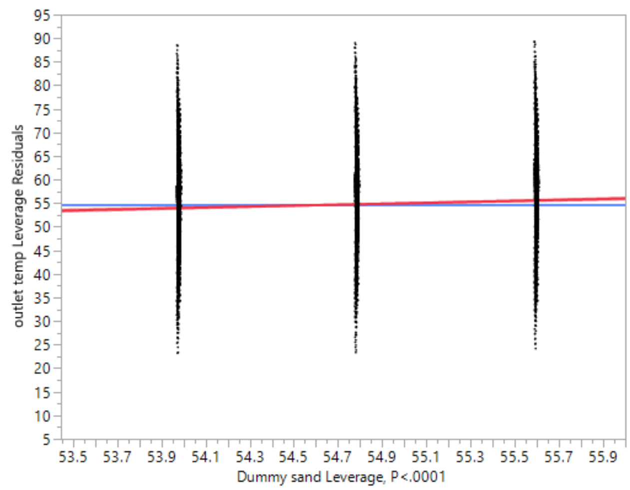

Figure 7-10: The Relation Between the Outlet Temperature and Soil Type (Sand) in Heating System

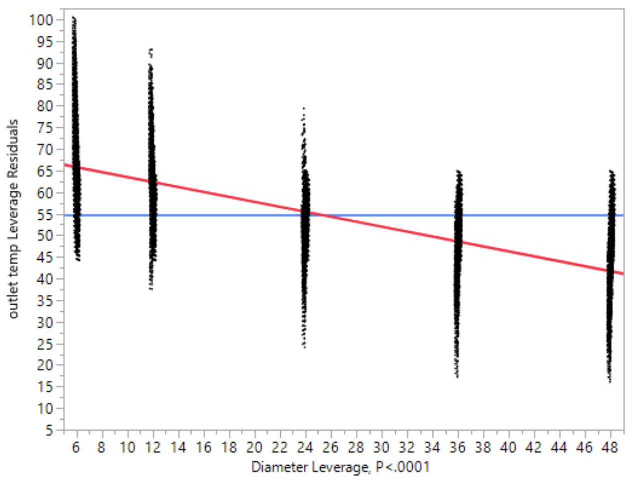

Figure 7-11: The Relation Between the Outlet Temperature and Pipe Diameter in Heating System

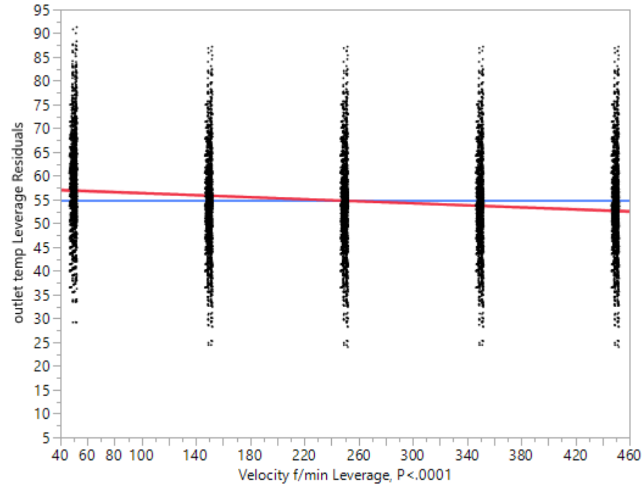

Figure 7-12: The Relation Between the Outlet Temperature and Airflow Velocity in Heating System

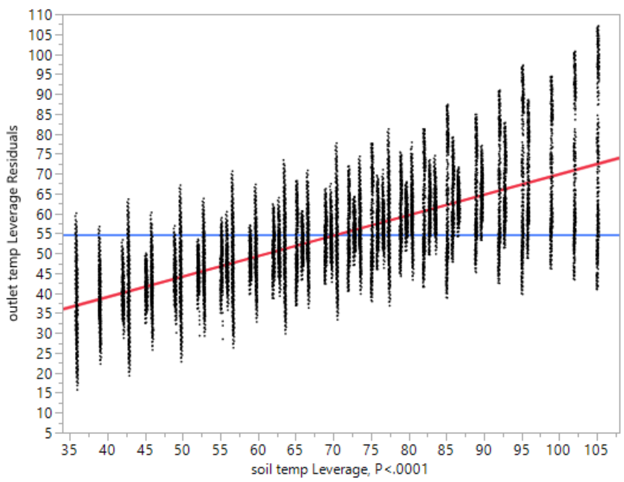

Figure 7-13: The Relation Between the Outlet Temperature and Soil Temperature in Heating System

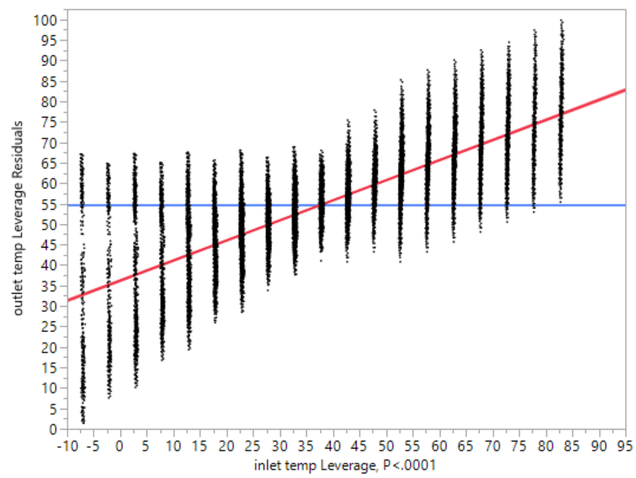

Figure 7-14: The Relation Between the Outlet Temperature and Inlet Temperature in Heating System

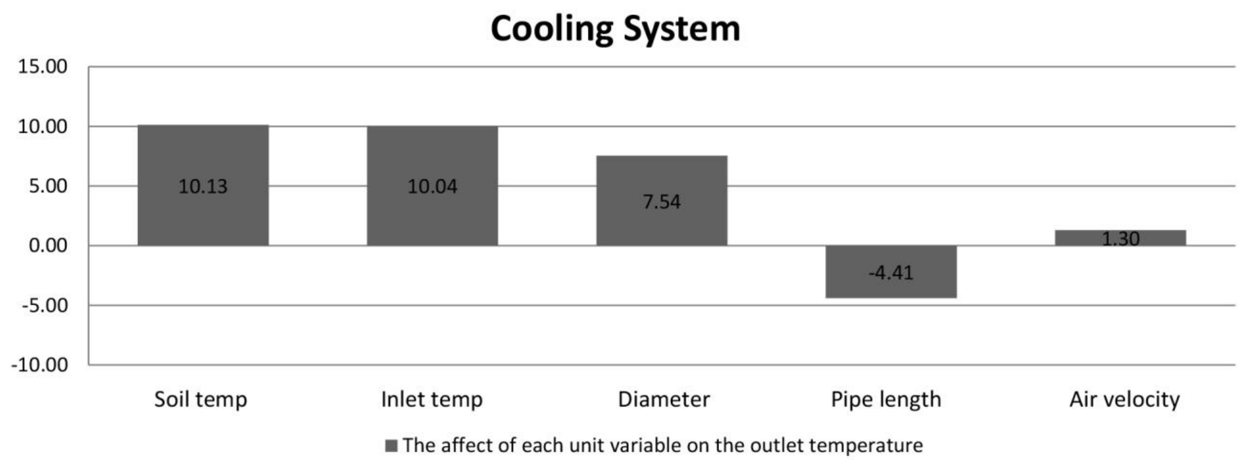

Figure 7-15: The Relations Between GCV System Variables in Cooling System

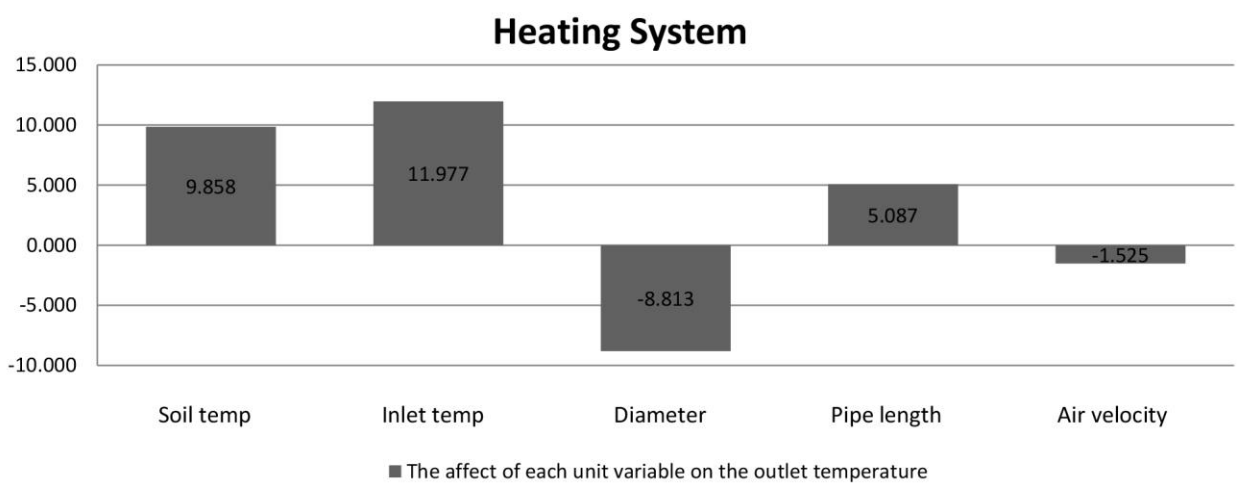

Figure 7-16: The Relations Between GCV System Variables in Heating System

Table 37: Multivariate Cooling System

Row	Diameter	Velocity f/min	Soil temp	Pipe length	Inlet temp	Outlet temp
Diameter	1	0	0	0	0	0.362364608
Velocity f/min	0	1	0	0	0	0.062675493
Soil temp	0	0	1	0	0.430082665	0.694020098
Pipe length	0	0	0	1	0	-0.211757052
Inlet temp	0	0	0.430082665	0	1	0.691564318
Outlet temp	0.362364608	0.062675493	0.694020098	-0.211757052	0.691564318	1

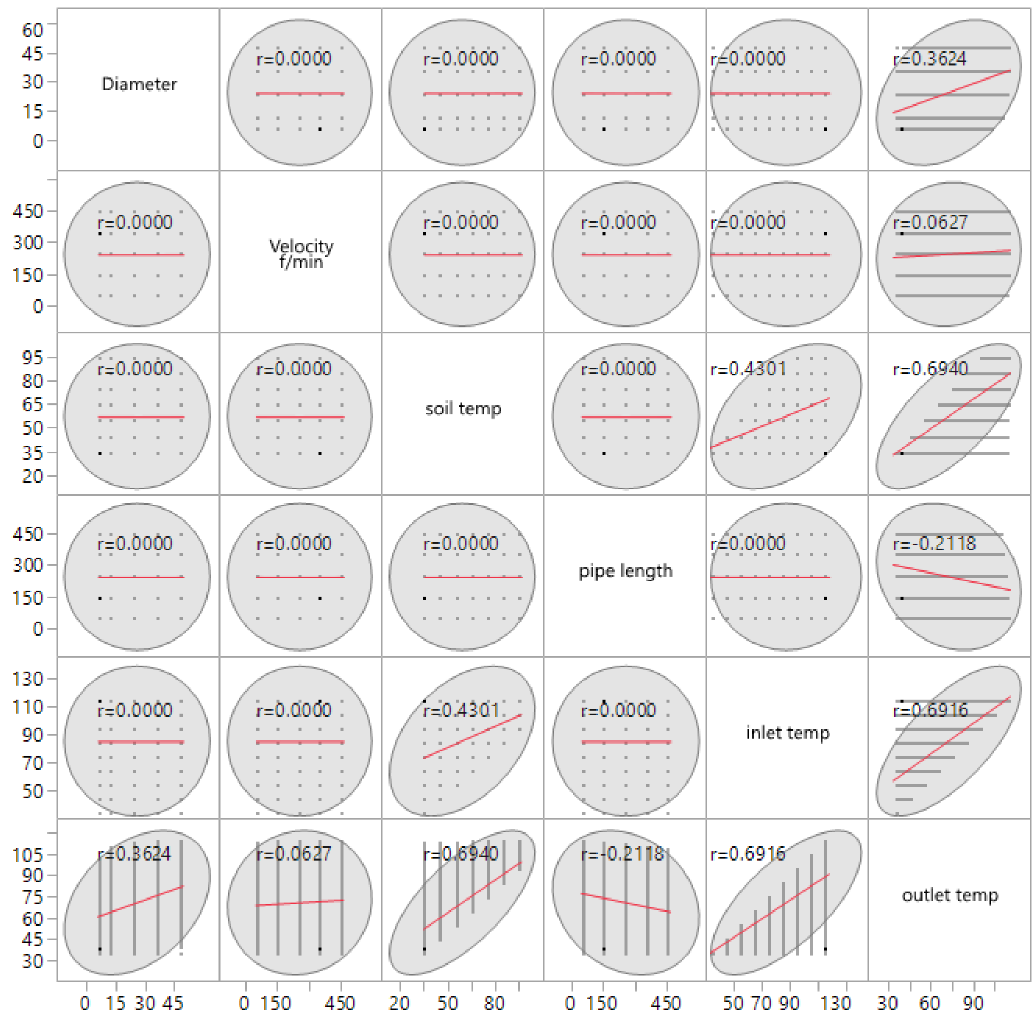

Figure 7-17: Correlation in Cooling System Variables

Table 38: Multivariate Heating System

Row	Diameter	Velocity f/min	Soil temp	Pipe length	Inlet temp	Outlet temp
Diameter	1	0	0	0	0	-0.385955785
Velocity f/min	0	1	0	0	0	-0.066766448
Soil temp	0	0	1	0	0.393919299	0.638312672
Pipe length	0	0	0	1	0	0.222778717
Inlet temp	0	0	0.393919299	0	1	0.694556078
Outlet temp	-0.385955785	-0.066766448	0.638312672	0.222778717	0.694556078	1

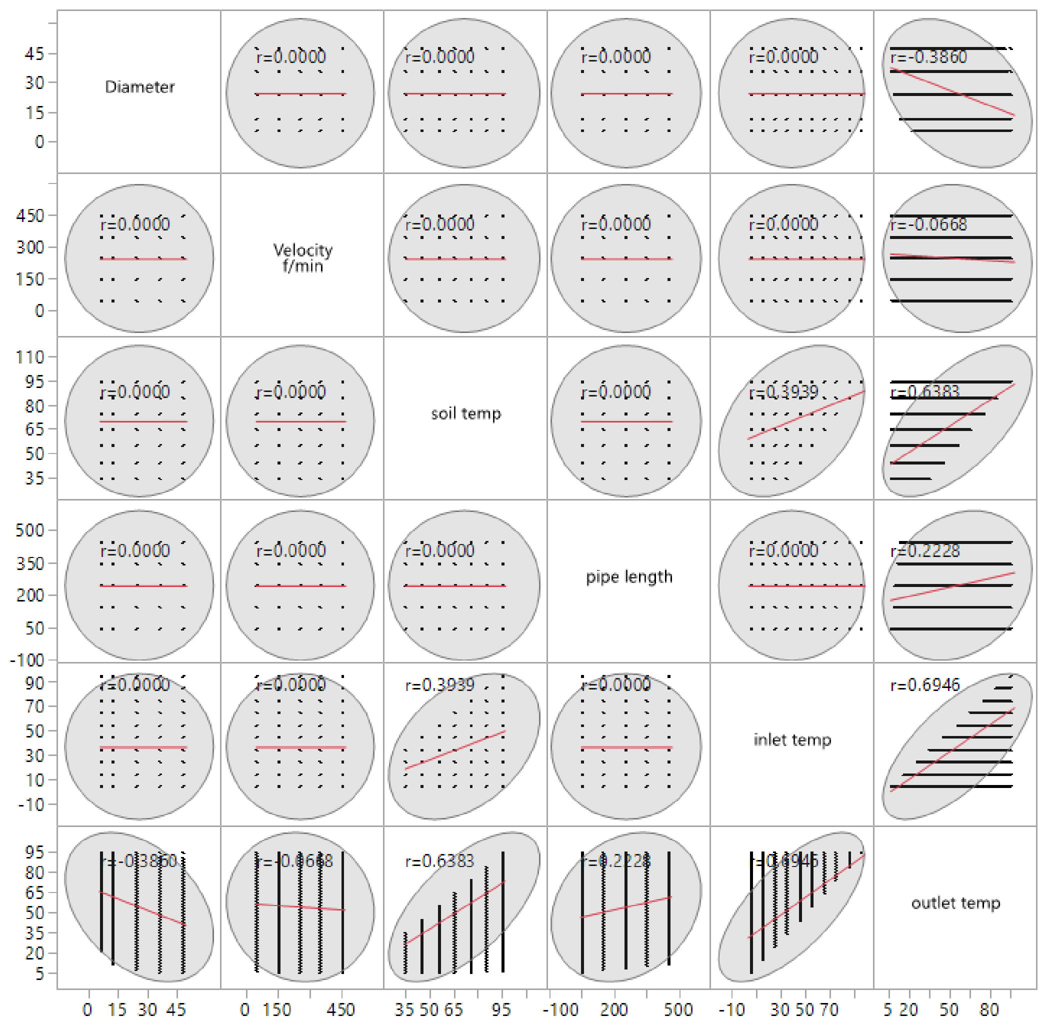

Figure 7-18: Correlation in Heating System Variables

7.2 Regression Analysis

JMP software was used to perform the regression analysis. Overall, 90% of the cooling and heating data from the GCV system simulation were analyzed to create the regression models. The remaining 10% was held out for use in the validation process. Since the relations between the GCV system variables were linear, a multiple linear regression was applied. Equation 10 and Equation 11 show the regression models for cooling and heating system. Table 39 and Table 40 show that all of the cooling and heating variables for the regression models were significant because the p-value is zero. The variance inflation factor (VIF) was small, which indicates that there was no multicollinearity between the variables. The cooling regression model predicted 85.21% of the variance in outlet temperature with a RMSE of 7.99^{o}F, as Table 41 shows. The heating regression model predicted 84.28% of the variance in outlet temperature with a RMSE of 9.04^{o}F, as Table 42 shows. Finally, as Equation 10 and Equation 11 show, the regression equation needed to be validated using the remaining 10% of the data.

Moreover, the cooling and heating system residuals (a residual is the distance between the predicted best fit line and a data point) in Figure 7-21 and Figure 7-22 were bell shaped, so they followed a normal distribution. The variance of these models was random, as shown (see Table 41 and Table 42). Finally, these regression equations needed to be validated using the remaining 10% of the data.

Table 39: Cooling System Regression Variables

Term	Estimate	Std Error	t Ratio	Prob>|t|	VIF
Intercept	-6.94	0.36	-19.34	<.0001	
Dummy limestone[0]	0.31	0.08	3.73	0.00	1.33
Dummy sand[0]	0.72	0.08	8.74	<.0001	1.33
Diameter	0.49	0.00	111.83	<.0001	1.00
Velocity f/min	0.01	0.00	19.87	<.0001	1.00
Soil temp	0.54	0.00	136.19	<.0001	1.23
Pipe length	-0.03	0.00	-65.55	<.0001	1.00
Inlet temp	0.46	0.00	135.11	<.0001	1.23

Table 40: Heating System Regression Variables

Term	Estimate	Std Error	t Ratio	Prob>|t|	VIF
Intercept	8.44	0.34	24.47	<.0001	
Dummy limestone[0]	-0.33	0.09	-3.82	<.0001	1.330
Dummy sand[0]	-0.81	0.09	-9.40	<.0001	1.330
Diameter	-0.57	0.00	-125.39	<.0001	1.000
Velocity f/min	-0.01	0.00	-21.57	<.0001	1.000
Soil temp	0.51	0.00	128.72	<.0001	1.181
Pipe length	0.04	0.00	72.27	<.0001	1.000
Inlet temp	0.49	0.00	156.15	<.0001	1.181

Equation 10: Regression Model for the Cooling System

$$Outlet\ Temperature = (-6.93) + if\ \frac{Limestone = -0.30}{Sand\ or\ Clay = 0.30} + if\ \frac{Sand = -0.71}{Limestone\ or\ Clay = 0.71}$$

$$+(0.49 \times Pipe\ Diameter) + (0.0094 \times Air\ Velocity)$$

$$+(0.54 \times Soil\ Temperature) + (-0.036 \times Pipe\ Length) + (0.46 \times Inlet\ Temperature)$$

Equation 11: Regression Model for the Heating System

$$Outlet\ Temperature = (8.35) + if\ \frac{Limestone = 0.32}{Sand\ or\ Clay = -0.32} + if\ \frac{Sand = 0.80}{Limestone\ or\ Clay = -0.80}$$

$$+(0.57 \times Pipe\ Diameter) + (-0.010 \times Air\ Velocity)$$

$$+(0.51 \times Soil\ Temperature) + (0.036 \times Pipe\ Length) + (0.49 \times Inlet\ Temperature)$$

Table 41: Cooling System Fit Model Summary

RSquare	0.852221
RSquare Adj	0.852148
Root Mean Square Error	7.998117
Mean of Response	71.45054
Observations (or Sum Wgts)	14175

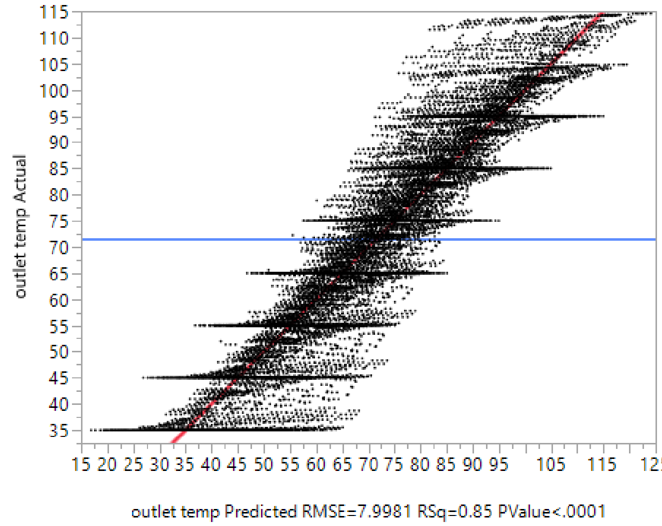

Figure 7-19: Actual vs. Predicted Outlet Temperature for Cooling System Regression Model

Table 42: Heating System Fit Model Summary

RSquare	0.8429
RSquare Adj	0.8428
Root Mean Square Error	9.0442
Mean of Response	54.7851
Observations (or Sum Wgts)	16537.0000

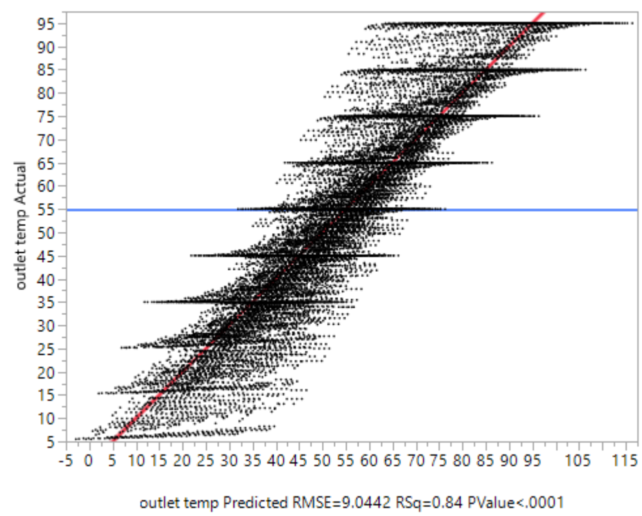

Figure 7-20: Actual vs. Predicted Outlet Temperature for Heating System Regression Model

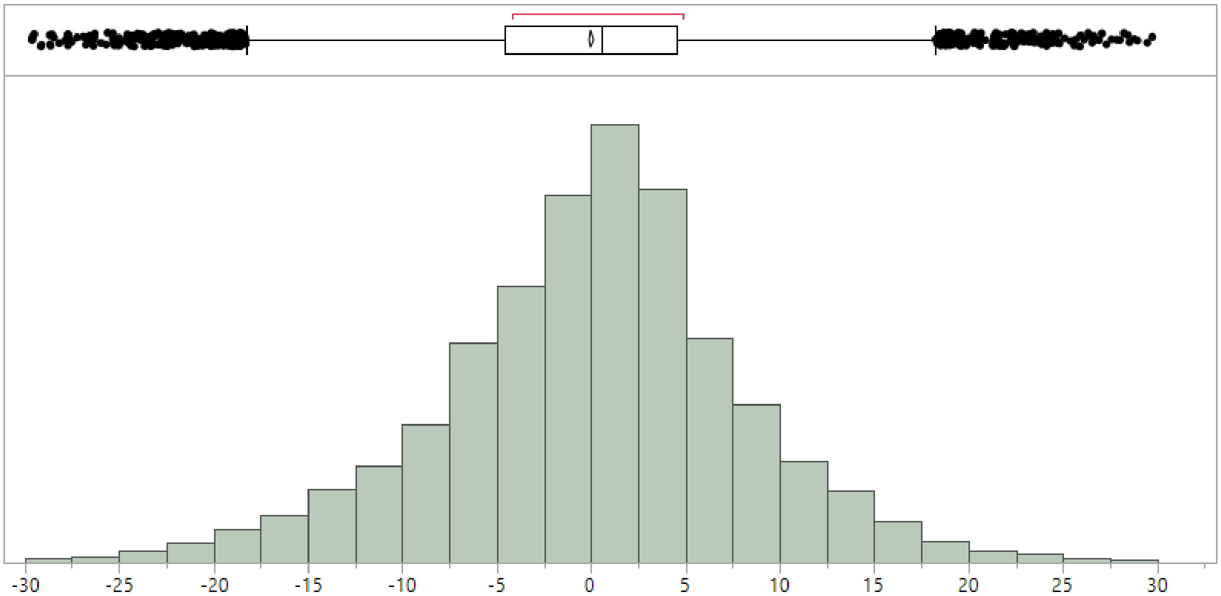

Figure 7-21: Cooling System Regression Residuals

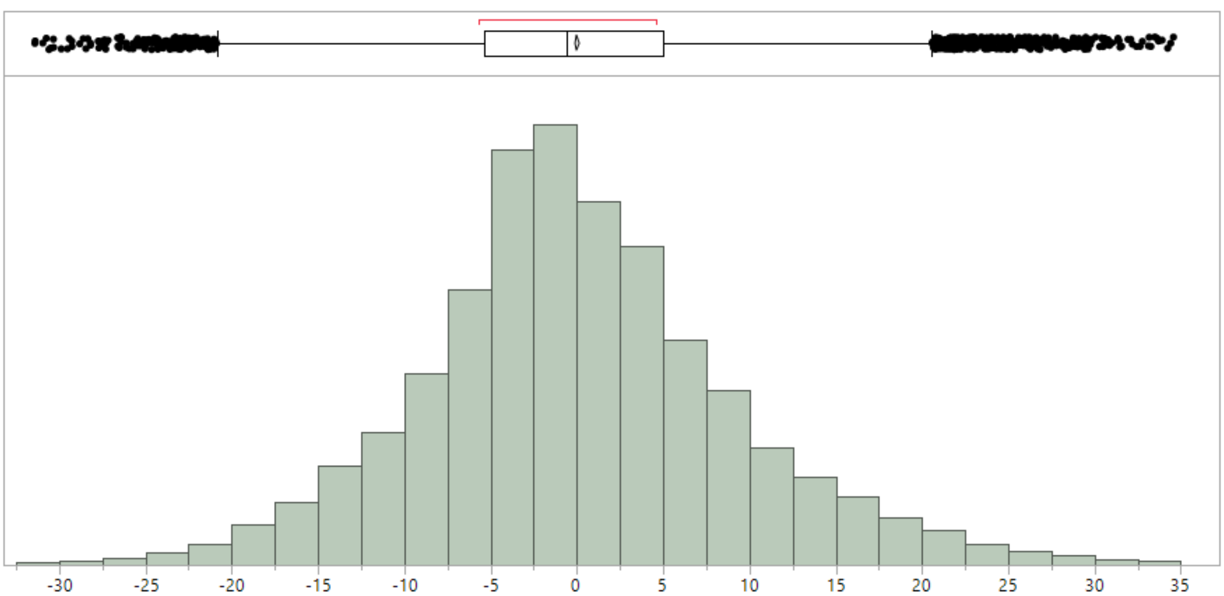

Figure 7-22: Heating System Regression Residuals

7.3 Regression Validation

The regression models for the cooling and heating systems needed to be validated using the remaining 10% of the GCV system simulation data. To perform this validation, a comparison was made between the outlet temperature predictions from the regression models and the values from the remaining 10% of the in-situ GCV system data. The soil type, soil temperature, airflow velocity, pipe length, pipe diameter, and inlet air temperature for the corresponding conditions of the 10% data were input to the regression models and the outlet temperatures were predicted and saved. A second regression analysis was then performed where the predictions from the regression models were correlated with the outlet temperatures from the simulation data (10%). The process is described by Equation 12 and Equation 13:

Equation 12: Regression Model Validation for Cooling System

$$Outlet\ Temp\ (10\%\ Simulation\ data)\ =\ 0.6368498\ +\ 0.9922883 * Outlet\ Temp\ (Regression\ model)$$

Equation 13: Regression Model Validation for Heating System

$$Outlet\ Temp\ (10\%\ Simulation\ data)\ =\ -1.249721\ +\ 1.0279206 * Outlet\ Temp\ (Regression\ model)$$

As a result of the validation, the predicted cooling model had a RMSE of 8.08^{o}F, and the predicted heating model had a RMSE of 8.08^{o}F. This indicated that the error in predicting the outlet temperature was ± 8.08 for the cooling model and ±8.08 for the heating model, respectively. The results from this analysis for the cooling and heating models can be summarized as Table 43, Figure 7-23, Table 44 and Figure 7-24 show. Accordingly, this provided confidence that the regression models are good predictors.

Table 43: Cooling System Regression Validation
Summary

RSquare	0.851134
RSquare Adj	0.851039
Root Mean Square Error	8.085743
Mean of Response	71.51067
Observations (or Sum Wgts)	1575

Table 44: Heating System Regression Validation Summary

RSquare	0.851134
RSquare Adj	0.851039
Root Mean Square Error	8.085743
Mean of Response	71.51067
Observations (or Sum Wgts)	1575

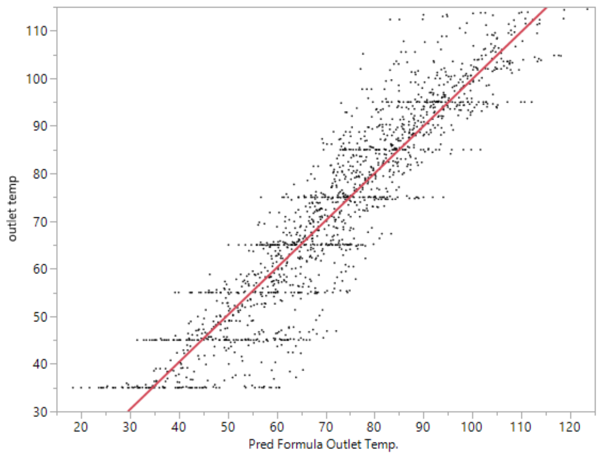

Figure 7-23: Cooling System's Actual vs. Predicted Outlet Temperature

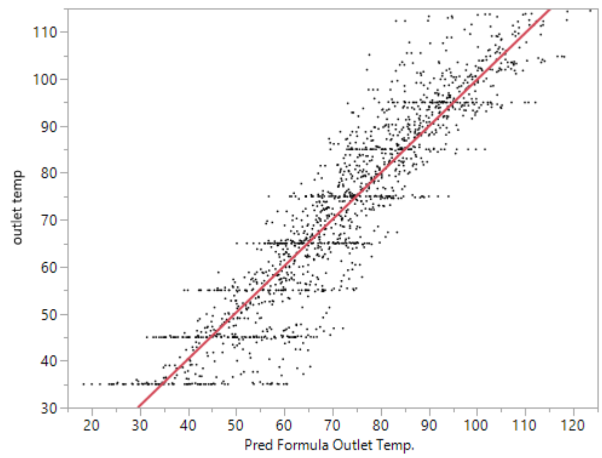

Figure 7-24: Heating System's Actual vs. Predicted Outlet Temperature

7.4 Summary

This chapter can be summarized as follows:

- **Simulation data analysis:** after collecting the 31,500 simulation data points, they were partitioned based on operation (either cooling or heating), both of which rely on the inlet and ground temperatures to see the relations between the variables. In the cooling system, there were positive linear relations between pipe diameter, airflow velocity, soil temperature, and inlet temperature with outlet temperature. There were negative linear relations between pipe length and outlet temperature. In the heating system, there were negative linear relations between pipe diameter, airflow velocity, soil temperature, and inlet temperature with outlet temperature. Also, there was a positive linear relation between pipe length and outlet temperature.
- **Regression analysis:** the reason to use the regression analysis is becasuse the regression model captured all CFD modeling runs to predict the outlet temperautre. Overall, 90% of the cooling and heating data from the GCV system simulation were analyzed to create the regression models. The remaining 10% was held out for use in the validation process. The regression indicated that there is no multicolilineraity between the variables. The cooling model predicted 85.21% of the variance in outlet temperature with a RMSE of 7.99^{o}F. The heating regression model predicted 84.28% of the variance in outlet temperature with a RMSE of 9.04^{o}F. Both models follow normal distirbution with a random variance.
- **Regrssion validation:** a comparison was made between the outlet temperature predictions from the regression models and the values from the remaining 10% of the GCV system data. As a result of the validation, the error in predicting the outlet temperature was ± 8.08 for the cooling model and ±8.08 for the heating model, respectively.

Chapter 8: GCV System Evaluation Tool

This chapter discusses the development of the GCV system evaluation tool, which was the primary goal of this research. The process for validation the GCV tool is also presented. Finally, guidelines are presented to help the user use the tool.

8.1 Tool Development

The GCV system evaluation tool predicts the performance based on the input of design parameters. This tool uses the cooling and heating regression models to predict the performance of a GCV system. MATLAB software was used for the interface and for algorithmic coding. For purposes of development, the tool was divided into three sections: tool input, processing, and output. Figure 8-1 shows a summary of the tool development process:

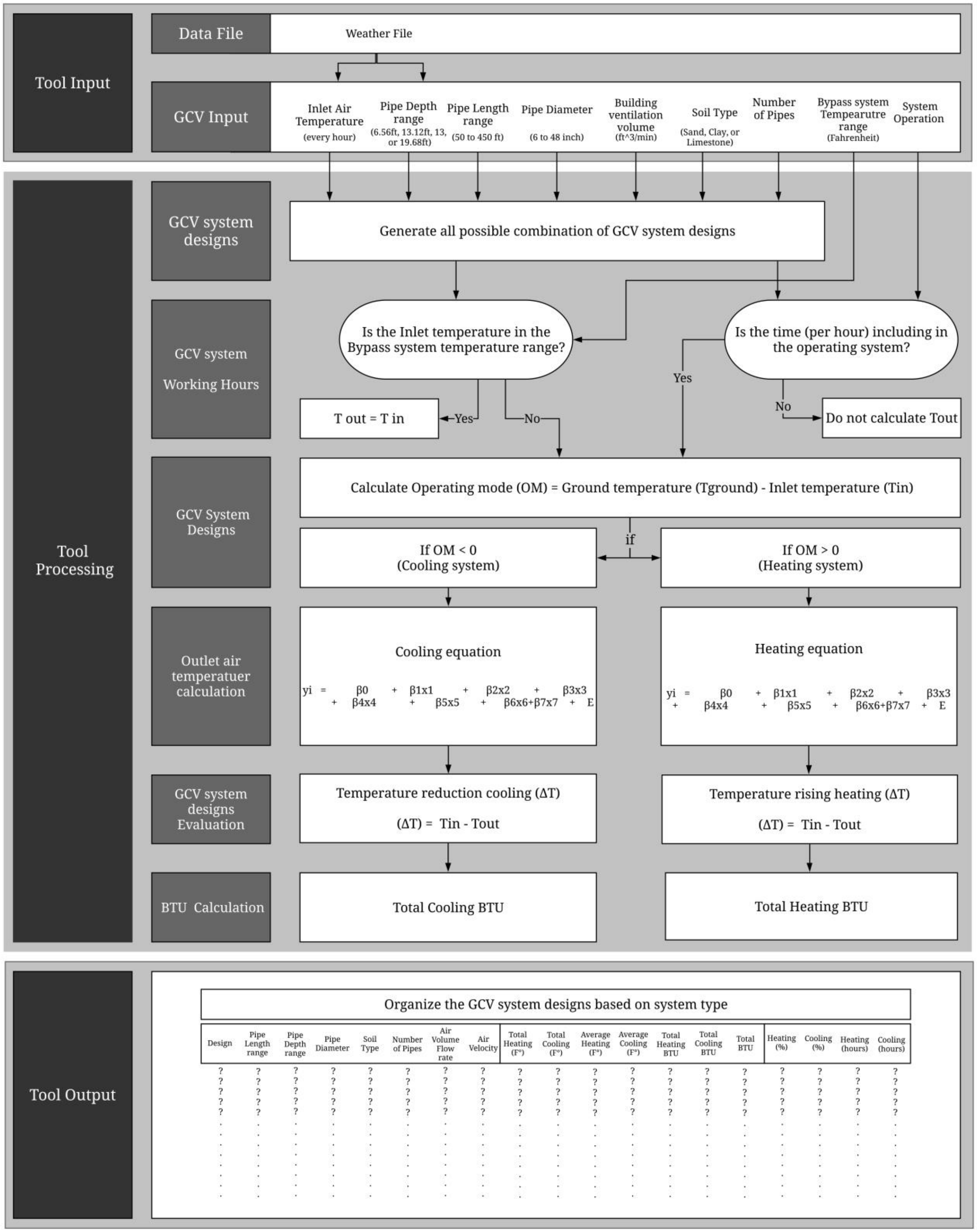

Figure 8-1: GCV System Evaluation Tool Processing

8.1.1 Tool input

The first phase involved the input logic and user interface. This was divided into two sections: importing the weather file and inputting the GCV system parameters. The tool was programmed to import and process data from a TMY (typical meteorological year) weather file (.xlsx). The file provides information about the location, latitude, longitude, source, and air and ground temperatures. The most critical information from the weather file is the air and ground temperatures. The weather file presents the ambient air temperature for each hour and the monthly mean ground temperature at three depths: 1.64, 6.56, and 13.12 feet. This information was used as input in the regression model.

The second input is the GCV system parameters. The tool is programmed to prompt for GCV system parameters including pipe length, pipe depth, pipe diameter, soil type, building volume flow rate, system operation time, and whether there is a bypass system or not. The pipe length input needs to be a fixed number (1 foot as a minimum input) or a range with an interval of 10 feet. There are three allowable pipe depths (1.64, 6.56, and 13.12 feet) corresponding to the ground temperatures from the weather file data. The pipe diameters range from 4, 6, 8, 10, 12, 15, 18, 21, 24, 27, 30, 32, 36, 39, 42, to 48 (which are the standard pipe diameters currently available on the market). There are three soil types: clay, sand, and limestone. However, the user may choose more than one type to see the performance differences if the soil is changed. For the volume flow rate, the user needs to calculate the required ventilation for the building using the American Society of Heating, Refrigerating and Air-Conditioning Engineers (ASHRAE) standard 55, or using energy modeling software, such as eQUEST. The last input is the bypass system, which is a system that allows the building to take in the outside air without using the GCV system when the outside air temperature is more beneficial than the air temperature from the GCV system. All inputs are used to define the performance of alternative GCV system designs.

8.1.2 Tool processing

After inputting the required information, there are six phases of processing: first, calculating the GCV system hours of operation; second, generating all possible design combinations; third, determining the operating mode (i.e., heating or cooling); fourth, calculating the outlet temperature; fifth, calculating the inlet-outlet temperature differences, respectively; and sixth, calculating the annual amount of energy reduction associated with the system operation, as Figure 8-2 shows.

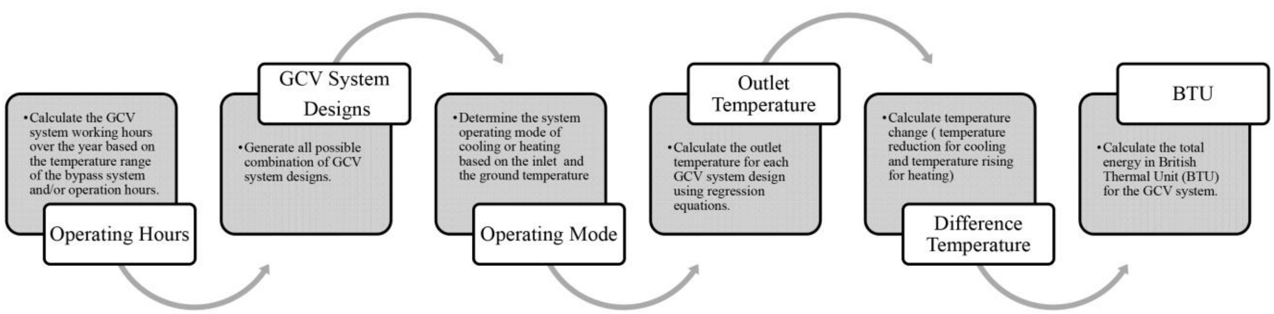

Figure 8-2: Tool Calculation Process

First, the tool calculates the GCV system hours of operation. The system working hours is determined based on the weather file that provides the hourly air temperature. As a default, the GCV system works the entire time unless the bypass system and/or the operation time setting affects it. Because the bypass system has a temperature range, the GCV system will not work if the inlet temperature is within the bypass system's temperature range. Therefore, the times at which the inlet temperature is in the bypass temperature range will not be calculated for the GCV system's working time. The operation time for the system can be set for each day in the week with working time range in a day. The selected days and time will be counted as the operation time of the system.

Second, based on the descriptive input all possible combinations of the GCV system, variables and ranges from pipe length, depth, diameter, soil type, volume flow rate, and number of pipes are determined. From this, the tool determines the volume flow rate in each pipe based on the number of pipes. MATLAB sorts all of these designs into a database for processing.

Third, the operating mode (heating or cooling) are determined for each hour by subtracting the inlet temperature from the ground temperature to determine whether heat is being removed or added to the air system. If the inlet temperature is greater than the ground temperature, the mode is cooling for that hour, while if the inlet temperature is less than the ground temperature, the system is heating.

Fourth, the outlet temperature is calculated for each GCV system design using the regression equations. If the operating mode is cooling, then the tool uses the cooling regression equation, and the converse for heating. The regression equations predict the hourly outlet temperature for each GCV system.

Fifth, the temperature differences between the inlet and outlet air are calculated. This calculation is performed for each hour, and when summed, shows the total temperature change.

Sixth, the GCV system energy reduction (BTU) is calculated for each GCV system. The total BTUs of energy reduction is calculated using the temperature differences, the total volume flow rate, and air properties for cooling and heating, as Equation 14 and Equation 15 show.

Equation 14: BTU heating calculation

$$BTU\ Heating = CFM \times \sum \Delta T \times 1.08$$

Equation 15: BTU cooling calculation

$$BTU\ Cooling = CFM \times \sum \Delta T \times 1.08$$

8.1.3 Tool output

In the third phase of development, the GCV system performance is presented to help the user decide which GCV system design to adopt. For this, the user must choose the system type—either cooling, heating, or both. Based on the selected system type, the tool shows a table of all possible combinations of designs sorted according to the greatest temperature change. This table includes valuable information about the GCV system and can be divided into three parts: GCV system design elements, temperature differences and energy, and cooling and heating time, as Table 45 shows. Thereafter, the user can compare up to three designs, which are presented in a scatterplot that shows the temperature change and a total BTU bar chart for each design.

Finally, the user can save a table of results for all GCV system designs and/or the selected GCV system designs as an Excel file. By saving all GCV system designs, the table presents general information about all GCV system designs regarding design elements, operation time, temperatures, and energy efficiency. Moreover, by saving the selected GCV system designs, the tables present detailed information including the GCV system design air, ground, and outlet temperature for each hour.

Table 45: GCV System Tool Output

Parameters	**Description**
Design ID	Unique number for each design (1-∞).
Pipe Length (ft)	Pipe length of the design based on the user inputs of pipe length range (50-450 ft)
Pipe Depth (ft)	Pipe depth of the design based on the user inputs of pipe depth range (6.56ft, 13.12ft, 19.58ft).
Pipe Diameter (in)	Pipe diameter of the design based on the user inputs of pipe diameter range (4,6,8,10,12,15,18,21,24,27,30,33,36,39,42,45,48 in).
Soil Type	Soil type of the design (Clay, Sand, Limestone).
Number of Pipes	Numbers of pipes for the design based on the user inputs range (1- ∞).
Volume Flow Rate (ft^3/min)	Volume flow rate for each pipe (Building volume flow rate/ Number of pipes).
Air Velocity (ft/min)	Air Velocity of the design. $Velocity = \frac{Volume\ flow\ rate\ for\ each\ pipe}{(\frac{Pipe\ Diameter\ (ft)}{2})^2 \times \pi}$
Total Heating (F°)	Total heating degrees over a year (total ΔT if OM is heating)
Total Cooling (F°)	Total cooling degrees over a year (total ΔT if OM is cooling)
Average Heating (F°)	Total average heating degrees over a year (total ΔT heating/ heating hours)
Average Cooling (F°)	Total average cooling degrees over a year (total ΔT cooling/ cooling hours)
Total BTU Heating	Total heating BTU over a year. $(BTU\ Heating = CFM \times \sum \Delta T \times 1.08)$
Total BTU Cooling	Total cooling BTU over a year. $(BTU\ Cooling = CFM \times \sum \Delta T \times 1.08)$
Total BTU	Total heating and cooling BTU over a year
Heating Hours over the year	Total heating hours of the design (Total hours if OM < 0).
Cooling Hours over the year	Total cooling hours of the design (Total hours if OM > 0).
Heating (%)	Heating percentage over the year (Total heating hours/ hours in a year).
Cooling (%)	Cooling percentage over the year (Total cooling hours/ hours in a year).

Key:
Inlet temperature (Tin)
Ground temperature (Tground)
Operating Mode (OM) (OM = Tground - Tin)
Temperature reduction (ΔT) (ΔT= Tground - Tin)
British Thermal Unit (BTU)

8.2 Tool Validation

After the GCV system evaluation tool was created, it needed to be validated to determine its accuracy. To do so, it was necessary to compare the predicted outlet temperatures with those of an actual GCV system. The GCV system at the Solar CM House was previously monitored, and the data was used for validation. By inputting the as-built GCV system design into the GCV tool and using the inlet and ground temperature data collected on site, the tool predicts the outlet temperature. To validate the tool predictions, three days (cold, mild, and hot) were chosen to compare the outlet temperatures from the GCV system at the Solar CM House to those that the GCV tool predicted—as Table 47, Figure 8-3, Figure 8-4, Figure 8-5, Figure 8-6 and Figure 8-7 show. As a result of this comparison, the highest RMSE for the tool is 3.96°F, as Table 46 shows. This confirms that the tool's error is not significant.

Table 46: Comparison of Outlet Temperature
(GCV System at the Solar CM House vs. GCV Tool)

		GCV Solar CM House Vs. GCV Tool	GCV Solar CM House Vs. GCV Tool
	Day	Pipe 100 fpm Outlet Air Temp (°F)	Pipe 200 fpm Outlet Air Temp (°F)
Root mean square error (Degree Fahrenheit)	24-Jul	3.7	3.96
	25-Oct	2.83	1.99
	20-Dec	3.66	3

Table 47: Outlet Temperature for GCV System at Solar CM House vs. GCV Tool

Date		Solar CM House	GCV Tool	Difference
Jul 24th				
Pipe 100 fpm	Min.	65.05	59.50	5.55
Outlet Air Temp (°F)	Max.	68.93	72.07	3.14
	Avg.	67.02	64.87	2.15
	Std dev.	1.31	4.46	3.15
Pipe 200 fpm	Min.	66.02	60.58	5.44
Outlet Air Temp (°F)	Max.	71.91	73.16	1.25
	Avg.	69.06	65.96	3.10
	Std dev.	1.98	4.46	2.48
Oct 25th				
Pipe 100 fpm	Min.	59.26	55.21	4.05
Outlet Air Temp (°F)	Max.	62.54	65.64	3.10
	Avg.	60.77	59.39	1.38
	Std dev.	1.00	2.85	1.85
Pipe 200 fpm	Min.	55.64	53.95	1.69
Outlet Air Temp (°F)	Max.	61.52	64.39	2.87
	Avg.	58.48	58.60	0.12
	Std dev.	1.82	2.88	1.06
Dec 20th				
Pipe 100 fpm	Min.	46.88	40.72	6.16
Outlet Air Temp (°F)	Max.	49.93	54.18	4.25
	Avg.	48.38	46.50	1.88
	Std dev.	0.84	3.96	3.12
Pipe 200 fpm	Min.	41.22	39.46	1.76
Outlet Air Temp (°F)	Max.	46.46	52.92	6.46
	Avg.	43.64	45.24	1.60
	Std dev.	1.52	3.96	2.44

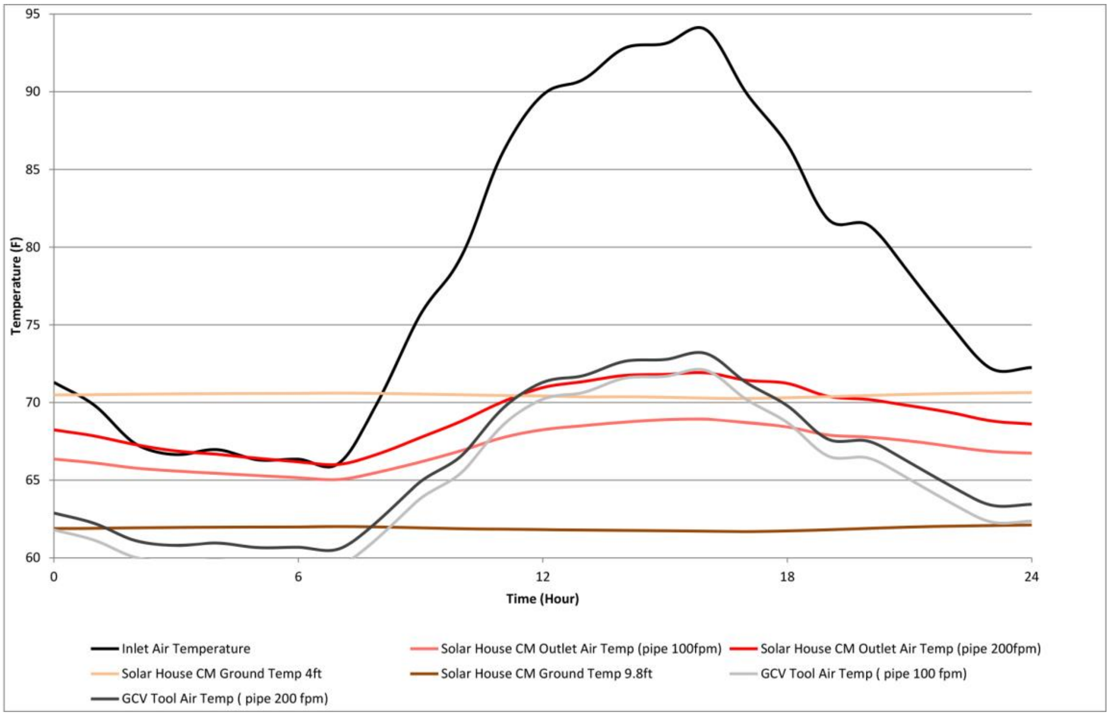

Figure 8-3: GCV Tool Prediction on Jul 24th

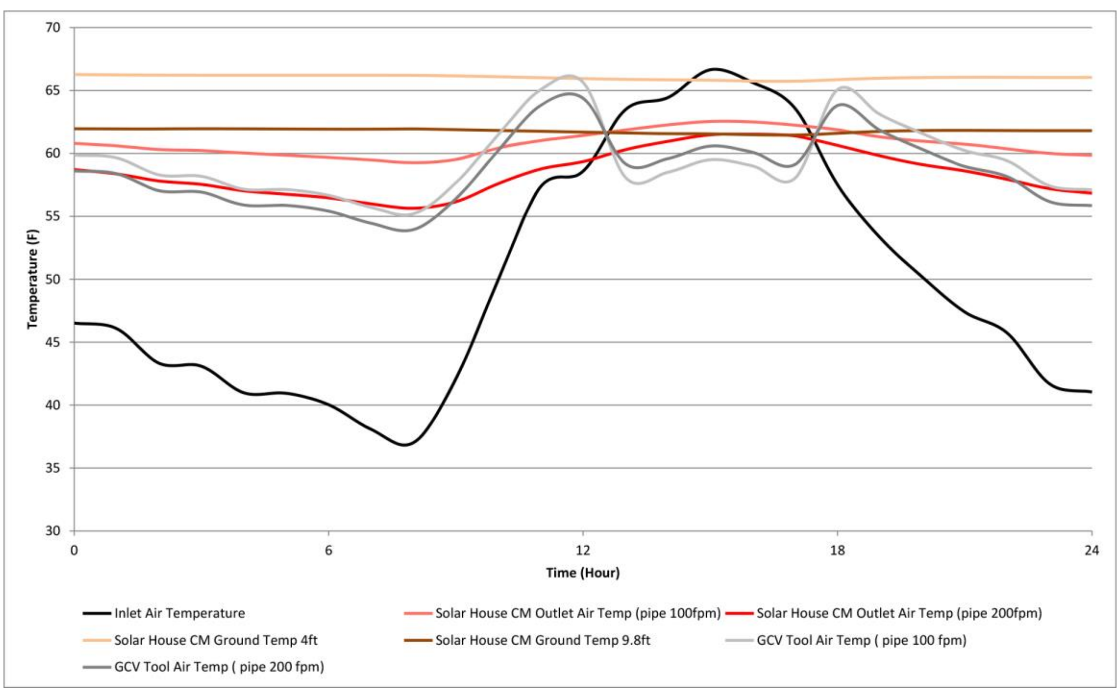

Figure 8-4: GCV Tool Prediction on Oct 25th

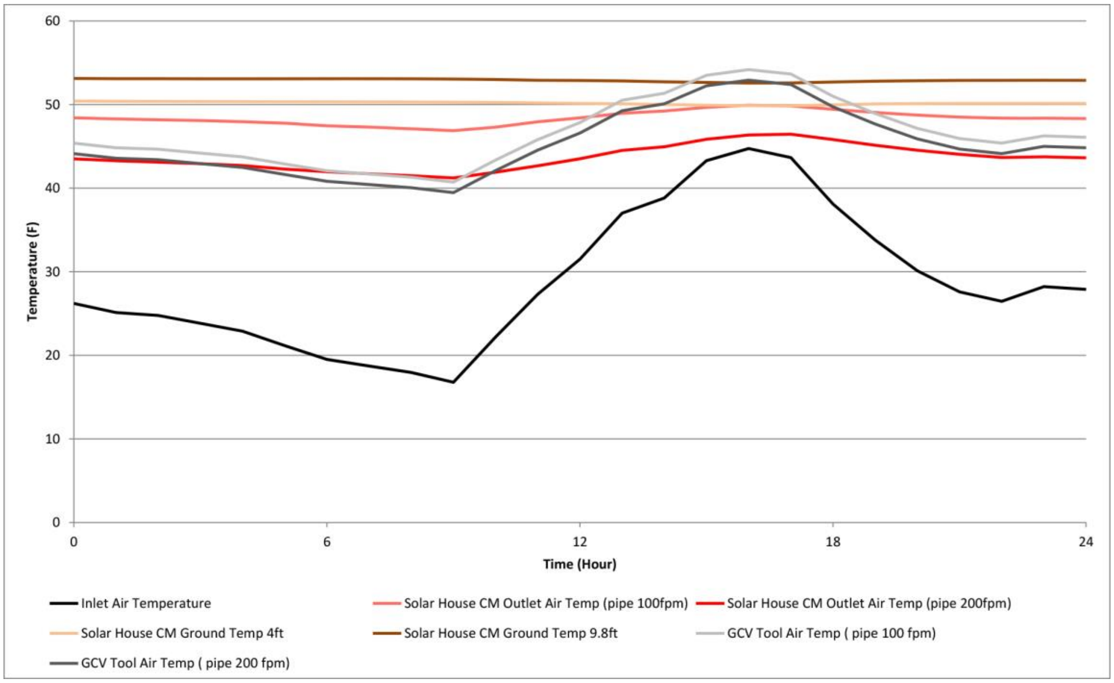

Figure 8-5: GCV Tool Prediction on Dec 20th

Figure 8-6: GCV Solar CM House vs. GCV Tool Outlet Temperature on Three Days (100fpm)

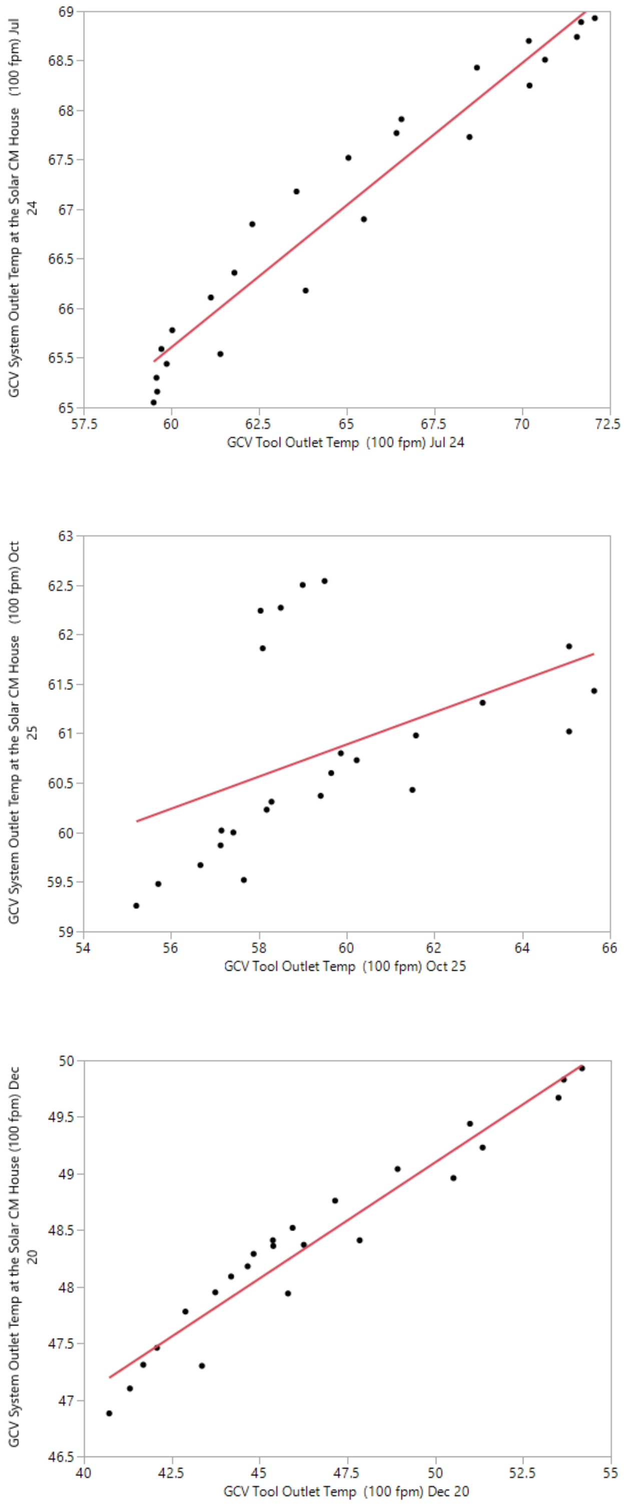

Figure 8-7: GCV Solar CM House vs. GCV Tool Temperature on Three Days (200fpm)

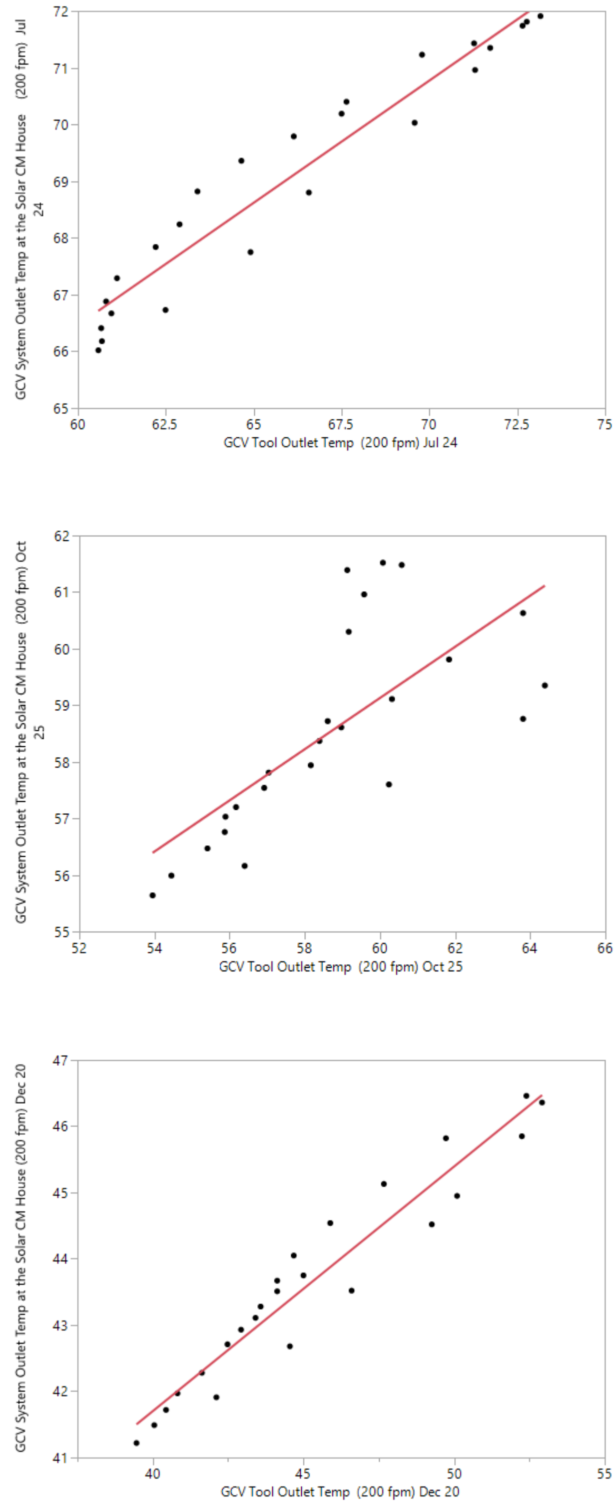

8.3 Tool Guidelines

The user needs to perform four steps to use the GCV system evaluation tool: first, calculate the required building ventilation; second, input the GCV system parameters; third, run the tool; and fourth, choose a GCV system design. Figure 8-8 shows the tool guidelines.

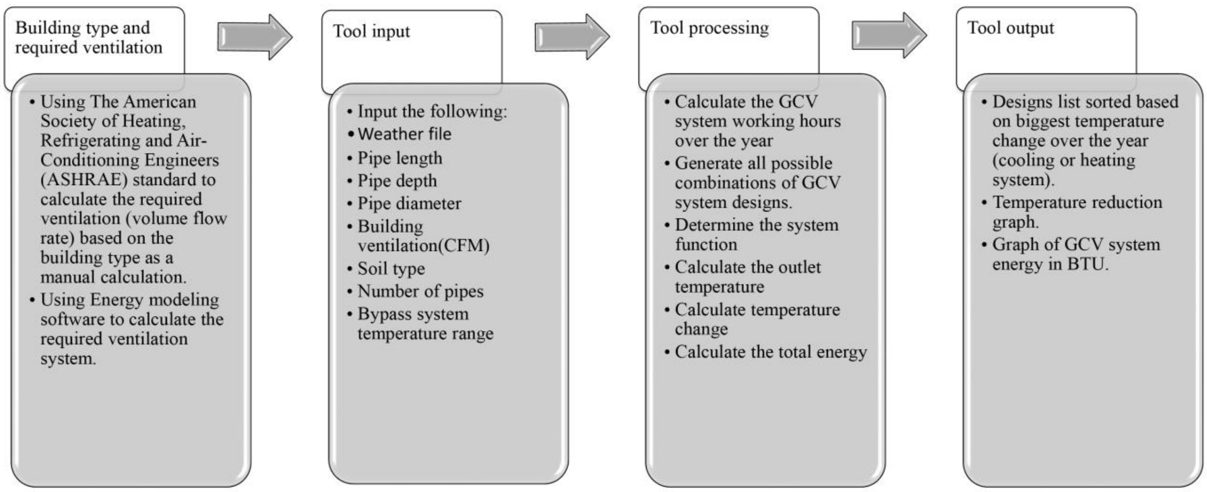

Figure 8-8: User Guidelines for the GCV System Evaluation Tool

8.3.1 Building ventilation volume requirements

Each building has a ventilation requirement. Building ventilation volume depends on building type and size, function, and the occupancy density. The ventilation rate may be calculated using energy modeling software or manually according to ASHRAE (2013) standard 62, as applied in the following equation (Equation 16).

Equation 16: Breathing zone outdoor airflow (ASHRAE, 2013)

$$V_{bz} = R_p P_z + R_a A_z$$

- V_{bz} Breathing zone outdoor airflow
- R_p Outdoor airflow rate required per person (from Table 50)
- P_z Zone population or the largest number of people expected to occupy the zone (from Table 50)
- R_a Outdoor airflow rate required by unit area (from Table 50)
- A_z Zone floor area

All of these variables must be determined for the user to calculate the ventilation air volume. Table 48 shows the effectiveness of the air distribution. For example, the ventilation for a selected office building, as Table 49 shows, requires 3,830 ft^3/min of ventilation based on the previous equation. The volumetric flow of ventilation air is typically the total air flow through the proposed GCV system.

Today, many computer programs are availabe to calculate the building heating and cooling loads. Software such as eQUEST, Carrier Building Hub, Energy Plus, and others can calculate the required cooling, heating, and ventilation based on many variables that depend on building type, occupancy, sensible loads attributable to the number of people, light loads, plug loads (such as computers and appliances), solar loads (from radiation and conductance), infiltration, latent heat, and building ventilation rates.

Table 48: Air Distribution Effectiveness (Table 6.2) (ASHRAE, 2013)

TABLE 6.2
Zone Air Distribution Effectiveness

Air Distribution Configuration	E_z
Ceiling supply of cool air	1.0
Ceiling supply of warm air and floor return	1.0
Ceiling supply of warm air at least 8°C (15°F) above space temperature and ceiling return.	0.8
Ceiling supply of warm air less than 8°C (15°F) above space temperature and ceiling return provided that the 0.8 m/s (150 fpm) supply air jet reaches to within 1.4 m (4.5 ft) of floor level. **Note**: For lower velocity supply air, E_z = 0.8.	1.0
Floor supply of cool air and ceiling return provided that the 0.8 m/s (150 fpm) supply jet reaches at least 1.4 m (4.5 ft) above the floor. **Note**: Most underfloor air distribution systems comply with this proviso.	1.0
Floor supply of cool air and ceiling return, provided low-velocity displacement ventilation achieves unidirectional flow and thermal stratification	1.2
Floor supply of warm air and floor return	1.0
Floor supply of warm air and ceiling return	0.7
Makeup supply drawn in on the opposite side of the room from the exhaust and/or return	0.8
Makeup supply drawn in near to the exhaust and/or return location	0.5

Notes for Table 6.2
1. "Cool air" is air cooler than space temperature.
2. "Warm air" is air warmer than space temperature.
3. "Ceiling" includes any point above the *breathing zone.*
4. "Floor" includes any point below the *breathing zone.*
5. As an alternative to using the above values, E_z may be regarded as equal to air change effectiveness determined in accordance with ASHRAE Standard 129 for all air distribution configurations except unidirectional flow.

Table 49: Ventilation Calculations for an Office Building (Stanke, 2004)

					Cooling		Heating	
Ventilation Zone	**People Outdoor Air Rate**	**Zone Population**	**Area Outdoor Air Rate**	**Zone Floor Area**	**Zone Ventilation Efficiency**	**Zone Outdoor Airflow**	**Zone Ventilation Efficiency**	**Zone Outdoor Airflow**
	R_p	P_z	R_a	A_z	E_z	V_{oz}	E_z	V_{oz}
	cfm/person		cfm/ft²	ft²		cfm		cfm
South Offices	5	20	0.06	2,000	1.0	220	0.8	275
West Offices	5	20	0.06	2,000	1.0	220	0.8	275
North Offices	5	20	0.06	2,000	0.9	244	0.8	275
East Offices	5	20	0.06	2,000	1.0	220	0.8	275
Interior Offices	5	100	0.06	20,000	1.0	1,700	0.8	2,125
North Conference Room	5	14.4*	0.06	2,000	0.9	213	0.8	240
South Conference Room	5	23.1**	0.06	3,000	0.9	328	0.8	369
Total Zone-Level Outdoor Airflow					ΣV_{oz} =	3,150	ΣV_{oz} =	3,830
Single-Zone Systems: Total Intake Air							ΣV_{oz} =	3,830
100%-Outdoor-Air System							V_{ot} =	3,830

* Average population (72% of 20-person peak population)
** Average population (77% of 30-person peak population)

Table 50: Standard Minimum Ventilation Rates in Breathing Zones (Table 6.1) (ASHRAE, 2013)

TABLE 6-1 MINIMUM VENTILATION RATES IN BREATHING ZONE *(continued)*
(This table is not valid in isolation; it must be used in conjunction with the accompanying notes.)

Occupancy Category	People Outdoor Air Rate R_p		Area Outdoor Air Rate R_a		Notes	Default Values: Occupant Density (see Note 4)	Default Values: Combined Outdoor Air Rate (see Note 5)		Air Class
	cfm/person	L/s·person	cfm/ft²	L/s·m²		#/1000 ft² or #/100 m²	cfm/person	L/s·person	
Office Buildings									
Office space	5	2.5	0.06	0.3		5	17	8.5	1
Reception areas	5	2.5	0.06	0.3		30	7	3.5	1
Telephone/data entry	5	2.5	0.06	0.3		60	6	3.0	1
Main entry lobbies	5	2.5	0.06	0.3		10	11	5.5	1
Miscellaneous Spaces									
Bank vaults/safe deposit	5	2.5	0.06	0.3		5	17	8.5	2
Computer (not printing)	5	2.5	0.06	0.3		4	20	10.0	1
Electrical equipment rooms	–	–	0.06	0.3	B	–			1
Elevator machine rooms	–	–	0.12	0.6	B	–			1
Pharmacy (prep. area)	5	2.5	0.18	0.9		10	23	11.5	2
Photo studios	5	2.5	0.12	0.6		10	17	8.5	1
Shipping/receiving	–	–	0.12	0.6	B	–			1
Telephone closets	–	–	0.00	0.0		–			1
Transportation waiting	7.5	3.8	0.06	0.3		100	8	4.1	1
Warehouses	–	–	0.06	0.3	B	–			2
Public Assembly Spaces									
Auditorium seating area	5	2.5	0.06	0.3		150	5	2.7	1
Places of religious worship	5	2.5	0.06	0.3		120	6	2.8	1
Courtrooms	5	2.5	0.06	0.3		70	6	2.9	1
Legislative chambers	5	2.5	0.06	0.3		50	6	3.1	1
Libraries	5	2.5	0.12	0.6		10	17	8.5	1
Lobbies	5	2.5	0.06	0.3		150	5	2.7	1
Museums (children's)	7.5	3.8	0.12	0.6		40	11	5.3	1
Museums/galleries	7.5	3.8	0.06	0.3		40	9	4.6	1
Residential									
Dwelling unit	5	2.5	0.06	0.3	F,G	F			1
Common corridors	–	–	0.06	0.3					1
Retail									
Sales (except as below)	7.5	3.8	0.12	0.6		15	16	7.8	2
Mall common areas	7.5	3.8	0.06	0.3		40	9	4.6	1
Barbershop	7.5	3.8	0.06	0.3		25	10	5.0	2
Beauty and nail salons	20	10	0.12	0.6		25	25	12.4	2
Pet shops (animal areas)	7.5	3.8	0.18	0.9		10	26	12.8	2
Supermarket	7.5	3.8	0.06	0.3		8	15	7.6	1
Coin-operated laundries	7.5	3.8	0.06	0.3		20	11	5.3	2

Table 50 continued: Standard Minimum Ventilation Rates in Breathing Zones (Table 6.1) (ASHRAE, 2013)

TABLE 6-1 MINIMUM VENTILATION RATES IN BREATHING ZONE *(continued)*
(This table is not valid in isolation; it must be used in conjunction with the accompanying notes.)

Occupancy Category	People Outdoor Air Rate R_p		Area Outdoor Air Rate R_a		Notes	Default Values: Occupant Density (see Note 4)	Default Values: Combined Outdoor Air Rate (see Note 5)		Air Class
	cfm/person	L/s·person	cfm/ft^2	L/s·m^2		#/1000 ft^2 or #/100 m^2	cfm/person	L/s·person	
Sports and Entertainment									
Sports arena (play area)	–	–	0.30	1.5	E	–			1
Gym, stadium (play area)	–	–	0.30	1.5		30			2
Spectator areas	7.5	3.8	0.06	0.3		150	8	4.0	1
Swimming (pool & deck)	–	–	0.48	2.4	C	–			2
Disco/dance floors	20	10	0.06	0.3		100	21	10.3	1
Health club/aerobics room	20	10	0.06	0.3		40	22	10.8	2
Health club/weight rooms	20	10	0.06	0.3		10	26	13.0	2
Bowling alley (seating)	10	5	0.12	0.6		40	13	6.5	1
Gambling casinos	7.5	3.8	0.18	0.9		120	9	4.6	1
Game arcades	7.5	3.8	0.18	0.9		20	17	8.3	1
Stages, studios	10	5	0.06	0.3	D	70	11	5.4	1

GENERAL NOTES FOR TABLE 6-1

1 **Related requirements:** The rates in this table are based on all other applicable requirements of this standard being met.
2 **Smoking:** This table applies to no-smoking areas. Rates for smoking-permitted spaces must be determined using other methods. See Section 6.2.9 for ventilation requirements in smoking areas.
3 **Air density:** Volumetric airflow rates are based on an air density of 0.075 lb_{da}/ft^3 (1.2 kg_{da}/m^3), which corresponds to dry air at a barometric pressure of 1 atm (101.3 kPa) and an air temperature of 70°F (21°C). Rates may be adjusted for actual density but such adjustment is not required for compliance with this standard.
4 **Default occupant density:** The default occupant density shall be used when actual occupant density is not known.
5 **Default combined outdoor air rate (per person):** This rate is based on the default occupant density.
6 **Unlisted occupancies:** If the occupancy category for a proposed space or zone is not listed, the requirements for the listed occupancy category that is most similar in terms of occupant density, activities and building construction shall be used.
7 **Health-care facilities:** Rates shall be determined in accordance with Appendix E.

ITEM-SPECIFIC NOTES FOR TABLE 6-1

A For high school and college libraries, use values shown for Public Assembly Spaces—Libraries.
B Rate may not be sufficient when stored materials include those having potentially harmful emissions.
C Rate does not allow for humidity control. Additional ventilation or dehumidification may be required to remove moisture.
D Rate does not include special exhaust for stage effects, e.g., dry ice vapors, smoke.
E When combustion equipment is intended to be used on the playing surface, additional dilution ventilation and/or source control shall be provided.
F Default occupancy for dwelling units shall be two persons for studio and one-bedroom units, with one additional person for each additional bedroom.
G Air from one residential dwelling shall not be recirculated or transferred to any other space outside of that dwelling.

8.3.2 Tool inputs

There are two inputs to the tool, the first of which is the weather file. This file can be downloaded from Energy Plus (https://energyplus.net/weather) based on the country and city in which the GCV system will be used. The user needs to convert the Energy Plus Weather file (EPW file) to an Excel file so the tool can read the information. To do so, the user opens the EPW file in Microsoft Excel and follows three steps, as Figure 8-9, Figure 8-10 and Figure 8-11 show. Then, the weather file is imported into the top box in the tool. The second input is the GCV system design parameters. The user must enter the design properties, including pipe length, pipe depth, pipe diameter, soil type, volumetric flow rate, time of operation, and whether there will be a bypass system. These variables can be entered as a single value or a range so that the tool can compare several designs. Figure 8-12 shows the way to import the weather file and the GCV system inputs.

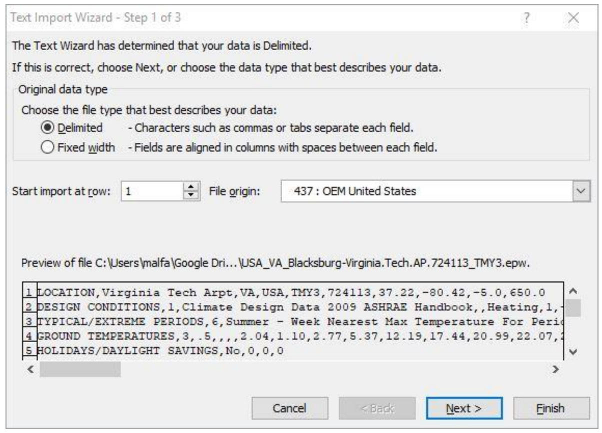

Figure 8-9: Step One: Convert EPW To Excel File

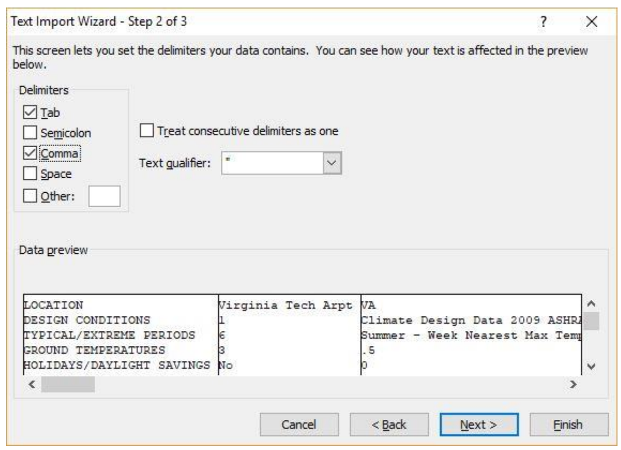

Figure 8-10: Step Two: Convert EPW To Excel File

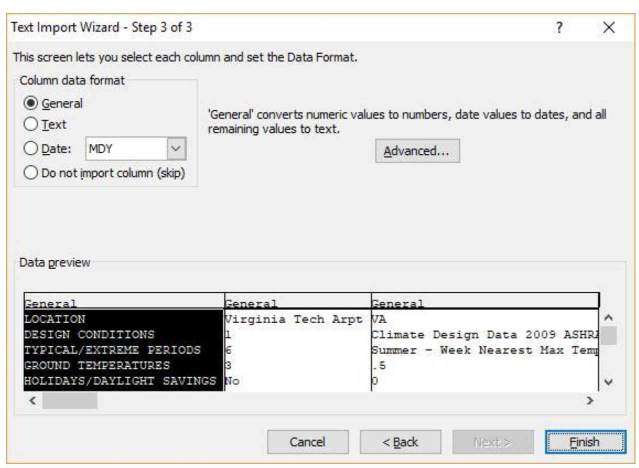

Figure 8-11: Step Three: Convert EPW To Excel File

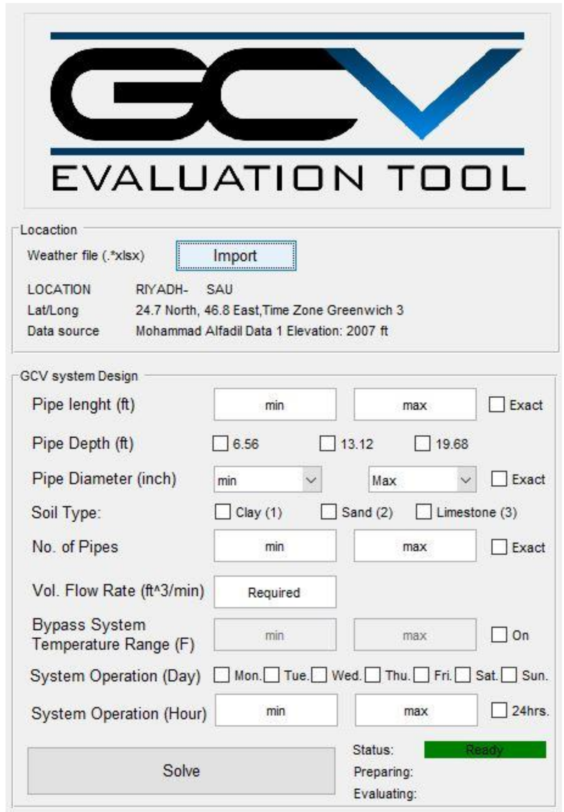

Figure 8-12: Import Weather File and GCV System Design Inputs

8.3.3 Tool processing

After all of the descriptive inputs are added, the user clicks on the **solve** button. The tool shows the percentage of data prepared for processing of the GCV system designs, as Figure 8-13 shows. Then, a second process status window will appear while calculating and evaluating the GCV system designs, as Figure 8-14 shows. If an error message appears, this indicates that an input is either missing or is invalid, as Figure 8-15, Figure 8-16, Figure 8-17, Figure 8-18, Figure 8-19, and Figure 8-20 show. The user simply clicks "**OK**," corrects the error specified in the message, and clicks "**Solve**."

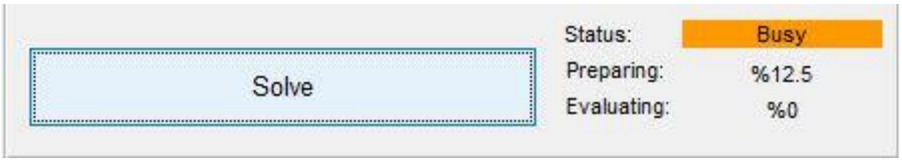

Figure 8-13: Loading Percentage in Preparing all GCV System Designs

Figure 8-14: Loading Percentage in Evaluating all GCV System Designs

Figure 8-15: Pipe Length Error

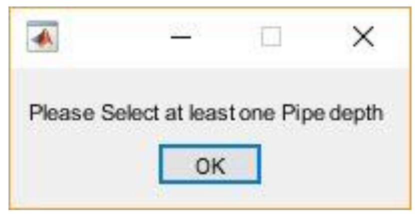

Figure 8-16: Pipe Depth Error

Figure 8-17: Pipe Diameter Error

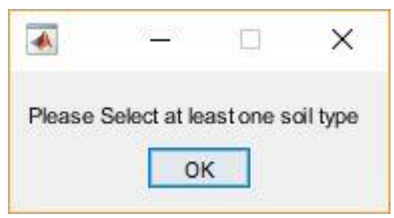

Figure 8-18: Soil Type Error

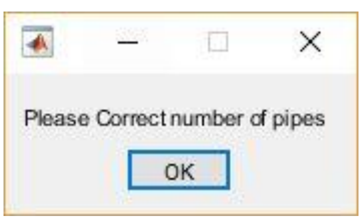

Figure 8-19: Number of Pipes Error

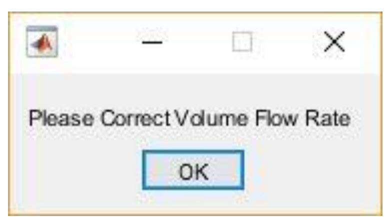

Figure 8-20: Volume Flow Rate Error

8.3.4 Tool output

To show the results, the tool sorts the GCV system designs from the highest to lowest total BTUs of heating and cooling system reduction for the ventilation air, and the user has the option to choose the system type: either cooling, heating, or both. Based on the type selected, a table will present the GCV system design with the highest to lowest temperature reduction (if cooling is selected) and temperature gain (if heating is selected), as Figure 8-21 shows. The second step is to choose multiple GCV system designs and compare them by entering the design ID number and pressing the "**Compare**" button. The results show a comparison of the GCV systems design performance over the year by the total energy reduction in BTU for cooling, heating, and overall total, as Figure 8-22 shows.

The user can save all of the GCV system designs in an Excel file by clicking "Save designs table" (Figure 8-23). Moreover, the user can save the data for the selected GCV designs' data in an Excel file by clicking "Save selected designs" (Figure 8-24).

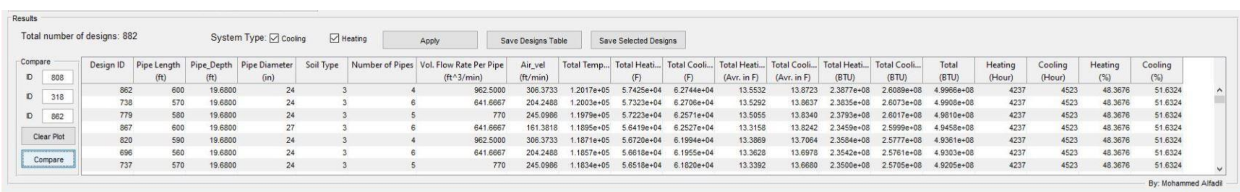

Design ID	Pipe Length (ft)	Pipe_Depth (ft)	Pipe Diameter (in)	Soil Type	Number of Pipes	Vol. Flow Rate Per Pipe (ft^3/min)	Air_vel (ft/min)	Total Temp...	Total Heati... (F)	Total Cooli... (F)	Total Heati... (Avr. in F)	Total Cooli... (Avr. in F)	Total Heati... (BTU)	Total Cooli... (BTU)	Total (BTU)	Heating (Hour)	Cooling (Hour)	Heating (%)	Cooling (%)
862	600	19.6800	24	3	4	962.5000	306.3733	1.2017e+05	5.7425e+04	6.2744e+04	13.5532	13.8723	2.3877e+08	2.6089e+08	4.9966e+08	4237	4523	48.3676	51.6324
738	570	19.6800	24	3	6	641.6667	204.2488	1.2003e+05	5.7323e+04	6.2706e+04	13.5292	13.8637	2.3835e+08	2.6073e+08	4.9908e+08	4237	4523	48.3676	51.6324
779	580	19.6800	24	3	5	770	245.0986	1.1979e+05	5.7223e+04	6.2571e+04	13.5055	13.8340	2.3793e+08	2.6017e+08	4.9810e+08	4237	4523	48.3676	51.6324
867	600	19.6800	27	3	6	641.6667	161.3818	1.1895e+05	5.6419e+04	6.2527e+04	13.3158	13.8242	2.3459e+08	2.5999e+08	4.9458e+08	4237	4523	48.3676	51.6324
820	590	19.6800	24	3	4	962.5000	306.3733	1.1871e+05	5.6720e+04	6.1994e+04	13.3869	13.7064	2.3584e+08	2.5777e+08	4.9361e+08	4237	4523	48.3676	51.6324
696	560	19.6800	24	3	6	641.6667	204.2488	1.1857e+05	5.6618e+04	6.1955e+04	13.3628	13.6978	2.3542e+08	2.5761e+08	4.9303e+08	4237	4523	48.3676	51.6324
737	570	19.6800	24	3	5	770	245.0986	1.1834e+05	5.6518e+04	6.1820e+04	13.3392	13.6680	2.3500e+08	2.5705e+08	4.9205e+08	4237	4523	48.3676	51.6324

Figure 8-21: GCV System Performance Results

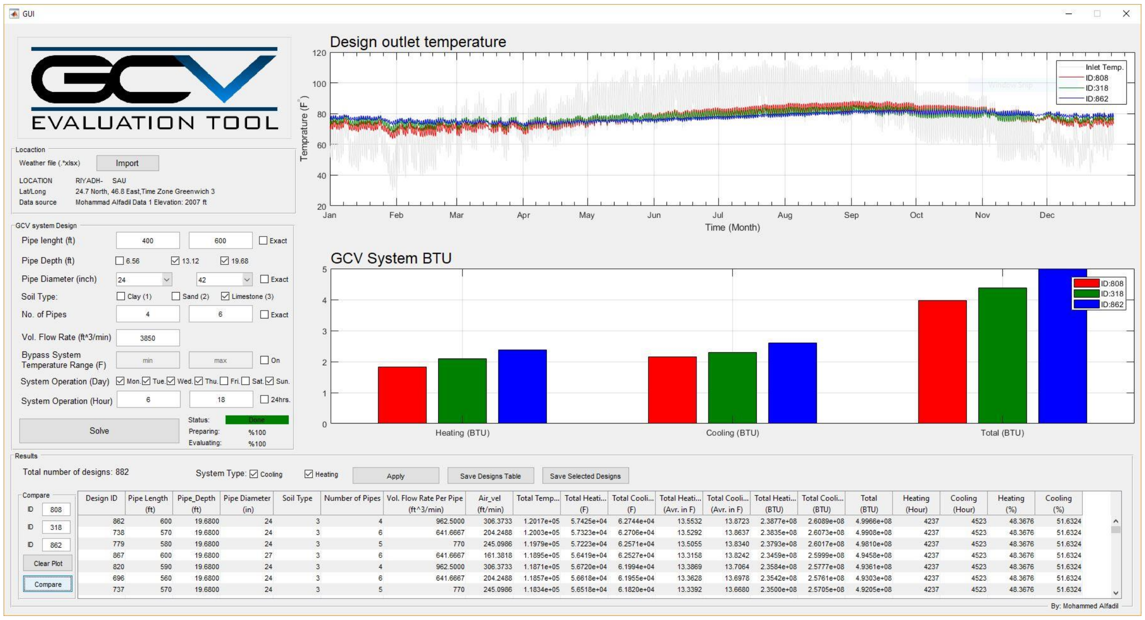

Figure 8-22: GCV Systems Performance Comparison

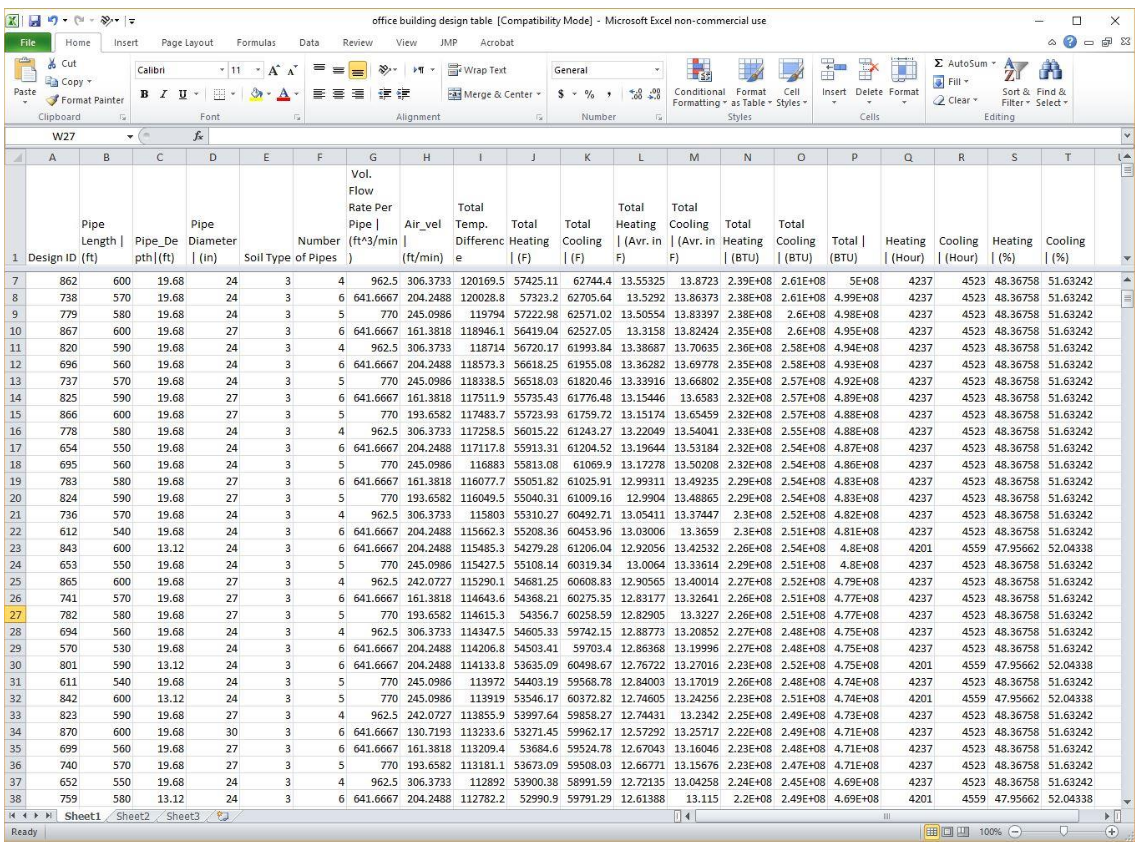

1	Design ID	Pipe Length | (ft)	Pipe_Depth|(ft)	Pipe Diameter | (in)	Soil Type	Number of Pipes	Vol. Flow Rate Per Pipe | (ft^3/min)	Air_vel | (ft/min)	Total Temp. Difference	Total Heating | (F)	Total Cooling | (F)	Total Heating | (Avr. in F)	Total Cooling | (Avr. in F)	Total Heating | (BTU)	Total Cooling | (BTU)	Total | (BTU)	Heating | (Hour)	Cooling | (Hour)	Heating | (%)	Cooling | (%)
7	862	600	19.68	24	3	4	962.5	306.3733	120169.5	57425.11	62744.4	13.55325	13.8723	2.39E+08	2.61E+08	5E+08	4237	4523	48.36758	51.63242
8	738	570	19.68	24	3	6	641.6667	204.2488	120028.8	57323.2	62705.64	13.5292	13.86373	2.38E+08	2.61E+08	4.99E+08	4237	4523	48.36758	51.63242
9	779	580	19.68	24	3	5	770	245.0986	119794	57222.98	62571.02	13.50554	13.83397	2.38E+08	2.6E+08	4.98E+08	4237	4523	48.36758	51.63242
10	867	600	19.68	27	3	6	641.6667	161.3818	118946.1	56419.04	62527.05	13.3158	13.82424	2.35E+08	2.6E+08	4.95E+08	4237	4523	48.36758	51.63242
11	820	590	19.68	24	3	4	962.5	306.3733	118714	56720.17	61993.84	13.38687	13.70635	2.36E+08	2.58E+08	4.94E+08	4237	4523	48.36758	51.63242
12	696	560	19.68	24	3	6	641.6667	204.2488	118573.3	56618.25	61955.08	13.36282	13.69778	2.35E+08	2.58E+08	4.93E+08	4237	4523	48.36758	51.63242
13	737	570	19.68	24	3	5	770	245.0986	118338.5	56518.03	61820.46	13.33916	13.66802	2.35E+08	2.57E+08	4.92E+08	4237	4523	48.36758	51.63242
14	825	590	19.68	27	3	6	641.6667	161.3818	117511.9	55735.43	61776.48	13.15446	13.6583	2.32E+08	2.57E+08	4.89E+08	4237	4523	48.36758	51.63242
15	866	600	19.68	27	3	5	770	193.6582	117483.7	55723.93	61759.72	13.15174	13.65459	2.32E+08	2.57E+08	4.88E+08	4237	4523	48.36758	51.63242
16	778	580	19.68	24	3	4	962.5	306.3733	117258.5	56015.22	61243.27	13.22049	13.54041	2.33E+08	2.55E+08	4.88E+08	4237	4523	48.36758	51.63242
17	654	550	19.68	24	3	6	641.6667	204.2488	117117.8	55913.31	61204.52	13.19644	13.53184	2.32E+08	2.54E+08	4.87E+08	4237	4523	48.36758	51.63242
18	695	560	19.68	24	3	5	770	245.0986	116883	55813.08	61069.9	13.17278	13.50208	2.32E+08	2.54E+08	4.86E+08	4237	4523	48.36758	51.63242
19	783	580	19.68	27	3	6	641.6667	161.3818	116077.7	55051.82	61025.91	12.99311	13.49235	2.29E+08	2.54E+08	4.83E+08	4237	4523	48.36758	51.63242
20	824	590	19.68	27	3	5	770	193.6582	116049.5	55040.31	61009.16	12.9904	13.48865	2.29E+08	2.54E+08	4.83E+08	4237	4523	48.36758	51.63242
21	736	570	19.68	24	3	4	962.5	306.3733	115803	55310.27	60492.71	13.05411	13.37447	2.3E+08	2.52E+08	4.82E+08	4237	4523	48.36758	51.63242
22	612	540	19.68	24	3	6	641.6667	204.2488	115662.3	55208.36	60453.96	13.03006	13.3659	2.3E+08	2.51E+08	4.81E+08	4237	4523	48.36758	51.63242
23	843	600	13.12	24	3	6	641.6667	204.2488	115485.3	54279.28	61206.04	12.92056	13.42532	2.26E+08	2.54E+08	4.8E+08	4201	4559	47.95662	52.04338
24	653	550	19.68	24	3	5	770	245.0986	115427.5	55108.14	60319.34	13.0064	13.33614	2.29E+08	2.51E+08	4.8E+08	4237	4523	48.36758	51.63242
25	865	600	19.68	27	3	4	962.5	242.0727	115290.1	54681.25	60608.83	12.90565	13.40014	2.27E+08	2.52E+08	4.79E+08	4237	4523	48.36758	51.63242
26	741	570	19.68	27	3	6	641.6667	161.3818	114643.6	54368.21	60275.35	12.83177	13.32641	2.26E+08	2.51E+08	4.77E+08	4237	4523	48.36758	51.63242
27	782	580	19.68	27	3	5	770	193.6582	114615.3	54356.7	60258.59	12.82905	13.3227	2.26E+08	2.51E+08	4.77E+08	4237	4523	48.36758	51.63242
28	694	560	19.68	24	3	4	962.5	306.3733	114347.5	54605.33	59742.15	12.88773	13.20852	2.27E+08	2.48E+08	4.75E+08	4237	4523	48.36758	51.63242
29	570	530	19.68	24	3	6	641.6667	204.2488	114206.8	54503.41	59703.4	12.86368	13.19996	2.27E+08	2.48E+08	4.75E+08	4237	4523	48.36758	51.63242
30	801	590	13.12	24	3	6	641.6667	204.2488	114133.8	53635.09	60498.67	12.76722	13.27016	2.23E+08	2.52E+08	4.75E+08	4201	4559	47.95662	52.04338
31	611	540	19.68	24	3	5	770	245.0986	113972	54403.19	59568.78	12.84003	13.17019	2.26E+08	2.48E+08	4.74E+08	4237	4523	48.36758	51.63242
32	842	600	13.12	24	3	5	770	245.0986	113919	53546.17	60372.82	12.74605	13.24256	2.23E+08	2.51E+08	4.74E+08	4201	4559	47.95662	52.04338
33	823	590	19.68	27	3	4	962.5	242.0727	113855.9	53997.64	59858.27	12.74431	13.2342	2.25E+08	2.49E+08	4.73E+08	4237	4523	48.36758	51.63242
34	870	600	19.68	30	3	6	641.6667	130.7193	113233.6	53271.45	59962.17	12.57292	13.25717	2.22E+08	2.49E+08	4.71E+08	4237	4523	48.36758	51.63242
35	699	560	19.68	27	3	6	641.6667	161.3818	113209.4	53684.6	59524.78	12.67043	13.16046	2.23E+08	2.48E+08	4.71E+08	4237	4523	48.36758	51.63242
36	740	570	19.68	27	3	5	770	193.6582	113181.1	53673.09	59508.03	12.66771	13.15676	2.23E+08	2.47E+08	4.71E+08	4237	4523	48.36758	51.63242
37	652	550	19.68	24	3	4	962.5	306.3733	112892	53900.38	58991.59	12.72135	13.04258	2.24E+08	2.45E+08	4.69E+08	4237	4523	48.36758	51.63242
38	759	580	13.12	24	3	6	641.6667	204.2488	112782.2	52990.9	59791.29	12.61388	13.115	2.2E+08	2.49E+08	4.69E+08	4201	4559	47.95662	52.04338

Figure 8-23: Save Designs Table Results

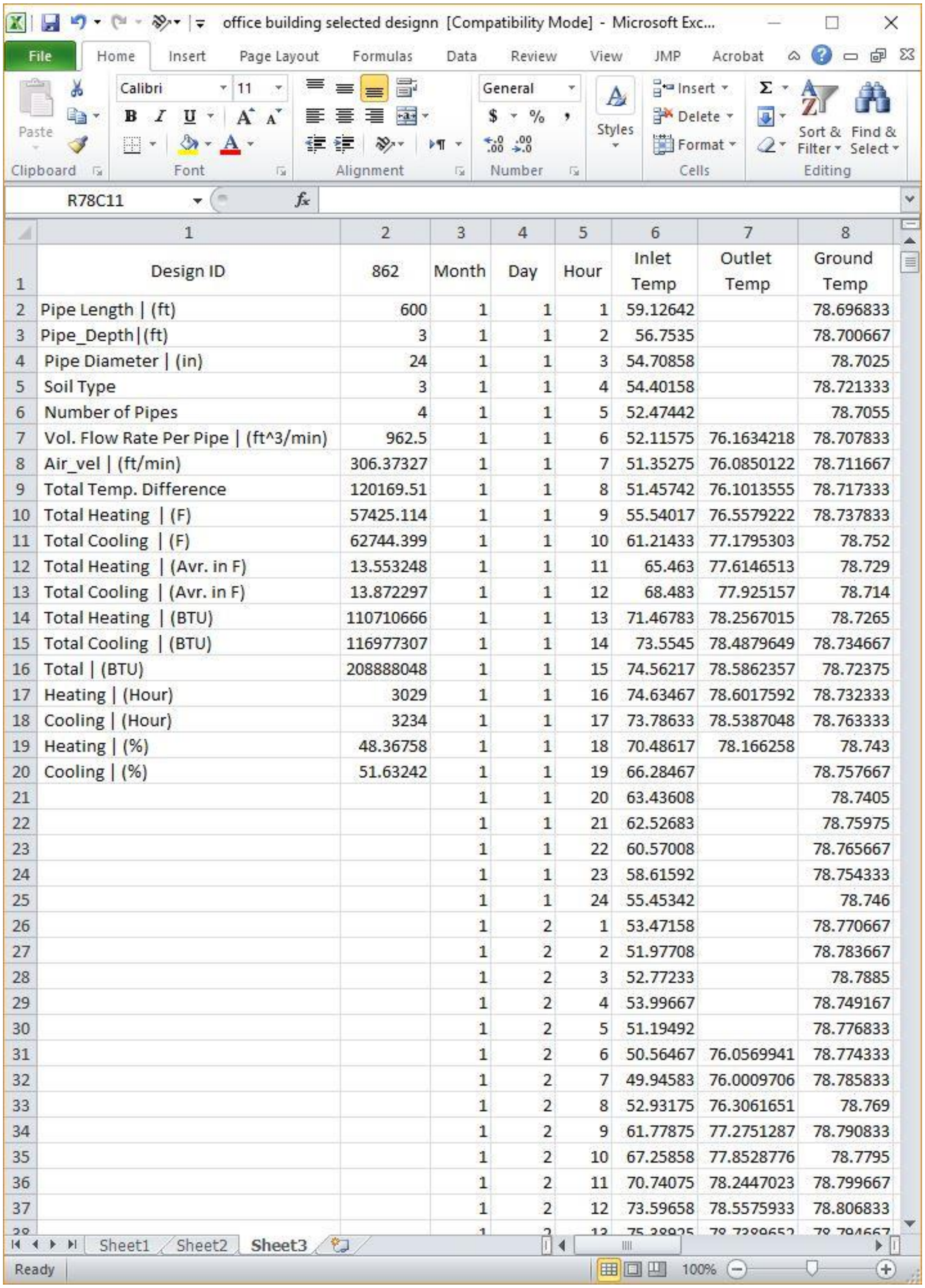

	1	2	3	4	5	6	7	8
1	Design ID	862	Month	Day	Hour	Inlet Temp	Outlet Temp	Ground Temp
2	Pipe Length | (ft)	600	1	1	1	59.12642		78.696833
3	Pipe_Depth|(ft)	3	1	1	2	56.7535		78.700667
4	Pipe Diameter | (in)	24	1	1	3	54.70858		78.7025
5	Soil Type	3	1	1	4	54.40158		78.721333
6	Number of Pipes	4	1	1	5	52.47442		78.7055
7	Vol. Flow Rate Per Pipe | (ft^3/min)	962.5	1	1	6	52.11575	76.1634218	78.707833
8	Air_vel | (ft/min)	306.37327	1	1	7	51.35275	76.0850122	78.711667
9	Total Temp. Difference	120169.51	1	1	8	51.45742	76.1013555	78.717333
10	Total Heating | (F)	57425.114	1	1	9	55.54017	76.5579222	78.737833
11	Total Cooling | (F)	62744.399	1	1	10	61.21433	77.1795303	78.752
12	Total Heating | (Avr. in F)	13.553248	1	1	11	65.463	77.6146513	78.729
13	Total Cooling | (Avr. in F)	13.872297	1	1	12	68.483	77.925157	78.714
14	Total Heating | (BTU)	110710666	1	1	13	71.46783	78.2567015	78.7265
15	Total Cooling | (BTU)	116977307	1	1	14	73.5545	78.4879649	78.734667
16	Total | (BTU)	208888048	1	1	15	74.56217	78.5862357	78.72375
17	Heating | (Hour)	3029	1	1	16	74.63467	78.6017592	78.732333
18	Cooling | (Hour)	3234	1	1	17	73.78633	78.5387048	78.763333
19	Heating | (%)	48.36758	1	1	18	70.48617	78.166258	78.743
20	Cooling | (%)	51.63242	1	1	19	66.28467		78.757667
21			1	1	20	63.43608		78.7405
22			1	1	21	62.52683		78.75975
23			1	1	22	60.57008		78.765667
24			1	1	23	58.61592		78.754333
25			1	1	24	55.45342		78.746
26			1	2	1	53.47158		78.770667
27			1	2	2	51.97708		78.783667
28			1	2	3	52.77233		78.7885
29			1	2	4	53.99667		78.749167
30			1	2	5	51.19492		78.776833
31			1	2	6	50.56467	76.0569941	78.774333
32			1	2	7	49.94583	76.0009706	78.785833
33			1	2	8	52.93175	76.3061651	78.769
34			1	2	9	61.77875	77.2751287	78.790833
35			1	2	10	67.25858	77.8528776	78.7795
36			1	2	11	70.74075	78.2447023	78.799667
37			1	2	12	73.59658	78.5575933	78.806833

Figure 8-24: Save Selected Designs Results

8.4 Summary

This chapter can be summarized as follows:

- **Tool development:** this tool uses the cooling and heating regression models to predict the performance of a GCV system. MATLAB software was used for the interface and for algorithmic coding. The tool was divided into three sections: tool input, processing, and output. First, importing the weather file and inputting the GCV system parameters as a tool input. Second, calculating operating hours, GCV system designs, operating mode, outlet temperature and energy reduction. Third, the tool presents GCV system designs based on design elements, temperature differences, and energy in table and graphs as output.
- **Tool Validation:** to validate the tool predictions, three days (cold, mild, and hot) were chosen to compare the outlet temperatures from the GCV system at the Solar CM House to those that the GCV tool predicted. As a result of this comparison, the highest RMSE for the tool is 3.96^{o}F.
- **Tool guidelines:** the user needs to perform four steps to use the GCV system evaluation tool: first, calculate the required building ventilation; second, input the GCV system parameters; third, run the tool; and fourth, choose a GCV system design based on the total energy reduction in BTU over the year.

Chapter 9: Riyadh GCV system

9.1 Overview

Based on Prince Mohammad bin Salman's 2030 vision to adopt alternative energy sources for Saudi Arabia, this research introduces GCV systems in Riyadh in an effort to realize his vision. This chapter discusses how the GCV system evaluation tool was used to select a GCV system for a non-residential building located in Riyadh. Because the EPW weather file data for Riyadh was old (from 1983), updated data for the air and ground temperature were required. For this, in-situ data for air and ground temperature were measured and recorded for a selected site in Riyadh.

9.2 In-situ Riyadh Data Collection

Air and ground temperature were collected at different depths every five minutes throughout the year 2016. Data were recorded with a HOBO analog logger (model UX120-HD). Table 51 describes the instruments used. Installing the instruments in-situ required a machine tool that dug a 19.68 feet deep hole. This digging machine had a crystal head that helps dig in hard ground, as the ground in the Riyadh region is limestone. Three temperature sensors were placed at different depths (6.56ft, 13.12ft, and 19.68ft) and one air temperature sensor was placed 4 feet above the surface while being protected from the sun and birds to determine the average temperature every five minutes as Table 52 shows.

Table 51: Instrument Type and Uses for Collection of the Riyadh Data

Data	Instrument	Description
Surface air temperature	Thermocouple wire (MC6-HD)	6 ft. Air/Water/Soil Temp (waterproof)
Ground temperature (6.56 ft. depth)	Thermocouple wire (MC6-HD)	6 ft. Air/Water/Soil Temp (waterproof)
Ground temperature (13.12 ft. depth)	Thermocouple wire (MC20-HD)	20 ft. Air/Water/Soil Temp (waterproof)
Ground temperature (19.68 ft. depth)	Thermocouple wire (MC20-HD)	20 ft. Air/Water/Soil Temp (waterproof)

Figure 9-1: Digging Process (photo by author)

Figure 9-2: Digging Machine (photo by author)

Figure 9-3: HOBO Analog Logger (photo by author)

Figure 9-4: Installation In-situ (photo by author)

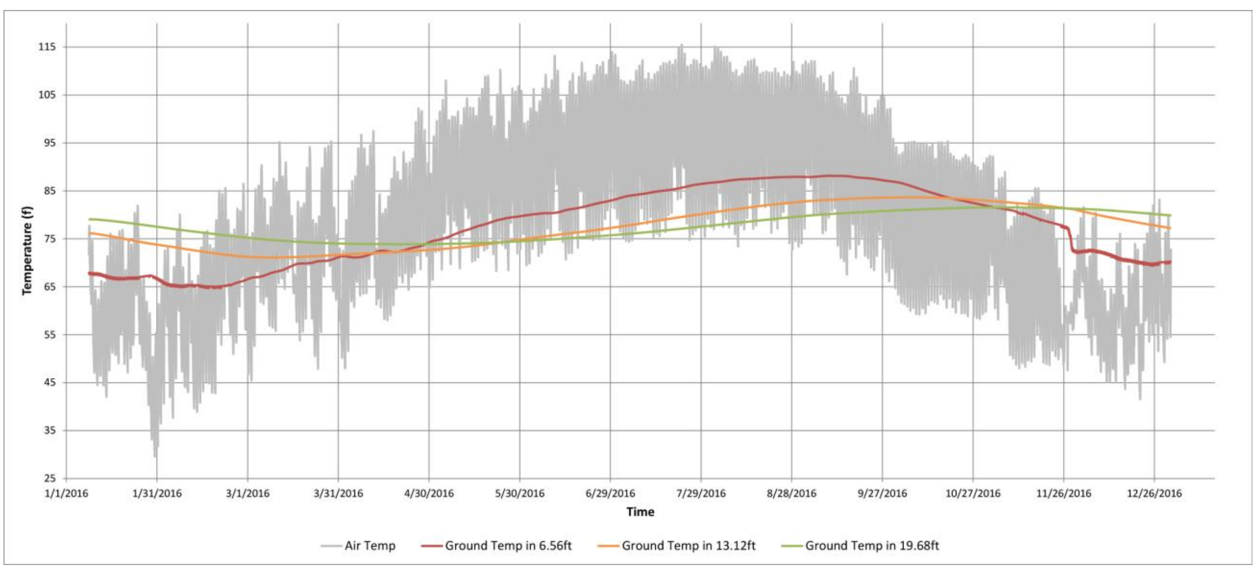

Figure 9-5: Riyadh Data for 2016

Table 52: Riyadh Data Collection

Date/ Time	Air Temp	Ground Temp at 6.56ft	Ground Temp at 13.12ft	Ground Temp at 19.68ft
1/8/16 11:42	71.56	67.93	76.13	79.06
1/8/16 11:47	72.70	67.84	76.13	79.06
1/8/16 11:52	72.31	67.77	76.13	79.06
1/8/16 11:57	72.70	67.80	76.13	79.06
1/8/16 12:02	72.96	67.86	76.13	79.06
1/8/16 12:07	73.05	67.85	76.13	79.06
1/8/16 12:12	72.79	67.84	76.13	79.06
1/8/16 12:17	72.97	67.72	76.13	79.06
1/8/16 12:22	73.61	67.82	76.13	79.06
1/8/16 12:27	75.20	67.77	76.13	79.06
1/8/16 12:32	75.54	67.85	76.13	79.06
1/8/16 12:37	75.27	67.84	76.13	79.06
1/8/16 12:42	75.32	67.84	76.13	79.06
1/8/16 12:47	75.94	67.91	76.13	79.06
1/8/16 12:52	75.42	67.80	76.13	79.06
1/8/16 12:57	75.80	67.87	76.13	79.06
1/8/16 13:02	75.96	67.91	76.13	79.06
1/8/16 13:07	75.75	67.68	76.13	79.06
1/8/16 13:12	75.52	67.88	76.13	79.06
1/8/16 13:17	76.46	67.91	76.13	79.06
1/8/16 13:22	76.15	67.85	76.13	79.06
1/8/16 13:27	76.29	67.77	76.13	79.06
1/8/16 13:32	76.30	67.85	76.13	79.06
1/8/16 13:37	76.46	67.90	76.13	79.06
1/8/16 13:42	76.96	67.90	76.13	79.06
1/8/16 13:47	77.25	67.91	76.14	79.06
1/8/16 13:52	77.23	67.95	76.14	79.06
1/8/16 13:57	77.32	67.89	76.14	79.06
1/8/16 14:02	77.39	67.91	76.14	79.06
1/8/16 14:07	77.14	67.92	76.14	79.07
1/8/16 14:12	77.32	67.85	76.14	79.07
1/8/16 14:17	77.42	67.75	76.14	79.07
1/8/16 14:22	77.16	67.93	76.14	79.07
1/8/16 14:27	77.38	67.89	76.14	79.07
1/8/16 14:32	77.36	67.84	76.14	79.07
1/8/16 14:37	77.36	67.96	76.14	79.07
1/8/16 14:42	77.72	67.80	76.14	79.07
1/8/16 14:47	77.54	67.85	76.14	79.07
1/8/16 14:52	77.50	67.84	76.14	79.07
1/8/16 14:57	77.62	67.83	76.14	79.07
1/8/16 15:02	77.47	67.86	76.14	79.07
1/8/16 15:07	77.68	67.83	76.14	79.07

9.3 Riyadh GCV System Design

The new tool was applied to design a GCV system design for an office building in Riyadh, as a case study, by following the tool guidelines. First, the required volume flow rate was calculated using the ASHRAE standard, followed by the tool input. Third, the tool processing was performed. Fourth, the recommended GCV system design was determined in the tool output. All of these steps are necessary to find the best recommended GCV system for any building.

Building ventilation volumetric flow rate

Using ASHRAE standard 62 (2013), the required ventilation flow for the office building was calculated. This depends on building type and size, function, and the occupancy density to calculate building ventilation. The results show that the required volumetric flow rate for the office building was 3,830 CFM, as Table 53 shows; this was rounded up to 3,850 CFM.

Table 53: Ventilation Calculations for an Office Building (Stanke, 2004)

					Cooling		Heating	
Ventilation Zone	People Outdoor Air Rate	Zone Population	Area Outdoor Air Rate	Zone Floor Area	Zone Ventilation Efficiency	Zone Outdoor Airflow	Zone Ventilation Efficiency	Zone Outdoor Airflow
	R_p	P_z	R_a	A_z	E_z	V_{oz}	E_z	V_{oz}
	cfm/person		cfm/ft²	ft²		cfm		cfm
South Offices	5	20	0.06	2,000	1.0	220	0.8	275
West Offices	5	20	0.06	2,000	1.0	220	0.8	275
North Offices	5	20	0.06	2,000	0.9	244	0.8	275
East Offices	5	20	0.06	2,000	1.0	220	0.8	275
Interior Offices	5	100	0.06	20,000	1.0	1,700	0.8	2,125
North Conference Room	5	14.4*	0.06	2,000	0.9	213	0.8	240
South Conference Room	5	23.1**	0.06	3,000	0.9	328	0.8	369
Total Zone-Level Outdoor Airflow					ΣV_{oz} =	3,150	ΣV_{oz} =	3,830
Single-Zone Systems: Total Intake Air							ΣV_{oz} =	3,830
100%-Outdoor-Air System							V_{ot} =	3,830

* Average population (72% of 20-person peak population)
** Average population (77% of 30-person peak population)

Tool input

The second step in the case study was to input the Riyadh weather file and GCV design parameters. For the weather file, the previously collected hourly in-situ data were saved in an Excel file. These data included air and ground temperatures at a depth of 6.56 feet, 13.12 feet, and 19.68 feet, respectively. For GCV design parameters, some parameters were limited based on land size (as Figure 9-6 shows), such as pipe length, pipe depth, and soil type. The pipe length parameters ranged from 400 feet to 600 feet, and pipe depth was input for deeps of 13.12 feet and 19.68 feet. The pipe diameters ranged from 24 to 42 inches. The soil type at the site is limestone. There were four to six pipes in the GCV system, and the volume flow rate was entered as 3,850 CFM (based on the previous calculation). The operation system was set to work five days a week for 12 hours a day, from 6 am to 6 pm. Figure 9-7 shows all the tool inputs for the office building.

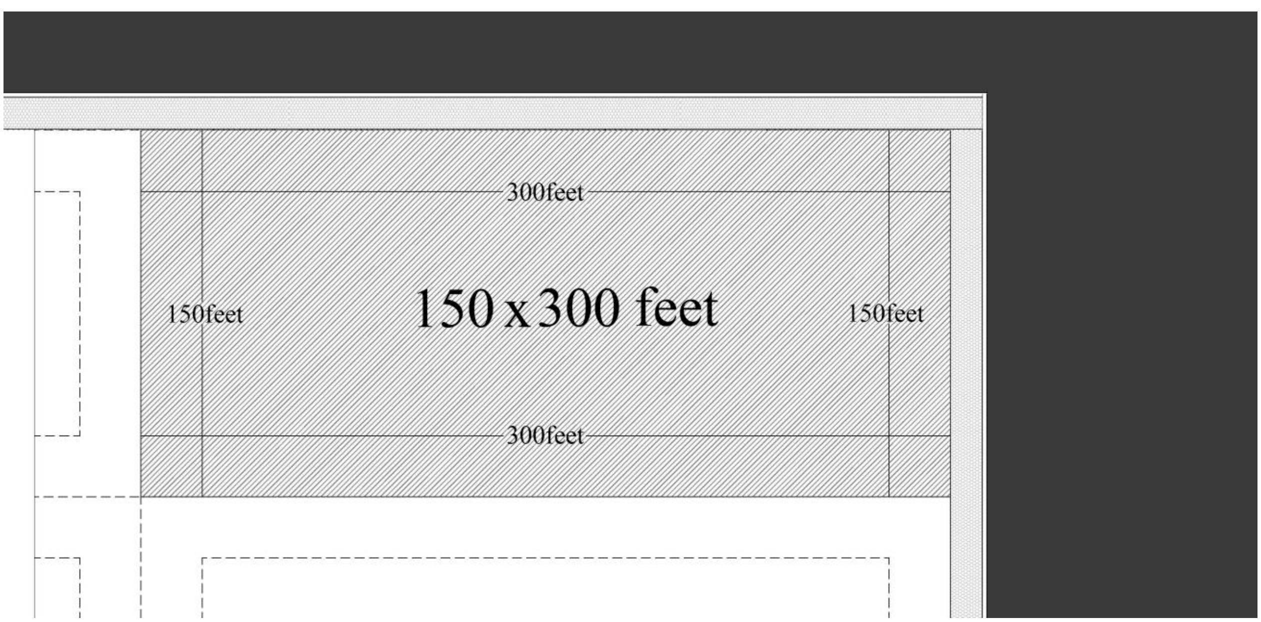

Figure 9-6: Office Building Site Plan

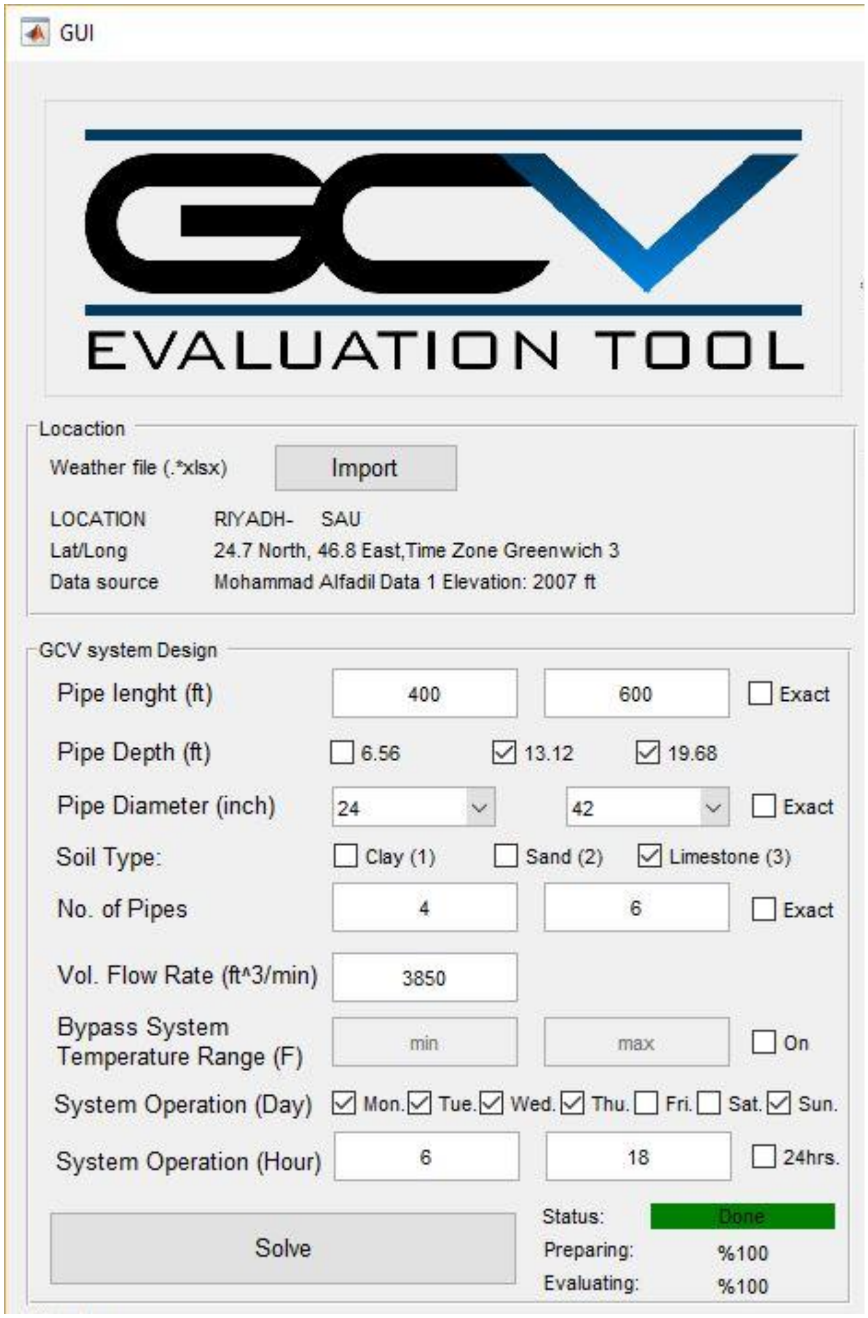

Figure 9-7: Tool Input for the Office Building

Tool processing

Following the descriptive inputs, the tool calculated the temperature changes for the GCV systems. All of the inputs were checked. The results were presented after loading was completed.

Tool output

The output is shown in a table organized by system type. The design that produced the greatest temperature change between the inlet and outlet temperatures, design ID: 862, was selected, and compared with other designs to see whether they differed significantly. Figure 9-8 shows the GCV system comparisons. Design ID: 862 has four pipes with a pipe length of 600 feet, at a depth of 19.68 feet, and with a diameter of 24 inches, which provides a total energy reduction of 208,888,048 BTU over the year and works five days a week for 12 hours a day as an open loop system to ventilate the building. Figure 9-9 shows the outlet temperature of the GCV system design during the operation time.

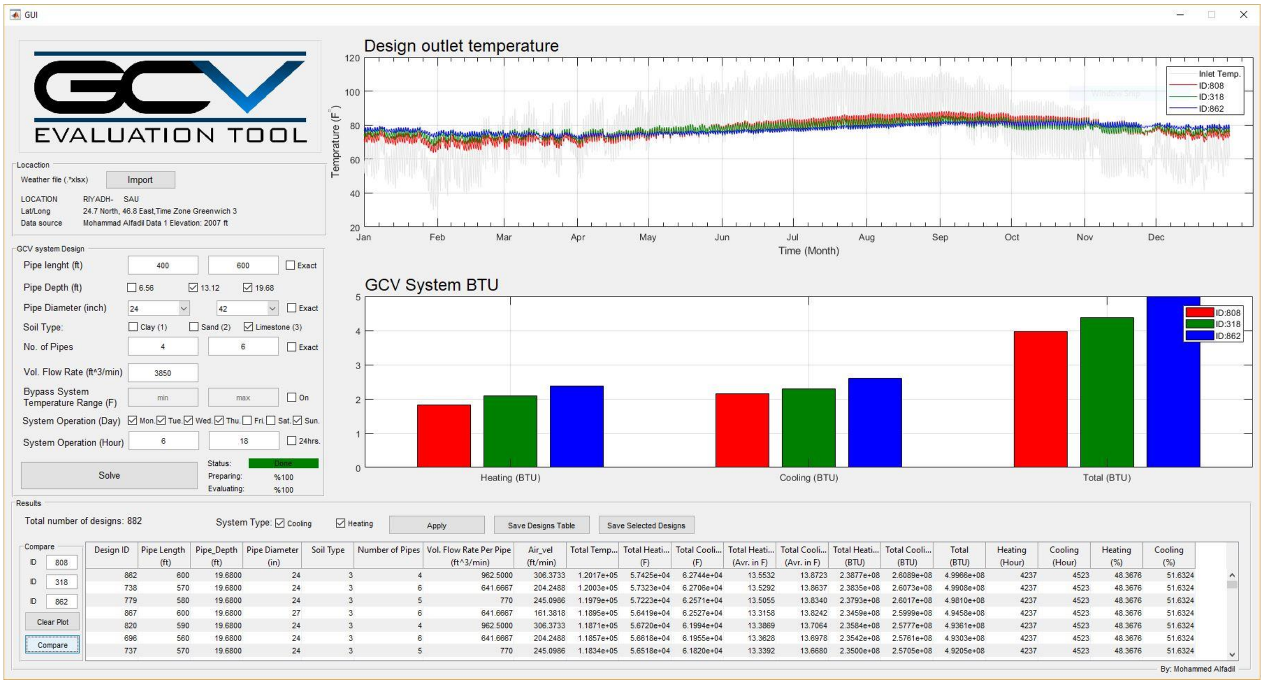

Figure 9-8: GCV System Design Comparison for the Office Building (Open Loop)

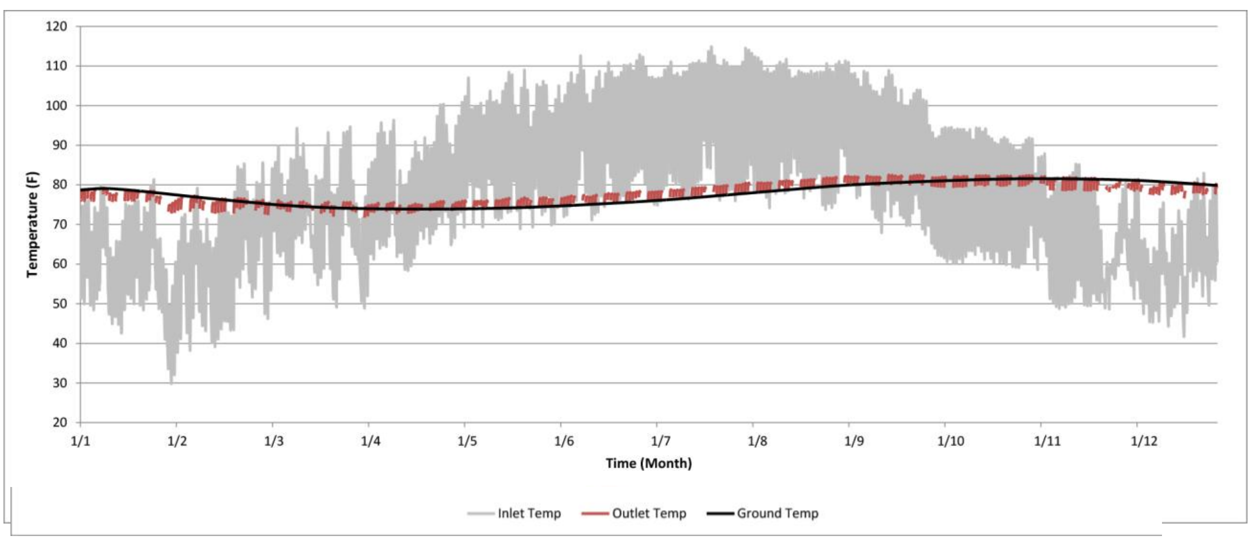

Figure 9-9: GCV System Design Performance for the Office Building

9.4 Summary

This chapter can be summarized as follows:

- **In-situ Riyadh data collection:** because the EPW weather file data for Riyadh was old (from 1983), updated data for the air and ground temperature were required. Air and ground temperatures were collected at different depths (6.56ft, 13.12ft and 19.68ft) every five minutes throughout the year 2016 using a HOBO analog logger (model UX120-HD).
- **Riyadh GCV system design:** the new tool was applied to determine a GCV system design for an office building in Riyadh by following the tool guidelines. First, the required volume flow rate was calculated using the ASHRAE standard, followed by the tool input. Third, the tool processing was performed. Fourth, the recommended GCV system design was determined in the tool output. As a result, the recommended GCV design has four pipes with a pipe length of 600 feet, at a depth of 19.68 feet, and with a diameter of 24 inches, which provides a total energy rduction of 208,888,048 BTU over the year and works five days a week for 12 hours a day as an open loop system to ventilate the building of cource a final recommendation would include a cost comparison which is planned for further development of the tool.

Chapter 10: Conclusion

Using a GCV system to take advantage of natural phenomena in the ground helps buildings reduce their energy consumption. The problem is that there is no standard design for GCV systems because the design parameters differ from place to place. Predicting a GCV system's performance takes time because it is necessary to run the simulations for a single design over one year. Moreover, a powerful computer is required to run the simulation. Thus, how is it possible to know the system performance if there are many GCV system designs? The answer is that the GCV system evaluation tool created during the course of this research can save time, money, and effort, and better predict and compare GCV system designs' performance.

This research achieved its goals by identifying the recommended GCV system for an office building in Riyadh and creating a GCV system evaluation tool that predicts performance based on research design variables. Furthermore, this research answered the research questions by finding the relations between GCV system variables and using the GCV system tool to confirm that the GCV system works well in Riyadh by reducing the total energy of 208,888,048 BTU over the year in a purposefully selected case study.

10.1 Methodology

This research used several quantitative methods to achieve its goals:

- **In-situ monitoring:** the GCV system at Solar CM House was monitored for eight months. The system had two pipes with different airflows (100 fpm and 200 fpm). Inlet and outlet air temperature and ground temperature at various depths were collected to determine the GCV system temperature changes.

- **Modeling GCV system at the Solar CM House:** the GCV system at the Solar CM House was simulated using CFD and GAEA to see how well the tool predicted temperature reduction. The GCV system simulation was run every two hours for three days (36 hours) at different temperatures—hot, cold, and mild. Both the CFD and GAEA used the GCV design, inlet air temperature, ground temperature, and soil properties from the GCV system at the Solar CM House to calculate the outlet air temperature change that the system achieved.

- **CFD and GAEA validation:** the GAEA and CFD simulations of the GCV system at the Solar CM House were validated by calculating the RMSE to determine the accuracy of the tool's predictions compared to as-built data. The results of this comparison were shown in Table 29 (see Chapter five).
- **GCV parameter modeling:** GCV system parametric models were evaluated through ranges of multiple variables using Autodesk CFD simulation to predict performance of each system. Moreover, a number of boundary conditions were considered for each design, and can be found in Table 54. All of these designs gave a total of 103,500 outlet temperature data points collected for the GCV system designs.

Table 54: GCV System Model Parameters

Variable	Min value											Max value	Unit
Air flow	50		150			250			350			450	fpm
Pipe length	50		150			250			350			450	feet
Pipe diameter	6		12			24			36			48	inch
Soil type	Clay					Sand						Limestone	
Air temperature	5	15	25	35	45	55	65	75	85	95	105	115	Fahrenheit
Ground Temperature	35		45		55		65		75		85	95	Fahrenheit

- **Simulation data and regression analysis:** the simulation data were analyzed to identify the relations between the GCV system design variables. Regression analyses were performed for the cooling and heating systems to derive the regression models using 90% of the data, and the remaining 10% of the data were used to validate the models.
- **Tool development:** the GCV system evaluation tool was developed using MATLAB. This tool predicts the GCV system performance by inputting the GCV system design parameters into the regression models. It also compares different designs and helps the user to choose the recommended cooling or heating design.

- **Riyadh GCV system:** after collecting air and ground temperatures at different depths throughout the year, these data were used as inputs in the GCV system evaluation tool to find the most suitable GCV system design for an office building in Riyadh. Thereafter, the recommended GCV system for this type of building was presented.

10.2 Research Findings

10.2.1 GAEA, CFD simulation, GCV tool accuracy

It is important to predict the GCV system outlet temperature accuracy. The results of the comparison of the GCV system's performance at the Solar CM House as a real model with the predictions from such tools as CFD simulation, GAEA software, and the GCV system evaluation tool can be found in Table 55. Moreover, based on the comparisons of the outlet temperatures over the course of three days, the most accurate tool to predict the outlet temperature was the CFD simulation, followed by the GCV system evaluation tool, and finally the GAEA software. Figure 10-1 and Figure 10-2 show the outlet temperatures as predicted by the GCV tool, GAEA, and CFD with the in-situ recording for the GCV system at the Solar CM House.

Table 55: Outlet Temperature Differences Between Solar CM House, CFD, GAEA, and GCV Tool

		GCV Solar CM House Vs. CFD	GCV Solar CM House Vs. GAEA	GCV Solar CM House Vs. GCV Tool	GCV Solar CM House Vs. CFD	GCV Solar CM House Vs. GAEA	GCV Solar CM House Vs. GCV Tool
	Day	Pipe 100 fpm Outlet Air Temp (°F)			Pipe 200 fpm Outlet Air Temp (°F)		
Root mean square error (Degree Fahrenheit)	24-Jul	0.56	9	3.7	1.15	10.45	3.96
	25-Oct	0.72	4.33	2.83	0.9	4.76	1.99
	20-Dec	0.73	10.8	3.66	1.3	10.63	3

Figure 10-1: GCV Solar CM House vs. All Predicted (CFD, GAEA and GCV Tool) Outlet Temperature on Three Days (100fpm)

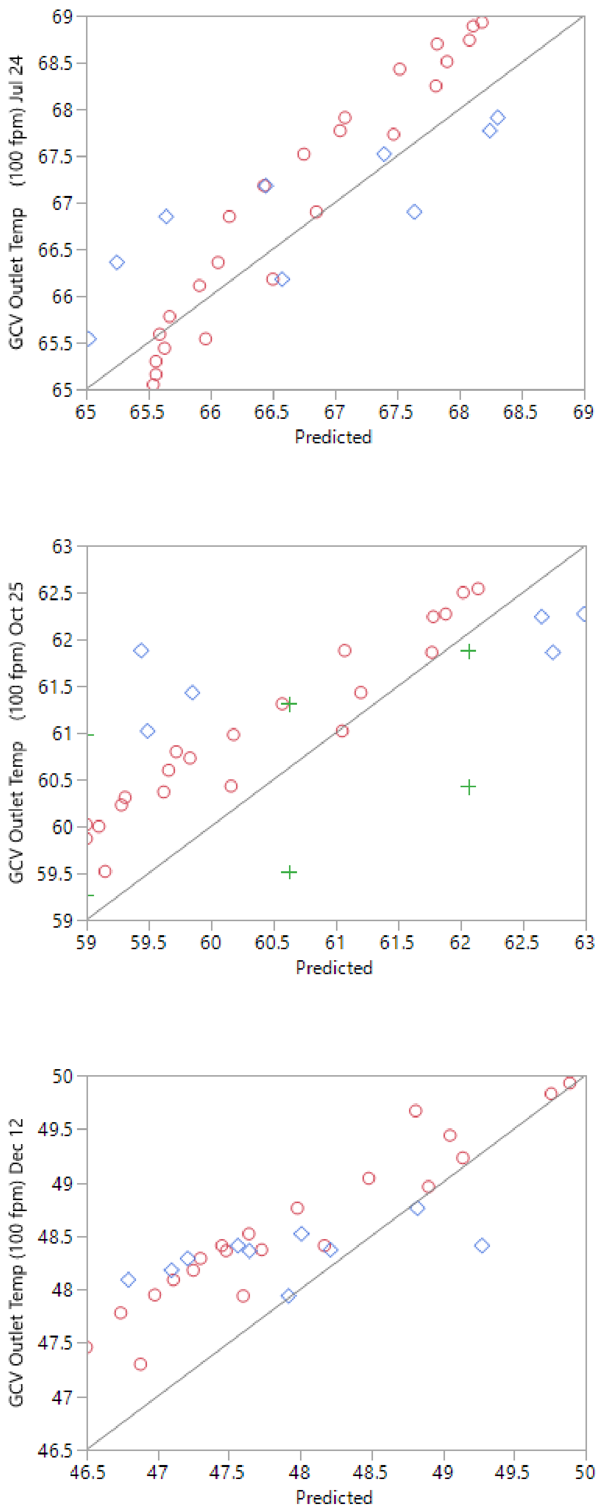

Figure 10-2: GCV Solar CM House vs. All Predicted (CFD, GAEA and GCV Tool) Outlet Temperature on Three Days (200fpm)

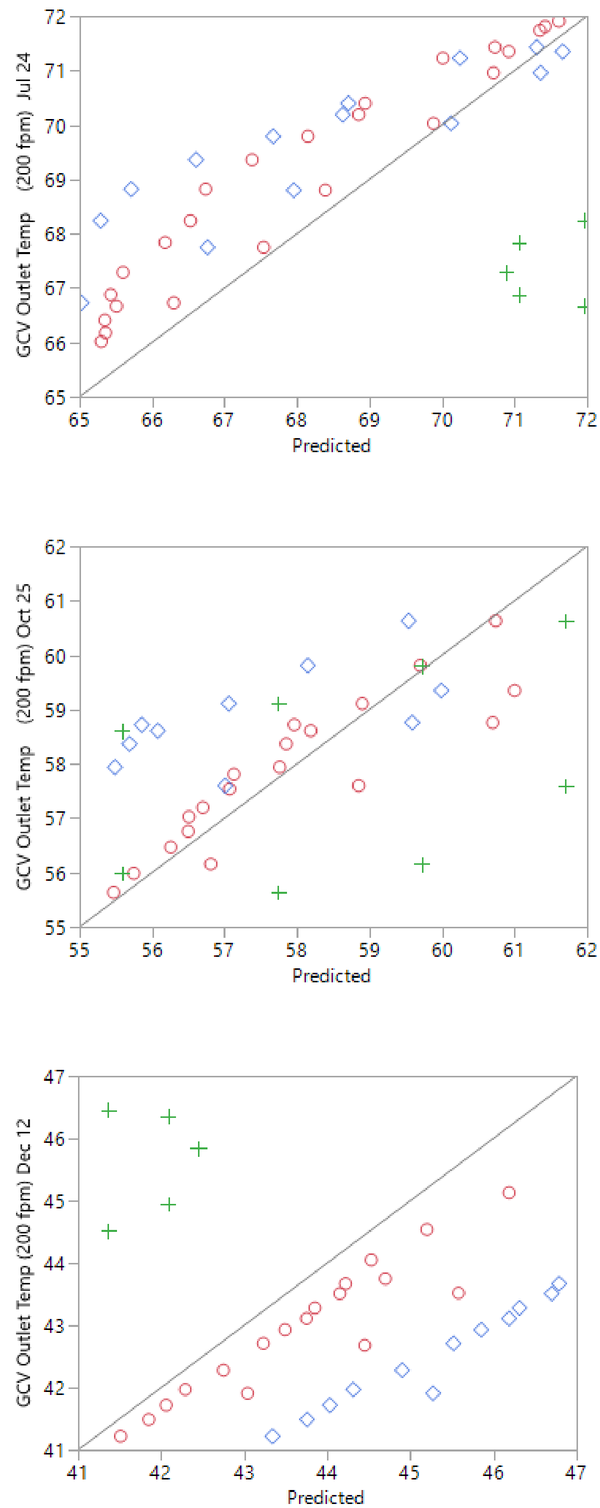

Predictors: ○ CFD + GAEA ◇ GCV Tool

10.2.2 GCV system variable relations

The relations among the variables depend on the operation mode (i.e., whether it is cooling or heating). In the cooling system, there were negative linear relations between pipe diameter, airflow velocity, soil temperature, and inlet temperature with the outlet temperature, and there were positive linear relations between pipe length and the outlet temperature (Figure 10-3). In the heating system, there were negative linear relations between pipe diameter, airflow velocity, and the outlet air temperature, and there were positive linear relations between inlet temperature, ground temperature, and pipe length with the outlet temperature (Figure 10-4).

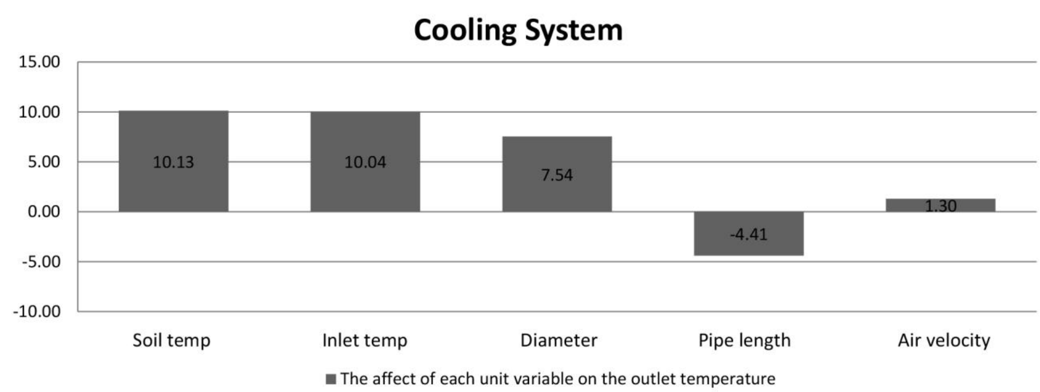

Figure 10-3: Cooling System Variable Relations

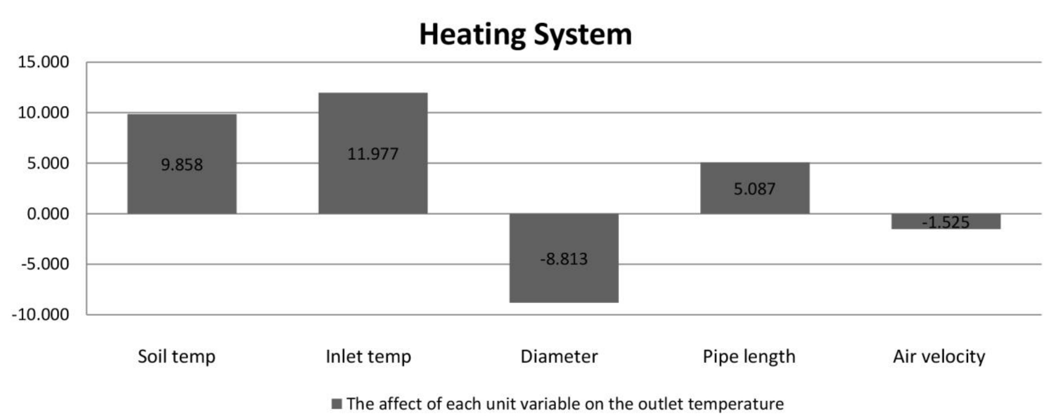

Figure 10-4: Heating System Variable Relations

10.2.3 Regression equation

Based on the operation mode, there are two regression equations—one each for the cooling and heating systems. These equations predict the outlet temperature based on the GCV system variables input into the equation. In the cooling system, the equation predicted 85.21% of the variance in outlet temperature with ±7.99°F error, as Equation 17 shows. In the heating system, the equation predicted 84.28% of the variance in outlet temperature with ±9.04°F error, as Equation 18 shows.

Equation 17: Regression Model for the Cooling System

$$Outlet\ Temperature = (-6.93) + if\,\frac{Limestone = -0.30}{Sand\ or\ Clay = 0.30} + if\,\frac{Sand = -0.71}{Limestone\ or\ Clay = 0.71}$$

$$+(0.49 \times Pipe\ Diameter) + (0.0094 \times Air\ Velocity)$$

$$+(0.54 \times Soil\ Temperature) + (-0.036 \times Pipe\ Length) + (0.46 \times Inlet\ Temperature)$$

Equation 18: Regression Model for the Heating System

$$Outlet\ Temperature = (8.35) + if\,\frac{Limestone = 0.32}{Sand\ or\ Clay = -0.32} + if\,\frac{Sand = 0.80}{Limestone\ or\ Clay = -0.80}$$

$$+(0.57 \times Pipe\ Diameter) + (-0.010 \times Air\ Velocity)$$

$$+(0.51 \times Soil\ Temperature) + (0.036 \times Pipe\ Length) + (0.49 \times Inlet\ Temperature)$$

10.2.4 GCV system evaluation tool

The GCV system evaluation tool software uses the cooling and heating regression models to predict the performance of a GCV system. MATLAB software was used for the interface and for algorithmic coding. The tool recommends a GCV system design to the user based on the system energy performance in BTU. Moreover, it compares multiple GCV system designs' performance based on a range of design variables, including pipe length, pipe depth, pipe diameter, number of pipes, soil type, and volume flow rate over the year. Figure 10-5 shows the GCV system evaluation tool interface.

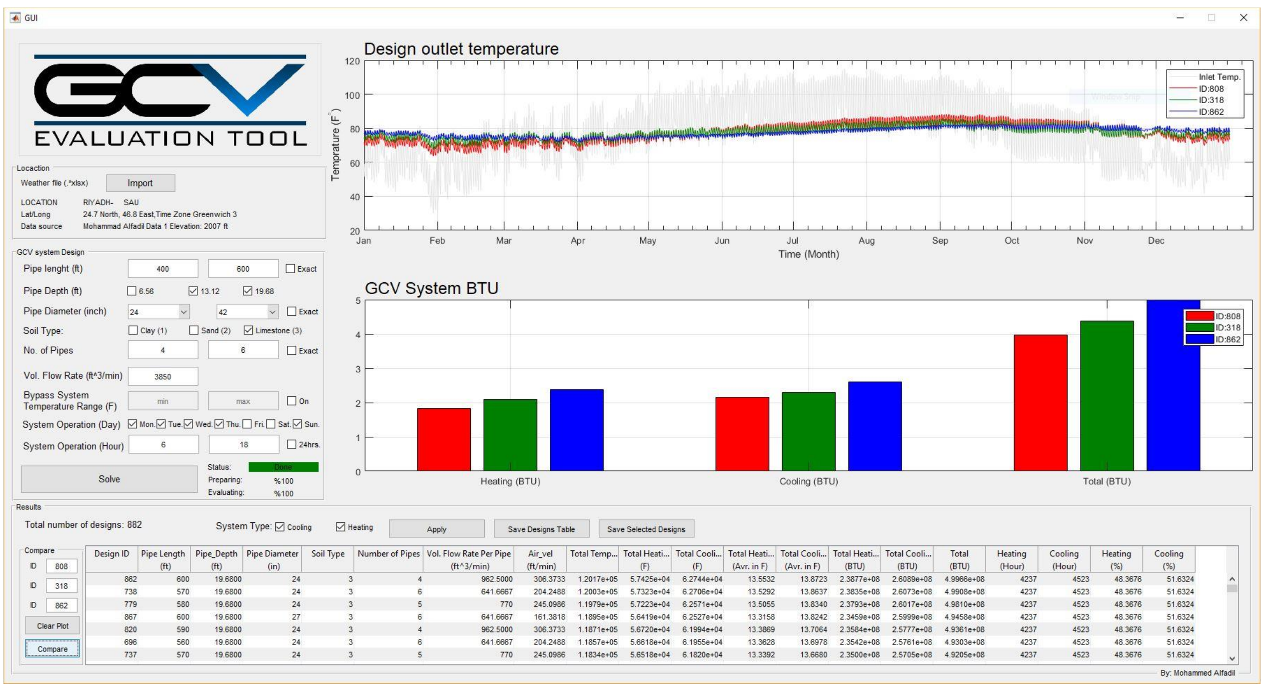

Figure 10-5: GCV System Evaluation Tool Interface

10.2.5 Riyadh GCV system

GCV system open loop design

The GCV system evaluation tool was used to determine the recommended GCV system for an office building in Riyadh. This GCV system design is an open loop system with a pipe length of 600 feet, diameter of 24 inches, depth of 19.68 feet, and four pipes that provides a total of 208,888,048 BTU for cooling and heating over the year. Figure 10-6 shows the GCV system performance for the office building.

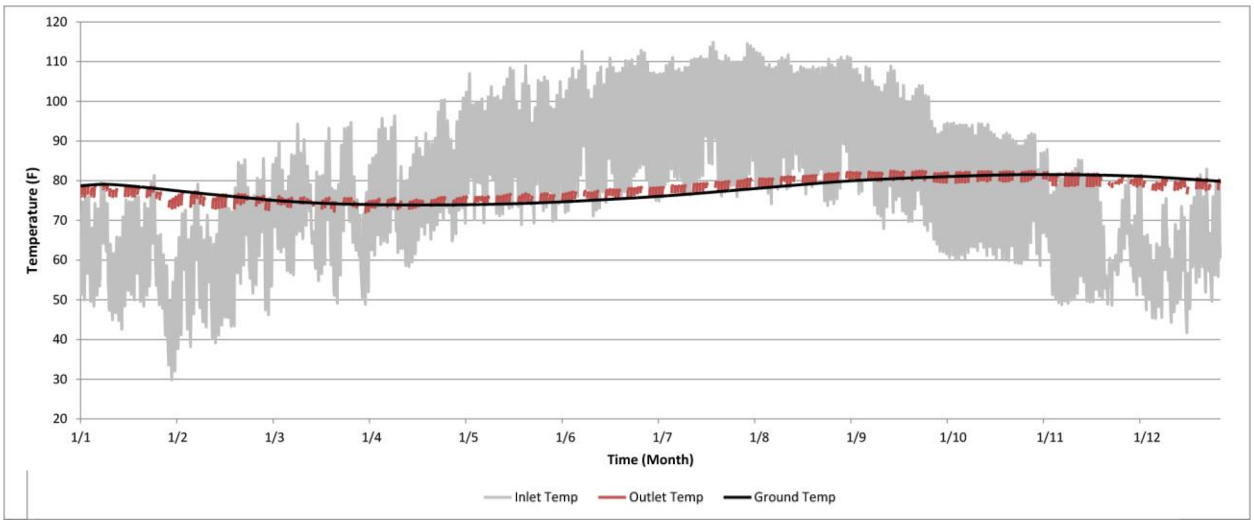

Figure 10-6: GCV System Design (Open Loop) Performance for the Office Building

GCV system closed loop design

The GCV system closed loop is not suitable for non-residential buildings in Saudi Arabia because the GCV system reduces the return air only by approximately four degrees in the hot season. Appendix C shows more details about the closed loop outlet temperature. It is clear that the open loop is more beneficial than the closed loop for ventilation in Riyadh.

10.3 The contributions to the body of knowledge

This research contributes to the body of knowledge in four ways. First, since the HVAC system represents the highest energy consumption in most buildings, by using the GCV system, the energy consumption may be reduced. Second, because the GCV system design varies from place to place, there is no standard design for the GCV system. The outcome of this research is a GCV system tool that predicts the performance of the GCV system, which helps to find the recommended GCV system design for a given building in a particular place. Third, the GCV evaluation tool helps the designer to save time predicting the performance of the GCV system. Fourth, the GCV system evaluation tool is more accurate than the GAEA tool because it relies on regression equations that were derived from parametric GCV modeling from CFD.

10.4 Future Uses for This Research

This research presented regression equations to predict the temperature change in GCV systems' cooling and heating functions. These equations were used in the standalone GCV system evaluation software tool to evaluate multiple GCV systems. In the future, this tool could be further developed in several ways:

- **GCV system cost:** calculating GCV system cost is important to check if the system is significant based on the cost and efficency. Adding the cost of the GCV system and operation cost in the tool would help the user make a decision by showing the life-cycle cost assessments for the GCV system.
- **GCV system design variables:** there are many variables that affect the performance of the GCV system. This research covered some variables including inlet temperature, ground temperature, soil type, pipe diameter, pipe length, and air flow rate. Adding more design variables, such as pipe material or additional soil types to the regression models, would make the tool more accurate and suitable for special GCV system designs.

- **System type:** currently, this tool uses an open loop system because calculations are based on the ambient air temperature from the weather file; however, the tool can be developed to use both open and closed loop systems by setting the indoor temperature as an inlet temperature to calculate system performance.
- **System design:** as a vertical and horizontal design, the GCV evaluation tool was developed to cover the preformance of a horizontal GCV system because it relies on a certain depth of soil temperature in the weather file. Since, the ground temperatures are more stable as the depth increases, this tool could be developed to cover the performance of a vertical GCV system by adding a stable ground temperature to the weather file.
- **Energy modeling software add-ons:** presently, the GCV evaluation tool is a standalone tool. As further research, the regression models could be integrated into energy modeling software that would help calculate cooling and heating loads, compare GCV systems with other HVAC systems, and perform life-cycle cost assessments of the GCV system.
- **Charging soil temperature:** the GCV system will overtime thermally charge the surrounding soil close to the pipe. This charge relies on airflow rate in the pipe, as Appendix D shows. As further research, charging the soil temperature could be studied by comparing different GCV systems with different airflow rates. Also, future research could study charging the surrounding soil of the GCV system during the day and night, which may charge or discharge the soil at different airflow rates.

All of these points could be used in the future to add to the body of knowledge on GCV systems specifically and geo-exchange system in general.

References

Ahmed, A., Miller, A., & Gidado, K. (2009). Thermal performance of earth-air heat exchanger for reducing cooling energy demand of office buildings in the United Kingdom. In *11th Conference of international building performance simulation association* (Vol. 2009, pp. 2228–2235).

Albers, K. (1991). *Untersuchungen zur Auslegung von Erdwärmeaustauschern für die Konditionierung der Zuluft für Wohngebäude*. Universität Dortmund, Dortmund.

Alghamdi, J. K. (2008). *CFD simulation methodology for ground-coupled ventilation system*. Virginia Polytechnic Institute and State University.

Al-Saud, M. bin S. (2016). Foreword | Saudi Vision 2030. Retrieved July 1, 2017, from http://vision2030.gov.sa/en/foreword

ANSYS Inc. (2010). ANSYS CFX Features. Retrieved May 4, 2015, from http://www.ansys.com/Products/Simulation+Technology/Fluid+Dynamics/Fluid+Dynamics+Products/ANSYS+CFX/Features

ASHRAE. (2013). Standard 62.1-2013 Ventilation for Acceptable Indoor Air Quality. *American Society of Heating, Refrigerating and Air-Conditioning Engineers, Inc., Atlanta, GA.*

Autodesk. (2015a, December 28). Laminar Flow Over Heated Cylinder | CFD | Autodesk Knowledge Network. Retrieved May 21, 2018, from https://knowledge.autodesk.com/support/cfd/learn-explore/caas/CloudHelp/cloudhelp/2014/ENU/SimCFD/files/GUID-0047747C-6C44-4AC9-93F8-FB30E6C373F9-htm.html

Autodesk. (2015b, December 28). Non-Newtonian Flow Around a Cylinder Array | CFD | Autodesk Knowledge Network. Retrieved May 21, 2018, from https://knowledge.autodesk.com/support/cfd/learn-explore/caas/CloudHelp/cloudhelp/2014/ENU/SimCFD/files/GUID-D3877E27-D5D9-4CF3-A509-1DF87810EE5A-htm.html

Autodesk. (2015c, December 28). Turbulent Axisymmetric Pipe Flow. Retrieved May 21, 2018, from https://knowledge.autodesk.com/support/cfd/learn-explore/caas/CloudHelp/cloudhelp/2014/ENU/SimCFD/files/GUID-83D8E933-5803-44F3-99EB-5B97A73AC2AF-htm.html

Autodesk CFD. (2016). Compare Autodesk CFD, CFD Advanced, and CFD Motion. Retrieved September 29, 2016, from http://www.autodesk.com/products/cfd/compare

Benkert, S., Heidt, F. D., & Schöler, D. (1997). Calculation tool for earth heat exchangers GAEA. Presented at the Fifth International IBPSA Conference, Prague.

Bojic, M., Trifunovic, N., Papadakis, G., & Kyritsis, S. (1997). Numerical simulation, technical and economic evaluation of air-to-earth heat exchanger coupled to a building. *Energy*, *22*(12), 1151–1158.

CD-adapco. (2015). STAR-CCM+ v10: Brochure. Retrieved May 4, 2015, from http://www.cd-adapco.com/brochure/star-ccm-v10-brochure

Cengel, Y. A. (2012). *Fundamentals of thermal-fluid sciences* (4th ed.). McGraw-Hill New York.

De Paepe, M., & Janssens, A. (2003). Thermo-hydraulic design of earth-air heat exchangers. *Energy and Buildings*, *35*(4), 389–397.

De Paepe, M. (2002). 3D unstructured finite volume technique for modelling earth air heat exchangers. *Heat Transfer VII, Proceedings of the Seventh International Conference on Advanced Computational Methods in Heat Transfer, Halkidiki, 2002, WIT Press. - ISBN 1-85312-906-2*, 471–480.

Farouki, O. T. (1981). *Thermal properties of soils*. Hanover, N.H.: U.S. Army Corps of Engineers, Cold Regions Research and Engineering Laboratory

Flückiger, B., Monn, C., Lüthy, P., & Wanner, H.-U. (1998). Hygienic aspects of ground-coupled Air systems. *Indoor Air*, *8*(3), 197–202.

Gauthier, C., Lacroix, M., & Bernier, H. (1997). Numerical simulation of soil heat exchanger-storage systems for greenhouses. *Solar Energy*, *60*(6), 333–346.

Georgiou, G., Momani, S., Crochet, M. J., & Walters, K. (1991). Newtonian and non-Newtonian flow in a channel obstructed by an antisymmetric array of cylinders. *Journal of Non-Newtonian Fluid Mechanics*, *40*(2), 231–260.

Givoni, B. (1998). *Climate considerations in building and urban design*. New Yourk: Van Nostrand Reinhold.

Hollmuller, P., & Lachal, B. (2001). Cooling and preheating with buried pipe systems: Monitoring, simulation and economic aspects. *Energy and Buildings*, *33*(5), 509–518.

Holman, J. P. (1981). *Heat transfer* (5th ed). New York : McGraw-Hill.

International Energy Agency. (2015). Key World Energy Statistics. Retrieved March 16, 2016.

Kumar, R., Ramesh, S., & Kaushik, S. C. (2003). Performance evaluation and energy conservation potential of earth–air–tunnel system coupled with non-air-conditioned building. *Building and Environment*, *38*(6), 807–813.

Kuzmin, D. (2014). Introduction to computational fluid dynamics [PowerPoint presentation]. Retrieved from http://www.mathematik.uni-dortmund.de/~kuzmin/cfdintro/lecture1.pdf.

Mihalakakou, G., Santamouris, M., & Asimakopoulos, D. (1994). Modelling the thermal performance of earth-to-air heat exchangers. *Solar Energy*, *53*(3), 301–305.

Mihalakakou, G., Santamouris, M., Lewis, J. O., & Asimakopoulos, D. N. (1997). On the application of the energy balance equation to predict ground temperature profiles. *Solar Energy*, *60*(3–4), 181–190.

Mission Rubber Company LLC. (1951). Standard Pipe Sizes. Retrieved October 16, 2016, from http://www.missionrubber.com/StandardPipeSizes.php

Pérez-Lombard, L., Ortiz, J., & Pout, C. (2008). A review on buildings energy consumption information. *Energy and Buildings*, *40*(3), 394–398.

Peters-Lidard, C. D., Blackburn, E., Liang, X., & Wood, E. F. (1998). The effect of soil thermal conductivity parameterization on surface energy fluxes and temperatures. *Journal of the Atmospheric Sciences*, *55*(7), 1209–1224.

Reysa, G. (2005). Ground temperatures as a function of location, season, and depth. Retrieved April 7, 2015, from http://www.builditsolar.com/Projects/Cooling/EarthTemperatures.htm

Riley, J. F. (1984). *A multifunction wall system for application with solar heating and ground cooling*. Virginia Polytechnic Institute and State University.

Riley, J. F., & Schubert, R. P. (1985). A multifunction wall system for application with solar heating and ground cooling. *NASA STI/Recon Technical Report N*, *85*.

Stanke, D. (2004). Single-zone & dedicated-OA systems. *ASHRAE Journal*, *46*(10), 12.

Taylor, D. (2008, January). Ground cupled + air coupled energy.

The Animal House ~ The Incredible Termite Mound | Nature | PBS. (2011, October). Retrieved February 27, 2015, from Nature website: http://www.pbs.org/wnet/nature/the-animal-house-the-incredible-termite-mound/7222/

Thermal Conductivity of some common Materials and Gases. (2015). Retrieved November 17, 2016, from http://www.engineeringtoolbox.com/thermal-conductivity-d_429.html

Trząski, A., & Zawada, B. (2011). The influence of environmental and geometrical factors on air-ground tube heat exchanger energy efficiency. *Building and Environment*, *46*(7), 1436–1444.

White, F. M. (1994). *Fluid mechanics*. McGraw-Hill Ryerson, Boston, MA.

York County School Division - Green YCSD Geothermal Heating & Cooling. (2016). Retrieved November 24, 2016, from http://yorkcountyschools.org/greenYCSD/geothermal.aspx

APPENDICES

Appendix A: GCV system at Solar CM House inspection

The Sterrett Facilities Complex and Environmental Health and Safety at Virginia Tech inspected the GCV system at Solar CM House for cracks and mold. They used special equipment with cameras to check the surface of the pipes and took samples to determine whether there was any mold or bacteria in the pipes. The results showed that there were neither cracks nor mold in any pipes, although pipes 7 and 8 contained some gravel, as Figure 4 shows.

Figure 1: Inspection Equipment

Figure 2: Humidity Inspection

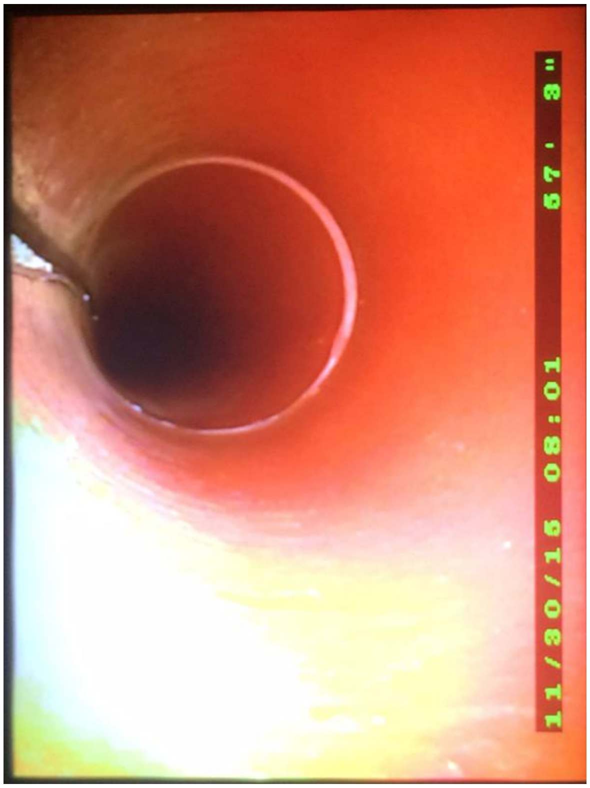

Figure 3: GCV System's Second Pipe

Figure 4: GCV System's Seventh Pipe

Appendix B: Boundary conditions:

Different volume flow rates

The boundary condition for volume flow rate was changed to determine temperature changes in the GCV system. The boundary condition for the simulation was set as shown in Table 56. The pipes differed, in that one had 118 CFM and the other had 353 CFM, as Figure 5 and Figure 6 show. As a result, the pipe with 118 CFM had a temperature reduction from 110^{o}F to 95^{o}F, while the pipe with 353 CFM had a temperature reduction from 110^{o}F to 103^{o}F. Figure 7, Figure 8, Figure 9 and Figure 10 show sections of the temperature changes. The results indicate that if the volume flow rate is reduced, the temperature is reduced more for cooling and raises more for heating.

Table 56: Boundary Condition for Different Volume Flow Rates

Domain	Elements	Variables	
Air		**Pipe 1**	**Pipe 2**
	Boundary condition		
	Turbulence	k-epsilon	k-epsilon
	Inlet temperature	110 F	110 F
	Volume flow rate	**118 ft^3/min**	**353 ft^3/min**
	Outlet heat flux	0 BTU/ft2/min	0 BTU/ft2/min
	Outlet pressure	0 Gage	0 Gage
	Physical properties		
	Density	Equation of state	Equation of state
	Conductivity	0.02563 w/m-k	0.02563 w/m-k
	Specific heat	1004 J/kg-k	1004 J/kg-k
	Viscosity	3.79148e-07 lbf-s/ft2	3.79148e-07 lbf-s/ft2
Pipe			
	Boundary condition		
	Thickness	1.12 in	1.12 in
	Diameter	12 in	12 in
	Material	Clay	Clay
	Shape	Cylinder	Cylinder
	Length	84 feet	As built
	Depth	19 feet	19 feet
	Physical properties		
	Conductivity	1.2 w/m-k	1.2 w/m-k
	Specific heat	900.16 J/kg-k	900.16 J/kg-k
	Density	2 g/cm3	2 g/cm3
Backfill			
	Boundary condition		
	Thickness	10 in	10 in
	Type	Gravel	Gravel
	Physical properties		
	Conductivity	0.7 w/m-k	0.7 w/m-k
	Specific heat	932 J/kg-k	932 J/kg-k
	Density	2 g/cm3	2 g/cm3
Soil			
	Boundary condition		
	Type	Ultisols	Ultisols
	Face 1 heat transfer	Temperature = 88.5Fahrenheit	Temperature = 88.5Fahrenheit
	Face 2 heat transfer	Temperature = 68.5Fahrenheit	Temperature = 68.5Fahrenheit
	Face 3 heat transfer	Heat flux = 0 BTU/ft2/min	Heat flux = 0 BTU/ft2/min
	Face 4 heat transfer	Heat flux = 0 BTU/ft2/min	Heat flux = 0 BTU/ft2/min
	Face 5 heat transfer	Heat flux = 0 BTU/ft2/min	Heat flux = 0 BTU/ft2/min
	Face 6 heat transfer	Heat flux = 0 BTU/ft2/min	Heat flux = 0 BTU/ft2/min
	Physical properties		
	Conductivity	1.2975 w/m-k	1.2975 w/m-k
	Specific heat	962.96 J/kg-k	962.96 J/kg-k
	Density	2.4 g/cm3	2.4 g/cm3

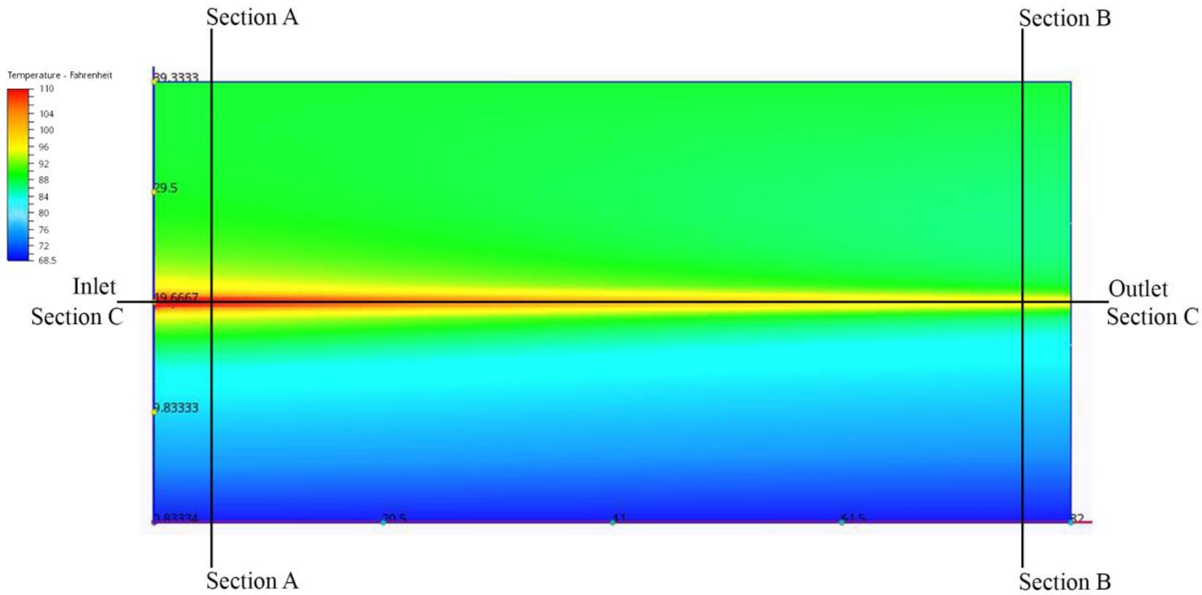

Figure 5: Pipe with 118 CFM

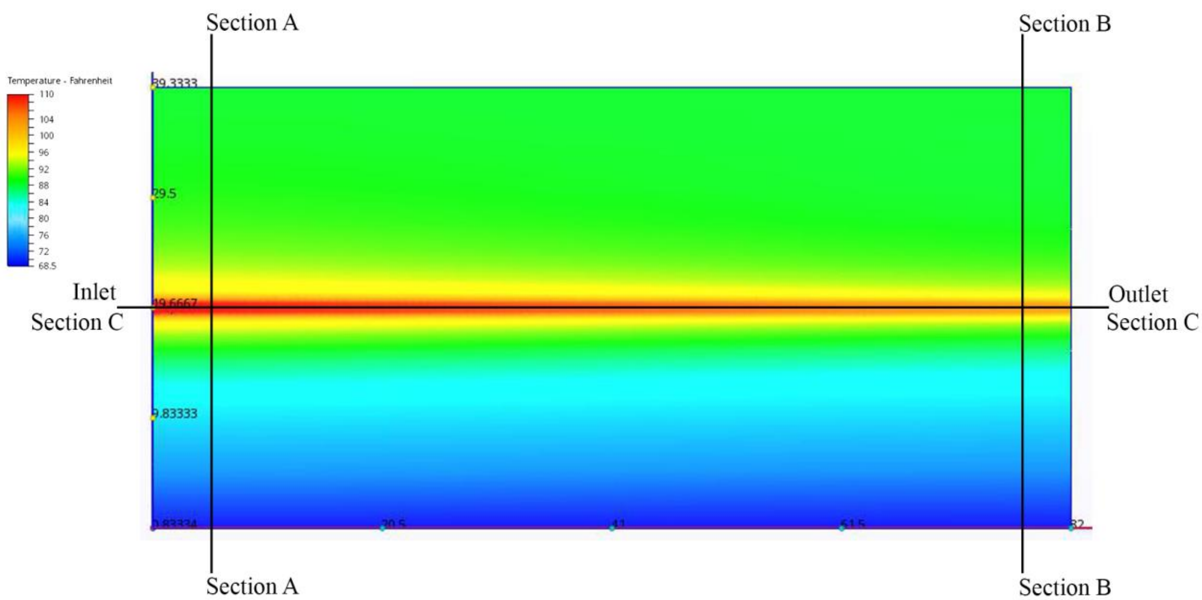

Figure 6: Pipe with 353 CFM

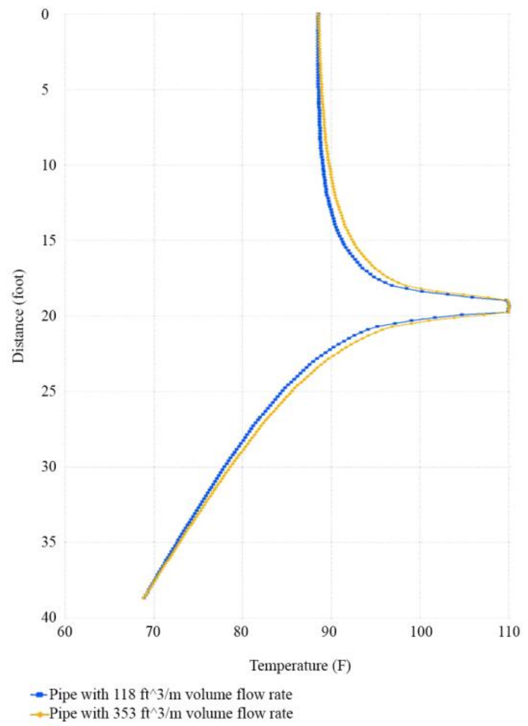

Figure 7: Section A

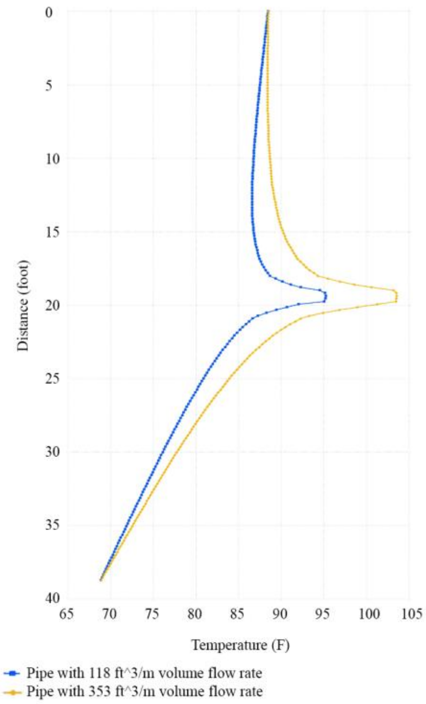

Figure 8: Section B

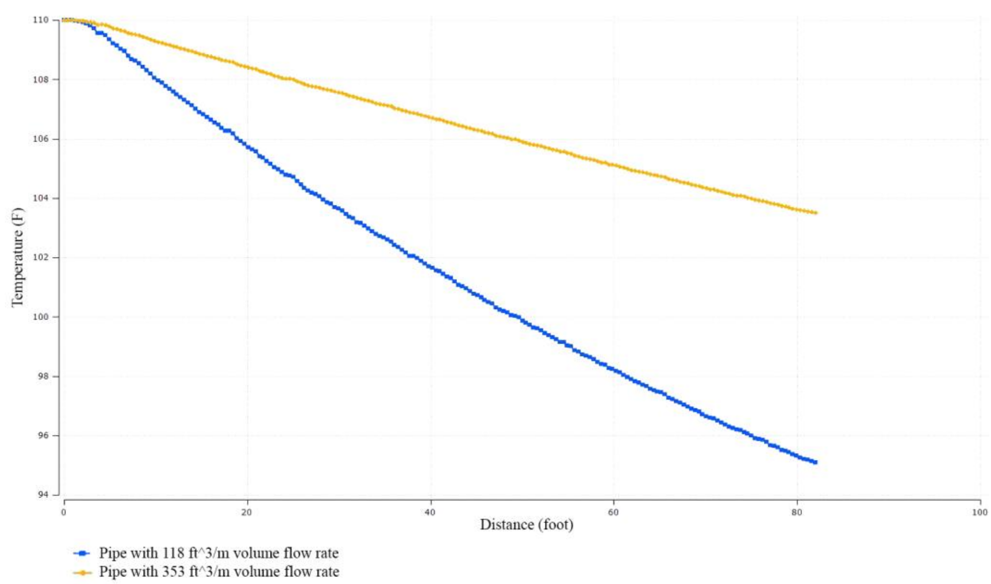

Figure 9: Section C

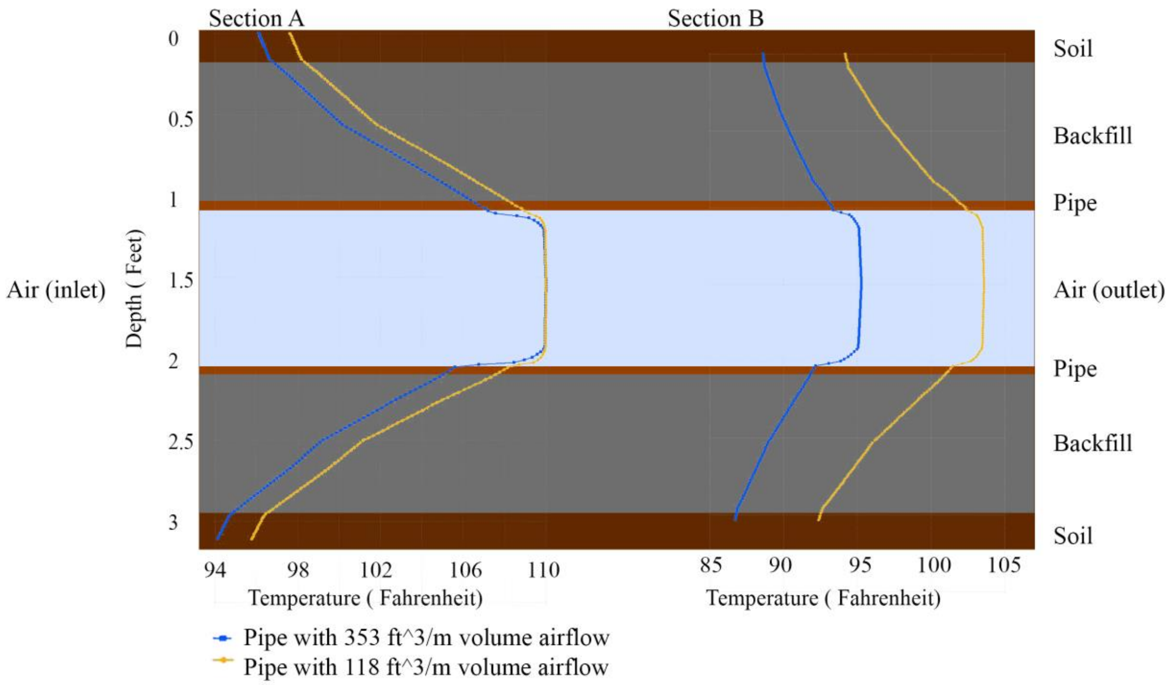

Figure 10: Detail of A and B Sections' Boundary Conditions

Different soil temperatures

The boundary condition for the soil was changed to determine the GCV system's temperature change. The boundary condition for the simulation was set, as shown in Table 57. The two boundaries differed in temperature (the top surface was 88.5°F and the bottom surface was 68.5°F), while the other was fixed at 78.5°F, as Figure 11 and Figure 12 show. As a result, both boundaries achieved the same temperature reduction of 83°F, as Figure 13, Figure 14, and Figure 15 show. Accordingly, this indicates that the soil temperature close to the pipe surface affects the GCV system.

Table 57: Boundary Condition for Different Soil Temperatures

Domain	Elements	Variables	
Air		**Pipe 1**	**Pipe 2**
	Boundary condition		
	Turbulence	k-epsilon	k-epsilon
	Inlet temperature	110 F	110 F
	Volume flow rate	118 ft^3/min	118 ft^3/min
	Outlet heat flux	0 BTU/ft2/min	0 BTU/ft2/min
	Outlet pressure	0 Gage	0 Gage
	Physical properties		
	Density	Equation of state	Equation of state
	Conductivity	0.02563 w/m-k	0.02563 w/m-k
	Specific heat	1004 J/kg-k	1004 J/kg-k
	Viscosity	3.79148e-07 lbf-s/ft2	3.79148e-07 lbf-s/ft2
Pipe			
	Boundary condition		
	Thickness	1.12 in	1.12 in
	Diameter	12 in	12 in
	Material	Clay	Clay
	Shape	Cylinder	Cylinder
	Length	84 feet	As built
	Depth	19 feet	19 feet
	Physical properties		
	Conductivity	1.2 w/m-k	1.2 w/m-k
	Specific heat	900.16 J/kg-k	900.16 J/kg-k
	Density	2 g/cm3	2 g/cm3
Backfill			
	Boundary condition		
	Thickness	10 in	10 in
	Type	Gravel	Gravel
	Physical properties		
	Conductivity	0.7 w/m-k	0.7 w/m-k
	Specific heat	932 J/kg-k	932 J/kg-k
	Density	2 g/cm3	2 g/cm3
Soil			
	Boundary condition		
	Type	Ultisols	Ultisols
	Face 1 heat transfer	**Temperature = 78.5Fahrenheit**	**Temperature = 88.5Fahrenheit**
	Face 2 heat transfer	**Temperature = 78.5Fahrenheit**	**Temperature = 68.5Fahrenheit**
	Face 3 heat transfer	Heat flux = 0 BTU/ft2/min	Heat flux = 0 BTU/ft2/min
	Face 4 heat transfer	Heat flux = 0 BTU/ft2/min	Heat flux = 0 BTU/ft2/min
	Face 5 heat transfer	Heat flux = 0 BTU/ft2/min	Heat flux = 0 BTU/ft2/min
	Face 6 heat transfer	Heat flux = 0 BTU/ft2/min	Heat flux = 0 BTU/ft2/min
	Physical properties		
	Conductivity	1.2975 w/m-k	1.2975 w/m-k
	Specific heat	962.96 J/kg-k	962.96 J/kg-k
	Density	2.4 g/cm3	2.4 g/cm3

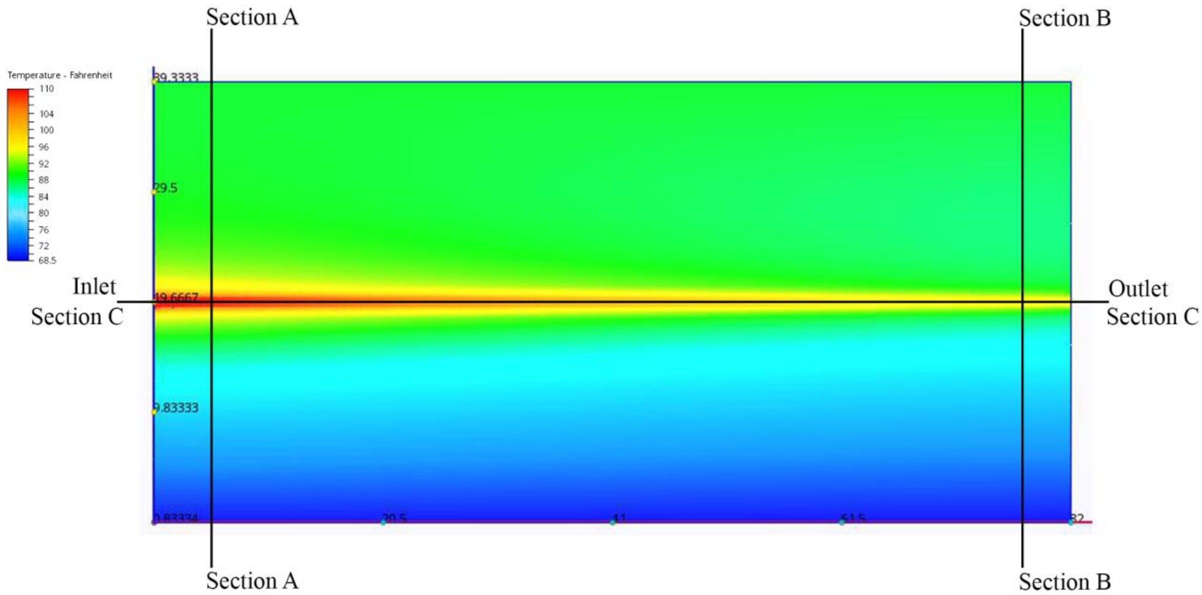

Figure 11: Pipe with Soil Temperature Difference (Top 88.5°F, Bottom 68.5°F)

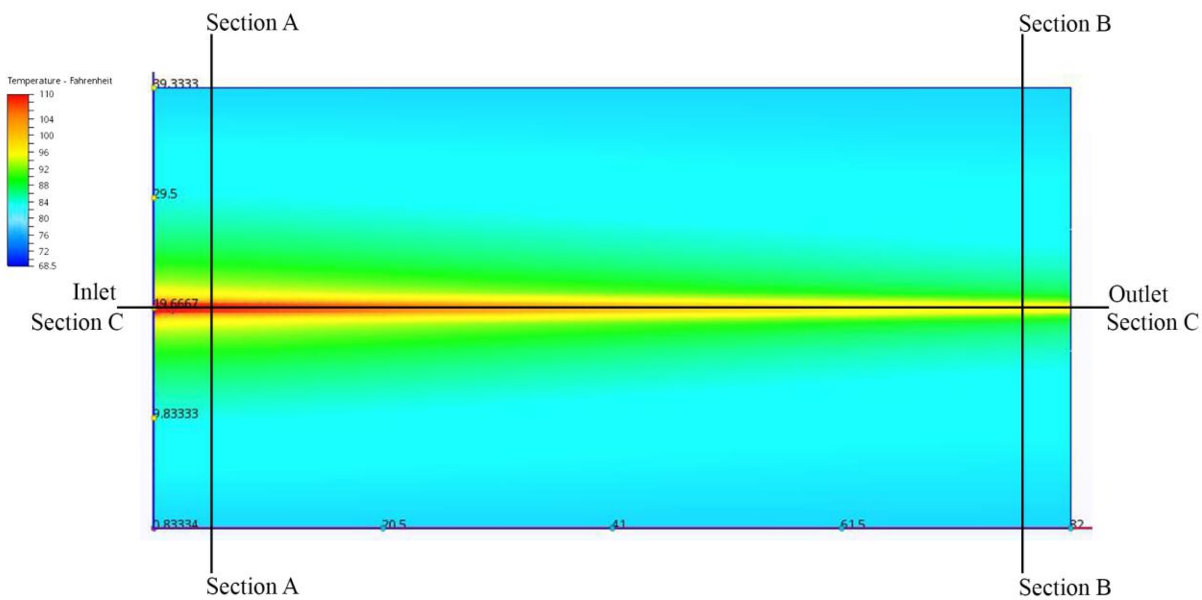

Figure 12: Pipe with Fixed Soil Temperature (78.5°F)

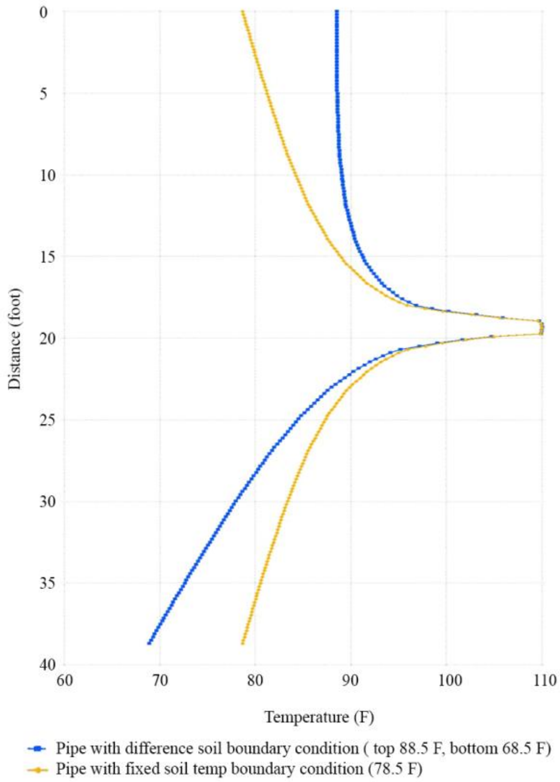

Figure 13: Section A

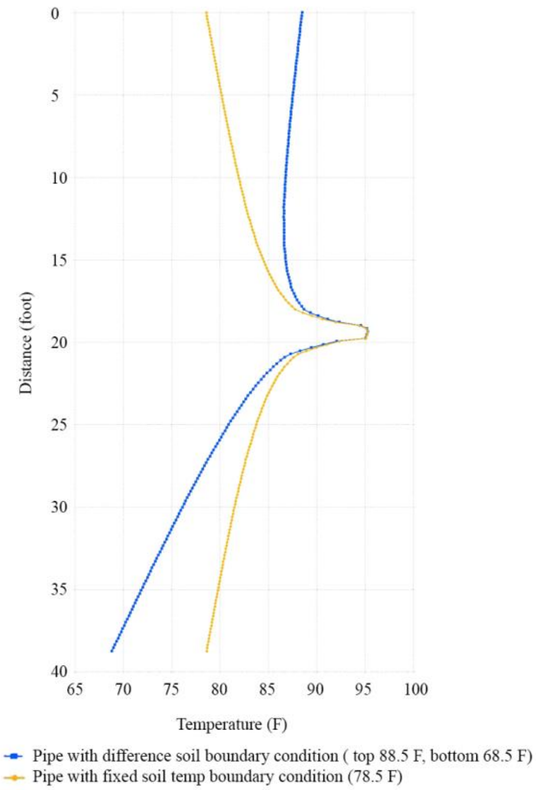

Figure 14: Section B

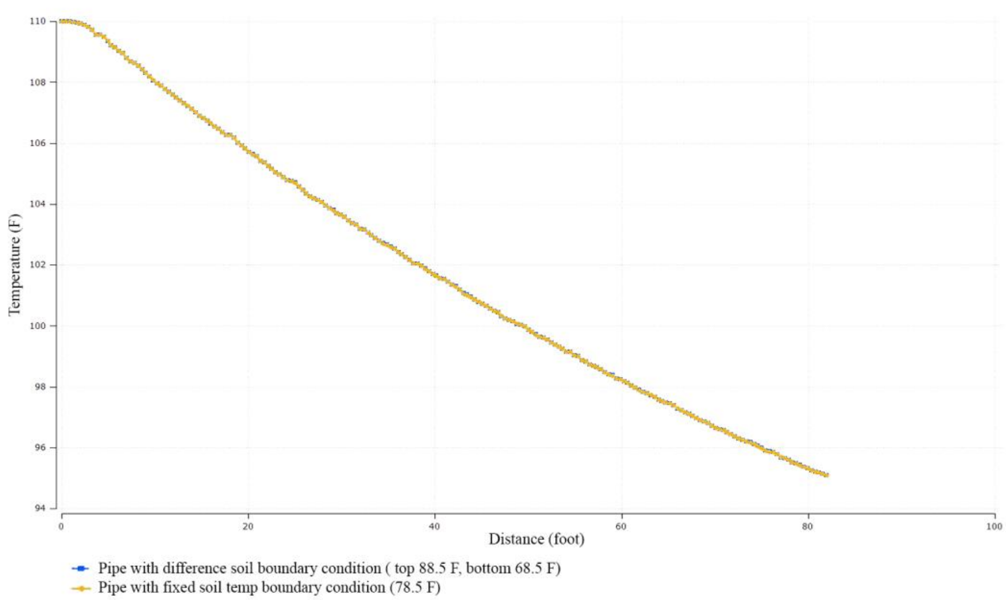

Figure 15: Section C

Appendix C: GCV system closed loop design

To test the GCV closed loop system in a residential building in Riyadh, we followed the GCV system evaluation tool guidelines to predict the temperature change. As the building's return air, the inlet temperature for the closed loop was fixed at 80^{o}F over the year. The GCV system was input with a pipe length from 400 to 600 feet and pipe depth of 13.12 feet and 19.68 feet. The pipe diameters range from 24 to 42 inches, and the soil type at the site is limestone. There were four to six pipes in the GCV system, and the volume flow rate was entered as 3,850 CFM. Figure 16 shows the GCV system design comparison for the non-residential building. The closed loop GCV system's performance in Figure 17 shows that the GCV system is inappropriate for non-residential buildings because it cools the return air by only four degrees Fahrenheit in the hot season.

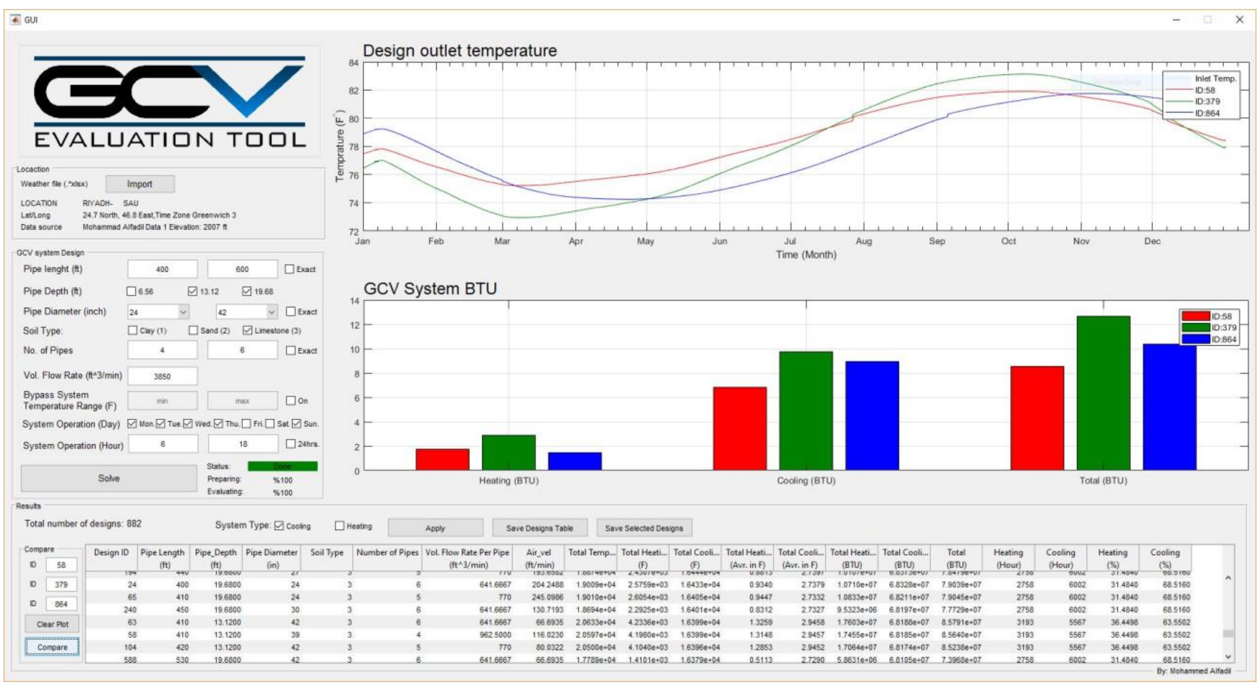

Figure 16: GCV System Design Comparison for Non-Residential Building (Closed Loop)

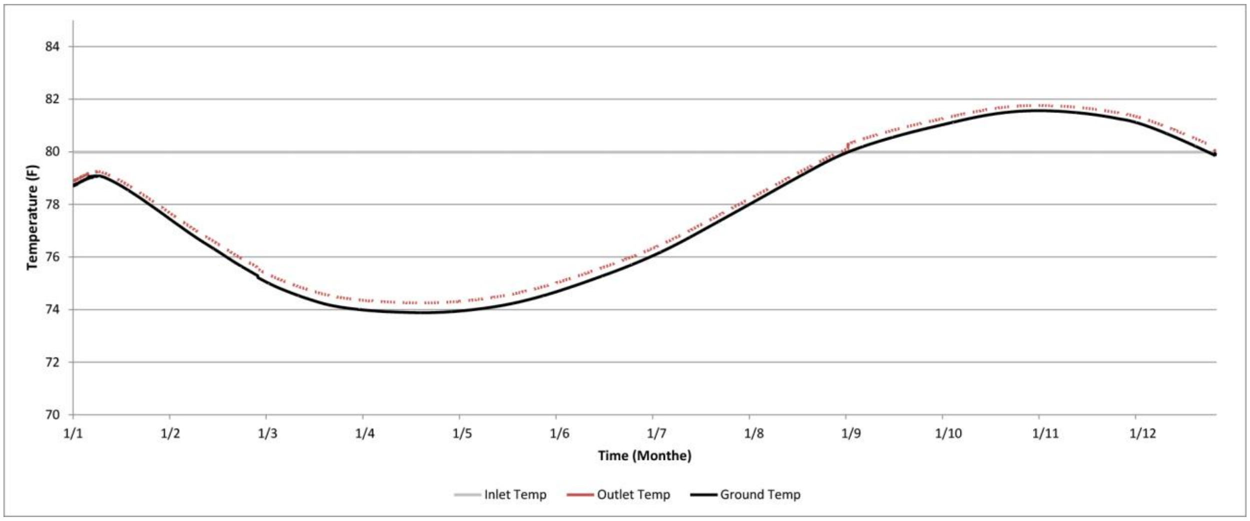

Figure 17: GCV System Design ID:864 Performance for Non-Residential Building (Closed Loop)

Appendix D: Soil temperature charged at Solar CM House

The GCV system affected the soil temperature that surrounded the pipe. To know the effect on the soil temperature, a thermocouple was installed at a depth of 9.8 feet, which is far away from the GCV system, in order to monitor soil temperature. Figure 18 shows the ground temperature close to the pipe surface (a pipe with airflow velocity of 200fpm) and ground temperature far away from the GCV system at Solar CM House over the period of seven days. The results indicate that the GCV system does not affect soil temperature daily, but the airflow rate charged the surrounding soil temperature an average of 4^{o}F.

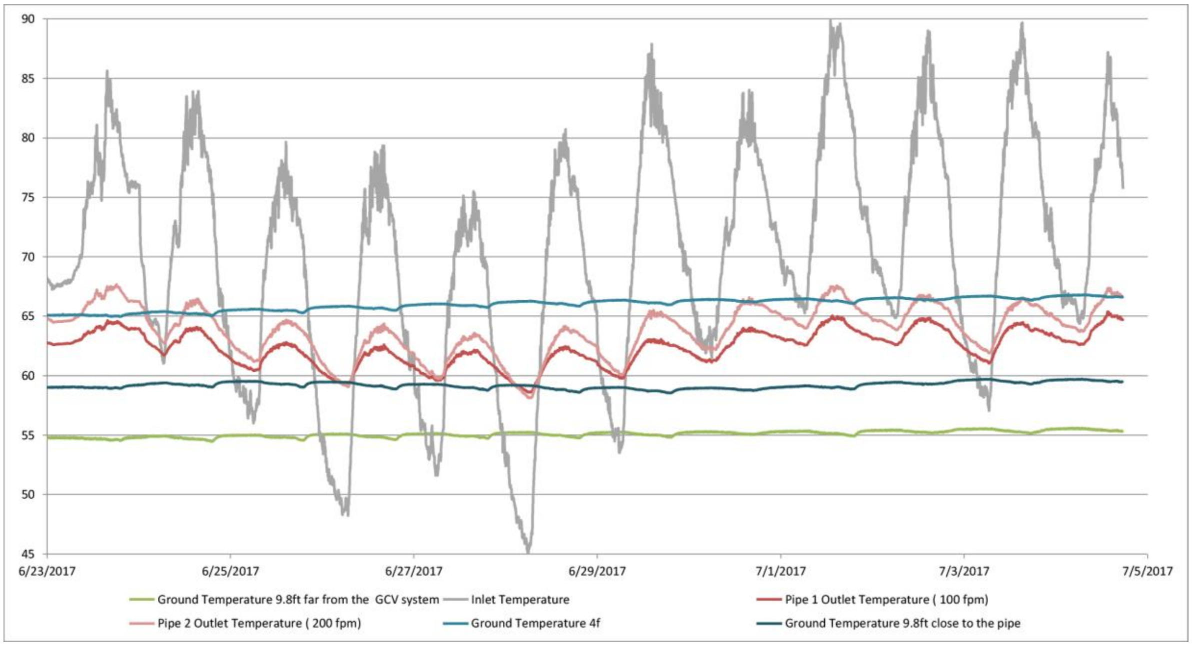

Figure 18: Soil Temperature Close and Far from the GCV System at a Depth of 9.8 Feet